# PHOSPHO-REGULATION OF THE DNA DAMAGE RESPONSE KINASE ATR

By

Edward Adam Nam

Dissertation

Submitted to the Faculty of the

Graduate School of Vanderbilt University

in partial fulfillment of the requirements

for the degree of

DOCTOR OF PHILOSOPHY

in

Cancer Biology

December, 2011

Nashville, Tennessee

Approved:

Dr. David Cortez

Dr. Graham Carpenter

Dr. Ellen Fanning

Dr. Albert Reynolds

Dr. Sandra Zinkel

*To my parents*

ACKNOWLEDGEMENTS

This dissertation is the culmination of a journey I began six years ago. Along the way I have run free, hobbled along, crawled, and sometimes just simply endured. I cannot say that I had the fortitude and will all on my own to accomplish what I have. Instead, I say thank you from the depths of my heart to the people that have supported me these last six years and throughout my life.

To my dissertation advisor David Cortez, thank you for seeing that I had stumbled down the wrong path and for setting me on course again. I am grateful for your belief, support, and mentorship. There are many aspects about your mentorship that I can thank you for, but you have impacted me most through your own example. Your work ethic and scientific acumen balanced with your family life are something I hope to have one day.

I thank my dissertation committee members: Drs. Graham Carpenter, Ellen Fanning, Albert Reynolds, and Sandra Zinkel. You all have graciously given your time and expertise to propel my research and career. Though my project was difficult, I am always encouraged by your enthusiasm for me as a scientist.

I have also received immense support from the Departments of Cancer Biology and Biochemistry, the Office of Biomedical Research Education and Training, and the Interdisciplinary Graduate Program. Special thanks to Tracy Tveit not only for making sure I have all my ducks in a row but also for your genuine care. Thank you to Drs. Roger Chalkley, Ann Richmond, Jin Chen, and Darrell Smith for your advice and guidance. With your wisdom, I persevered to continue down this road and have achieved what I thought was lost.

The Cortez lab has been fertile ground for me. Much of what I am as a scientist is due to my everyday interactions with lab members past and present. Courtney Lovejoy and Daniel Mordes, as senior students, I thank you for your knowledge and trade secrets. Jami Couch you are a newbie, but you are insightful beyond your years and have contributed to my success. My interactions with our honorary lab member Mahesh Chandrasekharan have contributed greatly to my growth. Thank you for your brilliance and for your jokes. Thank you to Nancy Zhao and Gloria Glick for keeping our lab running like a well-oiled machine. I am especially grateful to Nancy for her help in generating stable cell lines. Boundless thanks go to Gloria Glick, who goes above and beyond what is required everyday to ensure we have what we need to succeed. I thank you for your friendship and for your kindness and will always be grateful for our time together.

To my lab partners in crime, Bianca Sirbu and Carol Bansbach Robbins, you both have been a wellspring of encouragement and knowledge. I could not have asked for better colleagues. Bia, you inspire me with the passion and optimism you set to everything you do. CB, you keep me grounded and remind me of what is important. But enough of that, "It's the freaking weekend baby!" We have created a lot of great memories together. The inception of our lab dinner at PM and RoS + cooler should be enough to sum it up. Know that I cherish our friendships and that they have brightened my time in graduate school.

As much as it is a scientific and career journey, the path to the Ph.D. has granted me incredible richness in friendships. To my other friends in graduate school and beyond, I express nothing but gratitude for the support you have

given. Tarjani Thaker, you give your all to your friends, and I treasure you for that. Laura Titus Burns, you are just wholesome goodness, and I admire you for that. I expect to take a yoga class from you soon. Meghana Rao, I could not ask for a better work out buddy. You gave me the gift of spinning and yoga. More than that, you have enriched my life and my well-being. Finally to my friends Amy Park and Eun Young Son, thank you for being constants in my life. You both remind me there is another world outside this ivory tower. I will try to make it there soon.

Finally I am grateful for the support of my family. To my brother and sister, you both have influenced me with your lives and families. I know the two of you are always there if I need. Jim, thank you for your selflessness and care for our family. I can only aspire to have as much success in life as you. Susan, your ability and resoluteness to pursue what you desire has always prompted me to be courageous, to take more risks, and to experience new things. Mom, the gratitude I have for you is too manifold to enumerate here. Your love and support are beyond comparison. Your sacrifices gave me the opportunity to travel this path. Your strength, tenacity, and fearlessness are constant touchstones of what I need to keep moving forward. To my late father, I am grateful for your soundless love and support. I wish you were here to read this.

TABLE OF CONTENTS

Page

DEDICATION ..... ii

ACKNOWLEDGEMENTS ..... iii

LIST OF TABLES ..... x

LIST OF FIGURES ..... xi

LIST OF ABBERVIATIONS ..... xiv

Chapter

I. INTRODUCTION ..... 1

Cell cycle and genome duplication ..... 2
G1 phase ..... 2
S phase ..... 4
G2 and M phases ..... 5
DNA damage checkpoints ..... 5
G1 and G2 checkpoints ..... 6
S phase checkpoint and DNA replication stress ..... 8
DNA replication stress and cancer ..... 11
ATR regulation ..... 15
ATR and RPA-ssDNA ..... 15
ATR-ATRIP complex ..... 17
The Rad9-Rad1-Hus1 DNA damage clamp ..... 19
TopBP1-mediated activation of ATR ..... 21
Chk1 ..... 23
ATR-Chk1 and S phase checkpoint ..... 24
Common mechanisms of PIKK regulation ..... 26
Phospho-regulation of ATR ..... 30

II. MATERIALS AND METHODS ..... 34

DNA constructs and siRNA ..... 34
Genetic complementation of $ATR^{flox/-}$TR cell lines ..... 36
Verification of exogenous ATR expression in integrants ..... 37
Adenovirus infection ..... 38
PCR genotyping, RT-PCR, and sequencing of products ..... 38
Western blots and immunoprecipitations ..... 40
Immunofluorescence ..... 41
Colony formation and cell viability ..... 42
G2 checkpoint ..... 42

Completion of DNA synthesis after replication stress .....43
BrdU incorporation.....44
Mass spectrometry and sequence alignments .....44
ATR kinase reactions .....45
Phospho-peptide analysis.....46
Cell synchronization.....49
Yeast strain construction.....49
Yeast western blotting and spot assay .....50

III. T1989 PHOSPHORYLATION MARKS AN ACTIVE ATR KINASE .....52

Introduction .....52
Results.....53
ATR T1989 is a DNA damage-induced phosphorylation Site .....53
T1989 phosphorylation depends on ATR kinase activity. ....57
T1989 phosphorylation requires ATR activation ..... 62
Functional characterization of T1989 phosphorylation.....64
Discussion .....73
Regulation of T1989 phosphorylation.....73
Mechanistic implications of T1989 phosphorylation.....76
Research and Clinical Applications.....77

IV. ANALYSIS OF MUTATIONS THAT DISSOCIATE G2 and ESSENTIAL S PHASE FUNCTIONS OF HUMAN ATR .....78

Introduction .....78
Results.....79
Identification of an ATR separation of function mutant.....79
16A-ATR mutations result in replication stress response defects .....82
S944 .....86
S2143 .....86
3A-ATR phenocopies 16A-ATR replication stress response defects .....89
A conserved extended inter-HEAT repeat loop is important for ATR function .....94
Phospho-peptide analysis of ATR mutants .....96
T1589 is important for ATR function .....99
Discussion .....104
ATR phosphorylation.....104
Separation of Essential S phase functions of ATR from G2 checkpoint activity .....105
A potential novel ATR regulatory region.....108

V. FURTHER CHARACTERIZATION OF 16A-ATR MUTANTS .....110

Introduction .....110
Results.....110

Analysis of the 3A-ATR regulatory region in *S. cerevisiae* ....110
Hyper-stimulation of ATR does not segregate with viability and S phase defects ....112
Discussion ....118

VI. CHARACTERIZATION OF A NOVEL ATR KINASE INHIBITOR ....121

Introduction ....121
Results ....122
Characterization of AZ20-mediated ATR inhibition ....122
AZ20 inhibits ATR but not ATM ....124
AZ20 inhibits ATR rapidly ....124
AZ20 perturbs DNA replication ....125
AZ20 disrupts recovery from replication stress ....127
AZ20 delays entry into S phase ....132
AZ20 delays RB phosphorylation ....137
Replication stress potentiates AZ20 cytotoxic effects ....141
ATM deficiency increases AZ20 sensitivity ....143
Discussion ....145
Temporal requirements for ATR activity after replication Stress ....145
Clinical implication of AZ20 ....146
mTOR inhibition ....147

VII. SUMMARY AND FUTURE DIRECTIONS ....149

Summary ....149
ATR T1989 phosphorylation marks an active kinase ....150
S and G2 functions of ATR are separable ....150
Identification of a novel regulatory region ....150
Additional regulatory steps exist in TopBP1-mediate activation of ATR ....151
ATR kinase activity is important during replication fork stalling and completion of replication following fork stalling ....151
Determinants of ATR inhibition sensitivity ....151
Future Directions ....153
ATR activation ....153
Recruitment of ATR-ATRIP and ATR signaling factors ....153
How does TopBP1 activate ATR? ....158
Regulation of TopBP1-mediated activation ....160
Other ATR activating proteins? ....161
Phospho-regulation of DNA damage PIKKs ....162
A novel regulatory region ....166
T1989 phosphorylation ....168
Conflicting evidence for T1989 function ....170
Other post-translational modifications ....171
ATR function at replication forks ....172

ATR signaling in the clinic.....173
ATR function at the centrosome .....173

Appendix

A. ATR S428 and S435 .....178

S428 .....178
S435 .....180

REFERENCES.....182

LIST OF TABLES


| Table | | Page |
|---|---|---|
| 1. | Primers used for mutagenesis | 35 |
| 2. | Yeast strains | 50 |
| 3. | *MEC1* primer sequences | 50 |
| 4. | List of ATR phosphorylation sites and peptides identified by mass Spectrometry | 53 |

LIST OF FIGURES

Figure Page

1. Cell cycle progression is controlled by Cyclin-CDK activity .....3
2. G1 and G2 DNA damage checkpoints .....7
3. S phase checkpoint .....10
4. Oncogene-induced replication stress as a model for tumorigenesis .....13
5. DNA replication stress causes the formation of single-stranded DNA .....16
6. ATRIP domains and their functions .....18
7. ATR activation process .....20
8. TopBP1 domains and their functions .....22
9. PIKKs share common domain architecture .....27
10. Common modes of PIKK regulation .....29
11. ATR is phosphorylated on T1989 .....54
12. DNA damage induces ATR T1989 phosphorylation .....56
13. The pATR antibody is specific to T1989 .....58
14. T1989 phosphorylation depends on ATR kinase activity .....60
15. Chk1 and CDK2 are not required for T1989 phosphorylation .....61
16. T1989 phosphorylation requires ATR activation via the PRD .....63
17. Flow chart describing the ATR genetic complementation strategy .....65
18. ATR T1989 phosphorylation is dispensable for cellular recovery from replication stress .....66
19. T1989 phosphorylation causes a mild viability defect .....68
20. WT-ATR$^{del/-}$TR and T1989A-ATR$^{del/-}$TR derived clones do not differ significantly in S phase percentage .....70
21. Chk1 phosphorylation correlates with T1989A ATR protein levels .....72
22. Identification of an ATR separation of function mutant .....81

23. 16A-ATR mutations result in replication stress response defects .....84

24. 16A-ATR exhibits normal protein stability, basal kinase activity, and normal localization .....85

25. S944 is dispensable for ATR function .....87

26. S2143 is dispensable for ATR function .....88

27. 3A-ATR mutations perturb viability .....90

28. 3A-ATR phenocopies 16A-ATR replication stress response defects .....92

29. 3A-ATR mutations do not disrupt ATR-Claspin interactions.....93

30. A conserved extended inter-HEAT repeat loop is important for ATR function.....95

31. Phospho-peptide analysis of ATR mutants .....97

32. Mutation of T1566 and T1578 is not sufficient to disrupt ATR function ..100

33. Mutation of T1589 is sufficient to disrupt ATR function .....102

34. T1989 phosphorylation is intact in 3A-ATR.....103

35. Clustal alignment of 3A-ATR inter-HEAT repeat region of ATR orthologues .....111

36. An FRVF1349AAAA-Mec1 mutant cannot rescue *mec1Δsml1Δ* replication stress sensitivity .....113

37. 6A-ATR mutations increase TopBP1-mediated stimulation of ATR.....114

38. 16A-ATR exhibits increased binding to the AAD of TopBP1.....116

39. Increased Chk1 phosphorylation in 6A-ATR cells.....117

40. AZ20 inhibits ATR .....123

41. AZ20 perturbs cell cycle progression.....126

42. ATR inhibition in S phase disrupts DNA replication.....128

43. ATR inhibition following a transient exposure to replication stress disrupts completion of DNA synthesis .....129

44. ATR inhibition during prolonged replication fork stalling prevents completion of DNA synthesis ....131

45. AZ20 treatment during G0/G1 delays S phase entry ....133

46. AZ20 treatment during G1 delays S phase entry ....135

47. AZ20 treatment of asynchronous U2OS cells perturbs DNA replication and delays S phase entry ....136

48. AZ20 inhibits mTOR ....138

49. AZ20 inhibits ATR and mTOR at similar concentrations ....140

50. DNA replication stress potentiates AZ20 cytotoxicity ....142

51. ATM-deficiency sensitizes cells to AZ20 treatment ....144

52. Model of ATR activation ....154

53. Alternative mechanisms for ATR-ATRIP recruitment ....156

54. Activating mutations in PI3K and TOR ....159

55. Proposed model of ATM activation ....164

56. Alignment of ATR activation loop ....165

57. An extended inter-HEAT repeat loop is a novel regulatory region shared among DNA damage PIKKs ....167

58. Centrosome position and asymmetric stem cell division ....175

59. Centrosome and chromosome duplication cycles ....177

60. S428 and S435 are dispensable for ATR function ....179

LIST OF ABBREVIATIONS

| | |
|---|---|
| 9-1-1 | Rad9-Hus1-Rad1 |
| AA | amino acid |
| AAD | ATR activation domain |
| ABCDE | DNA-PK autophosphorylation cluster T2609, S2612, T2638, T2647 |
| ATM | ataxia-telangiectasia mutated |
| ATR | ATM and Rad3-related |
| ATRIP | ATR interacting protein |
| BLM | Bloom's Syndrome Helicase |
| BRCA1 | breast and ovarian cancer gene 1 |
| BRCT | BRCA1 C-terminal |
| BrdU | bromodeoxyuridine |
| CDK | cyclin-dependent kinase |
| CKI | cyclin-dependent kinase inhibitor |
| Chk1 | checkpoint kinase 1 |
| Chk2 | checkpoint kinase 2 |
| DDK | Cdc7/Dbf4-dependent kinase |
| DDR | DNA damage response |
| DNA-PK | DNA-dependent protein kinase |
| DSB | double-strand break |
| FACS | fluorescence activated cell sorting |
| FAT | FRAP-ATM-TRAPP |
| FATC | FAT C-terminal |

| | |
|---|---|
| FBS | fetal bovine serum |
| GST | glutathione s-transferase |
| HA | hemagglutin |
| HEAT | Huntingtin, Elongation factor 3, A subunit of protein phosphatase 2A and TOR1 |
| hTERT | human telomerase reverse transcriptase |
| HU | hydroxyurea |
| IR | ionizing radiation |
| MCM | mini-chromosome maintenance protein |
| MRN | Mre11-Rad50-Nbs1 |
| mTOR | mammalian target of rapamycin |
| mTORC1 | mTOR complex 1 |
| ORC | origin recognition complex |
| RB | retinoblastoma protein |
| PAGE | polyacrylamide gel electrophoresis |
| PI | propidium iodide |
| PI3K | phosphoinositide-3 kinase |
| PIKK | PI3K related kinase |
| PRD | PIKK regulatory domain |
| pre-RC | pre-replication complex |
| RPA | replication protein A |
| ssDNA | single-stranded DNA |
| S/TQ | serine/threonine-glutamine |
| TopBP1 | topoisomerase II-beta binding protein I |
| TR | tetracycline repressor |

| | |
|---|---|
| UV | ultraviolet irradiation |
| WRN | Werner's Syndrome helicase |
| WT | wild type |

# CHAPTER I

## INTRODUCTION

The average human body contains trillions of cells that initially arose from one dividing zygotic cell. The decision to divide is carefully regulated throughout a human lifespan by the cell cycle. Except for cells in specific niches in the adult body, cells in adult humans are quiescent and not actively dividing.

Improper control of cell division can lead to aberrant proliferation of cells and under certain conditions to the formation of a tumor and eventually a carcinoma. Many mutations linked to human cancers disrupt control of the cell cycle and cause cells to divide aberrantly (1). Changes in the cellular genome occur in every tumor, and genomic instability is a hallmark of cancer (2, 3).

Where do these genetic changes come from? With each cell division, DNA must be faithfully replicated. In human cells there are six billion bases of DNA to copy each time the cell divides, and trillions of cell divisions occur in a human lifespan. The amount of DNA itself that must be perfectly copied in a lifetime is a daunting task, and mistakes can occur. Cellular processes also produce reactive metabolites and oxidation products that damage DNA. Finally, exogenous sources of DNA damage like radiation and other genotoxins are prevalent in the environment. This combined assault on DNA yields tens of thousands of DNA lesions per day in every human cell.

In response to DNA damage, an evolutionarily conserved DNA damage response (DDR) elicits DNA damage checkpoints to coordinate cell cycle progression, DNA repair, DNA replication, DNA transcription, and even

programmed cell death to promote genome maintenance. Genome maintenance via the DDR is essential to prevent disease. Disruption of many DDR genes results in lethality, cancer susceptibility syndromes, neurodegenerative disorders, and premature aging syndromes (4).

## Cell cycle and genome duplication

The cell cycle controls cell division and, except for during embryonic development, consists of Gap 1 (G1), DNA Synthesis (S), Gap 2 (G2), and Mitotic (M) phases. Modulation of cyclin-dependent kinase (CDK) activity controls cell cycle progression. CDK activity is controlled at several levels including, requisite activation by cyclins, regulation of cyclin levels (Figure 1a), inhibition by CDK inhibitors (CKIs), and phosphorylation. The following overview of each of the cell cycle phases highlights some of these mechanisms and serves to introduce pathways that are also regulated by the DDR. It is by no means a comprehensive overview.

### *G1 phase*

The decision to divide is determined in the G1 phase of the cell cycle. External mitogenic signals and nutrient availability are integrated by the cell, and expression levels of cyclin D rise. Cyclin D binds and activates CDK4/6. Inhibitory phosphates are also removed from CDK4/6 by the CDC25 family of phosphatases. Cyclin D-CDK4/6 phosphorylates the tumor suppressor retinoblastoma (RB) pocket protein (5, 6). RB binds and inhibits the E2F family of transcription factors (Figure 1b, orange panel).

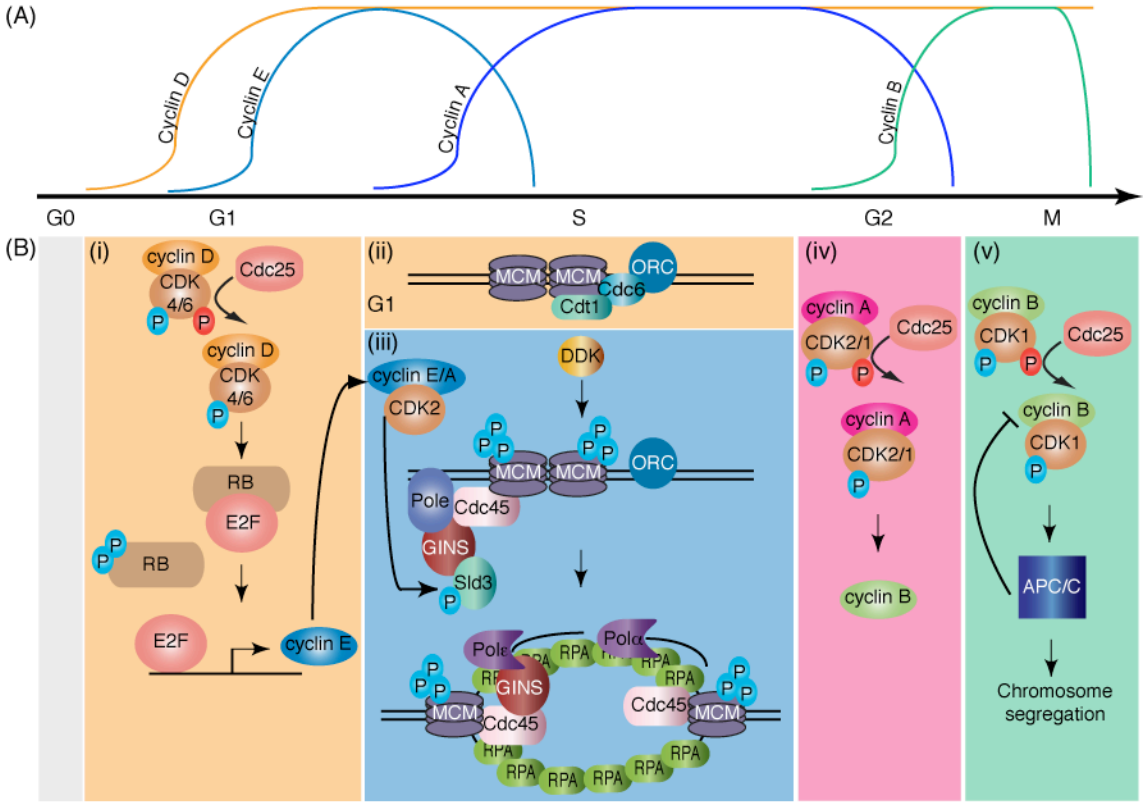


**Figure 1. Cell cycle progression is controlled by Cyclin-CDK activity.** (A) Cyclin-dependent kinase (CDK) activity is controlled by regulating levels of requisite cyclins. The rise and fall of cyclin levels through each cell cycle phase is depicted in graph form. (B) (i) Mitogenic signaling causes an increase in cyclin D levels. Inhibitory phosphates are removed from cyclin D-CDK4/6 by CDC25. Cyclin D-CDK4/6 regulate the G1/S transition by phosphorylating RB, alleviating inhibition of E2F. E2F-mediated transcription of cyclin E promotes cyclin E-CDK2 activity, which further phosphorylates RB to promote S phase entry. (ii) To replicate DNA, pre-replication complexes (pre-RCs) are formed at origins of replication in G1. (iii) In S phase cyclin E/CDK2 and DDK activities promote recruitment of additional replication factors to pre-RCs to form the pre-initiation complex and replication initiation. (iv) In G2, cyclin A-CDK2/1 activity promote an increase in nuclear cyclin B to mediate the transition from G2 to M phase. (v) In mitosis, cyclin B-CDK1 is activated in part by removal of inhibitory phosphates by CDC25. Cyclin B/CDK1 activates the anaphase promoting complex (APC/C), which is required for chromosomal segregation. APC/C activity also results in degradation of cyclin B, which is required for exit from mitosis.

Phosphorylation of RB relieves this inhibition allowing transactivation of E2F target genes, which include cyclin E and proteins required for genome duplication in S phase (6, 7).

*S phase*

Following G1, DNA synthesis occurs in S phase. DNA replication requires formation of a pre-replication complex (pre-RC) in the G1 phase (Figure 1b, small orange panel). Pre-RC formation includes binding of origin recognition complexes (ORCs) to replication origins, ORC-dependent recruitment of Cdc6 and Cdt1, and loading of the mini-chromosome maintenance (MCM) helicase complex (8-10). Pre-RCs remain inactive in this state until S phase when cyclin E-CDK2 and cyclin A-CDK2 activity is high. CDK2 and Cdc7/Dbf4-depedent kinase (DDK) activities initiate replication origin firing at pre-RCs through recruitment of Cdc45 and GINS, which activate the MCM helicase and promote DNA unwinding and polymerase recruitment (Figure 1b, blue panel) (11). DNA synthesis occurs in a bi-directional manner. These replication structures are called replication forks, and the replication proteins associated at these forks are collectively called the replisome (12, 13).

Loading of pre-RCs and initiation of DNA synthesis occur in separate phases of the cell cycle to ensure DNA is replicated only once. CDK activity is low in G1 when pre-RCs are formed but high throughout the rest of the cell cycle. Once an origin has fired in S phase, it will not be re-replicated, since pre-RCs can only form in G1. This is because CDK activity inhibits pre-RC formation at origins by phosphorylating all components of the pre-RC and negatively regulating these proteins through proteolysis and subcellular localization (14).

Preventing re-replication of DNA is essential to maintain genome integrity, as replicating certain regions more than once would change DNA copy number and perturb chromosome segregation (15).

*G2 and M phases*

Following DNA synthesis, the G2 phase of the cell cycle serves to prepare the cell for segregation of chromosomes in mitosis. This includes synthesis of proteins required for mitosis including cyclin B. The transition from G2 to mitosis occurs when a threshold of activated nuclear cyclin B-CDK1 is reached (Figure 1b, pink panel). In addition to complexing with cyclin B, removal of inhibitory phosphorylation on CDK1 by the CDC25 phosphatase is required for CDK1 activity (16). Once cyclin B-CDK1 activity levels are high, mitosis occurs, which includes segregation of duplicated chromosomes into to two daughter cells. Exit from mitosis is enacted by degradation of cyclin B (Figure 1b, green panel) (16).

## DNA damage checkpoints

Each phase of the cell cycle is tightly regulated through control of cyclin-CDK activity to ensure proper progression. The penultimate goal of this complex system is to ensure the genome is duplicated only once and properly segregated into two cells (17). Yet in each phase of the cell cycle, DNA is susceptible to damage, and this damage could be replicated and propagated to daughter cells. To prevent this, the DDR enacts checkpoints that inhibit many of the cell cycle components in addition to regulating DNA repair and cell death.

At the apex of the DDR are three related protein kinases, Ataxia-telangiectasia Mutated (ATM), ATM and Rad3-related (ATR), and DNA-dependent protein kinase (DNA-PK). While DNA double-strand breaks (DSBs) activate ATM and DNA-PK, many types of DNA damage activate ATR, including DNA replication stress, DNA DSBs, base adducts, and crosslinks (18). Once activated, these kinases preferentially phosphorylate serines and threonines followed by a glutamine (S/TQ) (19, 20) in hundreds of protein substrates to halt cell cycle progression, regulate DNA repair, and elicit cell death. In the next section I will introduce how the DDR enacts cell cycle checkpoints to halt progression in the presence of DNA damage.

*G1 and G2 checkpoints*

If DNA damage occurs in G1, activation of the DDR prevents progression into S phase primary through ATM-mediated stabilization of the tumor suppressor protein p53 (Figure 2a) ATM directly phosphorylates p53 and the ubiquitin ligase MDM2, which targets p53 for proteolysis. ATM also phosphorylates and activates the effector kinase Chk2, which also phosphorylates p53. ATM and Chk2 phosphorylation of p53 in both cases functions to stabilize p53. p53 transactivates expression of the CKI, p21, which binds and inhibits cyclin E-CDK2. Chk2 also phosphorylates CDC25, targeting the CDK-activating phosphatase for degradation (21). Inhibition of cyclin E-CDK2 prevents phosphorylation of RB and initiation of DNA synthesis and induces a G1 arrest. p53 also transactivates programmed cell death genes and promotes genome maintenance through culling of cells with DNA damage (22).

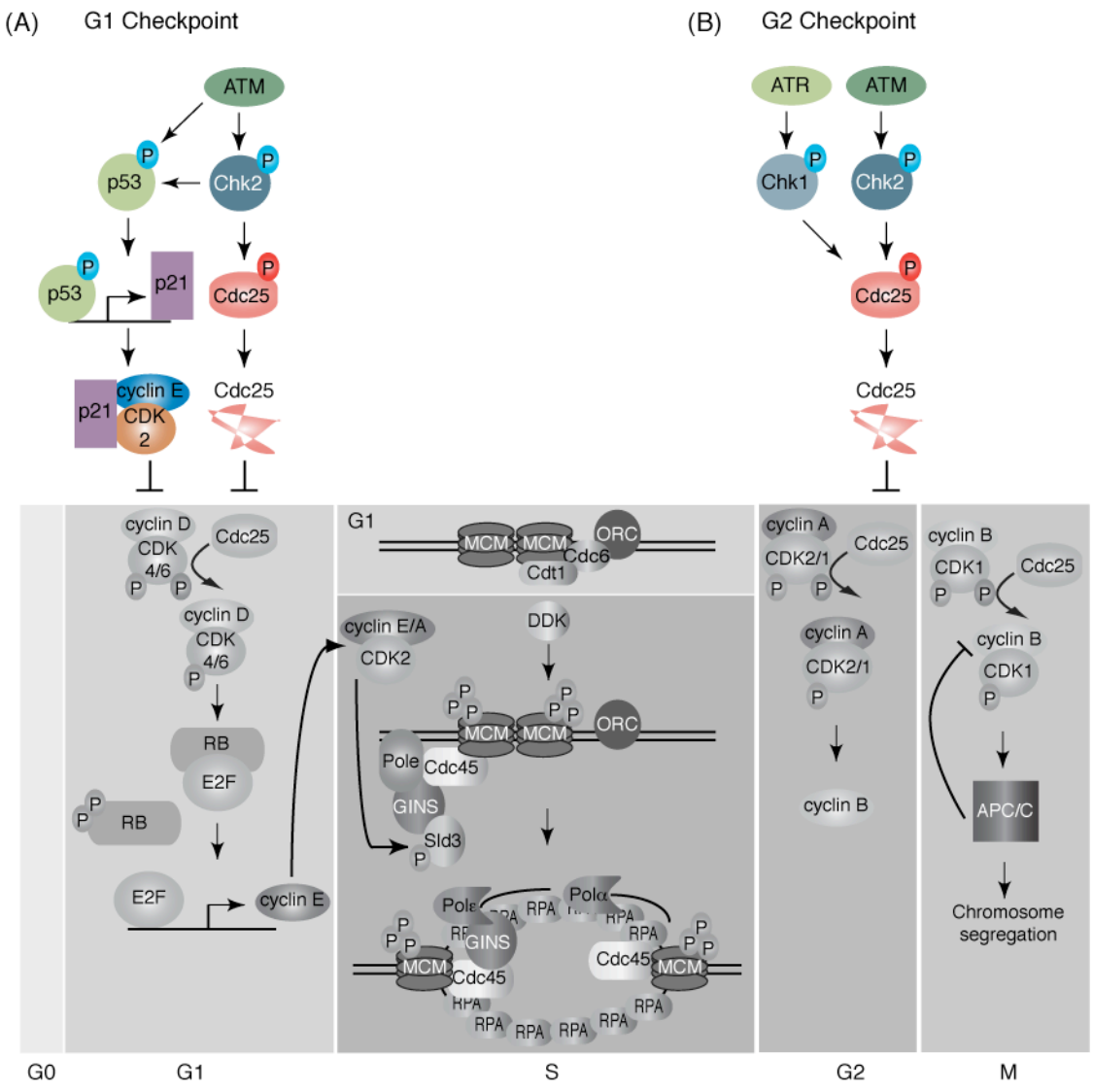


**Figure 2. G1 and G2 DNA damage checkpoints.** (A) In G1, DNA damage activates the ATM kinase which phosphorylates many substrates including p53 and Chk2. Once activated by ATM, Chk2 also phosphorylates p53. p53 phosphorylation stabilizes the protein and promotes transactivation of p53 target genes, including the cyclin-dependent kinase inhibitor p21. p21 binds and inhibits cyclin/CDKs. Chk2 also phosphorylates the CDC25 family of phosphatases targeting them for degradation, which also prevents cyclin/CDK activation. (B) In G2, DNA damage activates ATR and ATM, and they phosphorylate and activate Chk1 and Chk2 respectively. Both Chk1 and Chk2 phosphorylate CDC25 phosphatases to promote their degradation.

Aberrant regulation in all of these components is found in many types of cancer (23-26).

A DNA damage checkpoint also occurs in G2 to prevent entry into mitosis with damaged DNA. This checkpoint is mediated by the ATM-Chk2 and ATR-Chk1 pathways. ATM and ATR activation leads to the phosphorylation of the effector kinases Chk2 and Chk1, respectively. Both Chk2 and Chk1 phosphorylate the CDC25 phosphatase targeting it for proteasome-mediated degradation. Degradation of CDC25 prevents removal of inactivating phosphorylations on cyclin B-CDK1, which is required for entry into mitosis (Figure 2b) (23, 27-29).

*S phase checkpoint and DNA replication stress*

DNA is particularly vulnerable during the process of DNA replication. DNA is normally double-stranded, wrapped around proteins called histones, and compacted into higher order structures. During replication histones are removed, and DNA is unwound to a single-stranded state to facilitate semi-conservative replication. Furthermore, unwinding DNA creates topological problems. Enzymes nick and break the DNA in order to relieve this topological stress. These processes alone put the genome in a precarious state during DNA replication. The possibility of DNA damage further increases during replication, as the replisome can encounter obstacles on the DNA that can prevent replication fork progression (30).

Impeding replication fork progression causes what is collectively termed DNA replication stress. DNA damage, proteins tightly bound to DNA, lack of sufficient deoxynucleotides, and even difficult to replicate sequences are all

sources of DNA replication stress (31-33). In response to DNA replication stress, the ATR kinase is activated and enacts the intra-S phase checkpoint by phosphorylating the effector kinase Chk1 and other substrates to block cell cycle progression, regulate origin firing, stabilize stalled replication forks, restart collapsed forks, and prevent premature chromatin condensation in the presence of incomplete DNA replication (Figure 3) (18, 34, 35). ATR, unlike ATM and DNA-PK, is an essential gene in replicating cells (36-38). This probably is due to ATR activation by replication stress in every S phase and perhaps regulation of specific aspects of DNA replication such as origin firing or nucleotide production.

Replication stress often results in the generation of excess ssDNA. In addition, replication stress can lead to collapse of replication forks and generation of DNA double-strand breaks (DBSs) (39-42). Both ssDNA and DNA DSBs are highly recombinogenic. If they are not properly resolved, illicit recombination and genome rearrangements can occur. Disruption of replication proteins, such as DNA ligase, DNA polymerases, MCM4, and replication protein A (RPA), increases spontaneous chromosomal exchanges (43-47). Disruption of S phase checkpoint proteins, including the *S. cerevisiae* homolog of ATR, Mec1, causes an increase in chromosomal rearrangements (48, 49). In addition anti-recombinational helicases are regulated by ATR as part of the S phase checkpoint to suppress aberrant HR of replication intermediates. Deletion of these helicases results in human diseases and hyper-recombination in cells derived from these patients (50-52).

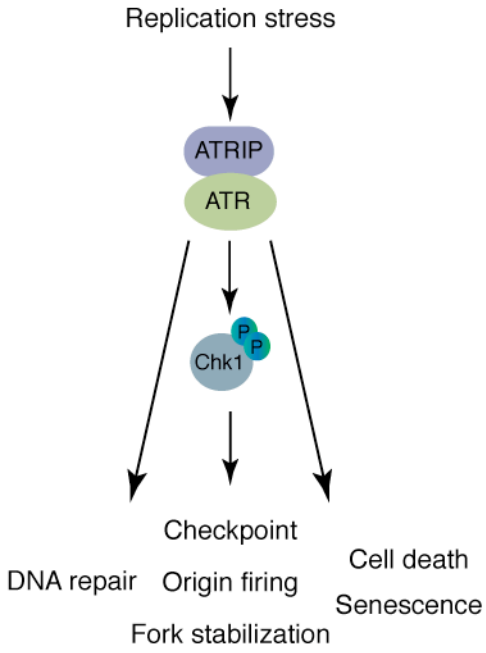


**Figure 3. S phase checkpoint.** In response to DNA replication stress, the ATR kinase phosphorylates Chk1 and numerous substrates. This signaling cascade regulates replication fork stability, origin firing, DNA repair, and cell death. The mechanisms through which ATR mediates these activities are complex and much is still unclear.

Because ATR is essential, homozyogous loss of function mutations are not compatible with life. Mice with *ATR* deleted die before embryonic day E7.5. Mouse embryonic fibroblasts from *ATR* null mice undergo cell cycle arrest and cell death in the absence of exogenous DNA damage (36-38). However, hypomorphic alleles of ATR that cause reduced protein levels due to a splicing error cause a rare disease called Seckel Syndrome. Seckel Syndrome patients exhibit short stature, microcephaly, and mental retardation thought to be attributed to proliferation defects during development (53, 54). In addition, ATR is a haploinsufficient tumor suppressor in certain genetic backgrounds. Hypomorphic *ATR* mutations in microsatellite instability tumors are associated with reduced overall survival and disease-free survival (55, 56), and mutations of ATR substrates are associated with cancer (57, 58). Thus responding to replication stress via the ATR pathway is essential to prevent genetic changes and disease. The functions of ATR in responding to replication stress will be discussed in depth later.

**DNA replication stress and cancer**

Inactivation of many DNA repair genes in the germline results in hereditary cancer predisposition syndromes (59). Disruption of DNA repair pathways, especially error-free repair pathways like homologous recombination, leads to increased genetic changes that can promote cancer development (Figure 4a). This paradigm is often referred to as the "mutator hypothesis." The source of genomic instability in this case comes from an inherited defect in DNA repair (60-63).

Chromosomal instability is also a hallmark in sporadic cancers. However in sporadic non-hereditary cancers, the source of genetic changes is unclear. Sequencing studies in sporadic cancers before treatment reveal that very few genes, including DNA repair genes, are mutated at high frequency (64-68). This suggests that in sporadic cancers early inactivation of DNA repair genes is a rare event. Interestingly, the few genes mutated at frequencies over 20% included *P53*, *EGFR*, *RAS*, *p16*, and *PTEN* (69). These genes encode for classical oncoproteins or negative regulators of oncoprotein activity.

Because oncogenes are frequently mutated in sporadic cancers, it has been hypothesized that oncogene activation leads to genomic instability. How can oncogenes cause DNA damage? It is now known that oncogene-driven proliferation in tumor-derived cell lines and xenograft models causes DNA replication stress, activation of the ATR-Chk1 pathway, loss of heterozygosity, and genome rearrangements (70-72). These data have led to the "oncogene-induced replication stress" hypothesis, which predicts that 1) mutations in genes that regulate entry into S phase occur at a high frequency, 2) DNA replication stress is present in early non-malignant neoplasias, 3) the DDR is activated and prevents tumor development, and 4) bypass of the DDR promotes progression to malignancy (73, 74).

In support of the first prediction, mutations in oncogenes (EGFR, RAS) that drive S phase entry and tumor suppresors (PTEN, p16, p53) that function to oppose these oncogenes are mutated at high frequency (69). Evidence also supports that DNA replication stress is present in early precancerous lesions. Common fragile sites are difficult to replicate regions of the genome.

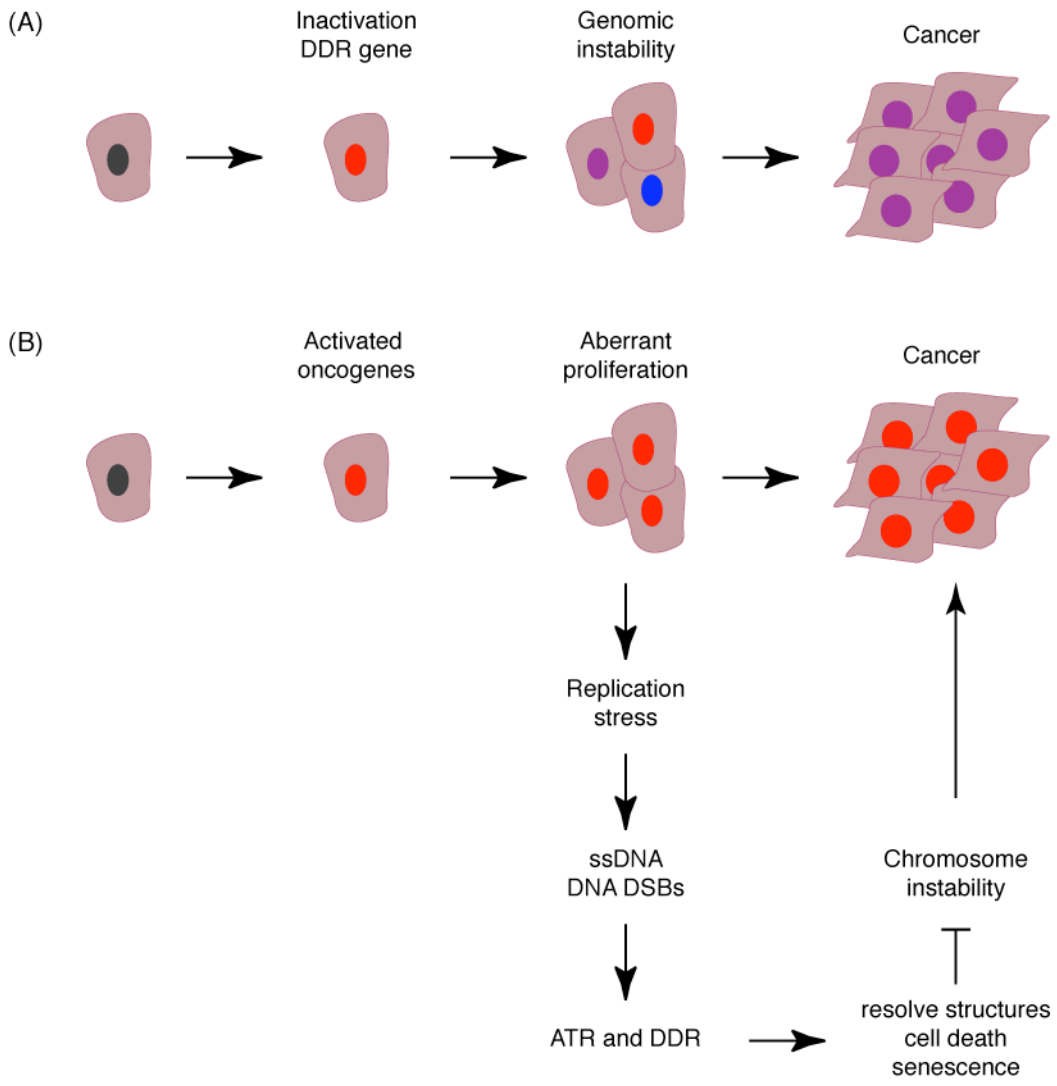


**Figure 4. Oncogene-induced replication stress as a model for tumorigenesis.** (A) Hereditary mutations in DNA repair genes lead to cancer predisposition likely because of the mutator hypothesis. Increased genomic instability is the result of an inability to properly repair DNA damage. This allows the accumulation of many genetic changes that may eventually select for cells with characteristics that can form a malignant tumor. (B) In contrast to hereditary tumors resulting from germline mutations in DNA repair genes, oncogene-induced replication stress is thought to contribute to genomic instability. Increased levels of replication due to oncogenes in early neoplasias cause replication stress which activate the ATR and DNA damage response. DNA damage response signaling is thought to prevent accumulation of cells with chromosomal instability through cell death pathways potentially mediated by p53.

DNA replication stress causes DNA breaks and gaps at common fragile sites leading to their rearrangement and can be considered a signature for replication stress (75). Two independent studies show that common fragile sites exhibit allelic imbalance in precancerous lesions (71-74). Importantly, allelic imbalance is not increased at other chromosome loci that frequently exhibit allelic imbalance in advanced cancers (71-74).

DDR activation occurs in precancerous neoplasias but not in adjacent normal tissue in several studies supporting prediction three (71-74). In support of prediction four, p53 protein levels were increased and apoptotic cells were observed in premalignant neoplasias. While DDR activation was still present in advanced cancers, apoptosis was suppressed and correlated with p53 mutations (71-74). Thus while p53 deletions in mouse models and human cells does not cause aneuploidy, it may be that bypass of the DDR occurs frequently through p53 inactivation, accounting for the high frequency of p53 mutations in cancers.

These data have led to a new paradigm in cancer biology and genome maintenance, whereby DNA replication stress induced by oncogene activation is a major contributor to genomic instability in tumors (Figure 4b). Replication stress generates ssDNA and DNA DSBs, which activate ATR and the DDR to facilitate proper replication, DNA repair, cell cycle arrest, and cell death or senescence. Thus ATR and the DDR are thought to be a barrier to tumor development. Bypass of this barrier via p53 mutations, for instance, may allow for selection of cells with genetic changes due to improper repair of ssDNA and DNA DSBs.

However, bypass of the DDR may be a double-edged sword for the cancer cell. There may be an increased dependency on the ATR pathway, analogous to

oncogene addiction, to continue to replicate in the presence of oncogene-induced replication stress. Understanding how cells maintain genome integrity during replication stress is necessary to gain insights into the pathology of cancer and other diseases. Furthermore, because many cancer cells experience increased replication stress, we may be able to develop therapies targeting ATR and the replication stress response.

## ATR regulation

It is clear that ATR is essential as one of the major controllers of the DDR to replication stress. I have focused my dissertation studies on understanding how ATR is regulated in order to gain insights into how cells maintain their genomes. In the follow section, I will outline major points known about ATR regulation.

### *ATR and RPA-ssDNA*

Replication protein A (RPA) is a single-stranded DNA (ssDNA) binding protein that consists of three subunits, RPA32, RPA14, and RPA70. RPA affinity for ssDNA is high, and RPA binding stabilizes ssDNA. In addition, protein interactions with RPA serve to recruit DNA replication, ATR, and other DDR proteins to RPA-ssDNA (76). RPA is normally associated with ssDNA even during replication, but it becomes hyperphosphorylated by the DDR (77-79).

The most common signal to activate ATR in response to replication stress is likely to be RPA-ssDNA (80). This is because while replication stress blocks

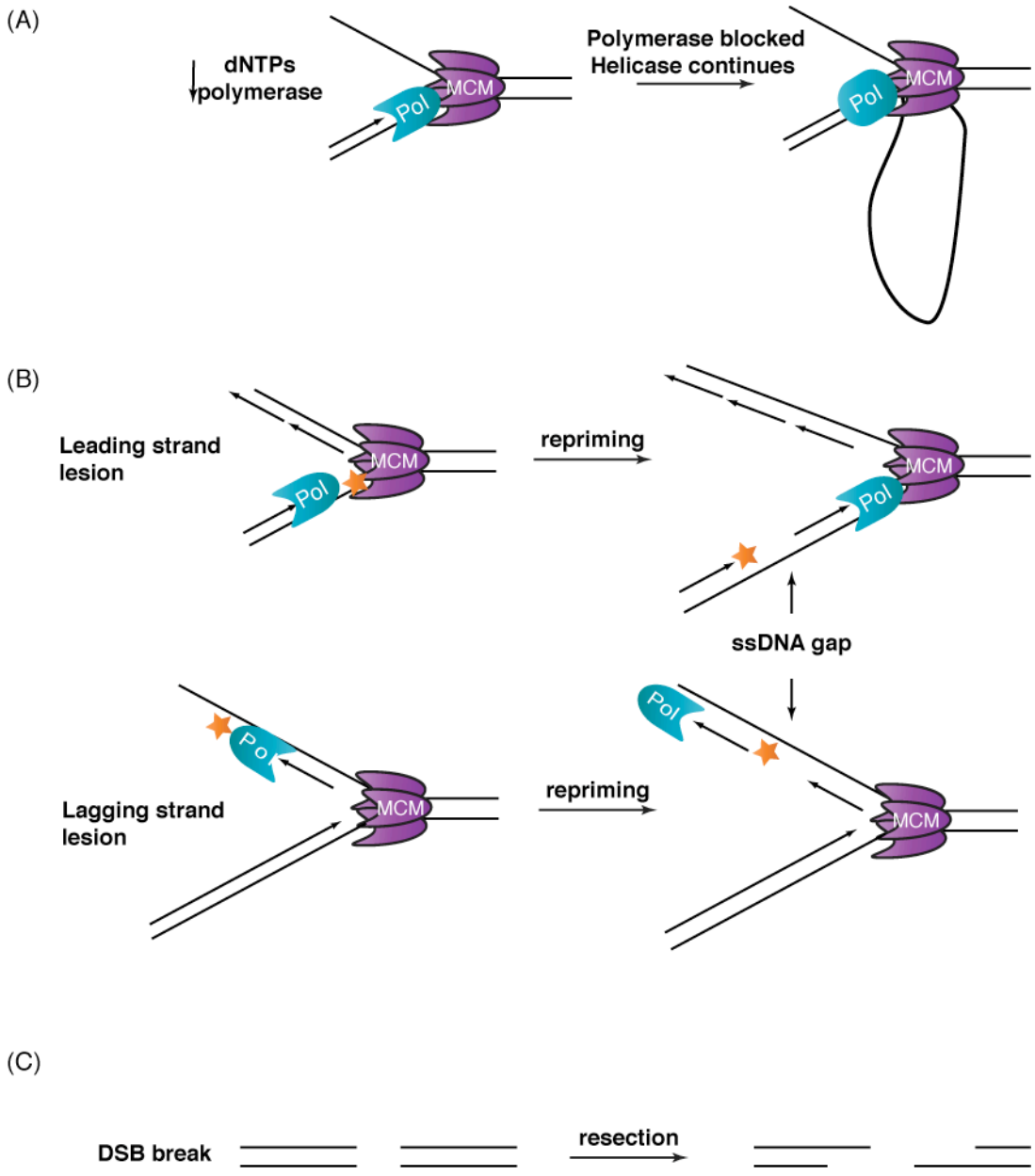


**Figure 5. DNA replication stress causes the formation of single-stranded DNA.** (A) Inhibition of polymerase activity or depletion of dNTPs leads to stalling of the polymerase while not affecting helicase activity. This can lead to functional uncoupling of the two enzymatic activities and generation of single-stranded DNA due to continued unwinding without DNA synthesis. (B) Depicted are lesions on the leading or lagging strands that block the polymerase but not the helicase. Re-priming allows continued DNA synthesis but leaves a single-stranded DNA gap behind. Of note, re-priming can also occur in the situation drawn in A. (C) Processing of many types of DNA damage also lead to single-stranded DNA intermediates. Resection of a DNA double-strand break to single-stranded DNA occurs as part of homologous recombination.

replication forks in many ways, RPA-ssDNA can be generated directly or indirectly from many types of replication stress. For example, some types of replication stress stall the DNA polymerase but not the replicative helicase (81). This functional uncoupling of enzymatic activities allows the helicase to continue to unwind DNA while the polymerase remains blocked, generating stretches of unreplicated ssDNA that becomes bound by RPA (Figure 5a). Functional uncoupling of the replisome occurs in cases of nucleotide depletion, polymerase inhibition, UV-generated thymidine dimers, and any type of lesion that blocks the polymerase but not the helicase. Re-priming can occur and only a small gap may be left behind (Figure 5b) (33, 82). While lesions, such as interstrand crosslinks, block both the polymerase and helicase, enzymatic remodeling of the blocked replication fork by helicases and nucleases also creates ssDNA. Similarly, nuclease-mediated resection of DNA double-strand breaks (DSBs) produces ssDNA (Figure 5c) (83). These are just a few ways in which ssDNA is generated by replication stress.

*ATR-ATRIP complex*

ATR forms an obligate complex with the ATR Interacting Protein (ATRIP) (36). ATRIP directly interacts with the 70N subunit of RPA (Figure 6) and facilitates the recruitment of ATR-ATRIP to RPA-ssDNA (Figure 7) (84, 85). ATR activity, though it is unclear why, is required for ATR-ATRIP recruitment to RPA-ssDNA (86). There may also be RPA independent modes of ATR-ATRIP recruitment (84, 87-89). In addition to recruitment, ATRIP is required for ATR protein stability (36). Localization of ATR-ATRIP is not sufficient to activate the kinase. Additional protein factors are required, namely the Rad9-Rad1-Hus1

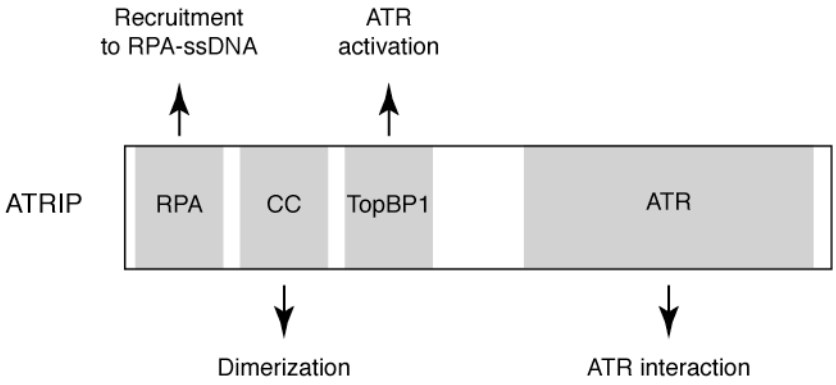


**Figure 6. ATRIP domains and their functions.** ATRIP interacts with replication protein A (RPA) via its N-terminus. The coiled-coil (CC) domain mediates oligomerization of ATRIP, which is important for ATR-dependent checkpoint signaling. ATRIP also interacts with the ATR activating protein TopBP1. This interaction is required for ATR activation by TopBP1. In the C-terminus, ATRIP interacts with ATR. ATRIP interaction with ATR is critical for ATR localization to stalled replication forks and protein stability.

complex and the ATR activator TopBP1. ATRIP directly interacts with TopBP1, and this interaction is necessary for TopBP1 to activate ATR (90). Finally ATRIP post-translational modifications regulate ATR function in the G2 DNA damage checkpoint (91, 92).

*The Rad9-Rad1-Hus1 DNA damage clamp*

Independently of ATR-ATRIP localization to RPA-ssDNA, the DNA damage clamp Rad9-Rad1-Hus1 (9-1-1) is loaded onto RPA-ssDNA (Figure 7). While 9-1-1 loading can occur on both 5′ and 3′ DNA ends, loading preferentially occurs at 5′ ssDNA-dsDNA junctions in the presence of RPA (93, 94). This preferential loading to the 5′ end is likely mediated by an interaction with the RPA70N subunit and Rad9 (95). RPA subunits bind ssDNA with 5′-3′ polarity, placing the RPA70 subunit adjacent to a 5′ ssDNA-dsDNA junction (96-98). 5′ ssDNA-dsDNA junctions are present in the lagging strand at Okazaki fragments during normal replication. However, during replication stress, re-priming of the leading strand by primase can also generate a 5′ssDNA-dsDNA junction, and primase activity is important for checkpoint activity (81, 99, 100). The loading of the 9-1-1 complex requires a specialized DNA damage clamp loader RFC-Rad17 and ATP hydrolysis (93, 94). The Rad9 subunit of the 9-1-1 clamp functions to recruit the ATR activator TopBP1. The C-terminal tail of Rad9 is constitutively phosphorylated. Phosphorylated Rad9 is recognized by the phospho-binding BRCA1 C-terminal (BRCT) repeats 1 and 2 of TopBP1 (Figure 8a). This interaction serves to concentrate TopBP1 in proximity to ATR-ATRIP (101, 102). In yeast, the Rad9 homolog, Ddc1, can activate the ATR homolog Mec1 (103), and artificial tethering of Ddc1 to chromatin can activate Mec1 in the absence of DNA

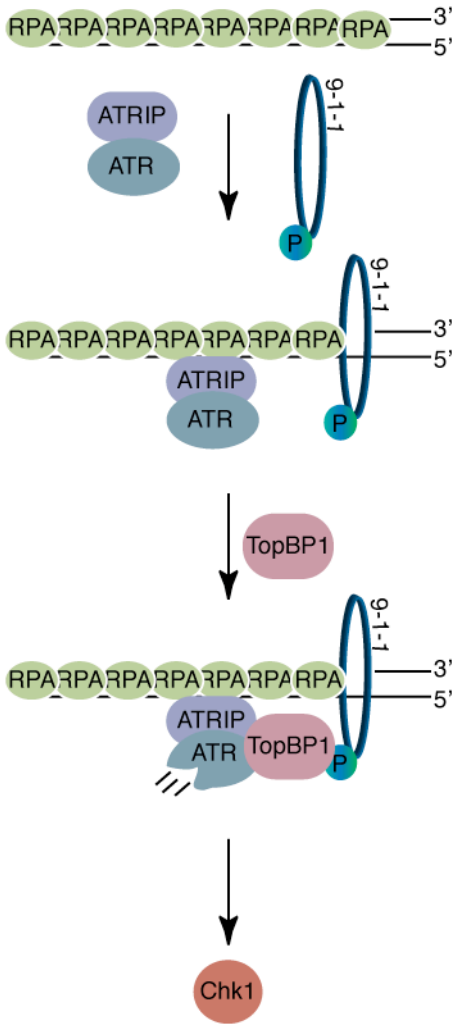


**Figure 7. ATR activation process.** An interaction between RPA and ATRIP localizes ATR to RPA-coated single-stranded DNA. In an independent process, a specialized DNA damage clamp loader Rad17-RCF1-5 loads the Rad9-Rad1-Hus1 (9-1-1) DNA damage clamp to a 5′-recessed ssDNA-dsDNA junction in an ATP-dependent manner. This process also depends on RPA-ssDNA. The phosphorylated C-terminal tail of Rad9 mediates an interaction with the ATR activator TopBP1. TopBP1 interacts with ATR and ATRIP, and this interaction stimulates ATR activity towards its substrate.

damage (104). However, in mammalian systems, Rad9 is not sufficient to activate ATR. TopBP1 fusions with chromatin proteins alleviate the requirement of Rad9 and Rad17 in checkpoint signaling in human cells (101, 105). Based on this, the primary function of the 9-1-1 complex in human cells is likely to recruit TopBP1.

*TopBP1-mediated activation of ATR*

ATR activity in response to DNA damage and replication stress requires TopBP1 (90, 106-109). Once localized to chromatin, a distinct region of TopBP1 termed the ATR Activation Domain (AAD) interacts with surfaces on both ATR and ATRIP and stimulates ATR kinase activity (Figure 7) (90). TopBP1 binding of ATR-ATRIP increases the affinity of ATR for substrates, though how is unknown (110). Disruption of interaction surfaces on ATR or ATRIP individually disrupts activation (90). Ectopic expression of the AAD in human cells is sufficient to activate ATR signaling in the absence of DNA damage (84, 109, 111). Additionally, tethering of TopBP1 to chromatin in human cells is also sufficient to activate ATR signaling (105). Thus, the recruitment of TopBP1 to chromatin is sufficient for ATR signaling and is an important regulatory step. TopBP1-mediated activation of ATR is evolutionarily conserved. The *S. cerevisiae* homolog of TopBP1, Dpb11, activates *S. cerevisiae* $Mec1^{ATR}$, and this activating activity is localized to the extreme C-terminal tail of Dpb11 (Figure 8b) (112, 113).

Recent research has made it clear that recruitment of TopBP1 is complex and can occur through multiple mechanisms. These mechanisms may be context specific. In *Xenopus* extracts, TopBP1 can localize to chromatin independently of Rad9 after replication stress (114). In response to ionizing radiation (IR), a new

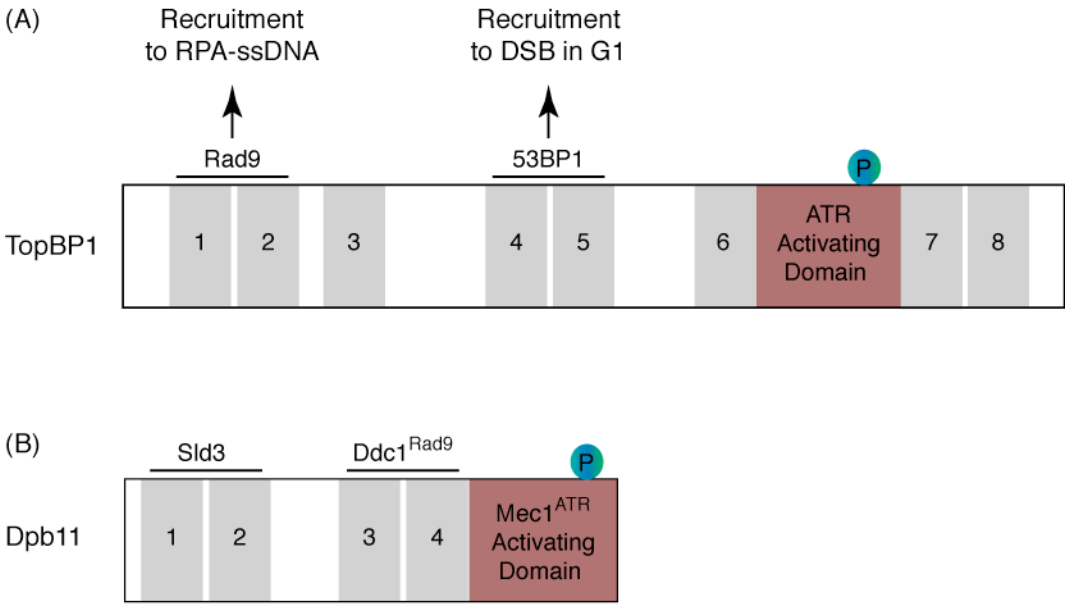


**Figure 8. TopBP1 domains and their functions.** (A) Human TopBP1 consists of eight BRCA1 C-terminal repeats (BRCT). BRCTs function in tandem as phospho-binding motifs. BRCTs 1-2 mediate an interaction with Rad9 and serve to recruit TopBP1 to sites of DNA damage. BRCTs 4-5 recruit TopBP1 to DNA damage foci specifically in G1 cells but not S phase cells. A region between BRCTs 6 and 7 is sufficient to activate ATR. This region is phosphorylated by ATM and potentiates TopBP1-mediated activation of ATR after DNA double-strand breaks. (B) TopBP1 functions are conserved in the S. cerevisiae homolog Dpb11. BRCT repeats 3-4 mediate interaction with the Rad9 homolog Ddc1. Dpb11 also contains a region that is sufficient to activate the ATR homolog Mec1, and phosphorylation of this region may also potentiate Mec1 activation.

protein RHINO interacts with both Rad9 and TopBP1 via distinct domains. This interaction is important for ATR signaling after IR, suggesting RHINO may bridge the two proteins on chromatin (115). Finally, new evidence suggests that BRCTs 4 and 5 are required for TopBP1 DNA damage foci in G1 but not for DNA replication stress (Figure 8b) (116). Thus, TopBP1 recruitment can occur through multiple mechanisms depending on the DNA damage context.

In addition to recruitment to chromatin, TopBP1 is regulated at the level of phosphorylation. ATM phosphorylation of S1138 of TopBP1 potentiates TopBP1-mediated activation of ATR after ionizing radiation (117, 118). In addition, T731 in the AAD of $Dpb11^{TopBP1}$ is likely phosphorylated by $Mec1^{ATR}$. A T731A mutation mildly reduces the ability of Dpb11 to activate Mec1 at low salt concentrations. However at physiological salt concentrations, the T731A mutation greatly reduces the ability of $Dpb11^{TopBP1}$ to activate $Mec1^{ATR}$. A phospho-mimicking mutation T731E partially restores $Mec1^{ATR}$ activation at physiological salt concentrations, supporting that T731 phosphorylation promotes the ability of $Dpb11^{TopBP1}$ to activate $Mec1^{ATR}$ (112).

TopBP1 is essential for DNA replication as well (119-124). However, mutations in the AAD of TOPBP1 that perturb ATR signaling after replication stress do not affect DNA replication (107, 124). Therefore the functions are separable, and for clarity I will not introduce TopBP1 functions in replication.

*Chk1*

Proteomic screens reveal that ATR phosphorylates hundreds of substrates in response to DNA damage (125-128). The function of the majority of these substrates in the replication stress response remains unknown. However, the

best characterized ATR substrate is the kinase Chk1. Similar to *ATR*, *CHK1* deletion results in embryonic lethality and replication stress response defects (129, 130). ATR phosphorylates Chk1 on serines 317 and 345 (34, 130). Chk1 phosphorylation increases its kinase activity and the kinase undergoes subsequent autophosphorylation (131, 132).

In contrast to other ATR substrates, ATR-dependent Chk1 phosphorylation has unique protein requirements. Claspin functions as an adaptor protein for Chk1 but not other ATR substrates (108, 133). There may be multiple cooperating mechanisms to localize Claspin to stalled replication forks. Claspin associates with the replisome via an interaction with the replication protein Cdc45 and may monitor replication as the fork progresses (134). Claspin also interacts with Timeless of the Tipin-Timeless complex, and this interaction mediates Chk1 signaling in the S phase checkpoint. Tipin contains an RPA binding motif, which localizes Claspin at RPA-ssDNA (135-138).

*ATR-Chk1 and S phase checkpoint*

The function of the ATR-Chk1 axis has been intensely studied in many systems. However studies in the budding yeast *S. cerevisiae* are the most extensive and have provided the foundation of much of what we understand about ATR and Chk1. In budding yeast $Mec1^{ATR}$ and $Rad53^{Chk1}$ regulate fork stability and late origin firing (139, 140). Replication forks irreversibly collapse in *MEC1* and *RAD53* deleted strains cultured in replication stress agents. Analysis of replication forks in Rad53 mutants after replication stress showed structures indicative of collapsed replication forks (141, 142). Additionally in *RAD53* null strains the failure to stabilize replication forks during replication stress is

irreversible. This was shown in studies where wild type Rad53 was inducibly expressed after release from replication stress in *RAD53* null cells. The re-expression of Rad53 could not rescue DNA replication after removal of replication stress (142).

In *S. cerevisiae* replication fork stability and origin firing functions of $Mec1^{ATR}$ are genetically separable. A *mec1-100* allele is viable and does not exhibit sensitivity to replication stress agents. The mec1-100 protein cannot suppress late origin firing but can stabilize replication forks in the presence of replication stress (143). Thus at least in yeast, suppressing late origin firing is dispensable while replication fork stabilization is essential. Whether this is also true in mammalian cells is not known. Many studies indicate that suppression of late origin firing is an important function of ATR-Chk1 in mammalian systems (144-147).

The targets of Mec1 and Rad53 that preserve replication fork stability are not well understood, differ in experimental systems, and are not necessarily overlapping. For instance, polymerase chromatin association in yeast during replication stress is dependent on S phase checkpoint activity (40, 148, 149). However in *Xenopus*, polymerase reloading can occur in an ATR/ATM dependent manner (150). Also the MCM helicase is phosphorylated by ATR (151, 152), and it is hypothesized that this slows unwinding of the DNA. In addition, ATR and Chk1 stabilize replication forks by preventing unwanted remodeling of replication forks by nucleases and recombinases. ATR phosphorylates anti-recombinogenic helicases such as WRN and BLM (153, 154). Mutation of BLM and WRN causes hyper-recombination supporting that preservation of fork stability is important to prevent aberrant recombination of

fork structures (52, 155). ATR and Chk1 also target nucleases such as Mus81 and Exo1 (156). Irreversible fork collapse in *RAD53* null cells is rescued by *EXO1* deletion (143), suggesting that in the absence of checkpoint signaling nucleases aberrantly process replication forks and convert them to a collapsed double-strand break state. This is further supported by evidence that markers of homologous recombination do not form in the presence of replication stress agents in wild type yeast but only when the checkpoint is defective (157).

Of note, *MEC1* deficiency causes cells to be more sensitive to replication stress than *RAD53* deletion (141, 158). This suggests that not all ATR functions are through Chk1 signaling. For instance while *EXO1* deletion can rescue *RAD53* deletion, it cannot rescue *MEC1* deletion(143). Other cases of Chk1-independent functions of ATR in responding to replication stress have been reported in other systems as well (159).

*Common mechanisms of PIKK regulation*

ATR belongs to the phosphoinositide 3-kinase (PI3K)-like kinase (PIKK) family of protein kinases, which includes ATR, ATM, DNA-PK, mTOR, and SMG1. ATR and ATM mediate the DDR, and DNA-PK also functions to preserve genome maintenance through its control of DSB repair. mTOR regulates cell growth through nutrient sensing, and SMG1 functions in mRNA surveillance. While their functions are diverse, common themes in PIKK regulation have emerged from research. New modes of ATR regulation may be garnered by exploring these shared mechanisms.

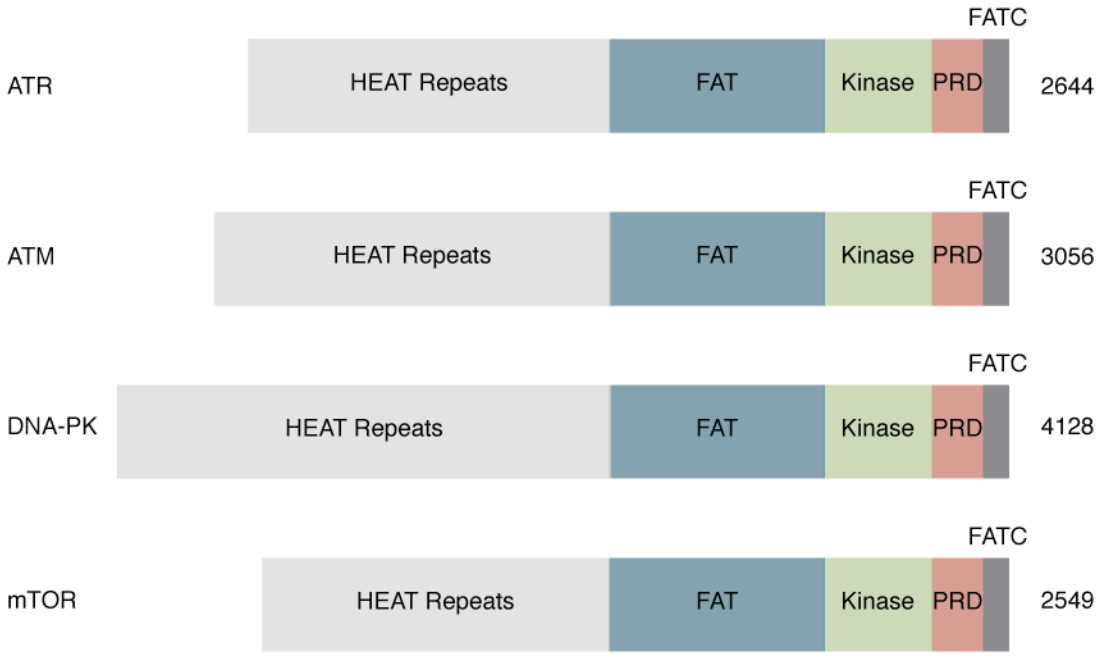


**Figure 9. PIKKs share common domain architecture.** Depicted are the three DNA damage PIKKs and the related PIKK mTOR. Each kinase contains an extensive array of N-terminal HEAT repeats that mediate protein-protein interactions. The C-terminal portion of the kinases exhibit the closest sequence conservation, with the catalytic kinase domain displaying the highest similarity. Surrounding the kinase domain are the FAT, PIKK Regulatory Domain (PRD), and FATC domains. HEAT repeats also comprise the FAT domain. Phosphorylation in the FAT domain modulates activity of some of the kinases, and the FATC domain is required for kinase activity. The PRD of ATR directly interacts with TopBP1 and is required TopBP1-mediated activation of ATR. The PRD also functions in the activation process of the other kinases.

The PIKKs share domain architecture with a conserved catalytic domain. The catalytic domain has sequence homology with the PI3K kinase domain. While PI3K is a lipid kinase, the PIKKs are serine/threonine protein kinases. Surrounding the C-terminal kinase domains are two regions flanking the kinase domain, the FAT and FATC, that exhibit sequence homology among family members (110, 160) (Figure 9). Studies show that the FATC domain is required for kinase activity of all the PIKKs (161). Additionally, modifications and protein interactions in the FAT domain modulate kinase activity (162-164). N-terminal to the kinase domain, the PIKKs consist of long arrays of anti-parallel helices called HEAT repeats. HEAT repeats are similar but distinct to ARM-repeats (165). The function of HEAT repeats in classical HEAT repeat proteins is to bind proteins. However, Rubison et al demonstrate that HEAT repeats also can mediate interactions with DNA (166).

In addition to domain architecture, the PIKKs also share several modes of regulation. ATR, ATM, DNA-PK, and mTOR are regulated by changes in subcellular localization. Subcellular localization is mediated by protein binding partners (Figure 10a). mTORC1, one of the distinct mTOR complexes, interacts with Raptor. mTORC1 localizes to distinct lysosomal membranes via an interaction between Raptor and Rag GTPases found in lysosomal membranes (167, 168). ATR, ATM, and DNA-PK interact with ATRIP, the Mre11-Rad50-Nbs1 (MRN) complex, and Ku70/80 respectively. These binding partners interact with specific nucleic acid structures and localize the kinases to sites of DNA damage (Figure 10a and b) (84, 87, 169).

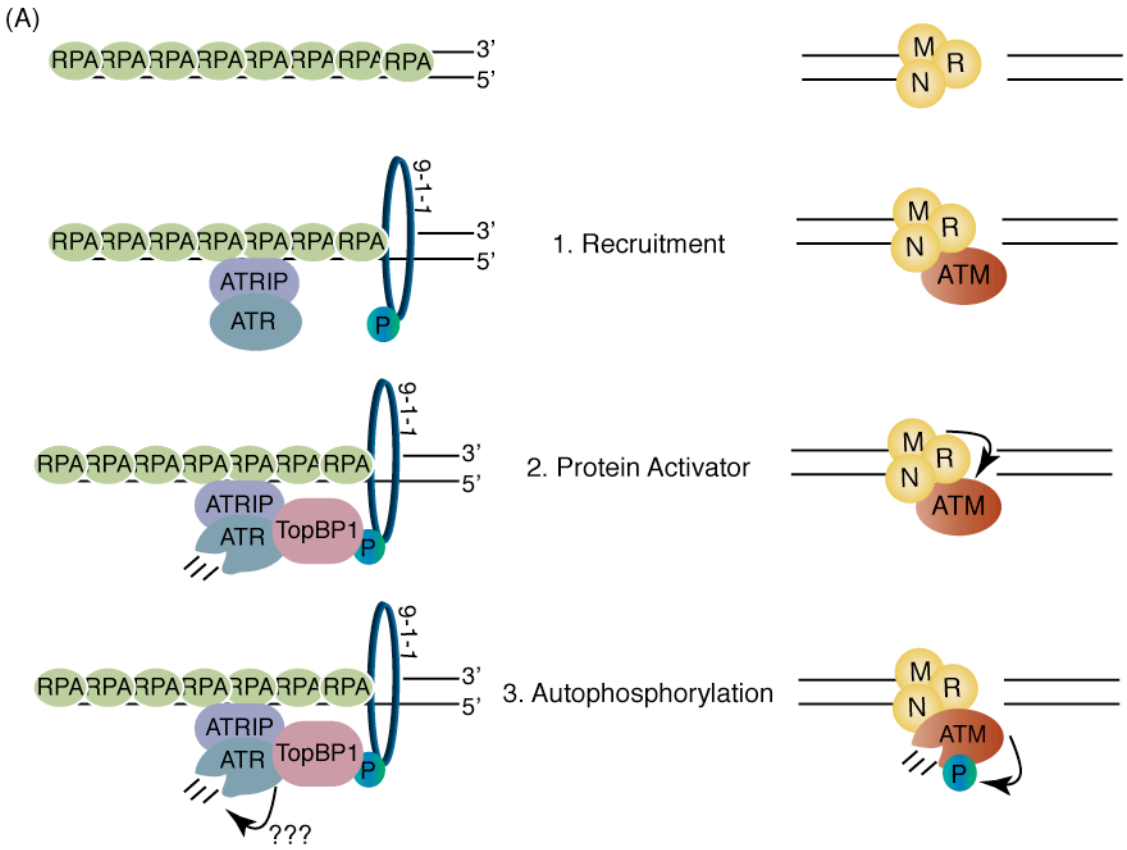


(B)

| PIKK | Partner | Localization | Activator | Autophosphorylation |
|---|---|---|---|---|
| ATR | ATRIP | ATRIP-mediated RPA-ssDNA | TopBP1 | unknown |
| ATM | MRN complex | MRN-mediated DSB end | Mre11-Rad50 bound to DSB | S367, S1893, S1981 |
| DNA-PK | Ku70/Ku80 | Ku70/Ku80-mediated DSB end | Ku70/Ku80 bound to DSB | T2609, 2612, 2620, 2624, 2647 |
| mTORC1 | Raptor | Raptor-mediated Rag GTPases lysosome membranes | Rheb | S2481 |

**Figure 10. Common modes of PIKK regulation.** (A) The PIKKs share several modes of regulation. (1) Recruitment to distinct structures occurs through the PIKK and a binding partner. ATRIP binding of RPA recruits ATR to ssDNA while Mre11-Rad50-Nbs1 (MRN) binding to DNA double-strand breaks (DSBs) localizes ATM to DSBs. (2) A protein or protein-nucleic acid activator activates the kinase. TopBP1 activates ATR and similarly Mre11-Rad50 bound to DNA ends activates ATM. (3) The PIKKs ATM, ATR, and mTOR autophosphorylate as part of their activation process. These autophosphorylation sites are critical for kinase function. It is not known whether autophosphorylation also regulates ATR. (B) Each PIKK is listed with its binding partner, how the binding partner localizes the PIKK, protein activator, and several known functional autophosphorylation sites.

Localization to distinct structures likely functions to concentrate the kinases with other regulatory inputs, such as protein activators. TopBP1 activates the ATR-ATRIP complex (90, 109). Similarly, ATM is activated by DNA-bound MRN complexes (170, 171), and the Ku70/Ku80 heterodimer bound to DNA ends activates DNA-PK (172, 173). The Rheb GTPase also stimulates mTORC1 activity (174). Kinase activation is mediated by the PIKK Regulatory Domain (PRD), which occurs between the kinase domain and the FATC domain (Figure 9). PRD sequences in PIKKs are divergent, suggesting that these variations allow the kinases to respond to different regulatory inputs or protein activators. While the sequences are different, the function of the PRD to mediate kinase activation seems to be conserved. In ATR, the PRD serves as a binding surface for the ATR activator TopBP1 (90). Likewise, mutations in the DNA-PK PRD disrupt kinase activation following DNA damage (90). In addition to protein binding, the PRD also is post-translationally modified. ATM acetylation in the PRD is required for kinase activation in response to DSB breaks (175, 176). mTOR phosphorylation and autophosphorylation also has been mapped to the PRD domain (177-179). The mechanism of how the PRD mediates kinase activity is unknown.

**Phospho-regulation of ATR**

Phosphorylation also regulates PIKK kinase activity. ATM, DNA-PK, and mTOR undergo phosphorylation (Figure 10). These phosphorylation events are critical regulatory events, as ablation of the phosphorylation sites results in cellular defects. ATM is phosphorylated on several residues, including four autophosphorylation sites S367, S1893, S1981, and S2996 (162, 180, 181). Over 30

DNA-PK phospho-residues have been identified and many are autophosphorylation sites (182). Ablation of both ATM and DNA-PK autophosphorylation sites causes DNA damage sensitivity (180, 181, 183, 184). Furthermore, both ATM and DNA-PK autophosphorylation require their protein activators and are direct markers of activated kinases (170, 171, 173).

The mechanism of how these phosphorylation sites regulate kinase activity is not well understood. The function of ATM S1981 autophosphorylation remains controversial. The initial report of S1981 autophosphorylation purports that S1981 phosphorylation mediates transition of inactive ATM dimers to active monomers (162). However, later studies show that S1981 is not required for transition to a monomer state (171) and that the murine equivalent of S1981 is not required for murine ATM activity (185).

Two clusters of DNA-PK autophosphorylation have been extensively studied and mutation of either of these clusters results in DNA damage sensitivity and defective DNA repair. Mechanistically these phosphorylation sites have been linked to modulating DNA association of the kinase, suggesting autophosphorylation causes a conformational change in the kinase (186-188). Low resolution structures support that there is a shift in protein conformation upon kinase activation (189, 190).

ATR also autophosphorylates *in vitro* and is a phospho-protein *in vivo* (36). However, the identity of these sites and whether they are DNA damage-regulated and functional remains unknown. In my dissertation research I explore the possibility that phosphorylation is also an ATR regulatory mechanism. I hypothesize that like ATM and DNA-PK, ATR is phosphorylated in response to DNA damage and that this phosphorylation would be a marker

for an activated kinase. I also explore a novel ATR inhibitor and its efficacy as an anti-tumor agent.

In Chapter III, I identify and characterize T1989 as the first DNA damage-regulated ATR phosphorylation site. T1989 phosphorylation occurs concurrently with ATR-dependent Chk1 phosphorylation and depends on ATR kinase activity in cells. Mutation of the ATR PRD, which is required for TopBP1-mediated activation of ATR, disrupts T1989 phosphorylation suggesting ATR phosphorylation occurs downstream of TopBP1 activation of ATR (191). This supports that T1989 phosphorylation occurs on an activated ATR kinase and can be used to directly monitor ATR activity in cells. Although I observed a mild viability defect with T1989 mutation, the function of T1989 phosphorylation remains unclear.

I continue exploring potential ATR autophosphorylation sites in Chapter IV by mutating and characterizing 16 conserved candidate ATR autophosphorylation sites. A 3A-ATR mutant dissociates essential functions of ATR from its G2 checkpoint activities. Disruption of essential functions of ATR correlates with replication stress response defects, suggesting that the essential function of ATR in mammalian cells is to respond to replication stress. This is the first separation of function mutant in human ATR reported. In addition, these mutations occur in a distinct region of ATR that is analogous to regions in ATM and DNA-PK that are targeted for autophosphorylation. However, whether ATR is phosphorylated at these residues remains unknown.

My analysis of the 16A-ATR mutations in Chapter IV uncovered a potential regulatory region in ATR and an unexpected hyper-stimulation phenotype. In Chapter V, I explore whether conserved residues in this potential

regulatory region are also functional in yeast. I also identify the sites within the 16 mutations that contribute to the hyper-stimulation phenotype and find they are distinct from the 3A-ATR residues. Preliminary experiments also suggest that the hyper-stimulation of ATR by TopBP1 may be due to increased TopBP1 AAD binding.

In Chapter VI, I characterize and explore the use of a novel ATR inhibitor for basic and translational studies. Transient inhibition of ATR supports that ATR kinase activity is important to stabilize replication forks and to promote replication fork restart after replication stress. Replication stress agents, as well as ATM-deficiency, sensitized cancer cells to ATR.

# CHAPTER II

# MATERIAL AND METHODS

*DNA constructs and siRNA*

Flag-$HA_3$-WT-ATR was subcloned into the BamHI site of a modified pCDNA5/TO vector (Invitrogen). The BamHI-XhoI fragment (9668-9724) of the multiple cloning site was deleted, making the NotI and BstXI sites of the ATR cDNA unique. Two fragments of the ATR cDNA, NotI-BstXI (1-3385) and BstXI-AgeI (3374-6689), were subcloned into pBSKII(-) with a multiple cloning site modified to contain a BstXI site matching the BstXI site found in ATR (pEN3). ATR mutants were generated using the QuikChange Site-Directed Mutagenesis (Agilent Technologies) method using the primers in Table 1. Mutated fragments were subcloned back into the full length cDNA and verified by sequencing. In some cases the Flag-$HA_3$ epitope was replaced with a single Flag epitope (destroys BamHI site) to facilitate purification of HA-ATRIP/Flag-ATR complexes by HA-immunoprecipitation. siGENOME SMARTpool TopBP1 siRNAs were purchased from Dharmacon. Plasmid and reverse siRNA transfections were carried out with Lipofectamine2000 using the manufacturer's protocol (Invitrogen).

**Table 1. Primers used for ATR mutagenesis.** + indicates the restriction site is created by mutagenesis. – indicates that restriction site is destroyed by mutagenesis. Unless noted, primers prime wild-type ATR or do not overlap with other mutated residues.

| Site | Primer name | Primer sequence | Notes |
|---|---|---|---|
| S749A | S749A F | 5'-gtaggaacttgaaagccactgctcaacatgaatgttcatct | No sites |
| S756A | S756A F2 | 5'-cacttctcaacatgaatgttcatcagcgcaactaaaagcttctgtc tgcaag | + HhaI |
| S756A | S756A F3 | 5'-cactgctcaacatgaatgttcatcagcgcaactaaaagcttctgt ctgcaag | pEN19 tem-plate +HhaI |
| S927A | S927A F | 5'-aaaagtgttaaactgcaaagtttttcgcgcagtataagaaaccca tctgtcagttt | +HhaI; +BstUI |
| S1333A | S1333A F | 5'-tgaaacagtagaacctattatcgcacaattggtgacag tgcttttgaaag | +MfeI |
| S1348A | S1333A F | 5'-ttgaaaggttgccaagatgcgaatgctcaagctcggttgctctgt | +BsmI |
| T1376A | T1376A F | 5'-gtcgattagatttctcaacaactgaagcgcaaggaaaa gattttacatttgtgac | -SmlI; +HhaI; +BstUI |
| S1464A | S1465A F | 5'-ctaaataccagatacaagagtgcacagaagtcaaccgattggtct | +ApaLI |
| T1566A | T1566A F | 5'-catgacgatcagcataccataaatgcccaagacattgc | No sites |
| T1566E | T1566E F | 5'-taaagcatgacgatcagcataccataaatgaacaaga cattgcatctgatctgtg | No sites |
| T1578A | T1578A F | 5'-atctgtgtcaactcagtgcacagactgtgttctcc | +ApaLI |
| T1578D | T1578D F | 5'-atctgatctgtgtcaactcagtgatcagacagtgttctcc atgcttgaccatc | +BclI |
| T1589A | T1589A F | 5'-catgcttgaccatctcgcccagtgggcaaggcaca | +BglI |
| T1589E | T1589E F | 5'-ttctccatgcttgaccatctcgagcagtgggcaaggcacaaattt | +SmlI; +XhoI |
| T1754A | T1754A F | 5'-agctgtctactgttatcgctcaagtgaatggagtgcatgc | +SmlI |
| S1782A | S1782A F | 5'-aagcagcttggaaattggcacagtgggatttggtg | No sites |
| S1876A | S1876A F | 5'-cattctccaggtgacagtgctcaggaagattctctaaactgg | -SmlI |
| T1890A | T1890A F | 5'-gtagctcgactagaaatggcccaaaattcctacagagccaag | -EcoRI |
| S2143A | S2143A F | 5'-ctccatatcaatttttgactgcttttgcacagttgatctctcgaatttgtcatt | -MfeI |
| T1989A | T1989A F | 5'-ggtgttgaattatgttttcctgaaaatgaggcgccacctgagggtaag | +HhaI |
| T1989E | T1989E F | 5'-gttcttcaaaaaggtgttgaattatgttttcctgaaaat gaagagcctccggagggtaagaacatgttaatcc | +BspEI |

*Genetic complementation of ATR$^{flox/-}$TR cell lines*

Parental HCT116 ATR$^{flox/-}$TR cells contain one *ATR* allele disrupted by a neomycin cassette, a conditional *ATR* allele flanked by loxP sites, and an integrated cDNA expressing the tetracycline repressor, which confers blasticin resistance (90). To generate clonal ATR$^{flox/-}$TR stable cell lines expressing tetracycline-inducible Flag-HA$_3$-epitope tagged ATR, ATR cDNAs with a tetracycline responsive promoter conferring hygromycin B resistance were linearized with FspI. Linearized cDNAs were separated on a 0.8% agarose gel, excised, and purified with the QIAquick Gel Extraction Kit. Extracted DNA was further purified by ethanol precipitation. 8 μg of linearized plasmid was transfected into 5x10$^6$ ATR$^{flox/-}$TR cells in a 60 mm dish according to the Lipofectamine2000 reverse transfection protocol. 24 hours after transfection, cells were trypsinized, plated into 100 mm dishes at different dilutions (ie. 1:20, 1:40), and selected for stable integrants by maintaining cells in and 10 μg/mL blasticin and 300 μg/mL hygromycin B. Selection media was replaced every 3 days until colonies were visible by eye, usually 2-3 weeks.

To expand single colonies, media was aspirated from dishes, and 5 mL of PBS was added to plates. Using a P200 set for 100 μL, single colonies were pipetted off the plate into the tip and transferred to a 12 well dish containing 100 μL of trypsin. Cells were pipetted several times in the trypsin. After several minutes, 1 mL of selection media was added and cells were allowed to expand. Media was replaced every 2-3 days. Once wells reached 70-80% confluency, integrants were screened for expression of exogenous ATR (see below).

*Verification of exogenous ATR expression in integrants*

An in-cell western was used initially to screen stable integrants for exogenous expression of Flag-$HA_3$-epitope tagged ATR. 500 μL of trypsin was added to each 80% confluent 12 well, and then 1 mL of media was added to inactivate trypsin. 100 μL of cells were transferred to a 96 well plate containing 50 μL of media containing tetracycline (final concentration of 1 μg/mL) to induce expression of integrated ATR cDNAs. The remaining 1400 μL of cells were transferred to a 6 well plate containing selection media and allowed to expand.

After 24 hours of growth in tetracycline, medium was aspirated from 96 well plates and cells were washed once with 100 μL of PBS. 150 μL of 3.7% formaldehyde/PBS was to each well for 20 minutes at room temperature. After fixation, cells were washed 5 times with 200 μL of 0.1% Triton-X 100/PBS for 5 minutes each. The washes were removed manually with a pipet to prevent excessive drying out by aspiration. 150 μL of Odyssey Blocking Buffer was added to each well and cells were blocked at room temperature for 1.5 hours. 50 μL of primary antibodies in Odyssey Blocking Buffer was added to each well (HA 1:100 and GAPDH 1:500) for 2 hours at room temperature or overnight at 4°C. Cells were washed 5 times with 200 μL 0.1% Tween-20/PBS for 5 minutes each time. 50 μL of secondary antibodies in Odyssey Blocking Buffer (anti-mouse 680 1:500 and anti-goat 800 1:500) was added for 1 hour at room temperature. Cells were again washed 5 times with 0.1% Tween-20/PBS for 5 minutes each time. After the final wash, the 96-well plate was inverted and firmly tapped onto a kimwipe to remove residual liquid. Plates were scanned

on a Licor Odyssey System using the microplate setting with a 3.0 mm focus offset.

Integrants with in-cell western HA-ATR signals similar to the WT-ATR$^{flox/-}$TR cell line were carried forward for western blot analysis and immunofluorescence. Western blotting was used to verify that integrants expressed full length ATR to similar levels in the WT-ATR$^{flox/-}$TR cell line. Immunofluorescence was also conducted on integrants for HA expression and compared to the WT-ATR$^{flox/-}$TR cell for similar percentages of cells expressing integrated cDNAs. Two stable integrants expressing similar levels of full length Flag-HA$_3$-ATR in a similar percentage of cells were analyzed when possible to account for potential clonal differences.

*Adenovirus infection*

To delete the *ATR$^{flox}$* allele, 1x10$^6$ cells were plated in a 100 mm tissue culture dish the day before infection in media containing 1 μg/mL tetracycline. The next day, 0.42 μL of adenovirus encoding for Cre-recombinase (AdCre) or GFP (AdGFP) was added to cells in 10 mL of media contain tetracycline. 24 hours after adenovirus addition, adenovirus media was replaced with media containing tetracycline. Functional analysis was conducted 72-96 hours post-infection.

*PCR genotyping, RT-PCR, and sequencing of products*

Genomic DNA was harvested from cells using the Qiagen DNeasy Blood and Tissue Kit. 300 ng of genomic DNA was used in PCR reactions containing

Taq DNA polymerase (Invitrogen), 1.5 mM $MgCl_2$, 200 μM dNTPs, and 200 nM primers. Primers used were: ATR8961: 5′-GTCTACCACTGGCATAACAGC and sfiloxpseq: 5′-CAGCGGGAGCAGGCATTTCC. Cycling parameters used were: 95°C 2′; [95°C 45″, 58°C 45″, 72°C 70″]x33; 72°C 5′. Products were run on a 0.8% ethidium bromide agarose gel and visualized on a BioRad gel documentation system.

RNA was extracted from $ATR^{flox/-}$TR, WT-$ATR^{del/-}$TR and T1989A-$ATR^{del/-}$TR cell lines using the Qiagen RNeasy Kit. RT-PCR reactions contained 1 μg of RNA, either 5 μM $oligo(dT)_{23}$ or 7.5μM hexamer primers (USB First-Strand cDNA Synthesis Kit), 500 μM dNTPs, 10 units RNase inhibitor, and 1μL M-MLV RT in a 20 μL reaction volume. Cycling parameters were: 44°C 60′; 92°C 10′; 4°C as needed. To amplify across the coding region of ATR T1989, RT-PCR and genomic DNA products were amplified using the following primer pairs:

1. ATR5877: 5′-GGCAAAGTGGCTCTGGTCCAAG
   ATR6041rev: 5′-GCTGTTTCTTCCATAAATCGGCCC

2. ATR5902: 5′-GATGTTCACCAGGCACTAATTGTTC
   ATR6099rev: 5′-TGGCAGGCACGCGGTCACATC

3. ATR5902: 5′-GATGTTCACCAGGCACTAATTGTTC
   ATR6041rev: 5′-GCTGTTTCTTCCATAAATCGGCCC.

PCR products are: primer pair 1 – 165 base pairs, primer pair 2 – 198 base pairs, and primer pair 3 – 140 base pairs. Mutation of ATR T1989 to alanine creates an HhaI restriction site within the PCR products. In addition to cleavage by HhaI, amplified RT-PCR and genomic DNA products were sequenced using either ATR5877 or ATR5902 to verify that T1989A-ATR$^{del/-}$TR cell lines express only the integrated mutant cDNA.

*Western blots and immunoprecipitations*

Drugs were added to cells at the following concentrations: 2mM HU, 50J/m$^2$ UV, 5Gy IR, 10mM caffeine, 10□M ATM inhibitor (KU55933) (192), 1μM DNA-PK inhibitor (NU7441) (193), 50μM Roscovitine, 100nM Chk1 inhibitor (AZD7762) (194), and 3μM ATR inhibitor (AZ20). Cell lysates were prepared by resuspending pellets in NP-40 buffer (1% NP-40, 200mM NaCl, 50mM Tris pH 8.0), incubating on ice for 20 minutes, and centrifuging at 16xg for 20 minutes at 4ºC. Protein quantification was done using a BSA standards and the BioRad Bradford reagent system. Immunoprecipitations were performed overnight at 4ºC using 5 μg of antibody and protein G agarose (Santa Cruz), washed three times with NP-40 buffer, and separated by SDS-PAGE prior to immunoblotting. For lambda phosphatase experiments, ATR immunoprecipitates were washed three times with NP-40 buffer and then incubated with lambda phosphatase (NEB) for 30 minutes at 37ºC.

For dot blots, peptides were dissolved in 50% acetonitrile, serial diluted in water, and spotted directly onto nitrocellulose membranes. Antibodies used included: ATR-N19 (Santa Cruz), Chk1-G4 (Santa Cruz), phosphorylated-S317

Chk1 (Cell Signaling), phosphorylated-S345 Chk1 (Cell Signaling), phosphorylated-S296 Chk1 (Cell Signaling), HA (Covance), Flag-M2 (Sigma), ATRIP-403 (36), and phosphorylated-S428 ATR (Cell Signaling). The phosphorylated-ATR antibody was generated by Bethyl Laboratories using a 13 amino acid human ATR peptide antigen with phosphorylated T1589 at position 7. A cysteine was added to the N-terminus to facilitate conjugation to a carrier. All immunoblotting was performed with infrared-conjugated secondary antibodies (LiCor) and quantified using an Odyssey system.

*Immunofluorescence*

Cells were seeded on glass coverslips in 6 well plates in media containing tetracycline to induce expression of integrated ATR cDNAs. 24 hours later, cells were treated with 2mM HU for 6 hours to examine ATR recruitment to stalled replication forks. Prior to fixation, the soluble fraction was extracted with 1mL of Triton X-100 solution (0.5% Triton-X 100, 20mM HEPES pH 7.4, 50mM NaCl, 3mM $MgCl_2$, 300mM sucrose) for 10 minutes on ice. Cells were carefully washed 3 times with 1mL of PBS and fixed with 2mL of 3% paraformaldehyde for 10 minutes at room temperature. 2mL of cold Triton-X 100 solution was added for 5 minutes on ice and then washed 5 times with PBS. Cells were blocked in 5% BSA/PBS for 15 minutes at room temperature. Coverslips were incubated cell side down onto 40μL of primary antibodies diluted in 5% BSA/PBS for 1 hour at 37°C on parafilm. After primary incubation cells were washed 2 times with 2mL of PBS and then incubated with 40μL of secondary antibodies for 30 minutes at 37°C cell side down on parafilm. Cells were washed

3 times with PBS and then mounted with Prolong Gold antifade mounting reagent containing DAPI. Antibodies and dilutions used were: HA 1:100 (Covance), Flag-M2 1:100 (Sigma), ATRIP-403 1:1000 (36), anti-mouse FITC 1:100 (Jackson Laboratories), and anti-rabbit rhodamine red 1:300 (Jackson Laboratories).

*Colony formation and cell viability*

For colony formation assays, $1x10^3$, $5x10^3$, and $1x10^4$ cells were plated in triplicate in 60 mm dishes containing media and tetracycline after AdCre or AdGFP infection. Colonies were allowed to form over 2 weeks and then were stained with methylene blue. Colonies were manually counted and percent viability is reported as a ratio of AdCre/AdGFP to correct for plating efficiency differences among cell lines.

For AZ20 experiments, cell viability was assessed by sub$G_0/G_1$ DNA content by propidium idodide staining. Viability was also determined using the Alamar blue reagent. 2000 cells were plated in 96 wells in triplicate. 24 hours later, AZ20 was added at 0.001, 0.01, 0.0333, 0.1, 0.333, 1.0, 3.333, and 10 μM.

*G2 checkpoint*

For G2 checkpoint assays, cells were irradiated with 8 Gy ionizing radiation and 30 minutes after irradiation were transferred to media containing nocodazole. 8 hours after release into nocodazole both the media and cells were harvested and fixed in 70% ice cold ethanol at -20ºC for at least 1 hour. To quantify the mitotic index, ethanol fixed cells were pelleted at 1.8xg for 5 minutes. Pellets were resuspended in 1mL of cold PBS and incubated on ice for

10 minutes. Cells were pelleted and resuspended in 1mL of ice cold 0.25% Triton-X 100/PBS and incubated on ice for 15 minutes to permeabilize. Cells were pelleted and rinsed once in 1% BSA/PBS and were incubated for 1.5 hours at room temperature with 100μL of phospho-S10 Histone H3 (Bethyl) diluted 1:2000 in 1% BSA/PBS. Cells were washed 2 times without resuspending with 1mL of 1% BSA/PBS and then incubated with 100μL of anti-rabbit FITC secondary (Jackson Laboratories) diluted 1:75 in 1% BSA/PBS for 1 hour at room temperature. Cells were washed once in 1% BSA/PBS and once in PBS without resuspension. To stain DNA, cells were incubated with 1mL of PBS containing 25μg/mL propidium iodide and 0.1mg/mL RNase A for 30 minutes at 37°C. Samples were filtered and analyzed by flow cytometry. Mitotic cells were determined to be FITC positive cells with 4N DNA content.

*Completion of DNA synthesis after replication stress*

For analysis of completion of DNA synthesis after exposure to replication stress, cells were arrested with 2mM HU for 24 hours. HU was removed and cells were washed 2 times with equilibrated media. Cells were released into media containing 100ng/mL nocodazole and media and cells were harvested at indicated time points. Cells were fixed in 70% ethanol at -20°C for at least 1 hour. To analyze DNA content, cells were pelleted and resuspended into 1mL of PBS containing 25μg/mL propidium iodide and 0.1mg/mL RNase A for 30 minutes at 37°C. DNA content by propidium iodide was then determined by flow cytometry.

*BrdU incorporation*

For BrdU incorporation experiments, cells were incubated with equilibrated media containing 10μM BrdU for 15 minutes and collected. Cells were fixed by adding 70% ice cold ethanol dropwise while vortexing and then incubating cells at -20ºC for at least 1 hour. Cells were pelleted at 1.8xg for 5 minutes and washed once in 0.5% BSA/PBS. Cells were permeabilized and DNA was denatured by adding 1mL of 2N HCl/0.5% Triton-X 100/PBS dropwise while vortexing and incubating for 30 minutes at room temperature. Cells were pelleted and incubated in 1mL of 0.1M sodium borate for 2 minutes. Cells were washed once with 1mL of 0.5%BSA/PBS and then incubated with 100μL of BrdU-Alexafluor488 antibody diluted 1:20 in 0.5% BSA/PBS/0.5% Tween-20 for 30 minutes at room temperature in the dark. Antibody was removed and 1mL of 0.5% BSA/PBS was added to wash one time. 1mL of PBS containing 5μg/mL propidium iodide and 0.1mg/mL RNase A was added and incubated for 30 minutes at 37ºC. Samples were then analyzed by flow cytometry.

*Mass spectrometry and sequence alignments*

Endogenous ATR-ATRIP complexes immunoprecipitated from HU treated HeLa cells with an anti-ATRIP antibody was excised from an SDS-PAGE gel, reduced and alkylated with DTT and iodoacetamide, and subjected to in-gel digestion using a variety of proteases including trypsin, chymotrypsin, endo-AspN and elastase using standard procedures. Peptides were extracted with 60% acetonitrile, 0.1% formic acid, dried by vacuum centrifugation, and

resuspended in 0.1% formic acid for analysis by liquid chromatography coupled with tandem mass spectrometry using an LTQ linear ion trap mass spectrometer (ThermoScientific) operated using standard data-dependent (top-five) acquisition including neutral loss ms3 acquisition. Spectra were searched against the human uniprot_kb databse (v155, July 2009) concatenated with the reverse database using the Sequest algorithm allowing for +80 mass shifts on serine, threonine and tyrosine residues.

For T1989 conservation, full length protein sequences were aligned with ClustalW2 (195). Conservation of S/TQ residues was determined by sequence alignment of ATR orthologs using ClustalW2. Secondary structure alignments by HEAT repeats is described in (165). DNA-PK secondary structure predictions were determined by Jpred3 (196).

*ATR kinase reactions*

All ATR kinase reactions were carried out on beads. For TopBP1-mediated activation of ATR *in vitro*, ATR-ATRIP complexes were HA-immunopurified from nuclear extracts prepared from 293T cells transiently expressing Flag-ATR and HA-ATRIP. HA-immunoprecipitations were carried out at 4ºC for no more than 3 hours and were washed 3 times with 1mL of TGN lysis buffer (50mM Tris pH 7.5, 150mM NaCl, 10% glycerol, and 1% Tween-20), 1 time with TGN lysis buffer containing 500mM LiCl, and 2 times with kinase buffer (10mM HEPES pH 7.5, 50mM NaCl, 10mM $MgCl_2$, 1mM DTT, 50mM Beta-glycerophosphate). To the purified kinases 10pmol of recombinant GST or GST-TopBP1-AAD (ATR Activation Domain) was added and then 30μL of kinase buffer containing 0.5μg of recombinant GST-MCM2 substrate, 10μM cold ATP,

and 1μL of $\gamma^{32}$P-ATP (Perkin Elmer) was added to the complexes. Reactions were incubated at 30°C for 20 minutes, and reactions were stopped by addition of 30μL of 2X LSB and boiling for 5 minutes. For phospho-peptide maps of GST-AAD stimulated ATR-ATRIP complexes, reactions were carried out in the absence of GST-MCM2 substrate and for 30 minutes at 30°C.

For ATR autophosphorylation kinase reactions, Flag-ATR was immunopurified from 293T cells transiently expressing Flag-ATR and HA-ATRIP. Flag immunoprecipitations were carried out in TGN lysis buffer overnight at 4°C. Immunoprecipitations were washed 3 times with TGN lysis buffer, 1 time with TGN lysis buffer containing 500mM LiCl, and 2 times with kinase buffer. Kinase complexes were incubated with 30μL of kinase buffer containing 10μM cold ATP and 1μL of $\gamma^{32}$P-ATP for 30 minutes at 30°C. Reactions were stopped with addition of 30μL of 2X LSB and boiled for 5 minutes. All reactions were separated by SDS-PAGE and protein levels were determined by Coomassie blue staining or by western blot. $^{32}$P incorporation was analyzed by phosphorimaging or by autoradiography.

*Phospho-peptide analysis*

For *in vitro* phospho-peptide analysis, ATR-ATRIP complexes were immunopurified, subjected to kinase reactions, and prepared for phospho-peptide mapping. GST-AAD stimulated complexes were phosphorylated for 30 minutes. For *in vivo* phospho-peptide analysis, two 10 cm plates of 293T cells overexpressing Flag-$HA_3$-ATR and myc-ATRIP constructs were washed twice with equilibrated phosphate-free DMEM. Cells were incubated in equilibrated

phosphate-free DMEM containing 10% dialyzed FBS for 3 hours. During this time, a betashield box was also placed in the incubator to equilibrate. To label cells, 0.5mCi/mL of $^{32}$P-orthophosphate in phosphate-free DMEM containing 10% dialyzed FBS and 2mM HU was added for 2 hours and dishes placed in the betashield box. Cells were washed once with PBS and 700µL of trypsin added to each plate for 5 minutes. 700µL of media was added to trypsinized cells, cells were transferred to a 1.5mL screw cap microcentrifuge tube and pelleted at 1000 rpm for 5 minutes. Pellets were washed once with PBS and combined into a single tube and pelleted. Cells were lysed in 700µL of TGN lysis buffer containing inhibitors for 20 minutes on ice and then cleared at 4ºC for 20 minutes at 16.1xg. 30µL of protein G agarose (Santa Cruz) and 5µg of mouse IgG were added to the cleared lysate for 30 minutes rotating at 4ºC. Protein G agarose was pelleted and lysates were transferred to 60µL of HA-beads and rotated at 4ºC for 3 hours. HA-beads were then washed 3 times with 1mL of RIPA lysis buffer (150mM NaCl, 1% NP-40, 0.1% SDS, 0.5% deoxycholate, 50mM Tris pH 8.0) containing inhibitors, 1 time with RIPA buffer containing 500mM LiCl, and 2 times with RIPA buffer containing inhibitors. 30µL of 2X LSB was added to beads and boiled for 10 minutes. HA-immunoprecipitates were separated by SDS-PAGE on an 8% acrylamide gel and transferred to PVDF at 0.2 Amps for 8 hours. PVDF membranes were exposed to film for 1 hour to visualize proteins with $^{32}$P incorporated. Film was aligned to the membrane, and a syringe was used to perforate the membrane around radiolabeled ATR. Membrane was cut and transferred to a 1.5mL centrifuge tube. 1mL of 100% methanol was added to the membrane for 1 minute and then removed. Membranes were washed

with 1mL of 0.05M of ammonium bicarbonate containing 0.1% Tween-20 once and then incubated in 1mL of the solution for 30 minutes at 37ºC. Membranes were washed onced with 1mL of 0.05M ammonium bicarbonate without Tween-20. 20µL of 0.05M ammonium bicarbonate was added to cover the membrane, and 10µL of sequencing grade trypsin (10mg/mL stock, Promega) was added. Proteins were digested at 37ºC for 3 hours, and another 10µL of trypsin was added for an additional 3 hours. 400µL of milliQ water was added to digested proteins and dried in a speed vacuum over night. 400µL of milliQ water was added to dried samples, vortexed well, and then dried in a speed vacuum for 3 hours or until completely dry. Digested proteins were then resuspended in 400µL of pH 1.9 electrophoresis buffer (2.5% formic acid, 7.8% glacial acetic acid), vortexed well, transferred to a new tube, and lyophilized again. After lyophilizing, centrifuge tubes were placed with caps open in a dry scintillation vial and $^{32}P$ was counted in a scintillation counter. Peptides were resuspended in pH 1.9 buffer to equalize counts/volume. Equal counts were then spotted onto cellulose coated glass thin layer chromatography plates according the standard protocol (197). In the case of GST-AAD stimulated maps, counts were not equalized. Instead equal amounts of peptide were spotted. Plates were electrophoresed at 1000V for 30 minutes on a Hunter Box in pH 1.9 buffer and then completely dried in the fume hood for several hours. Plates were then transferred to a chromatography tank containing phosphochromatography buffer (7.5% glacial acetic acid, 25% pyridine, 37.5% *n*-Butanol) over night. Plates were dried and then exposed to film (197).

*Cell synchronization*

To contact inhibit RPE cells, $3.5x10^6$ cells were seeded in a 100mm dish and allowed to contact inhibit for 96 hours. To relieve contact inhibition, cells were trypsinized and $3x10^5$ cells were replated in 6 well plates for cell cycle analysis

To arrest cells in early S phase, cells were treated with 2mM HU for 24 hours. To release cells, HU was removed and cells were washed twice with equilibrated media and fresh media containing 1μg/mL nocodazole was added to arrest cells in mitosis.

To arrest HeLa cells in mitosis, 20ng/mL nocodazole was added to media for 18 hours. Plates were tapped to release mitotic cells and media was harvested. Pellets were washed twice with 50mL of media and replated at $3x10^5$ cells/6 well in fresh media to release.

*Yeast strain construction*

Strain GA2895 (*mec1 Δsml1Δ*) was grown to $OD_{600}$ of 0.5 and pelleted for 2 minutes at 3000 rpm. Cells were washed with 5mL of 100mM lithium acetate in TE (10mM Tris pH 8.0, 1mM EDTA), pelleted, and resuspended in 1mL of 100mM lithium acetate in TE. 100μL of yeast was added to a centrifuge tube containing 1μg of plasmid. 25μL of boiled salmon sperm ssDNA and 700μL of 30% PEG-3500/100mM lithium acetate/TE were added to the tube and tubes vortexed well. Tubes were incubated at 30ºC for 30 minutes and transferred to a 42ºC water bath for 20 minutes. Yeast were pelleted for 30 seconds at 3000 rpm and supernatant carefully aspirated. Pellets were resuspended in 150μL of sterile water, plated on appropriate plates, and incubated for 2 days at 30ºC.

Strain genotypes, plasmids used to transform them, and mutagenesis primers are summarized in Table 2 and Table 3.

**Table 2. Yeast strains.** Strains used in this study and their genotypes.

| Strain | Genotype | Notes |
|---|---|---|
| GA2895 | MAT**a,** *ade2*-1, *trp1*-1, *his3*-11, -15, *ura3*-1, *leu2*-3,-112, *can1*-100 *mec1*::*HIS3, sml1*::*KanMX6* | (40) |
| yDC208 | GA2895 [pRS416: *URA3-CEN*] | pRS416 |
| yDC209 | GA2895 [pRS416:*MEC1-URA3-CEN]* | pBad45 |
| yDC211 | GA2895 [pRS416:*E1354R-mec1-URA3-CEN*] | pDC1141 |
| yDC212 | GA2895 [pRS416:*W1359R-mec1-URA3-CEN*] | pDC1138 |
| yDC213 | GA2895 [pRS416:*FRVF1349AAAA-mec1-URA3-CEN*] | pDC1142 |
| yEN10 | GA2895 [pRS416:*HA-MEC1-URA3-CEN*] | pEN184 |
| yEN11 | GA2895 [pRS416:*HA-FRVF1349AAAA-mec1-URA3-CEN*] | pEN186 |
| yEN12 | GA2895 [pRS416: *URA3-CEN*] | pRS416 |
| yEN13 | GA2895 [pRS426:*HA-FRVF1349AAAA-mec1-URA3-2μ*] | pEN186 |

**Table 3. *MEC1* primer sequences.** + denotes a restriction site is added by mutagenesis. – indicates the site is destroyed with mutagenesis.

| Primer | Sequence | Notes |
|---|---|---|
| W1359R | 5′-CAGAGTTTTCGAATATTGCAAAAAAGGGCA ACTGAATTTAAACAAAATTACATAAACTAC | -PmeI |
| E1354R | 5′-GAATCCATCTTCAGAGTTTTCAGATATTGCAAA AAATGGGCAACTGAG | -BstBI |
| FRVF-AAAA | 5′-CGTTAAGAATGTGCTATGAATCCATCGCC GCTGCGGCCGAATATTGCAAAAAATGGGC | -BstBI +EagI |

*Yeast western blotting and spot assay*

For Rad53 phosphorylation, logarithmically growing cultures were α-factor (1pM) arrested for 3 hours at 30ºC in YPD pH 3.5. Arrested cells were harvested and washed twice with 1mL of sterile water. 1.0 $OD_{600}$ of arrested cells was treated with 200mM HU for 1 hour at 30ºC. HU-treated cells were

pelleted, washed once with 1mL of 20% TCA, and frozen at -80°C. To lyse, 200μL of 20% TCA was added to pellets with glass beads and homogenized for 3 minutes using a bead beater. Supernatant was transferred to a new tube and 2X LSB was added. Lysates were neutralized with 1M Tris pH 8.0, boiled for 5 minutes, and cleared for 5 minutes at room temperature at max speed. Protein was quantified using the BioRad Bradford system (samples diluted 1:30) and 50μg of protein was separated by SDS-PAGE on an 8% acrylamide gel. A Rad53 antibody was used at 1:1000 and detected with an anti-rabbit 800 infrared-conjugated Licor secondary antibody.

For western blots of HA-Mec1, cells were homogenized in the presence of glass beads and NP-40 buffer 4 times 30 seconds each with 1 minute of rest in between. 30μL of HA-beads were incubated with cleared lysates over night at 4°C and separated by SDS-PAGE on an 8% polyacrylamide gel. anti-HA antibody (Covance) was used at 1:4000 and anti-mouse-HRP conjugated was used at 1:10,000.

For spotting assays, 5mL of each strain was grown overnight. 1 $OD_{600}$ of cells were transferred to a 1.5mL centrifuge tube and pelletted at 3000rpm for 1 minute. The supernatant was removed and cells were resuspended in 200μL of sterile water. 200μL of cells were added to the first column of wells in a 96-well round bottom plate. Five 10-fold serial dilutions were made in the adjacent columns. A spotter was used to transfer cells from the 96-wells to pre-warmed growth plates. Plates were dried and then incubated at 30°C until visible colonies formed.

# CHAPTER III

## T1989 PHOSPHORYLATION MARKS AN ACTIVE ATR KINASE[1]

### Introduction

ATM and DNA-PK, like ATR, are regulated by recruitment to sites of DNA damage (169) and by protein activators (170, 173). In addition, ATM and DNA-PK undergo autophosphorylation (162, 181, 184, 198). These kinases prefer to phosphorylate serines or threonines that are immediately followed by glutamine (S/TQ). Phosphorylation sites on ATM and DNA-PK are functionally significant and have been used as direct markers of activation (162, 181, 184, 198), allowing direct monitoring of ATM and DNA-PK activity in cells.

ATR autophosphorylates *in vitro* (36); however, direct evidence for ATR regulation by phosphorylation is lacking. Currently researchers monitor ATR activity in cells indirectly through phosphorylation of its substrates. This is problematic for several reasons. First many ATR substrates, such as RPA, H2AX, and p53, are phosphorylated by ATM and DNA-PK. To address this issue of overlapping substrates, investigators monitor Chk1 phosphorylation on S317 and S345. However, ATR-dependent Chk1 phosphorylation has a unique requirement for the protein adaptor Claspin. Therefore, Chk1 phosphorylation measures one distinct ATR phosphorylation event that does not necessarily reflect ATR activity towards all substrates. Here I identify and characterize T1989 as a DNA damage-regulated ATR phosphorylation site. T1989

[1] A portion of this chapter is published in (191)

phosphorylation depends on ATR kinase activity in cells and requires kinase activation. Ablation of T1989 phosphorylation causes a modest functional defect. This is the first characterization of an ATR phosphorylation site that can be used as a direct measurement of ATR activity in cells.

## Results

*ATR T1989 is a DNA damage-induced phosphorylation site*

To identify ATR phosphorylation sites, I purified endogenous ATR-ATRIP complexes from hydroxyurea (HU) treated HeLa cells using an anti-ATRIP antibody in a single-step immunoprecipitation. I separated the ATR protein from associated proteins by gel electrophoresis and subjected it to in-gel digestion followed by liquid chromatography-coupled tandem mass spectrometry. This method identified several ATR phospho-peptides (Table 4), including S428, S435 (See Appendix A), and T1989 (Figure 11a). Several phospho-proteomic screens also identified these phospho-residues (125, 126). However these groups did not determine how these sites are regulated and whether they are functionally significant.

**Table 4. List of ATR phosphorylation sites and peptides identified by mass spectrometry**

| Phosphorylation site | Peptide |
|---|---|
| S428 | NLSSNSDGI(p)SK |
| S435 | RL(p)SSSLNPSK |
| S944 | SLHS(p)SQMTALPNTPCQNADVR |
| T1989 | GVELCFPENE(p)TPPEGK |

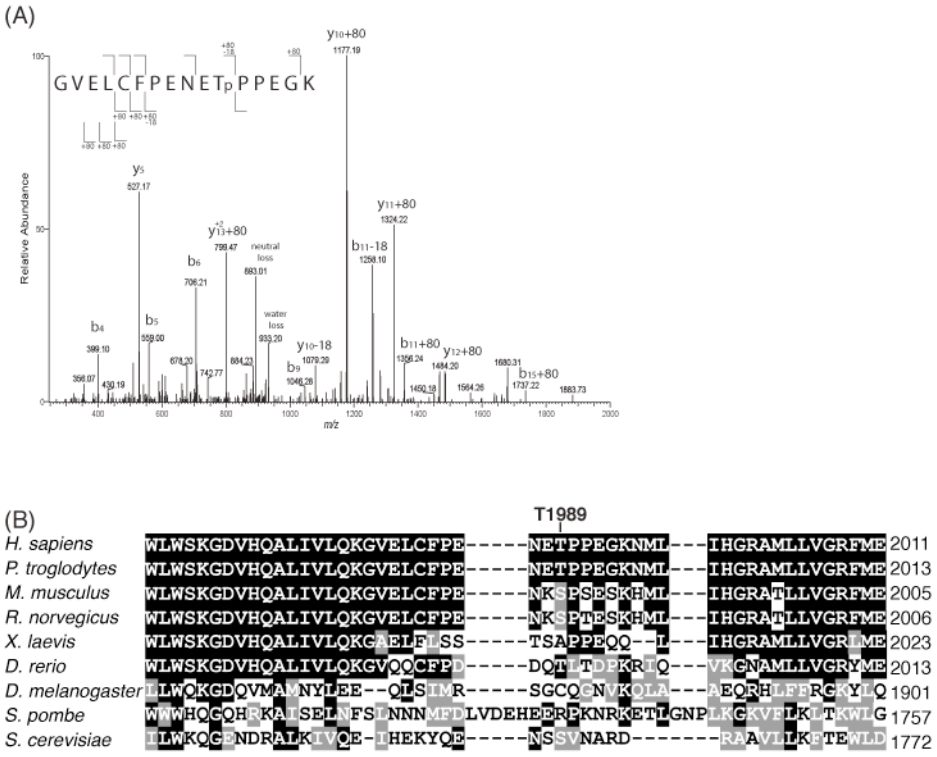


**Figure 11. ATR is phosphorylated on T1989.** (A) Annotated tandem mass spectrum of a doubly-charged peptide ion (m/z 942.10) consistent with the ATR sequence GVELCFPENETPPEGK with the threonine phosphorylated at position 1989 (Xcorr = 3.63). Labeled b-ions and y-ions are denoted by cleavage brackets above and below the sequence, respectively. (B) Sequence alignment of ATR orthologues. Black shaded boxes indicate conserved residues, and grey boxes denote residues with similar characteristics.

T1989 occurs within the ATR FAT domain. The FAT domain is composed of HEAT repeats and is generally highly conserved among ATR orthologues. However, sequence alignment revealed that T1989 is only conserved in primates, changed to a serine in rodents, and not conserved in frogs or flies (Figure 11b). The amino acids flanking T1989 are also poorly conserved.

To characterize phosphorylation of T1989 further, I generated a phospho-peptide specific antibody (pATR). This antibody recognizes an ATR peptide phosphorylated at position T1989 but not the corresponding unmodified peptide (Figure 12a). The antibody also recognizes ATR on immunoblots following immunoprecipitation (Figure 12b). It is specific to ATR, since excision of the floxed allele from $ATR^{flox/-}$TR cells eliminated reactivity (Figure 12b). Attempts to detect phosphorylated ATR by immunoblotting without prior immunoprecipitation were unsuccessful due to a cross-reacting protein near the same molecular weight as ATR.

Treating cells with HU increased T1989 phosphorylation (Figure 12c). Time-course experiments with HU, ultraviolet radiation (UV), and ionizing radiation (IR) revealed increased phosphorylation of T1989 in response to all of these agents within one hour of treatment (Figure 12d). I consistently observed the approximately two-fold induction of ATR phosphorylation in cells treated with HU for one hour (Figure 12e). A commonly used marker of ATR activation is phosphorylation of the ATR substrate Chk1. While Chk1 S317 and ATR T1989 both are phosphorylated within one hour of HU, UV, or IR exposure, Chk1 phosphorylation did not substantially increase at later times. In contrast, T1989 phosphorylation continued to increase at least until 3h after treatment (Figure 12d).

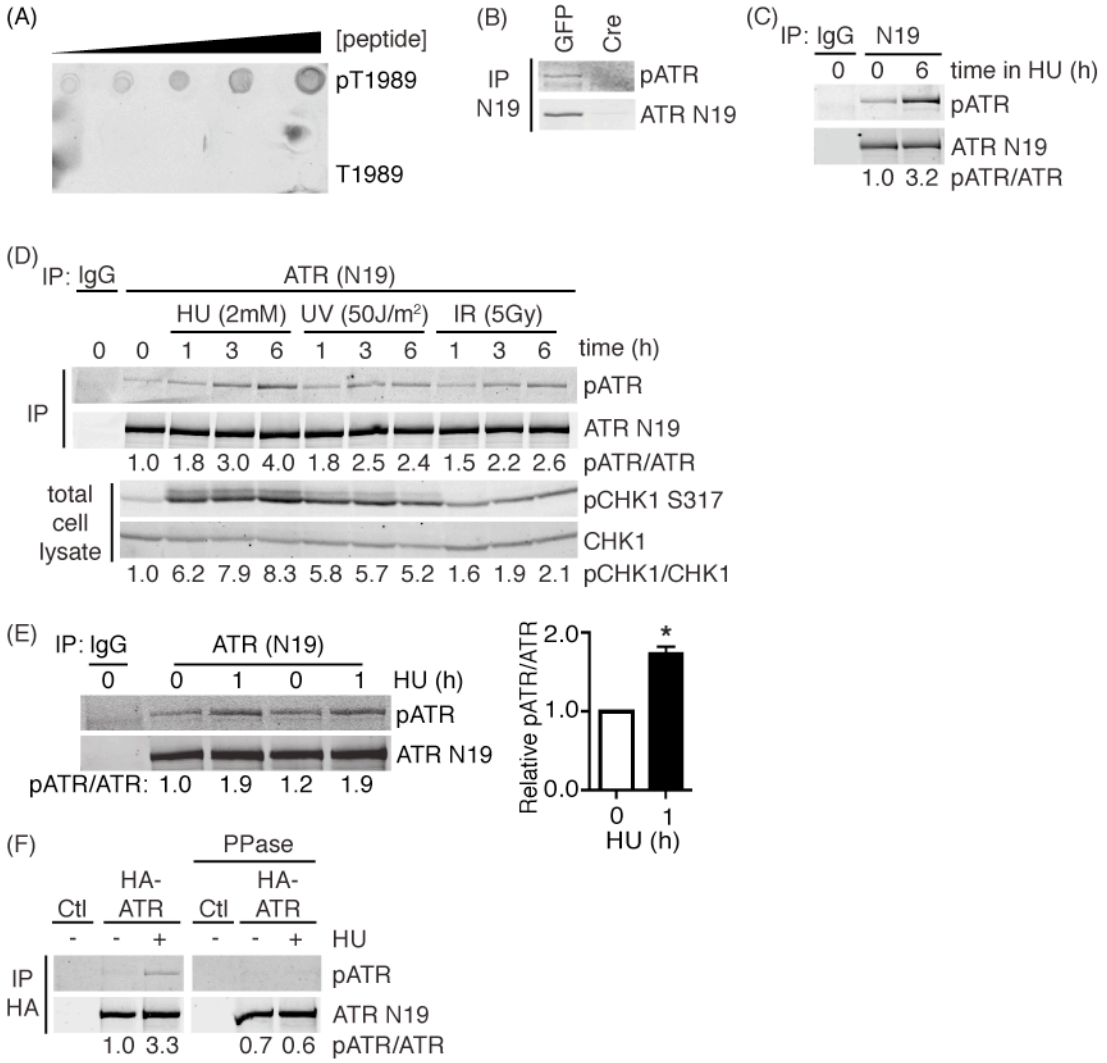


**Figure 12. DNA damage induces ATR T1989 phosphorylation.** (A) Dot blots of increasing amounts of phosphorylated CFPENE(pT)PPEGK (pT1989) and nonphosphorylated CFPENETPPEGK (T1989) peptides were immunoblotted with pATR antibodies. (B) $ATR^{flox/-}TR$ cells were infected with adenovirus encoding either GFP or Cre. ATR was immunoprecipitated and immune complexes separated by SDS-PAGE prior to immunoblotting with phospho-specific (pATR) or total (N19) ATR antibodies. (C – E) Anti-ATR or control IgG immunoprecipitates from cells treated with HU, UV, or IR for the indicated times were separated by SDS-PAGE and immunoblotted as indicated. CHK1 phosphorylation was examined in total cell lysates. (E) Quantification of pATR/ATR 1 hour post-HU treatment over three-independent experiments (*$p<0.01$). (F) Cells were mock or HU-treated for 6 hours. Anti-HA immunoprecipitates from control $ATR^{flox/-}TR$ (Ctl) or $ATR^{del/-}TR$ cells expressing Flag-HA-ATR were incubated with or without lambda phosphatase prior to immunoblotting.

Importantly, lambda phosphatase abolished detection of DNA damage-induced T1989 phosphorylation (Figure 12f).

To determine whether the pATR antibody is specific to phosphorylated T1989, I assessed its recognition of an ATR T1989A mutant protein. In contrast to wild-type ATR, the antibody did not recognize an HU-inducible phosphorylation on the ATR T1989A protein (Figure 13a). I did note some residual antibody recognition of a protein at the molecular weight of ATR after immunoprecipitation of Flag-ATR T1989A (Figure 13a). To further characterize the T1989 dependency of the antibody, we generated $ATR^{flox/-}$TR cells stably expressing Flag-HA-ATR or Flag-HA-ATR T1989A, immunopurified these proteins, and blotted with the phosphorylation specific antibody. In these circumstances there was significant recognition of the wild-type protein immunoprecipitated from HU-treated cells but no HU-inducible recognition of the T1989A mutant (Figure 13b). I conclude that the antibody is largely specific to phosphorylated T1989, and T1989 is hyper-phosphorylated when ATR is activated. The antibody may have some cross-reactivity to another phospho-epitope on ATR that is not regulated in response to HU.

*T1989 phosphorylation depends on ATR kinase activity*

ATM and DNA-PK undergo autophosphorylation, and ATR can autophosphorylate *in vitro* (36). Most characterized ATM, DNA-PK, and ATR phosphorylation sites are S or T followed by Q. T1989 does not fit this consensus; however, there are several characterized ATM and DNA-PK autophosphorylation sites that also fail to conform to this consensus sequence (180, 199). Therefore, I tested whether T1989 phosphorylation in cells depends

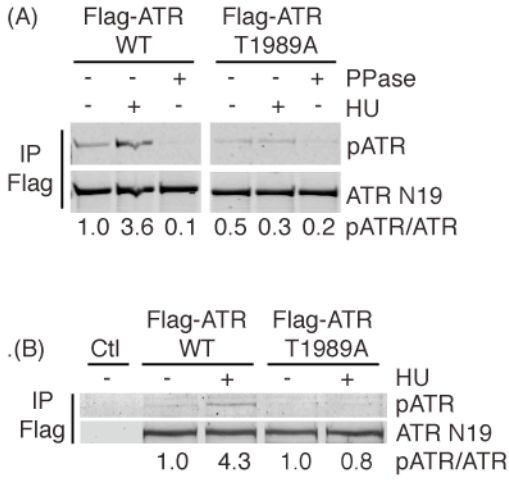


**Figure 13. The pATR antibody is specific to T1989.** Cells were mock or HU-treated for 6 hours. (A) Flag-ATR wild-type (WT) or T1989A were expressed in 293T cells. Flag immunoprecipitates were mock treated or treated with phosphatase prior to immunoblotting. (B) Flag-immunoprecipitates from $ATR^{flox/-}$TR (Ctl), Flag-HA-ATR WT, or Flag-HA-ATR T1989A expressing $ATR^{flox/-}$TR cells were immunoblotted.

on ATR kinase activity. First, I assayed whether a kinase-dead ATR mutant can be phosphorylated on T1989. Unlike wild-type ATR, the kinase-dead mutant did not exhibit HU-inducible T1989 phosphorylation (Figure 14a). I next used small molecule inhibitors to the PIKK family of kinases. Selective ATM (KU) and DNA-PK (NU) inhibitors did not reduce T1989 phosphorylation following HU treatment (Figure 14b). However, the non-selective ATR and ATM inhibitor caffeine significantly decreased T1989 phosphorylation in HU-treated cells and inhibited ATR signaling as measured by Chk1 phosphorylation. Finally, an agent that selectively inhibits ATR (AZ20) but not DNA-PK or ATM also abrogates HU-induced T1989 phosphorylation on both exogenous (Figure 14c) and endogenous ATR (Figure 14d). These results indicate that T1989 phosphorylation in cells requires ATR kinase activity.

Immunopurified ATR-ATRIP complexes failed to phosphorylate a small, recombinant ATR fragment containing T1989 purified from *E. coli* (not shown). We also failed to observe a significant increase in T1989 phosphorylation on purified full-length ATR subjected to *in vitro* conditions that allow autophosphorylation (not shown). Thus, it remains possible that the *in vivo* dependency on ATR kinase activity is due to an ATR-activated kinase rather than autophosphorylation. However, treating cells with a selective Chk1 inhibitor did not significantly impair HU-induced T1989 phosphorylation (Figure 15), indicating that if another kinase is involved, it is not Chk1-dependent. While T1989 is followed by a proline like many CDK substrates, treatment with the CDK inhibitor roscovitine also had no effect on T1989 phosphorylation (Figure 15)

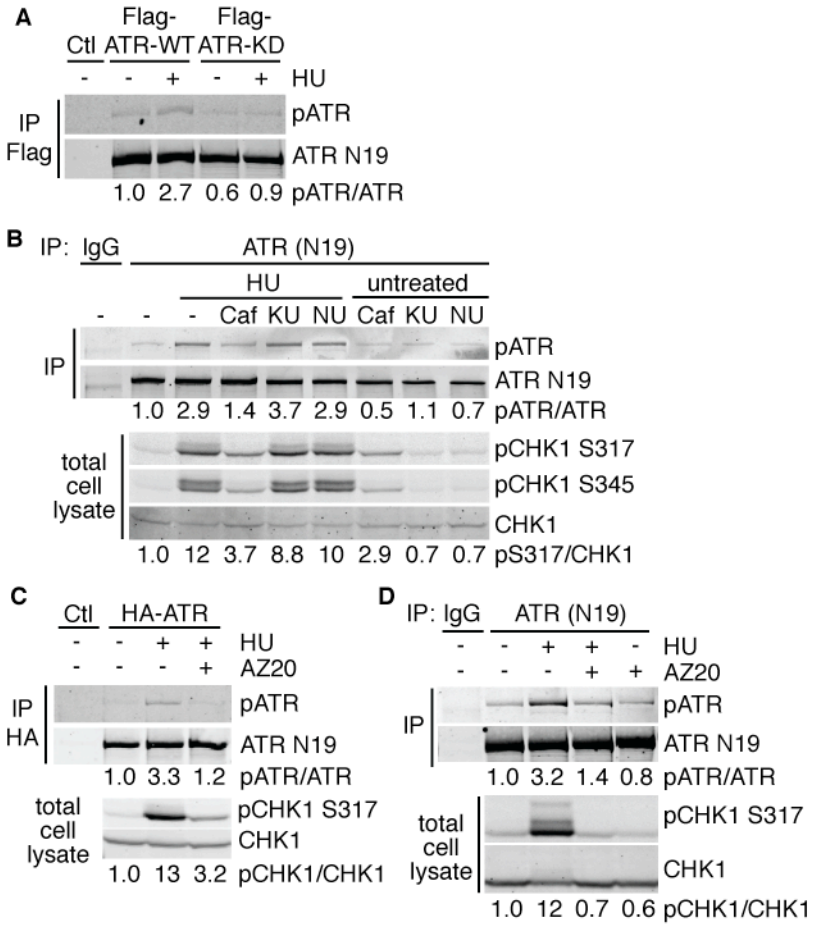


**Figure 14. T1989 phosphorylation depends on ATR kinase activity.** (A-D) Immunoprecipitates (IP) or total cell lysates were analyzed by immunoblotting with the indicated antibodies. (A) Flag-ATR (WT) or Flag-ATR kinase dead (KD) expressing 293T cells were treated with HU for 0 or 6h. Ctl is cells transfected with an empty vector. (B) 293T cells were treated with the following kinase inhibitors in the presence or absence of HU for 6 hours: 10mM caffeine (Caf), 10$\mu$M KU55933 (KU), or 1$\mu$M NU7441 (NU) (C) $ATR^{flox/-}$TR (Ctl) or $ATR^{del/-}$TR cells expressing Flag-HA-ATR were treated with 2mM HU and 5$\mu$M AZ20 for 6 hours as indicated. (D) 293T cells were treated with HU and 3 $\mu$M AZ20 for 6 hours.

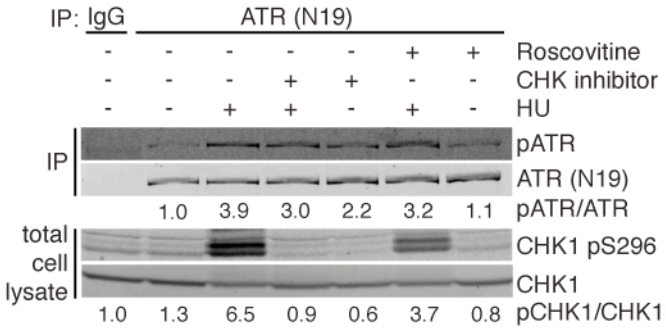


**Figure 15. Chk1 and CDK2 are not required for T1989 phosphorylation.** Cells were treated with HU, CHK1 inhibitor (AZD7762), or roscovitine as indicated for 6 hours. IgG control or ATR immunoprecipitates were separated by SDS-PAGE and immunoblotted with the indicated antibodies. For Chk1 inhibition, Chk1 S296 autophosphorylation was monitored.

*T1989 phosphorylation requires ATR activation*

ATM and DNA-PK activation and autophosphorylation require their protein activators Mre11-Rad50-Nbs1 (MRN) and Ku70/80, respectively (160). Thus, I first sought to determine whether T1989 phosphorylation requires the ATR activator TopBP1 (109). Transfection with TopBP1 siRNA alone caused increased T1989 phosphorylation even in the absence of a DNA damaging agent. This level of phosphorylation did not change upon addition of HU and remained below the level seen in HU-treated cells transfected with a control non-targeting siRNA (Figure 16a). I was unable to achieve complete knockdown of TopBP1 in these experiments and could still detect significant Chk1 phosphorylation in HU-treated TopBP1 siRNA cells (Figure 16a). The incomplete silencing of *TopBP1* expression and increased basal T1989 phosphorylation but lack of HU-inducible phosphorylation makes this siRNA experiment difficult to interpret. As an alternative approach, I examined T1989 phosphorylation on the ATR PIKK Regulatory Domain (PRD) mutant, which contains the point mutation K2589E. This mutation disrupts the ability of ATR to interact with and be activated by TopBP1 while retaining basal ATR kinase activity (90). The ATR-PRD mutant is not phosphorylated on T1989 in response to HU (Figure 16b), suggesting that T1989 phosphorylation depends on activation of ATR.

Since T1989 phosphorylation depends on ATR activation, phosphorylation is unlikely to be required for the activation process, and an ATR T1989A mutant should still be activated by TopBP1 *in vitro*. To test this hypothesis, I assayed whether the ATR activation domain (AAD) of TopBP1 could activate immunopurified wild-type, T1989A, and T1989E ATR-ATRIP complexes. All three of these proteins were activated to similar extents by

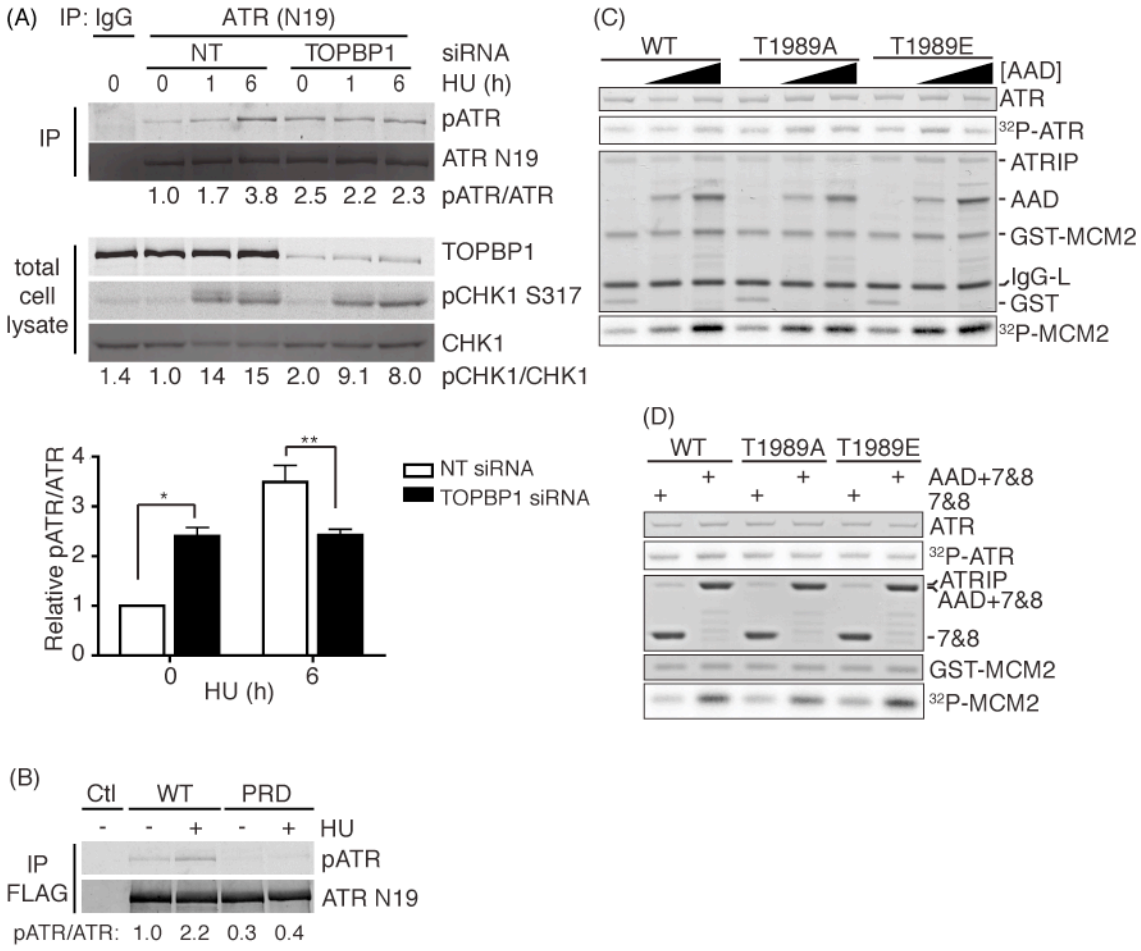


**Figure 16. T1989 phosphorylation requires ATR activation via the PRD.** (A) 293T cells transfected with either non-targeting (NT) or TOPBP1 siRNA were treated with HU for times indicated. Endogenous ATR was immunoprecipitated and examined for T1989 phosphorylation by immunoblotting. Expression levels of TOPBP1, CHK1, and pCHK1 S317 were also examined by immunoblotting the total cell lysates. Graph represents pATR/ATR levels from three independent siRNA experiments (*p<0.01, **p<0.04). (B) Empty vector (Ctl), FLAG-ATR-WT, or FLAG-ATR-PRD expression vectors were transfected into 293T cells. Cells were HU-treated or untreated for 6 hours, lysed, and Flag-immunoprecipitates immunoblotted to detect phosphorylated and total ATR. (C and D) Wild-type ATR (WT), ATR T1989A, or ATR T1989E proteins complexed with ATRIP were isolated from transfected 293T cells and incubated with MCM2 substrate, γ-32P-ATP, and (C) increasing concentrations of recombinant GST-TOPBP1-AAD or GST or (D) GST-TOPBP1-BRCT7&8 or GST-TOPBP1-AAD+BRCT7&8 as indicated. Kinase reactions were separated by SDS-PAGE and detected by phosphorimaging (32P-ATR and 32P-MCM2). The amount of ATR, ATRIP, TOPBP1, MCM2, and GST proteins in each reaction was detected by staining with Coomassie blue.

increasing concentrations of the GST-AAD protein but not by GST (Figure 16c). A GST-TopBP1 protein containing the AAD and the C-terminal BRCT domains of TopBP1 also activated all three proteins (Figure 16d). Therefore at least under these *in vitro* conditions, T1989 phosphorylation does not impact TopBP1-mediated ATR activation.

*Functional characterization of T1989 phosphorylation*

To examine the functional relevance of T1989 phosphorylation, I employed a genetic complementation strategy (Figure 17) using $ATR^{flox/-}$ cells harboring one conditional allele of *ATR* and a second allele disrupted by a neomycin cassette (36). These cells were also engineered to express the tetracycline repressor, creating the parental $ATR^{flox/-}$TR cell line. I then integrated either wild-type (WT) or ATR T1989A mutant expression vectors containing a tetracycline-response promoter, creating WT-$ATR^{flox/-}$TR and T1989A-$ATR^{flox/-}$TR cell lines. ATR cDNAs also contain an N-terminal Flag-$HA_3$ epitope tag to differentiate exogenous and endogenous proteins. After selection, I screened stable integrants for inducible expression of the ATR protein and selected only clones expressing similar protein levels for further analysis. In addition, I verified that the percentage of cells expressing tagged ATR in each clone was similar using immunofluorescence (Figure 18a). I also confirmed that the tagged protein correctly localized to the nucleus and can localize to stalled replication forks in response to HU-treatment (Figure 18b). This analysis confirms that the T1989A mutation does not interfere with the ATR-ATRIP complex, since ATRIP association is required for both the stability and

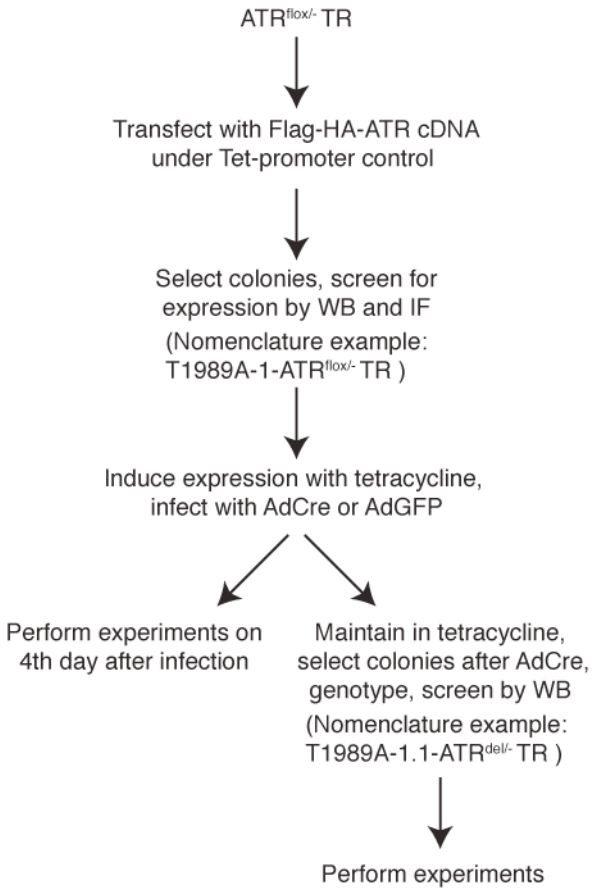


**Figure 17. Flow chart describing the ATR-genetic complementation strategy.**

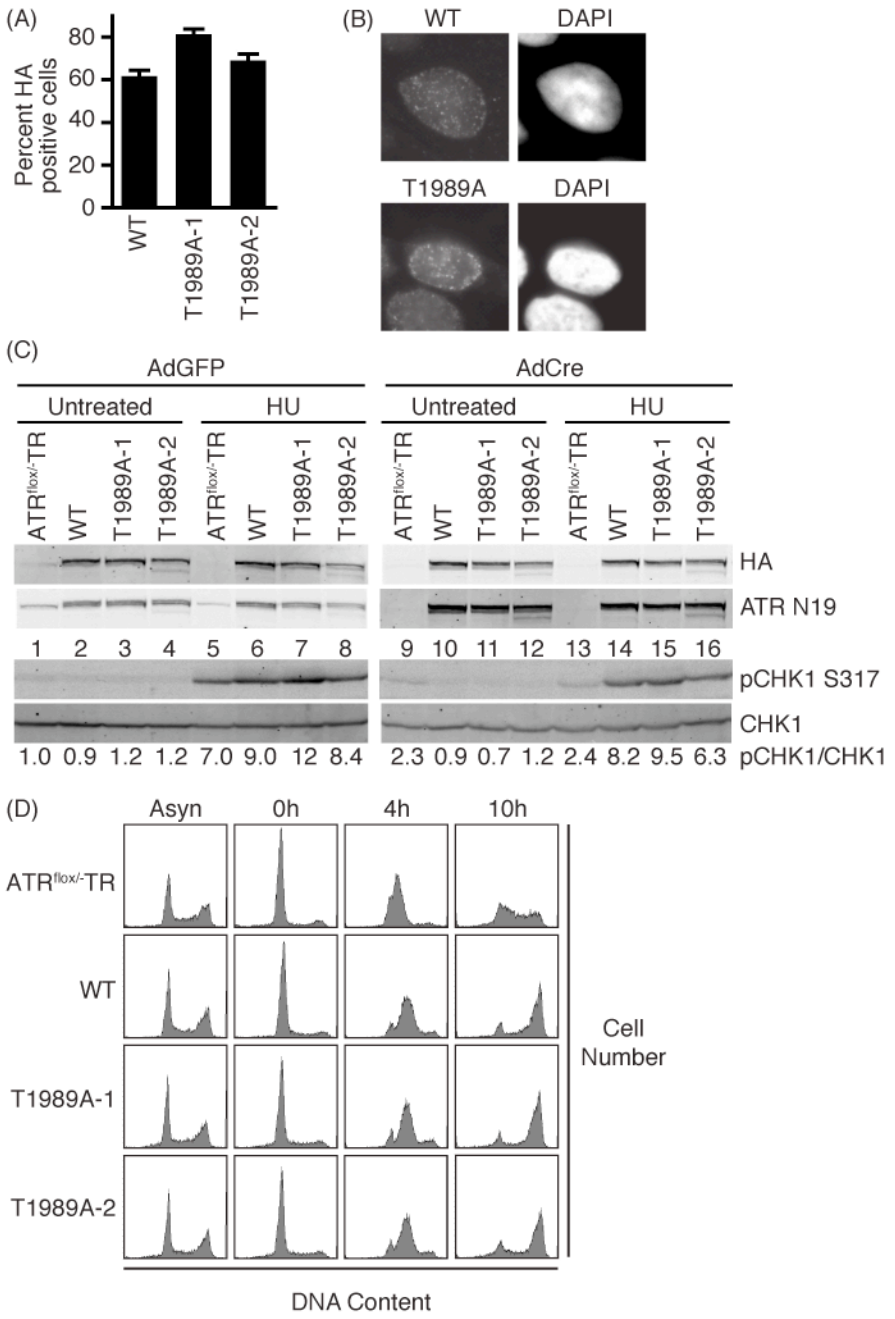


**Figure 18. ATR T1989 phosphorylation is dispensable for cellular recovery from replication stress.** (A) ATR$^{flox/-}$TR cells with an integrated tetracycline-responsive expression vector encoding FLAG-HA-ATR (WT) or FLAG-HA-T1989A proteins were analyzed by immunofluorescence after a transient induction of protein expression. (B) Localization of wild-type or T1989A ATR in HU-treated cells. (C and D) ATR$^{flox/-}$TR, WT-ATR$^{flox/-}$TR, or two independent clones of T1989A-ATR$^{flox/-}$TR cells were cultured in tetracycline media and infected with control (AdGFP) or Cre-expressing adenovirus (AdCre) to delete the floxed ATR allele. (C) Four days after infection, cells were treated with 0 or 2mM HU for 6 hours. Lysates were separated by SDS-PAGE and immunoblotted with the indicated antibodies. (D) AdCre infected cells were treated with HU for 24hrs, washed once, and released into growth media containing nocodazole for 0, 4, or 10h. Cells were fixed, stained with propidium iodide, and examined for DNA content by flow cytometry. Untreated (Asynchronous) cells were also analyzed.

localization of ATR (36, 84). In subsequent experiments, I characterized two independent mutant cell lines to account for any possible clonal differences.

Infecting the parental ATR$^{flox/-}$TR cells with an adenovirus encoding the Cre recombinase nearly ablated ATR protein expression within four days post infection (Figure 18c). Tetracycline-induced expression of the exogenous ATR cDNAs restored ATR expression with both WT-ATR and T1989A-ATR expressed at similar levels (Figure 18c).

To compare the signaling activities of the T1989A and WT ATR proteins, I deleted the floxed allele, expressed the WT or T1989A mutant, and treated the cells with HU. Deletion of *ATR$^{flox}$* in the parental cell line attenuates Chk1 phosphorylation (Figure 18c, compare lanes 5 and 13). WT-ATR restored Chk1 phosphorylation (Figure 18c, lane 14). Similarly, both T1989A-ATR clones also supported ATR-dependent Chk1 phosphorylation (Figure 18c, lanes 15 and 16), suggesting T1989 phosphorylation is not required for ATR signaling in response to replication stress.

ATR promotes completion of DNA synthesis following an HU challenge (18). To test whether T1989 phosphorylation regulates this activity, I monitored completion of DNA replication following a transient exposure to HU. After Cre-deletion of the floxed allele, both WT-ATR and T1989A-ATR cells have similar distributions of cells in each cell cycle phase (Figure 18d). HU synchronizes the cells in early S-phase. Cre-infected parental ATR$^{flox/-}$TR cells are unable to complete S phase when released from the HU arrest. In contrast, both WT-ATR$^{flox/-}$TR and T1989A-ATR$^{flox/-}$TR cells complete replication with similar kinetics (Figure 18d).

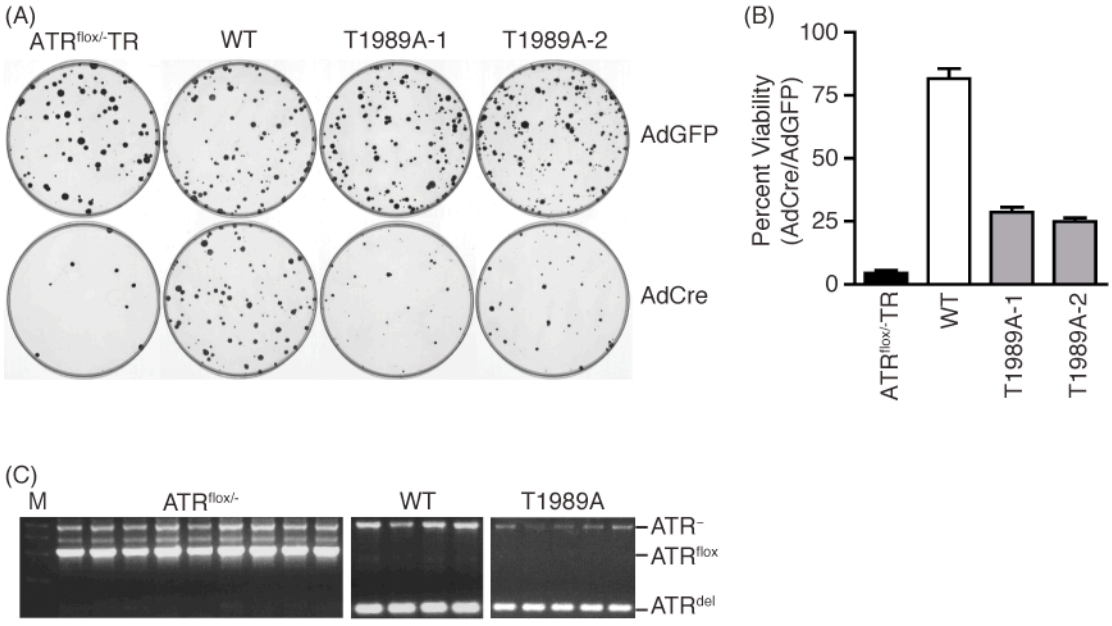


**Figure 19. T1989 phosphorylation causes a mild viability defect.** (A-C) ATR$^{flox/-}$TR, WT-ATR$^{flox/-}$TR, or two independent clones of T1989A-ATR$^{flox/-}$TR cells were cultured in tetracycline media and infected with control (AdGFP) or Cre-expressing adenovirus to delete the floxed ATR allele. The infected cells were plated at low density and then cultured for 14 days in the presence of tetracycline. Surviving colonies were stained (A), scored (B), and PCR genotyped (C).

*ATR* is an essential gene required for human cell viability even in the absence of exogenous DNA damage (36). To determine whether T1989 phosphorylation is required for the essential function of ATR, I grew ATR$^{flox/-}$TR, WT-ATR$^{flox/-}$TR, and T1989A-ATR$^{flox/-}$TR cells in the presence of tetracycline, infected with adenovirus encoding either GFP or Cre, and allowed single colonies to form over a period of 14 days. I visualized surviving colonies by methylene blue staining and counted colonies to determine survival fractions. Upon *ATR* deletion, 5% of AdCre infected parental ATR$^{flox/-}$TR cells were able to form colonies (Figure 19a and b). Wild-type ATR complements this viability defect with 82% of AdCre infected WT-ATR$^{flox/-}$TR cells forming colonies. In contrast, T1989A-ATR does not fully complement the viability defect caused by *ATR$^{flox}$* deletion with only 29% and 25% of AdCre infected T1989A-1 and T1989-2-ATR$^{flox/-}$TR cells forming colonies respectively.

I further confirmed the colony formation results by monitoring excision of the flox allele in colonies from AdCre infected cells by PCR genotyping. As expected, 100% of colonies (9 out of 9) obtained from the parental ATR$^{flox/-}$TR cell line contained an intact flox allele (Figure 19c). Thus, they survived only because Cre-catalyzed excision was not complete. In contrast, PCR genotyping showed excision of the floxed allele in every colony from AdCre infected WT cells (20 out of 20) and in nearly every colony obtained from T1989A-ATR$^{flox/-}$TR cells (53 out of 55). These results suggest that T1989 phosphorylation may be important but not essential for ATR to support cell viability.

Because the T1989A-ATR protein yielded a modest colony formation defect, I considered the possibility that a mild checkpoint signaling defect may not have been observed in the Cre infection experiments (Figure 18c) due to

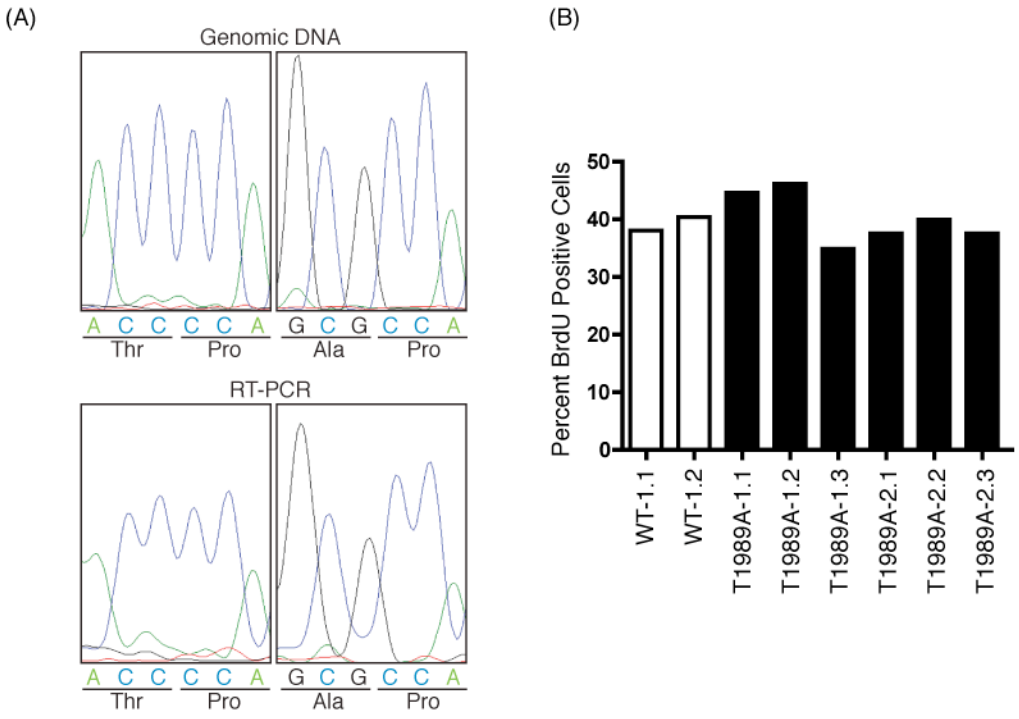


**Figure 20. WT-ATR$^{del/-}$TR and T1989-ATR$^{del/-}$TR derived clones do not differ significantly in S phase percentage.** (A) Sequence analysis confirms expression of wild-type or T1989A ATR in ATR$^{del/-}$TR cells. Genomic DNA or cDNA from either WT-1.1-ATR$^{del/-}$TR cells or T1989A-1.1-ATR$^{del/-}$TR cells was amplified by PCR. The primers used were: ATR5902: GATGTTCACC-AGGCACTAATTGTTC and ATR6099rev: TGGCAGGCACGCGGTCACATC. PCR products were sequenced using the ATR5902 primer. (B) Cell lines were pulsed with BrdU for 15 minutes and analyzed by flow cytometry using anti-BrdU antibodies and propidium iodide.

residual endogenous ATR protein expression following Cre-mediated excision of the flox allele. To address this possibility, WT and T1989A AdCre infected colonies determined to have an excised flox allele by PCR genotyping were expanded, creating WT-ATR$^{del/-}$TR and T1989A-ATR$^{del/-}$TR cell lines that have no intact *ATR* genes at the endogenous loci. I confirmed that the only ATR expressed in these cell lines comes from the integrated ATR wild-type or T1989A cDNAs (Figure 20a) and that the percentage of S phase cells was similar among cell lines (Figure 20b). I examined Chk1 phosphorylation in two WT-ATR$^{del/-}$TR and six T1989A-ATR$^{del/-}$TR clones with varying levels of ATR expression. T1989A ATR expression varied between 37% (T1989A2.2) and 122% (T1989A1.3) of the ATR level in the parental ATR$^{flox/-}$TR cells. For comparison, WT1.1 and WT1.2 expressed ATR at 80% and 64% of the ATR$^{flox/-}$TR expression level. Both WT clones supported Chk1 phosphorylation equally (Figure 21a). The amount of Chk1 phosphorylation varied in the T1989A-ATR$^{del/-}$TR cell lines (Figure 21a) and correlated with the amount of T1989A protein expressed (Figure 21b). The cell lines expressing the least amount of T1989A protein exhibited approximately 60% of wild-type Chk1 phosphorylation while cell lines expressing the most T1989A had 150% of wild-type Chk1 phosphorylation levels. Thus, I conclude that the T1989A-ATR protein signals to phosphorylate Chk1 as efficiently as wild-type ATR when expressed at similar levels.

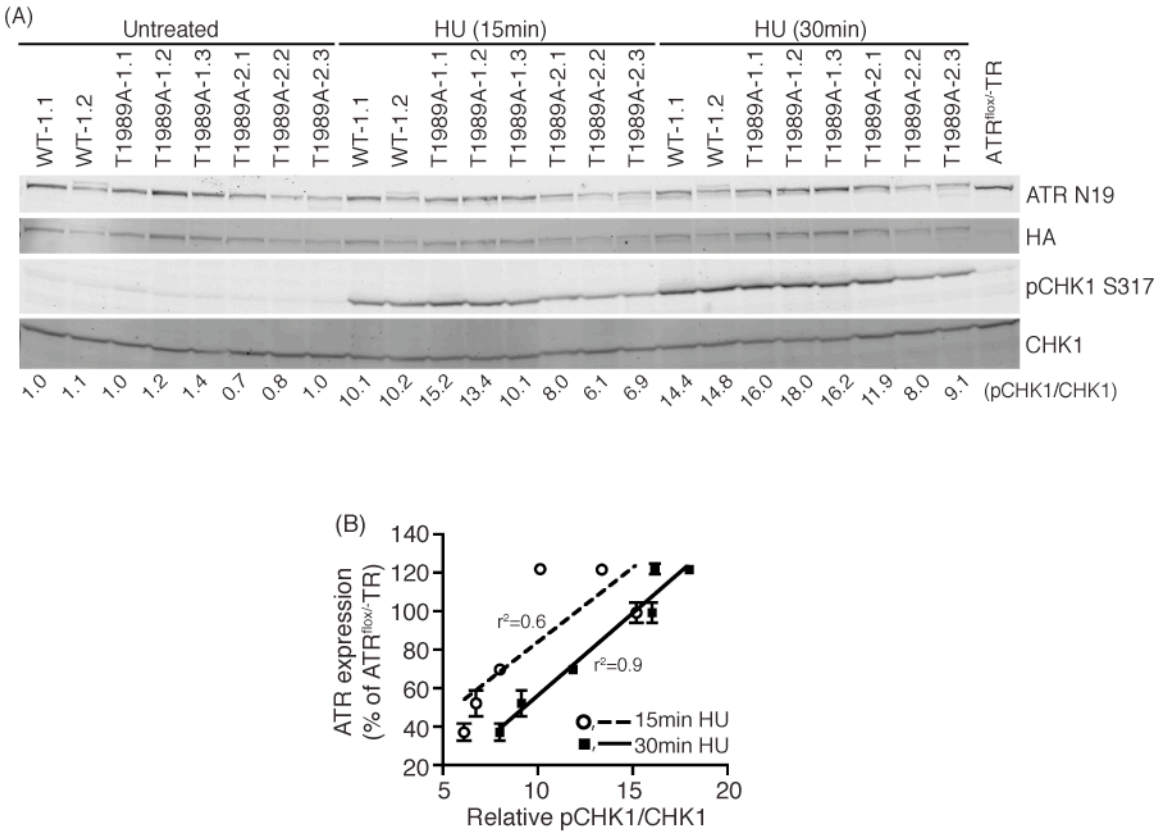


**Figure 21. Chk1 phosphorylation correlates with T1989A ATR protein levels.** (A and B). Surviving WT- ATR$^{del/-TR}$ and T1989A-ATR$^{del/-}$TR clones were challenged with 2mM HU for 0, 15, or 30 minutes. (A) Cell lysates were separated by SDS-PAGE and analyzed by quantitative immunoblotting. (B) The amount of T1989A ATR in each clone (expressed as a percentage of the level in the parental ATR$^{flox/-}$TR cells) was compared to the amount of CHK1 phosphorylation following the 15 or 30 minute HU treatment.

## Discussion

A challenge to studying ATR function has been the lack of a proximal biomarker to detect an active ATR kinase. Thus, researchers use Chk1 phosphorylation as a surrogate. However, ATR-dependent Chk1 phosphorylation requires proteins like Claspin that are not necessary for ATR to phosphorylate other substrates (133). There may also be instances in which Chk1 is phosphorylated by other kinases like ATM. My data on T1989 phosphorylation suggests it is a good biomarker for active ATR. T1989 phosphorylation is DNA damage-regulated, depends on ATR kinase activity, appears concurrently with ATR-dependent phosphorylation of Chk1, and requires activation of the ATR kinase. Functionally, T1989 phosphorylation is not essential for the ATR-Chk1 signaling axis following replication stress but has some function in supporting cellular viability.

### *Regulation of T1989 phosphorylation*

My cellular data indicate that T1989 phosphorylation requires ATR kinase activity suggesting it may be an autophosphorylation site. While T1989 does not conform to the typical ATR S/TQ phosphorylation consensus, there is precedence for nonconsensus ATM and DNA-PK autophosphorylation. Several DNA-PK autophosphorylation residues in the PQR cluster are tyrosine-directed (183), and ATM autophosphorylation sites S1893 (181) and S2996 (180) are glutamic and aspartic acid-directed respectively. I was unable to obtain evidence that T1989 is phosphorylated by ATR *in vitro.* However, these experiments are done in conditions that do not fully reconstitute the ATR activation mechanism, and two-dimensional phospho-peptide maps of *in vivo* and *in vitro* ATR

phospho-peptides have minimal similarities (Figure 31b-c). Thus, it is unclear whether the *in vitro* ATR kinase analysis mimics what happens *in vivo*. The other possibility is that an ATR-dependent kinase phosphorylates T1989. Only Chk1 is a well-defined ATR-dependent kinase, but my experiments indicate it is not required for T1989 phosphorylation. Further analyses will be necessary to unambiguously determine whether T1989 is truly an autophosphorylation site or phosphorylated by an ATR-activated kinase in an autoregulatatory circuit.

I noted that Chk1 phosphorylation remains constant after reaching a high level 1h after HU treatment whereas ATR T1989 phosphorylation continued to increase throughout the HU time course. The source of the difference is presently unclear but could be explained if different phosphatases act on these sites to cause the dynamic differences. Alternatively, it may take longer for most ATR molecules in the cell to be activated compared to Chk1 molecules. Future studies examining the timing and persistence of T1989 phosphorylation will help answer some of these questions. In addition, genetic and inhibitor experiments may reveal whether phosphatases regulate T1989 phosphorylation.

Mutation of the ATR PRD, which prevents TopBP1-dependent ATR activation (90), abolishes DNA damage-induced T1989 phosphorylation. Thus, T1989 phosphorylation requires ATR activation and suggests this site is downstream of TopBP1 function. Likewise, autophosphorylation of ATM and DNA-PK also requires activation by their protein activators (184, 200, 201). Though the only known function of the ATR PRD is to facilitate ATR activation by binding TopBP1, I cannot exclude the possibility that proteins other than TopBP1 function through the PRD to promote T1989 phosphorylation. It will be interesting to further probe the dependency of T1989 phosphorylation on other

known steps of ATR activation, namely the Rad9-Hus1-Rad1 complex. In mammalian cells, the 9-1-1 complex promotes TopBP1 recruitment. Based on PRD mutant data, I hypothesize that T1989 phosphorylation would also depend on the 9-1-1 complex. However, evidence in *Xenopus* suggests that there are modes of 9-1-1 independent recruitment for TopBP1.

Ablation of the ATM autophosphorylation site S1981 does not impact MRN-mediated activation of ATM (171). Similarly, mutation of T1989 to an alanine does not perturb TopBP1-mediated activation of ATR *in vitro*. Also in agreement with a lack of an ATR activation defect is the absence of strong signaling and functional defects in cells expressing only the unphosphorylatable T1989A ATR protein. ATR mutations that disrupt the activation process, such as the K2589E PRD mutant, exhibit severe cellular defects due to their inability to be activated (90).

Chk1 phosphorylation in multiple T1989A-ATR$^{del/-}$TR cell lines showed a strong correlation with ATR protein levels. When T1989A ATR is expressed at levels similar to those found in ATR$^{flox/-}$TR cells, it signals to Chk1 similar to wild-type ATR. ATR protein levels in the ATR$^{flox/-}$TR cells is approximately 30-40% of that found in the ATR$^{+/+}$ cell line due to the deletion of one *ATR* allele and the insertion of the loxP sites in the remaining expressed allele. Thus, the lack of an obvious ATR signaling defect in the T1989A mutant cell lines is not due to over-expression of this protein.

Despite the lack of a signaling defect, I observed a significant albeit partial decrease in the ability of T1989A ATR to maintain cell viability when challenged in a colony formation assay. A possible explanation is that T1989A ATR is expressed at variable levels in the clonal population. Low expression levels may

not support viability, since signaling under these circumstances is attenuated compared to cells with wild-type expression levels. The viability assay likely presents a stringent requirement for ATR function, since it requires colony growth from a single cell. However once the T1989A-ATR$^{del/-}$TR cells that survived were expanded, they showed no evidence of a continued survival or proliferation deficit, indicating T1989 is not essential for ATR function. The low conservation of T1989 even among vertebrate ATR orthologues and the lack of salient activation and signaling defects corroborate this conclusion.

The modest phenotypic consequence of the T1989A mutation is reminiscent of single mutants of DNA-PK autophosphorylation clusters (202). Mutation of multiple sites across clusters (203) or of a single cluster in entirety (202) is required to observe strong defects. Disruption of additional ATR phosphorylation sites may be needed to produce a significant biological defect. The functional significance of T1989 phosphorylation may also depend on specific cellular contexts. For instance, mutation of ATM S1981 to an alanine results in functional defects in human cells (162), yet there is no functional consequence of mutating this phosphorylation site in mouse cells (185).

*Mechanistic implications of T1989 phosphorylation*

Mechanistically it is difficult to hypothesize how T1989 phosphorylation may regulate ATR activity. I have strong evidence supporting that T1989 phosphorylation occurs after TopBP1-mediated activation and that T1989 is not essential for Chk1 phosphorylation in cells. Therefore, one possibility is that T1989 phosphorylation is not necessarily regulatory. ATR oligomerizes (204)

and the FAT domain where T1989 resides is adjacent to the kinase domain. Active ATR molecules may autophosphorylate in *trans* due to proximity.

However, cells expressing the T1989A mutant exhibited a modest viability defect, suggesting T1989 phosphorylation is functional. The ATR FAT domain, is thought to interact with the FATC domain to stabilize the intervening kinase domain. The FAT domain of DNA-PK also undergoes a considerable conformational shift upon kinase activation (182). T1989 phosphorylation may serve to further stabilize the complex after activation and function in signal amplification. Under conditions of exogenous stress where many ATR kinase molecules are activated, signal amplification may not be as critical to maintain signaling. During normal unperturbed rounds of replication where fewer molecules of ATR are activated such a mechanism may become important.

*Research and Clinical Applications*

Since T1989 is a damage-regulated phosphorylation site that requires activation of ATR, antibodies to this phosphorylation site will be useful to directly monitor an active ATR kinase in cells. In addition to facilitating future research on ATR function, monitoring ATR T1989 phosphorylation may also prove to be a useful biomarker for cancer treatment or as a measurement of oncogene-induced replication stress. For instance, many current therapies cause DNA replication stress and several groups have developed ATR-selective inhibitors for potential use in the clinic (205, 206). Monitoring T1989 phosphorylation in tumors may prove to be a predictive marker for treatment response and could be used to assess inhibition of ATR signaling after treatment.

# CHAPTER IV

# ANALYSIS OF MUTATIONS THAT DISSOCIATE G2 AND ESSENTIAL S PHASE FUNCTIONS OF HUMAN ATR

## Introduction

In the previous chapter, I tested the hypothesis that phosphorylation regulates ATR activity using mass spectrometry to identify ATR T1989 as a DNA damage-regulated phosphorylation site. It remains unclear whether ATR T1989 is an autophosphorylation site. However ATR autophosphorylates *in vitro,* suggesting ATR S/TQ consensus residues may be autophosphorylation sites. In this chapter, I test whether these candidate autophosphorylation sites are required for ATR function.

ATR contains 16 conserved candidate autophosphorylation sites that match the S/TQ consensus. A 16A-ATR mutant protein, which contains all 16 sites mutated to alanine, maintains kinase and G2 checkpoint activities. However, it fails to rescue the essential function of ATR in maintaining cell viability and fails to promote replication recovery from a transient exposure to replication stress. Further analysis identified T1566A/T1578A/T1589A (3A-ATR) as critical mutations causing this separation of function activity. Secondary structure predictions indicate these residues occur in a region between ATR HEAT repeats 31R and 32R. This region aligns with regions of ATM and DNA-PK containing regulatory autophosphorylation sites. It is unclear if ATR also autophosphorylates in this region. Nevertheless, my analysis identifies an important regulatory region of ATR that is shared among the DNA damage response PIKK kinases. Furthermore, my data indicates that

the essential function of ATR is linked to its function in promoting proper replication in the context of replication stress and is independent of G2 checkpoint activity.

## Results

*Identification of an ATR separation of function mutant*

Human ATR contains 19 putative autophosphorylation consensus sites (S/TQ). Primary sequence alignment of ATR orthologs revealed conservation of 16 of these residues to mouse with several conserved to *X. laevis* and *S. cerevisiae* (Figure 22a). To examine their functional significance, I mutated the 16 conserved residues to alanine within a single cDNA, generating a 16A-ATR mutant.

I characterized the 16A-ATR mutant in the same genetic complementation assay used to examine ATR T1989 phosphorylation (Figure 17). This assay utilizes the parental cell line $ATR^{flox/-}$TR, which harbors a conditional *ATR* allele, a second *ATR* allele disrupted by a neomycin cassette, and a stably integrated construct expressing the tetracycline repressor (TR) (90). I then integrated either wild type (WT) or 16A-ATR constructs with a tetracycline response promoter, creating WT-$ATR^{flox/-}$TR and 16A-$ATR^{flox/-}$TR cell lines. ATR cDNAs also contain an N-terminal Flag-$HA_3$ epitope tag to differentiate exogenous and endogenous proteins. I screened stable integrants for equal protein levels and verified that percentages of cells expressing tagged ATR were similar among clones. I characterized at least two independent mutant clones in subsequent experiments to account for possible clonal differences.

I induced expression of integrated *ATR* alleles and infected cell lines with adenovirus expressing Cre recombinase (AdCre) to delete the $ATR^{flox}$ allele or GFP (AdGFP) as a control. 96 hours post infection, excision of $ATR^{flox}$ in parental $ATR^{flox/-}$TR cells caused a substantial reduction in ATR protein levels (Figure 22b lanes 1 vs. 6). The integrated WT-ATR or 16A-ATR cDNAs express at comparable levels (Figure 22b, lanes 8-10), which is similar to the amount expressed from the endogenous locus in the heterozygous $ATR^{+/-}$ cells lacking a flox allele.

To test the proficiency of 16A-ATR to prevent progression into mitosis after DNA damage, I performed a G2 checkpoint assay. After tetracycline induction and adenovirus infection, I treated uncomplemented parental, WT-, and 16A-$ATR^{flox/-}$TR cells with ionizing radiation (IR) and cultured cells in nocodazole to block cells in mitosis. I determined the mitotic index by quantification of phospho-Ser10 Histone H3 positive cells using flow cytometry. Following deletion of the $ATR^{flox}$ allele, 37% of uncomplemented, parental $ATR^{flox/-}$TR cells progressed into mitosis after IR treatment. However, only 13% of WT-ATR integrants and 15% and 13% of the two 16A-ATR integrants entered mitosis post-IR (Figure 22c). These results demonstrate that 16A-ATR is proficient in maintaining the G2 checkpoint.

Since ATR is essential for cellular viability in mammalian cells even in the absence of DNA damage, I examined the ability of 16A-ATR to support viability using a colony formation assay. I induced expression of integrated ATR constructs, infected cells with AdGFP or AdCre, and allowed single colonies to form over a period of 14 days. 32% of the parental $ATR^{flox/-}$TR cells formed colonies upon $ATR^{flox}$ deletion (Figure 22d) while expression of WT-ATR

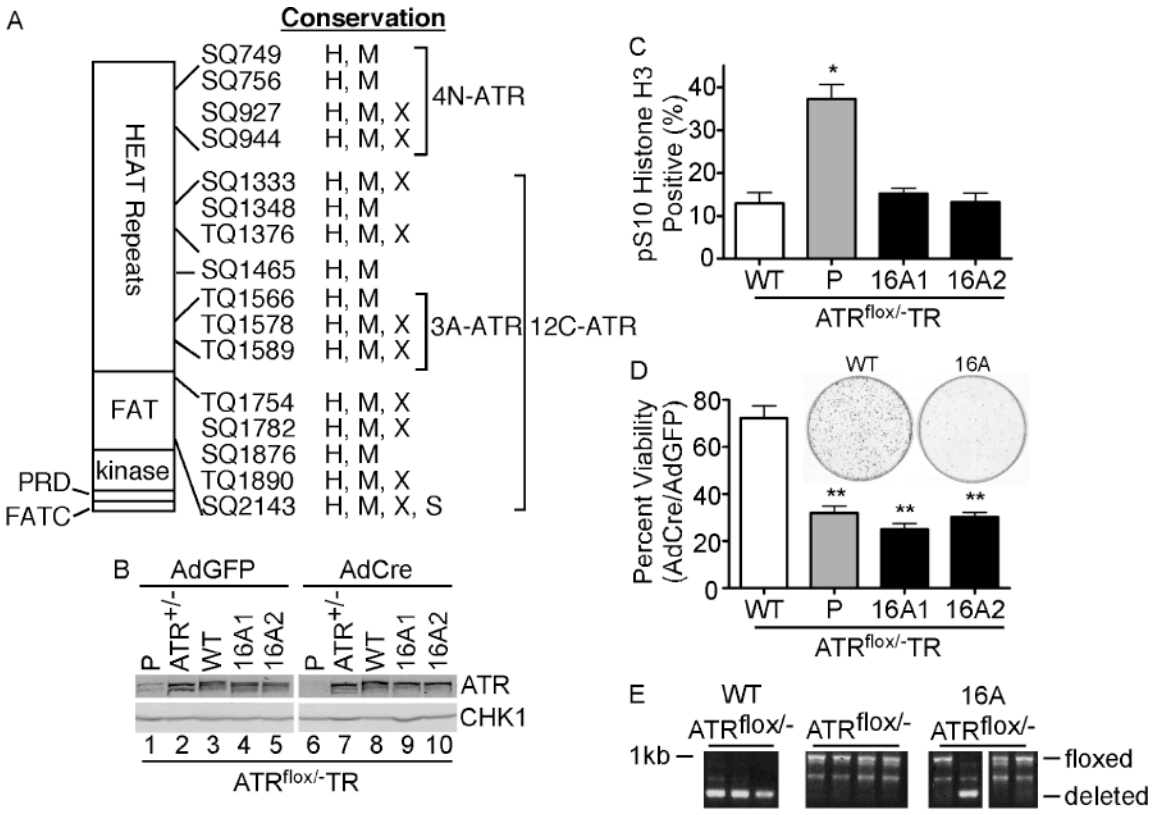


**Figure 22. Identification of an ATR separation of function mutant.** (A) Schematic depicting ATR domains, the 16 conserved S/TQ residues, and level of conservation (H=*H. sapiens*, M=*M. musculus*, X=*X. laevis*, and S=*S. cerevisiae*). Brackets denote residues mutated in ATR mutants. (B-E) Parental (P) ATR$^{flox/-}$TR cells integrated with tetracycline-inducible wild type (WT) and 16A-ATR were treated with tetracycline to express exogenous forms of ATR and infected with adenovirus expressing Cre recombinase (AdCre) or GFP (AdGFP) as a control. Two independent clones of 16A-ATR$^{flox/-}$TR cells are shown. (B) Cell lysates were separated by SDS-PAGE and blotted with ATR and CHK1 antibodies. ATR$^{+/-}$ is a heterozygous cell line lacking a flox allele. (C) Cells were irradiated with 8Gy ionizing radiation and incubated with nocodazole for 8 hours. Cells and media were collected, stained with propidium iodide (PI) and anti-phosphorylated-S10 Histone 3, and examined by flow cytometry to determine DNA content and percentage of mitotic cells. Shown are the results from three-independent experiments *$p<0.005$. (D) Equal numbers of AdCre and AdGFP infected cells were plated in triplicate for colony formation assays. 14 days later surviving colonies were stained with methylene blue and counted. (**$p<0.01$, $n\geq3$). Representative methylene blue stained colonies from AdCre infected WT and 16A-ATR$^{flox/-}$TR cells are also shown. (E) PCR was performed to monitor excision of the flox allele.

significantly improved viability with 72% of cells forming colonies. As previously reported, the surviving colonies of the parental $ATR^{flox/-}$TR cell line are due to incomplete Cre-excision of the flox allele (Figure 22e) (36). Unlike the WT-ATR cells, only 25% and 30% of cells in the two 16A-ATR cell lines formed colonies (Figure 22d).

Only 1 in 8 of the surviving 16A-ATR colonies from AdCre-infected cells actually successfully deleted the $ATR^{flox}$ allele (Figure 22e). Thus, most of the surviving colonies of 16A-ATR cells grew because they maintained expression of the endogenous wild-type ATR allele. In contrast, 5 of 5 colonies tested from the AdCre-infected WT-ATR cell line contained a deleted flox allele and only express the integrated WT-ATR cDNA. Thus, the 16A-ATR protein has a significantly diminished capacity to maintain cell viability after deletion of the endogenous *ATR* alleles. These data together with G2 checkpoint results indicate that 16A-ATR acts as a separation of function mutant.

*16A-ATR mutations result in replication stress response defects.*

The *mec1-100* allele of *S. cerevisiae* ATR is a separation of function mutant defective in S but not G2 checkpoint functions (207). Thus, I hypothesized that reduced viability but G2 checkpoint proficiency of 16A-ATR may be due to a separation of human ATR functions in S and G2 phases. To examine S phase functions, I investigated if 16A-ATR could support resumption of DNA synthesis following a transient exposure to replication stress. I treated WT- and 16A-$ATR^{del/-}$TR cells with hydroxyurea (HU) for 24 hours, removed the HU, and monitored DNA content. 16 hours after release from HU, WT-ATR cells proceeded through S phase and accumulated with 4N DNA content, since I

added nocodazole to the release media. However, a large portion of 16A-ATR cells did not complete replication upon release (Figure 23a), demonstrating 16A-ATR does not support the completion of DNA synthesis after a transient replication block.

In agreement with a replication stress response defect, 16A-ATR has a reduced ability to phosphorylate Chk1 in HU-treated cells (Figure 23b). Quantification of three independent experiments confirmed a 50% reduction that is reproducible and statistically significant (Figure 23c). This 16A-ATR signaling defect was not due to a difference in the number of cells in S phase, since BrdU incorporation indicated that 55% of WT-ATR$^{del/-}$TR and 53% of 16A-ATR$^{del/-}$TR cells were in S phase at the time of HU addition. These observations further indicate that the 16A mutation separates G2 and S phase functions of ATR.

16A-ATR defects could be due to changes in protein folding or stability. However, I did not detect a difference in protein stability or basal kinase activity (Figure 24a and b). 16A-ATR mutations also did not disrupt the ability of ATR to form higher order oligomers (Figure 24c) further suggesting it is properly folded. Finally, both WT and 16A-ATR localized to stalled replication forks (Figure 24d and e), which depends on an interaction with ATRIP. The 16A-ATR mutations actually reproducibly increased TopBP1-stimulated *in vitro* ATR kinase activity compared to WT-ATR (Figure 24f). However, this phenotype does not segregate with the minimal ATR mutations causing viability and replication stress response defects (see 3A-ATR below). These results indicate that the functional defects of the 16A-ATR protein in cells are not due to a defect in protein folding, stability, or interaction with protein partners.

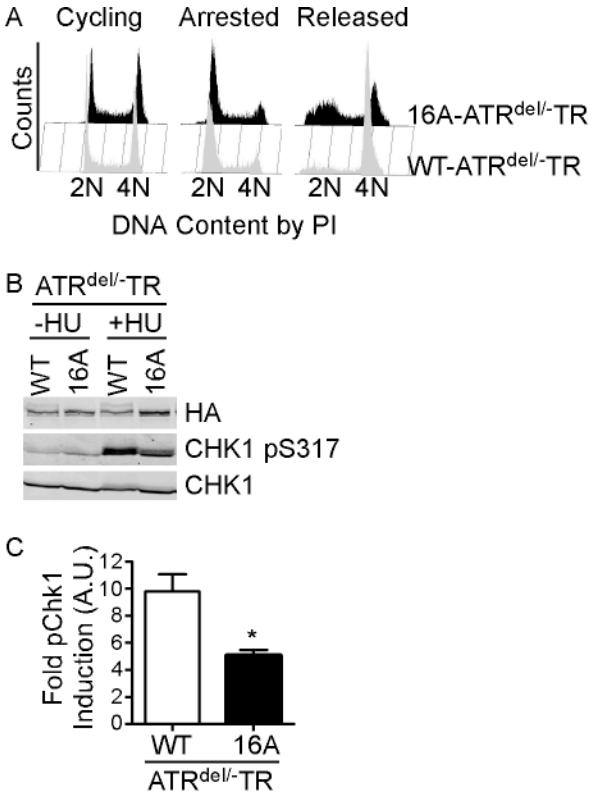


**Figure 23. 16A-ATR mutations result in replication stress response defects.** (A) WT-ATR$^{del/-}$TR and 16A-ATR$^{del/-}$TR cells expressing only Flag-HA3-tagged versions of ATR were exposed to 2mM HU for 24 hours. HU was removed and cells were released into nocodazole for 16 hours to allow completion of S-phase and arrest in mitosis. DNA content was determined by propidium iodide (PI) staining and flow cytometry. (B) WT and 16A-ATR$^{del/-}$TR cells were treated with 2mM HU for 6 hours. Cell lysates were separated by SDS-PAGE and immunoblotted with ATR, phosphorylated S317 CHK1, and CHK1 antibodies. (C) The fold induction of phosphorylated CHK1 (treated/untreated) following HU treatment was quantified in three independent experiments using an Odyssey instrument and infrared-conjugated secondary antibodies *p=0.02.

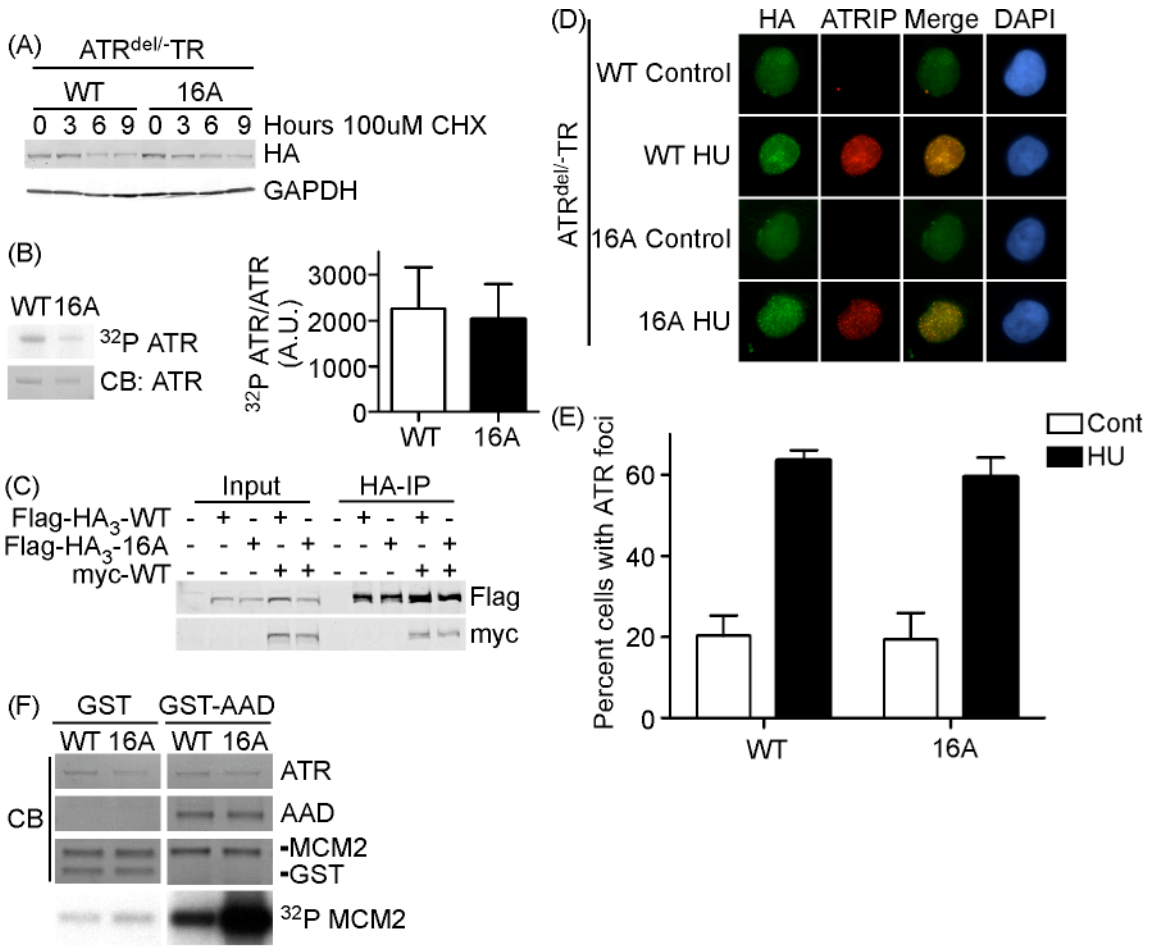


**Figure 24. 16A-ATR exhibits normal protein stability, basal kinase activity, and normal localization.** (A) WT and 16A-ATR$^{del/-}$TR cells expressing only Flag-HA3-ATR and Flag-HA3-16A-ATR were treated with cyclohexamide (CHX) for indicated time points. Cell lysates were separated by SDS-PAGE and immunoblotted with HA and GAPDH antibodies. (B) HEK293T cells were transiently co-transfected with the indicated ATR constructs. HA immunoprecipitates were separated by SDS-PAGE and immunoblotted with Flag and myc antibodies. (C) 293T cells were transiently co-transfected with Flag-HA3-WT or Flag-HA3-16A ATR and HA-ATRIP. ATR-ATRIP complexes were isolated by Flag immunoprecipitation and subjected to in vitro kinase reactions. $^{32}$P incorporation into ATR proteins was quantified on a phosphorimager and kinase input was determined by coomassie blue staining. Graph represents $^{32}$P incorporation normalized to ATR input for three independent experiments (D) Representative images of WT- and 16A-ATR$^{del/-}$TR cells treated with 10mM HU for 6 hours, Triton-X100 extracted, paraformaldehyde fixed, and immunostained with HA and ATRIP antibodies. Nuclei were visualized with DAPI. (E) Graph represents the percentage of nuclei with ATR foci in (D) (n=400). (F) WT and 16A-ATR complexed with ATRIP were isolated from transfected 293T cells and incubated with MCM2 substrate, γ-$^{32}$P-ATP, and GST or GST-TOPBP1-AAD. Kinase reactions were separated by SDS-PAGE and detected by phosphorimaging. The amount of ATR, GST, TOPBP1, and MCM2 was detected by Coomassie blue (CB).

*S944*

In the mass spectrometry analysis conducted in Chapter III, I identified one ATR phospho-peptide, SLHS(p)SQMTALPNTPCQNADVR, that potentially is phosphorylated at S944. However, there are several potential phospho-accepting residues in the peptide, and I did not obtain sufficient peptide fragmentation in subsequent mass spectrometry scans to unequivocally assign the identity of the modified residue. In addition to the mass spectrometry data, S944 is conserved in *H. sapiens, M. musculus, and X. laevis*, suggesting it may be functionally important. To test its functional significance, I generated WT-ATR$^{del/-}$TR and S944A-ATR$^{del/-}$TR cell lines that only express the integrated forms of ATR (Figure 25a) and examined DNA synthesis completion following a transient exposure to HU. Both WT and S944A cells completed DNA synthesis upon release from HU (Figure 25b), indicating that S944 is not required for S phase functions of ATR.

*S2143*

Of the sixteen conserved candidate ATR autophosphorylation sites, only S2143 is conserved in *H. sapiens, M. musculus, and X. laevis* and changed to a threonine in *S. cerevisiae*. Because this residue is highly conserved, I also examined its functional significance by assaying the ability of S2143A-ATR$^{del/-}$TR cells (Figure 26a) to complete DNA replication after a transient exposure to HU. S2143A expressing cells completed DNA synthesis after HU release similar to the WT-ATR expressing cell line (Figure 26b). Therefore S2143 is also dispensable for ATR function in S phase.

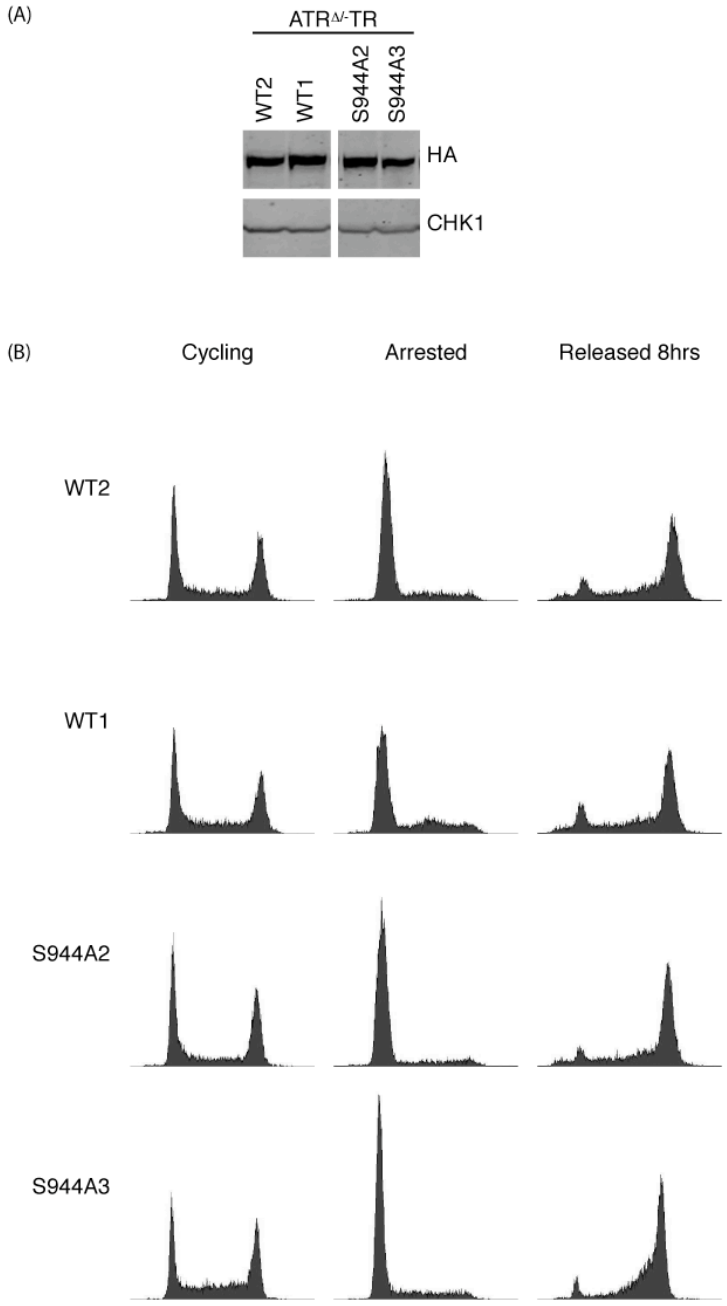


**Figure 25. S944 is dispensable for ATR function.** (A) Cell lysates from WT- and S944A-ATR$^{del/-}$TR cells were immunoblotted with the indicated antibodies. (B) Cells were exposed to 2mM HU for 24 hours. HU was removed and cells were released into nocodazole for 16 hours to allow completion of S-phase and arrest in mitosis. DNA content was determined by propidium iodide (PI) staining and flow cytometry.

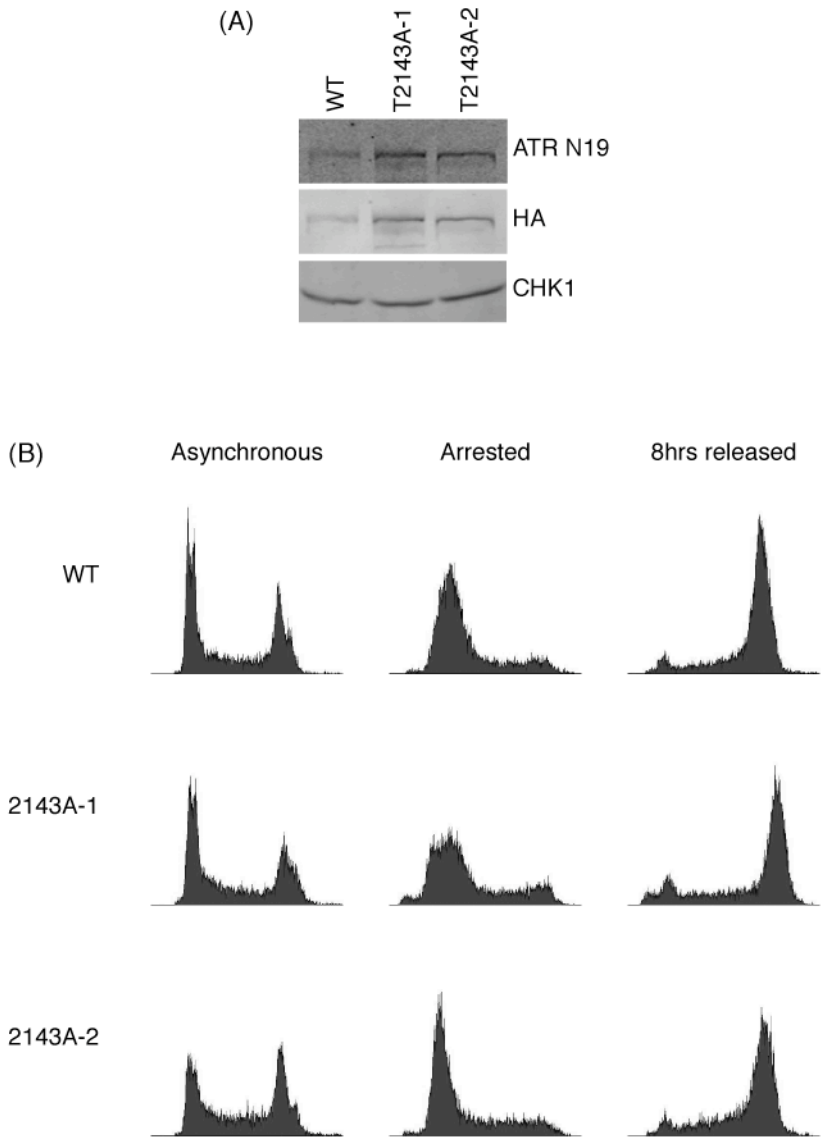


**Figure 26. S2143 is dispensable for ATR function.** (A) Cell lysates from WT- and S2143A-ATR$^{del/-}$TR cells were immunoblotted with the indicated antibodies. (B) Cells were exposed to 2mM HU for 24 hours. HU was removed and cells were released into nocodazole for 16 hours to allow completion of S-phase and arrest in mitosis. DNA content was determined by propidium iodide (PI) staining and flow cytometry.

*3A-ATR phenocopies 16A-ATR replication stress response defects*

To determine which of the 16 mutations within 16A-ATR cause the functional defects, I analyzed mutants containing a subset of the 16A mutations in the cellular complementation assay. First, I generated two mutants containing either the 4 N-terminal sites (Figure 22a; 4N-ATR) or the remaining 12 C-terminal sites mutated to alanine (Figure 22a; 12C-ATR) and integrated the mutant cDNAs into the $ATR^{flox/-}$TR cell line. I screened mutant cell lines as before and determined the protein levels to be at least equal to wild type expressing cells (Figure 27a). Colony formation assays revealed that two 4N-ATR expressing clones complemented the essential function of ATR similar to WT-ATR (61% and 51% viable 4N-ATR colonies compared to 64% WT). However, both 12C-ATR expressing clones exhibited significantly reduced viability (26% and 9%) in the colony formation assay (Figure 27b).

Further analysis identified a triple mutant, T1566A/T1578A/T1589A (3A-ATR), that phenocopies the reduced viability observed in the 16A-ATR mutant. Only 21% and 25% of cells from two independent 3A-$ATR^{flox/-}$TR cell lines formed colonies after excision of the flox allele compared to 80% of WT-$ATR^{flox/-}$TR cells despite similar protein expression (Figure 27c and d). Slight differences in colony formation by the parental $ATR^{flox/-}$TR cell line in Figure 27 is likely due to differences in adenovirus batch used to delete the floxed allele. However, within each group of experiments, the colony formation efficiencies were highly reproducible. PCR genotyping confirmed the reduced viability of the 3A-ATR clones after Cre-mediated excision of the $ATR^{flox}$ allele. 12 of 14 colonies from Cre-infected WT-ATR colonies contained a deleted flox allele compared to only 6 of 21 3A-ATR expressing clones.

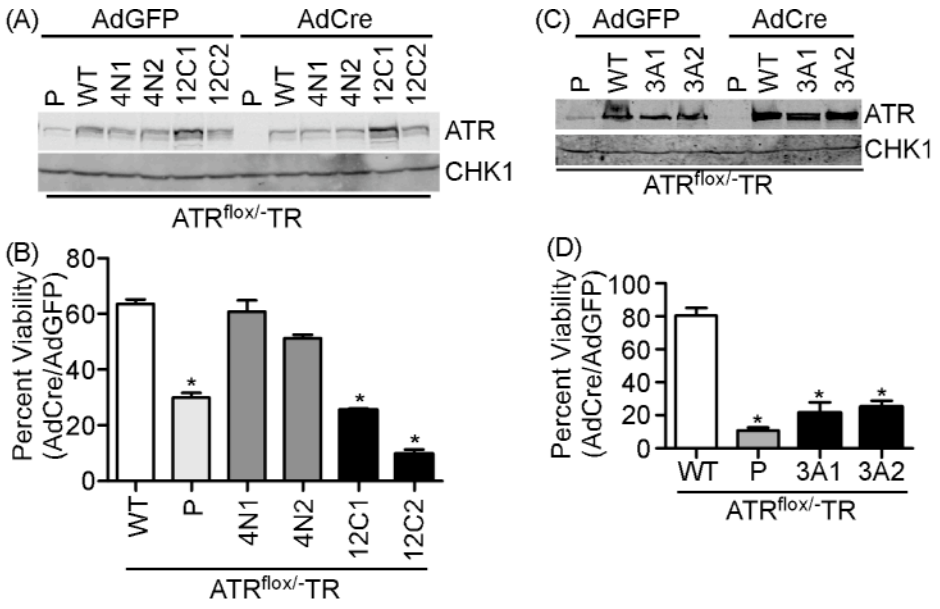


**Figure 27. 3A-ATR mutations perturb viability.** (A-B) Parental (P) ATR$^{flox/-}$TR, WT-ATR$^{flox/-}$TR, two clones of 4N-ATR$^{flox/-}$TR, and two clones of 12C-ATR$^{flox/-}$TR cells were induced with tetracycline and infected with AdCre to delete the flox allele or with AdGFP as a control. (A) Cell lysates were separated by SDS-PAGE and immunoblotted with ATR and CHK1 antibodies. (B) Equal numbers of AdCre and AdGFP infected cells were plated in triplicate for colony formation assays. 14 days later surviving colonies were stained with methylene blue and counted. Shown are the results from three independent experiments (*$p<0.01$, $n\geq3$). (C-D) Parental ATR$^{flox/-}$TR (P), WT-ATR$^{flox/-}$TR, and two clones of 3A-ATR$^{flox/-}$TR cells were tetracycline induced and infected with AdCre and AdGFP. (C) Cell lysates were analyzed by SDS-PAGE and immunoblotted for ATR and CHK1. (D) Colony formation analysis was conducted as in B (*$p<0.01$, $n\geq3$).

I next examined whether 3A-ATR also recapitulates 16A-ATR replication stress response defects. Three independent clones of 3A-ATR cells exhibited reduced Chk1 and SMC1 phosphorylation after HU treatment compared to WT (Figure 28a). BrdU incorporation assays showed that this difference in phosphorylation cannot be explained by differences in the percentage of S phase cells among clones at the time of the experiment (%BrdU positive: WT1 49%, WT3 52%, 3A1 49%, 3A2 44%, and 3A3 42%).

3A-ATR mutations also compromised completion of DNA synthesis following a transient replication block. Only 22%, 21%, and 22% of WT-ATR cells in three independent cell lines did not complete DNA synthesis 16 hours after HU removal while 36%, 49%, and 39% of the 3A-ATR cells failed to complete replication at the same time point (Figure 28b). In agreement with the 16A-ATR results, the G2 checkpoint also remained intact in the 3A-ATR mutant (Figure 28c). Together, these data confirm that the reduced viability observed in 3A-ATR cells correlates with a defect in S phase but not G2 checkpoint functions of ATR similar to the 16A-ATR phenotype. I also measured TopBP1-mediated activation of 3A-ATR and found it was similar to WT-ATR (Figure 28d). Therefore the increased *in vitro* ATR activation observed with the 16A-ATR mutations does not segregate with the viability and S phase defects.

ATR-dependent Chk1 phosphorylation requires the adaptor protein Claspin, which interacts with ATR. The requirement for Claspin in Chk1 phosphorylation is unique to Chk1. I examined whether 3A-ATR mutations disrupt the ATR-Claspin interaction by Flag-immunoprecipitating ATR from 293T cells transiently expressing Flag-WT, Flag-16A, and Flag-3A forms of ATR. Claspin co-immunoprecipitated with all three forms of Flag-ATR (Figure 29).

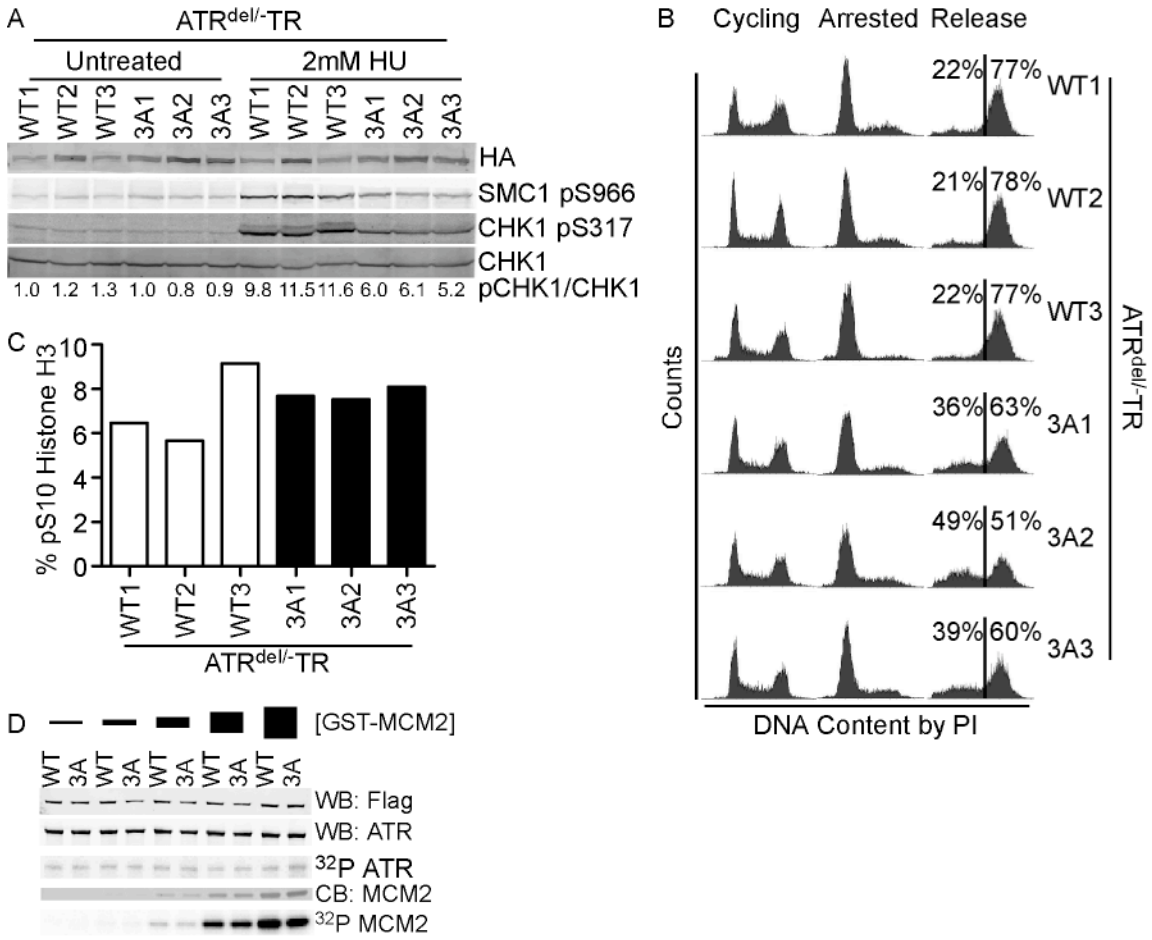


**Figure 28. 3A-ATR phenocopies 16A-ATR replication stress response defects.** (A-C) Three independent clones of WT-ATR$^{del/-}$TR and 3A-ATR$^{del/-}$TR cells expressing only Flag-HA$_3$-tagged versions of ATR were assessed for functional defects. (A) Cells were treated with 2mM HU for 6 hours, and cell lysates were separated by SDS-PAGE and immunoblotted with HA, phosphorylated S966 SMC, phosphorylated S317 CHK1, and CHK1 antibodies. Infrared-conjugated secondary antibodies and an Odyssey instrument were used to quantify signals. Numbers indicate pCHK1/CHK1 normalized to the WT1 control sample. (B) Cells were exposed to HU for 24 hours. HU was removed and cells were released into nocodazole for 16 hours to allow completion of S-phase and arrest in mitosis. DNA content was determined by propidium iodide (PI) staining and flow cytometry. Lines and percentages indicate <4N and 4N DNA content. (C) Cells were irradiated with 8 Gy ionizing radiation and incubated with nocodazole for 8 hours. Cells and media were collected and flow cytometry analysis using propidium iodide (PI) and anti-phosphorylated-S10 Histone 3 were used to determine DNA content and percentage of mitotic cells. (D) Flag-WT and Flag-3A-ATR complexed with HA-ATRIP were isolated from 293T cells transfected with Flag-ATR and HA-ATRIP constructs by HA-immunoprecipitation and incubated with γ-$^{32}$P-ATP, GST-AAD, and increasing concentrations of MCM2. Reactions were separated by SDS-PAGE and detected by phosphorimaging. Protein inputs were determined by immunoblotting or Coomassie blue staining.

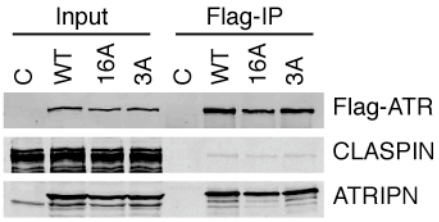


**Figure 29. 3A-ATR mutations do not disrupt ATR-Claspin interactions.** Flag-immunoprecipitates from 293T cells transiently expressing Flag-WT, 16A, or 3A-ATR were immunoblotted with the indicated antibodies. C denotes vector transfected cells.

This indicates that the reduction in Chk1 phosphorylation observed in 16A and 3A-ATR mutants is not due to a defect Claspin binding. This is in agreement with the reduction in SMC1 phosphorylation, which does not require Claspin, in 3A-ATR expressing cells.

*A conserved extended inter-HEAT repeat loop is important for ATR function*

Due to the functional defects observed with 3A-ATR, I was curious about the domain architecture surrounding the mutated residues. The PIKK kinases consist of a large number of helical HEAT repeats. A HEAT repeat consists of two anti-parallel helices. These HEAT repeats are connected by inter-HEAT repeat loops to form the large array of repeats found in PIKKs. While the primary sequence of ATR and ATM HEAT repeats differ, Perry and Kleckner aligned the two proteins by the secondary structure of these repeats. According to the HEAT repeat alignments designated by Perry and Kleckner (165), 3A-ATR residues occur in the inter-HEAT repeat loop between ATR HEAT repeats 31R and 32R (amino acid (aa) 1557-1628) and is just N-terminal to the FAT domain (aa1640) (Figure 30). Notably while inter-HEAT repeat loops are typically short 5-20aa linkers, the loop between 31R and 32R is 71aa long and predicted to be largely unstructured except for a short predicted helix.

ATR HEAT repeats 31R and 32R align with ATM HEAT repeats 34M and 35M (Figure 30)(165). Similar to ATR, the inter-HEAT repeat loop between 34M and 35M (aa1875-1927) is longer than a typical inter-HEAT repeat loop (52aa), predicted to be unstructured except for a single helix, and is just N-terminal of the ATM FAT domain (aa1960). Importantly, this region contains the regulatory ATM autophosphorylation site S1893 whose mutation to alanine results in

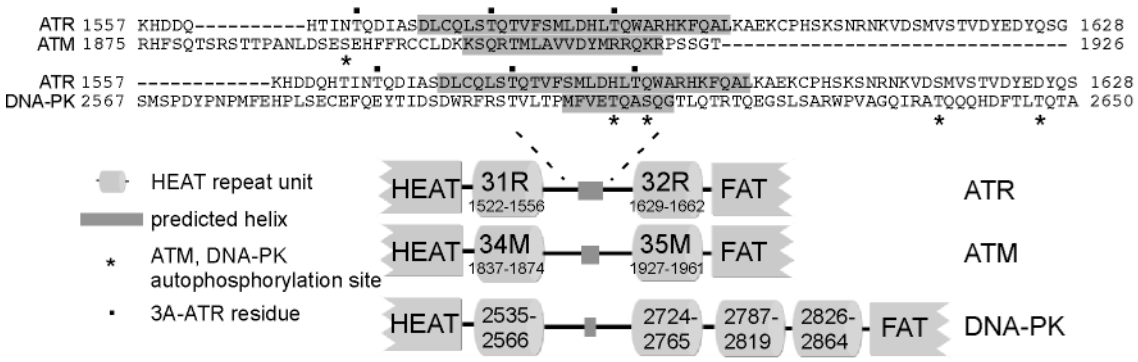


**Figure 30. A conserved extended inter-HEAT repeat loop is important for ATR function.** Alignment of ATR and ATM by HEAT repeats as described by Perry and Kleckner (165). Secondary predictions generated by Jpred were used to align DNA-PK with ATR and ATM.

radiosensitivity and loss of checkpoint activity (181). Secondary structure predictions of DNA-PK also reveal the presence of an extensive 158aa inter-HEAT repeat loop (aa2566-2723) N-terminal to the DNA-PK FAT domain that contains the regulatory ABCDE (T2609/S2612/T2638/T2647) autophosphorylation cluster (Figure 30) (184, 198). These similarities suggest that the region between ATR 31R and 32R is a conserved regulatory region among the DNA damage PIKKs, and several of these sites may be targeted for autophosphorylation.

*Phospho-peptide analysis of ATR mutants*

I analyzed purified ATR from undamaged and HU-treated cells for phosphorylation by mass spectrometry but was unable to detect a modified peptide containing T1566, T1578, or T1589 despite multiple attempts. This mass spectrometry analysis was limited by our ability to detect peptides spanning this region. I next assayed autophosphorylation of WT and 3A-ATR *in vitro.* I Flag-immunoprecipitated ATR from cells expressing Flag-WT or Flag-3A-ATR and allowed ATR to autophosphorylate. $^{32}$P incorporation was comparable between WT and 3A-ATR (Figure 31a), suggesting 3A-ATR mutations do not diminish ATR autophosphorylation under these *in vitro* conditions.

I reasoned that analysis of $^{32}$P incorporation into total ATR proteins may not be sensitive enough to detect loss of one or a few phospho-residues if there are many other autophosphorylation sites within ATR. I also postulated that phosphorylation of 3A-ATR residues may require TopBP1-mediated ATR activation. To address both of these considerations, I examined ATR phospho-peptides under conditions that included TopBP1-mediated ATR activation.

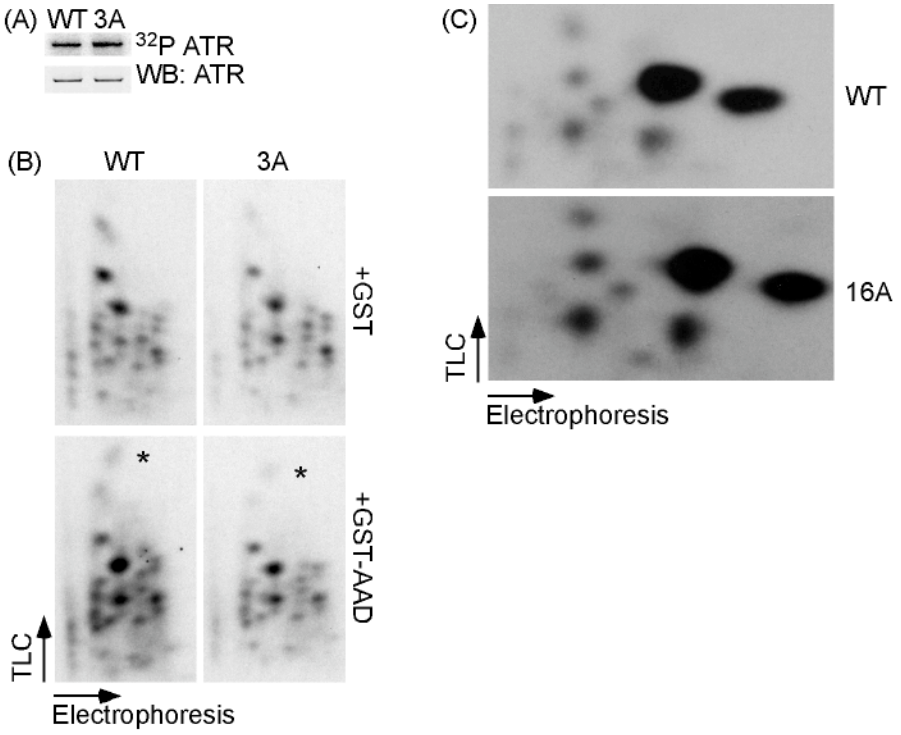


**Figure 31. Phospho-peptide analysis of ATR mutants.** (A) WT and 3A-ATR were Flag-immunoprecipitated from 293T cells transiently expressing Flag-ATR and HA-ATRIP constructs and incubated with γ-32P-ATP. Kinase reactions were separated by SDS-PAGE and detected by phosphorimaging. Protein inputs were determined by immunoblotting for ATR. (B) Flag-WT and Flag-3A-ATR complexed with HA-ATRIP were isolated from 293T cells transfected with Flag-ATR and HA-ATRIP constructs by HA-immunoprecipitation and incubated with γ-32P-ATP and GST or GST-AAD. Reactions were separated by SDS-PAGE and transferred to PVDF membranes. ATR bands incorporating 32P were excised from membranes, trypsin digested, and subjected to two-dimensional thin layer chromatography analysis. A new phospho-peptide visible after GST-AAD activation is marked with an asterisk. (C) 293T cells transiently expressing Flag-HA3-WT or Flag-HA3-16A-ATR were metabolically labeled with $^{32}$P-orthophosphate and simultaneously treated with 2mM HU for 3 hours. HA-ATR immunoprecipitations were prepared and analyzed for phospho-peptide mapping as in B.

I purified ATR-ATRIP complexes from cells expressing Flag-ATR and HA-ATRIP constructs and allowed ATR to autophosphorylate in the presence of recombinant GST or GST-TopBP1 ATR activating domain (GST-AAD) *in vitro.* I separated kinase reactions by SDS-PAGE, excised the ATR bands incorporating $^{32}P$, generated phospho-peptides by trypsin digestion, and compared phospho-peptides of WT and 3A-ATR using two-dimensional thin layer chromatography (2D-TLC) phospho-peptide mapping.

Comparison of WT and 3A-ATR phospho-peptides from GST maps did not reveal loss of a detectable phospho-peptide (Figure 31b compare top panels), although there is small variability in intensity of some phospho-peptides. Upon GST-AAD addition, one relatively low abundance phospho-peptide appeared (Figure 31b, asterisk in bottom panels). GST-AAD addition to 3A-ATR also induced this phospho-peptide. Therefore under these conditions, 3A-ATR mutations fail to eliminate a discernible phospho-peptide.

I also examined *in vivo* ATR phospho-peptides obtained from HU-treated $^{32}P$ metabolically labeled cells transiently overexpressing Flag-$HA_3$-WT or Flag-$HA_3$-16A-ATR. I did not observe loss of an *in vivo* phospho-peptide with 16A-ATR mutations (Figure 31c). Of note, the *in vivo* and *in vitro* WT-ATR phospho-peptide maps are dissimilar (compare maps in Figure 31b and c). The *in vivo* maps will include phosphorylation sites catalyzed by other kinases, which likely explains some of the difference. However, these results also indicate that *in vitro* and *in vivo* phosphorylation may be different.

*T1589 is important for ATR function*

While I could not determine the phosphorylation status of T1566, T1578, and T1589, my data suggests they are important for ATR function. I next sought to determine if any of these sites alone were sufficient to disrupt ATR function. I created T1566A-ATR$^{flox/-}$TR, T1578A-ATR$^{flox/-}$TR and T1589A-ATR$^{flox/-}$TR cell lines to examine the functional significance of each residue in the 3A-ATR mutant. Upon deletion of the floxed allele, WT-ATR and two T1578A-ATR expressing cell lines formed similar numbers of colonies (Figure 32a and b). One T1566A-ATR expressing cell line supported colony formation after deletion of *ATR$^{flox}$*; however the second cell line did not (Figure 32b). Therefore, it is inconclusive whether T1566 impacts viability.

To confirm viability results, I also analyzed DNA replication following HU exposure in WT-ATR$^{del/-}$TR, T1578A-ATR$^{del/-}$TR, and T1566A-ATR$^{del/-}$TR cell lines. After removal of HU, a similar percent of WT, T1578A, and T1566A expressing cells persisted with less than 4N DNA content (Figure 32c). These results support that mutation of T1578 alone cannot recapitulate replication stress response and viability defects observed in the 3A-ATR mutant. Also the lack of a replication stress response defect in T1566A-ATR$^{del/-}$TR cell lines suggest that the viability defect observed in one cell line may be clonal and that mutation of T1566 alone also is not sufficient to recapitulate 3A-ATR phenotypes.

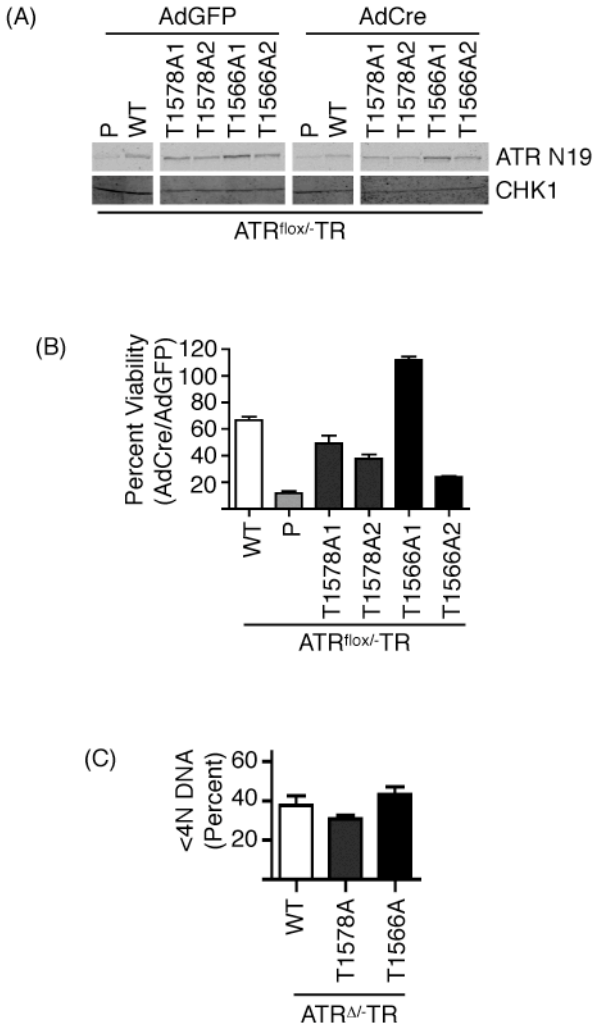


**Figure 32. Mutation of T1566 and T1578 is not sufficient to disrupt ATR function.** (A-B) Parental (P) ATR$^{flox/-}$TR, WT-ATR$^{flox/-}$TR, two clones of T1566A-ATR$^{flox/-}$TR, and two clones of T1578A-ATR$^{flox/-}$TR cells were induced with tetracycline and infected with AdCre to delete the flox allele or with AdGFP as a control. (A) Cell lysates were separated by SDS-PAGE and immunoblotted with ATR and CHK1 antibodies. (B) Equal numbers of AdCre and AdGFP infected cells were plated in triplicate for colony formation assays. 14 days later surviving colonies were stained with methylene blue and counted. (C) WT-, T1566A-, and T1578A-ATR$^{del/-}$TR cells were exposed to HU for 24 hours. HU was removed and cells were released into nocodazole for 16 hours to allow completion of S-phase and arrest in mitosis. DNA content was determined by propidium iodide (PI) staining and flow cytometry. The percent of cells with incomplete DNA replication (<4N content) are displayed in graphical form. Graphs represent the combined data for two independent clones for each genotype (n=4).

While the point mutants T1566A and T1578A were not sufficient to cause viability and replication stress response defects, mutation of T1589 to alanine resulted in viability defects (Figure 33 a and b). In addition, three independent T1589A-ATR$^{del/-}$TR cells exhibited replication stress response defects (Figure 33c). These data indicate that mutation of T1589 alone is sufficient to cause viability and replication stress response defects. A T1589E mutant also could not rescue viability (not shown). I examined ATR mutants for T1989 phosphorylation after HU treatment and did not detect a difference (Figure 34).

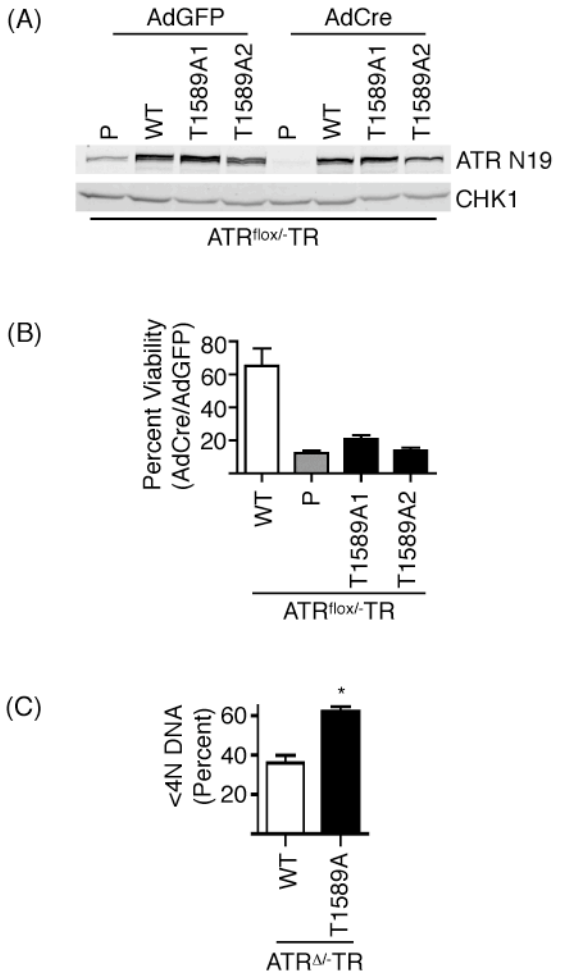


**Figure 33. Mutation of T1589 is sufficient to disrupt ATR function.** (A-B) Parental (P) ATR$^{flox/-}$TR, WT-ATR$^{flox/-}$TR, and two clones of T1589A-ATR$^{flox/-}$TR were induced with tetracycline and infected with AdCre to delete the flox allele or with AdGFP as a control. (A) Cell lysates were separated by SDS-PAGE and immunoblotted with ATR and CHK1 antibodies. (B) Equal numbers of AdCre and AdGFP infected cells were plated in triplicate for colony formation assays. 14 days later surviving colonies were stained with methylene blue and counted. (C) WT- and T1589A-ATR$^{del/-}$TR cells were exposed to HU for 24 hours. HU was removed and cells were released into nocodazole for 16 hours to allow completion of S-phase and arrest in mitosis. DNA content was determined by propidium iodide (PI) staining and flow cytometry. The percent of cells with incomplete DNA replication (<4N content) are displayed in graphical form. Graphs represent the combined data for three independent clones for each genotype (n=8, *p<0.0001).

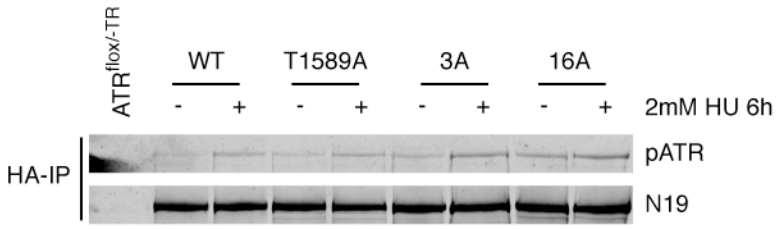


**Figure 34. T1989 phosphorylation is intact in 3A-ATR.** HA-immunoprecipitates from ATR$^{del/-}$TR cells expressing the indicated forms of HA-ATR were isolated from cells untreated and treated with 2mM HU for 6 hours. The ATR$^{flox/-}$TR cell line was used as a negative control. Immunoprecipitates were analyzed by western blot with the indicated antibodies.

## Discussion

My data demonstrate that the S and G2 phase functions of ATR can be separated by mutation of three candidate ATR autophosphorylation sites, T1566/T1578/T1589, within an S/TQ cluster. Based on HEAT repeat alignments, the mutated residues occur in a region of ATR that aligns to regions of ATM and DNA-PK containing functional autophosphorylation sites, although I have been unable to demonstrate ATR autophosphorylates any of these residues. ATR is essential for viability, promotes recovery from replication stress, and activates the G2 DNA damage checkpoint. Mutation of 3A-ATR residues perturbs viability and replication stress responses but not the G2 checkpoint. This is the first identification and characterization of a separation of function mutant in human ATR that dissociates S and G2 phase activities. The correlation between cell viability and S phase defects suggests that the essential function of ATR is to promote completion of DNA replication.

### *ATR phosphorylation*

Incomplete peptide coverage of ATR hindered detection of phosphorylation by mass spectrometry. I also did not detect loss of phosphorylation in phospho-peptide maps. These maps were generated using transiently overexpressed ATR, which may not be regulated the same as the endogenous protein. Indeed, Sancar and colleagues reported that they could only reconstitute ATR signaling *in vitro* by purifying endogenous, not overexpressed ATR complexes (208). I attempted to analyze phospho-peptides of endogenous ATR but was unable to obtain sufficient quantities of purified labeled protein. My *in vivo* phospho-peptide maps do suggest that there are

multiple regulatory phosphorylation sites on ATR. Identification of these phosphorylation sites will be necessary to understand the function of ATR phosphorylation.

The *in vitro* kinase activity of 3A-ATR is indistinguishable from WT-ATR. However, 3A-ATR does not phosphorylate Chk1 or SMC1 as well as the wild-type protein in cells. This observation is similar to the S1981A-ATM autophosphorylation mutant, which has *in vivo* but not *in vitro* substrate phosphorylation defects (162). Likewise, DNA-PK autophosphorylation mutants also do not show *in vitro* phosphorylation defects (202).

Mutation of a single site, T1589, is sufficient to cause viability defects. The inability of T1589E-ATR to rescue viability defects may indicate that the threonine residue and not phosphorylation is critical at this position. This has been implicated to be true for several putative phosphorylation sites in human Claspin (209). However, a glutamic acid may not effectively mimic phosphorylation, or constitutive phosphorylation may be detrimental to protein function. Phospho-mimicking mutations of DNA-PK ABCDE autophosphorylation sites in the analogous 3A-ATR region only partially rescue function (202). Phospho-specific antibodies generated against a phospho-peptide did not react with ATR in a T1589 dependent manner. Thus, it remains to be determined whether T1589 is an ATR phosphorylation site.

*Separation of Essential S phase functions of ATR from G2 checkpoint activity*

In *S. cerevisiae*, $MEC1^{ATR}$ deletion results in inviability in the absence of exogenous DNA damage (210). Deletion of *SML1*, which suppresses nucleotide production via inhibiting ribonucleotide reductase1 subunit (Rnr1), rescues

*MEC1* deletion (211) (212). Overexpression of Rnr1 also suppresses Mec1 deficiency (158), suggesting the essential function of Mec1 is to regulate nucleotide levels. However, *SML1* deletion does not rescue DNA damage sensitivity caused by *MEC1* deletion (212).

*ATR* deletion in mammalian cells also results in embryonic lethality. While nucleotide production is cell cycle regulated in human cells as well, DNA damage does not cause an increase in nucleotide levels (213). There is no evidence that ATR regulates nucleotide production in human cells or that ATR-deficiency can be rescued by increasing nucleotide levels. Thus, the essential function of ATR in human cells has been unclear. Nucleotide production in yeast occurs de novo while a nucleotide salvage pathway also exists in mammalian cells (214). This redundancy may explain why a clear link between nucleotide regulation and ATR function has not been made. My data suggest that the essential function of human ATR is to promote completion of DNA synthesis after a challenge to replication. The exact functions of ATR in S phase that are disrupted by 3A-ATR mutations remain unclear.

3A-ATR mutations cause defects in viability but only a 50% reduction in signaling to Chk1 and SMC1. A 50% reduction in phosphorylation may be sufficient to cause viability defects especially considering other ATR substrates are likely to be affected as well. Gene dosage is known to be important for ATR function. ATR is a haploinsufficient tumor suppressor in certain genetic backgrounds (215, 216), and reducing ATR protein levels can sensitize tumor cell lines to chemotherapies (217). Additionally, a hypomorphic allele of *ATR* found in Seckel Syndrome patients results in diminished ATR protein levels due to aberrant splicing (53, 54).

Why might low levels of ATR signaling be insufficient for cell viability and the replication stress response but sufficient for the G2 checkpoint? Redundancy in signaling is a likely explanation. ATM, DNA-PK, and ATR signal in response to DNA double strand breaks (DSB) or resected DSBs in the case of ATR. Reducing the contribution of ATR in checkpoint signaling following DSB generation may not cause G2 checkpoint defects due to this overlap in kinase response. A second layer of redundancy also occurs with the ATR and ATM effector kinases, Chk1 and Chk2 respectively, as both kinases phosphorylate overlapping substrates in the G2 checkpoint.

The *mec1-100* allele of the budding yeast *ATR* ortholog *MEC1* dissociates S and G2 phase functions, suggesting ATR signaling in different cell cycle phases may have distinct requirements (207). This allele contains the point mutations F1179S and N1700S, which correspond to L1405 and A1934 respectively in human ATR (207). Neither amino acid is close to 3A-ATR residues in primary sequence, though I do not know their relative proximity in three-dimensional space. Work by the Burgers group supports that there are distinct protein activators for Mec1 in G1, S, and G2 phases (103). Dpb11 the yeast homolog of TopBP1 activates $Mec1^{ATR}$ in G2 while the Rad9 homolog Ddc1 functions in both G1 and G2 phases (103, 112, 113). A double *ddc1Δdpb11-1* mutant does not fully abolish S phase activation of Mec1, suggesting there is an undefined S phase activator of Mec1. The 3A-ATR mutant is stimulated by TopBP1 and retains G2 but not S phase functions. Therefore it is possible that these mutations specifically disrupt regulation of ATR by an undefined protein activator in S phase.

*A potential novel ATR regulatory region*

There is a dearth of structural information on ATR. Structure function studies on ATR have also been difficult, as the ATR protein mislocalizes and is unstable when truncations or deletions are made. This has made assigning functions to domains of the ATR protein difficult. 3A-ATR mutational analysis may have serendipitously uncovered a novel regulatory region in ATR that appears to also exist in other DNA damage response PIKKs.

Cryo-EM and X-ray crystal structures of DNA-PK reveal a "crown" structure that consists of the FAT, kinase, and FATC domains (182, 218-220). The crown structure sits atop two "arms" consisting of the N-terminal HEAT repeats. Juxtaposed between the crown and arm structures are irregular regions in the DNA-PK structure predicted to be flexible hinges. Autophosphorylation produces a conformational shift in the DNA-PK structure possibly due to a shift in this flexible region. Notably, the regulatory ABCDE DNA-PK autophosphorylation (T2609/S2612/T2638/T2647) cluster occurs just before the DNA-PK FAT domain (begins at aa2881) and may reside in this predicted flexible region.

Indeed, by secondary structure prediction, the ABCDE cluster occurs between HEAT repeats in a 158aa inter-HEAT repeat loop (aa2566-2723) predicted to be unstructured except for a single short helix. Examining HEAT repeat alignments by Perry and Kleckner (165), an analogous loop between HEAT repeat units occurs just before the ATR and ATM FAT domains. ATM is autophosphorylated in the linker at S1893, and 3A-ATR residues occur in the region as well. Furthermore, alignment of ATR and DNA-PK by secondary structure places ATR T1589 within 1-2 amino acids of DNA-PK

autophosphorylation sites T2609 and S2612. These similarities among ATR, ATM, and DNA-PK suggest that the uncommonly long inter-HEAT repeat loops may be a shared regulatory region involved in controlling PIKK activity.

# CHAPTER V

# FURTHER CHARACTERIZATION OF 16A-ATR MUTATIONS

## Introduction

It remains unclear if 3A-ATR residues are phospho-residues. Secondary structure alignments suggest that the region containing these residues is regulatory in the related DNA damage kinases ATM and DNA-PK. The 3A-ATR region is also present in ATR orthologues. In this chapter, I briefly explore whether this region is also functional in *S. cerevisiae* $Mec1^{ATR}$.

16A-ATR mutations produce an interesting hyper-activation phenotype that does not segregate with 3A-ATR S phase defects. Here I also define 6 residues within 16A-ATR that cause to this phenotype. These residues are distinct from 3A-ATR residues. I also present preliminary evidence that hyper-activation may be due to increased TopBP1 binding.

## Results

*Analysis of the 3A-ATR regulatory region in S. cerevisiae*

While T1566, T1578, and T1589 are not conserved in *S. cerevisiae*, the extended inter-HEAT repeat loop is present in *S. cerevisiae* and other ATR orthologues. Alignment of ATR orthologues by HEAT repeat units show that several residues within this region are highly conserved (Figure 35). To determine if the functional importance of this region is conserved, I created three mutants, FRVF1349AAAA, E1354R, and W1359R, in the *S. cerevisiae* ATR

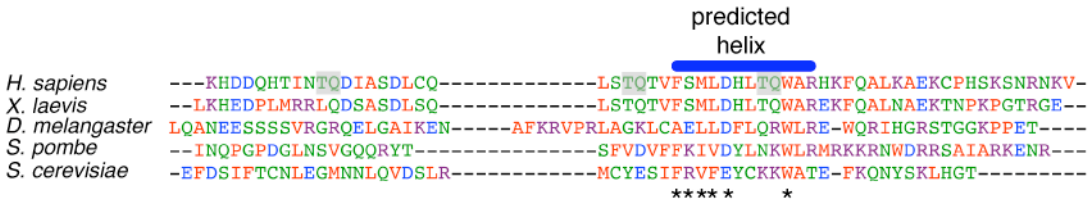


**Figure 35. Clustal alignment of 3A-ATR inter-HEAT repeat region of ATR orthologues.** Shaded residues indicate 3A-ATR residues. Asterisks denote residues mutated. Amino acid properties are as follows: red – small, hydrophobic, aromatic except Y, blue – acidic, purple – basic except H, and green – hydroxyl, sufhydryl, amine, and G.

orthologue Mec1. Because 3A-ATR exhibited replication stress response defects, I assayed the ability of these mutants to complement HU sensitivity in a *mec1Δsml1Δ* background. Strains harboring an emptor vector exhibit HU sensitivity (Figure 36a). WT-Mec1 rescues the HU sensitivity as does both the W1359R and E1354R mutants (Figure 36a). In contrast, the FRVF1349AAAA mutant strain exhibits HU sensitivity comparable to vector only (Figure 36a). In agreement with a defect in responding to replication stress, the FRVF1349AAAA mutant did not promote $Rad53^{Chk1}$ phosphorylation after HU treatment (Figure 36b). However, Mec1 protein expression levels of the FRVF1349AAAA mutant were reduced compared to WT-Mec1 in several independent strains tested (Figure 36c). Therefore, the inability to complement HU sensitivity may be due to lower levels of protein or improper protein folding. When I expressed the mutant from a high copy 2μ plasmid, it was still unable to rescue HU sensitivity (Figure 36d). This implies that protein levels may not be the cause of the defect; however, this experiment does not rule out the possibility of improper folding.

*Hyper-stimulation of ATR does not segregate with viability and S phase defects*

16A-ATR exhibits increased TopBP1-mediated activation *in vitro*. I also observed this hyper-stimulation in the 12C-ATR mutant (Figure 37a) but not with the 3A-ATR mutant. Instead a 6A-ATR mutant (S1333A/S1348A/T1376/S1782/T1890/S2143) with distinct mutations from 3A-ATR is sufficient to augment TopBP1-mediated stimulation of ATR (Figure 37b).

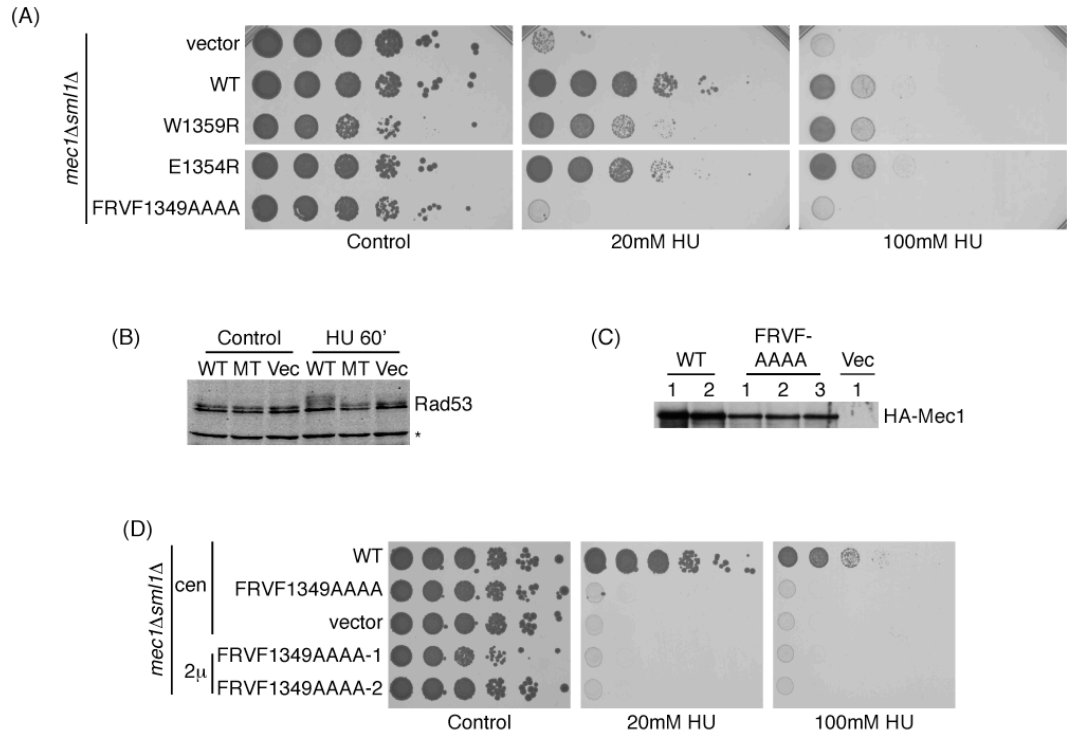


**Figure 36. An FRVF1349AAAA-Mec1 mutant cannot rescue *mec1*Δ*sml1*Δ replication stress sensitivity.** (A-B) The ***mec1*Δ*sml1*Δ** strain was transformed with empty, WT-Mec1, W1359R-Mec1, E1354R-Mec1, and FRVF1349AAAA vectors. (A) Strains were spotted onto plates containing hydroxyurea and allowed to grow for 3 days. (B) Strains were arrested in alpha-factor and then released into control or media containing 100mM HU for 60 minutes. Yeast lysates were immunoblotted with a Rad53$^{Chk1}$ antibody. MT denotes the FRVF1349AAAA mutant. (C) HA-immunoprecipitates from multiple clones of WT-HA-Mec1 and FRVF1349AAAA-HA-Mec1 transformed ***mec1*Δ*sml1*Δ** strains were immunoblotted with anti-HA antibodies. (D) ***mec1*Δ*sml1*Δ** strains transformed with WT-Mec1 and FRVF1349AAAA-Mec1 expressed from a low copy (CEN) or a high copy 2m plasmid were spotted onto plates containing hydroxyurea and allowed to grow for 3 days.

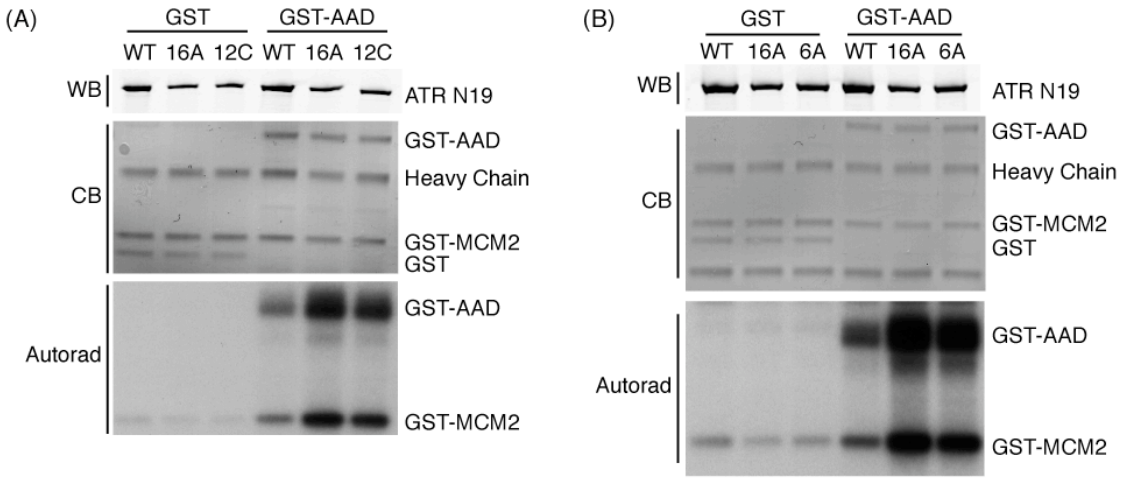


**Figure 37. 6A-ATR mutations increase TopBP1-mediated stimulation of ATR.** (A-B) Flag-epitope tagged WT, 16A, 12C, and 6A-ATR complexed with HA-ATRIP were isolated from 293T cells transfected with Flag-ATR and HA-ATRIP constructs by HA-immunoprecipitation and incubated with γ-$^{32}$P-ATP, GST-MCM2, and GST or GST-AAD. Reactions were separated by SDS-PAGE and exposed to film to detect $^{32}$P. Protein levels were detected by Coomassie blue staining (CB) and western blot (WB).

Because ATR activation requires ATR binding to the AAD of TopBP1, I next examined whether hyper-stimulation is due to increased TopBP1 binding. GST-TopBP1-AAD interacted with HA-WT-ATR from stable WT-ATR$^{del/-}$TR and transiently expressed constructs in 293T cells (Figure 38). Strikingly, 16A-ATR interaction with GST-TopBP1-AAD was increased (Figure 38). This suggests that 16A-ATR hyper-stimulation may be due to increased TopBP1 interaction.

It is not clear what functional consequences hyper-stimulation may have in cells. 16A-ATR$^{del/-}$TR cell lines exhibit increased basal Chk1 phosphorylation (Figure 23b), but 3A-ATR cells do not (Figure 28a). Preliminary results in 6A-ATR$^{del/-}$TR cell lines also show increased Chk1 phosphorylation in the absence of damage (Figure 39a). In contrast phosphorylated RPA is not increased in 6A cell lines, suggesting that the increase in Chk1 phosphorylation is not due to DNA damage. While more experiments are required, the increase in Chk1 phosphorylation also does not correlate well with ATR protein levels (Figure 39b). This supports that hyper-activation also occurs in cells. Whether this increase in Chk1 phosphorylation amounts to other functional consequences remains unclear. Additional 6A-ATR$^{flox/-}$TR cell lines with similar expression to WT cells are required for this analysis.

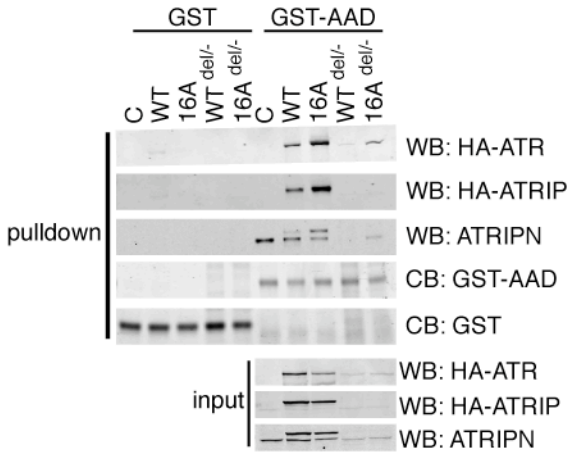


**Figure 38. 16A-ATR exhibits increased binding to the AAD of TopBP1.** Lysates from 293T transiently expressing HA-WT or HA-16A-ATR or lysates from WT-ATR$^{del/-}$TR or 16A-ATR$^{del/-}$TR cells were incubated with GST or GST-AAD bound to glutathione-beads. Beads were washed and bound proteins were analyzed by SDS-PAGE. Pulldowns were immunoblotted with the indicated antibodies and a duplicate gel was cooomassie blue stained to visual GST inputs.

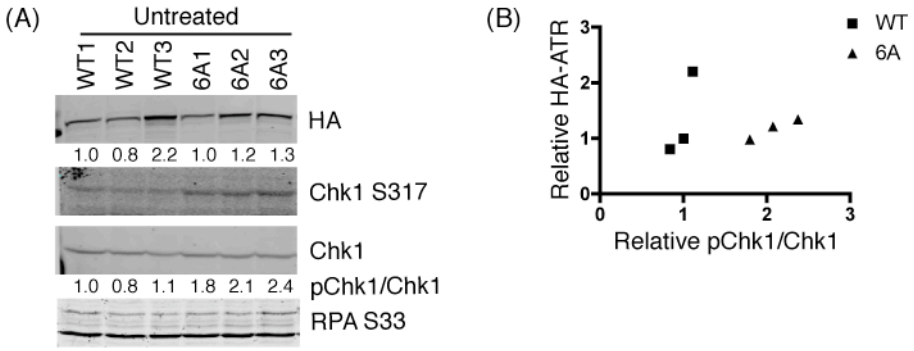


**Figure 39. Increased Chk1 phosphorylation in 6A-ATR cells.** (A) Lysates from undamaged $ATR^{del/-}TR$ cells expressing only HA-WT-ATR or HA-6A-ATR were immunoblotted for HA, phosphorylated Chk1 S317, total Chk1, and phosphorylated RPA S33. Blots were quantified using infrared conjugated Licor secondary antibodies and an Odyssey system. (B) Relative phosphorylated Chk1/Chk1 was graphed versus HA-ATR levels.

## Discussion

There are few defined regulatory regions in ATR, and structural information of ATR is lacking. Because of this, the inter-HEAT repeat loop where 3A-ATR mutations reside is an interesting region for future ATR studies especially since it is conserved among ATR orthologues and also occurs in ATM and DNA-PK. I was unsuccessful in determining whether 3A-ATR residues are phosphorylated. It is a good possibility that the mutations disrupt other forms of regulation, which the yeast FRVF-AAAA mutant data supports. It would be interesting to conduct a systematic analysis of the conserved residues in this region in yeast. Identifying other functional residues that do not disrupt protein levels when mutated would help future study of the region. Alternatively, confirming that the FRVF-AAAA mutant has normal basal kinase activity would alleviate protein folding issues. If other mutations that do not disrupt protein levels were identified, an overexpression suppressor screen could be conducted to identify proteins that function through this region.

To my knowledge, 6A-ATR mutations are the first mutations that produce a super-activatable ATR kinase. 6A-ATR mutations do not create a constitutively activated ATR kinase. Instead the mutations substantially potentiate TopBP1-mediated stimulation of kinase activity. This suggests there are additional regulatory steps in TopBP1-mediated activation of ATR mediated by 6A-ATR mutations. Three of the 6A-ATR mutations occur in the ATR FAT domain. Rapamycin binds mTOR in its FAT domain to inhibit mTOR activity (221). The model of ATM activation suggests that the FAT domain occludes the kinase domain in inactive dimers and autophosphorylation within the FAT domain relieves this inhibition by transitioning to a monomer state (162). It is possible

that the FAT domain of ATR also serves as a negative regulatory input whether through binding of an inhibitory protein, inhibitory post-translational modification, or auto-inhibitory interactions that are relieved allosterically upon kinase activation.

There are many tantalizing possibilities that could explain hyper-activation. ATR signaling to Chk1 in cells requires protein phosphatase 5 (PP5), and PP5 and ATR co-immunoprecipitate, suggesting that dephosphorylation of ATR contributes to ATR activation (222). One attractive hypothesis is that 6A-ATR residues are inhibitory phosphorylation sites. I have no evidence that 6A-ATR perturbs ATR phosphorylation. However, several alternative experiments to test this hypothesis are feasible. For instance, *PP5* silencing perturbs ATR-dependent Chk1 phosphorylation in cells. 6A-ATR expressing cells should be refractory to PP5-deficiency if 6A-ATR residues are dephosphorylated by PP5. In addition, phosphatase treatment of WT-ATR but not 6A-ATR should increase TopBP1 interaction in GST-pulldown assays. However, one consideration is that damaging cells prior to *in vitro* stimulation of ATR does not increase ATR activation (unpublished D.M.), possibly due to not preserving ATR phosphorylation during purification. Comparison of phospho-mimetic mutants may be a better approach.

My preliminary data shows that TopBP1 binding is increased with 16A-ATR. Hyper-activation may be due to an artifact, perhaps by creating an artificial TopBP1 binding surface on the mutant ATR protein or a "sticky" ATR. Defining the minimal mutations that produce hyper-activation will alleviate some of these concerns. Interestingly, screens for activating mutations in yeast TOR identified many activating mutations in the TOR FAT domain that

conferred growth in the absence of the TOR activator Rheb or in the presence of the nonspecific mTOR inhibitor caffeine (223, 224). Therefore it is possible that TopBP1 binding may also be regulated by residues in the FAT domain.

# CHAPTER VI

# CHARACTERIZATION OF A NOVEL ATR KINASE INHIBITOR

## Introduction

Ectopic oncogene expression both in cultured human cells and in xenograft models drives aberrant proliferation and leads to activation of the ATR-Chk1 pathway. Work at the single DNA fiber level suggests activation of ATR is due to DNA replication stress. ATR also is activated in neoplasias but not in adjacent normal tissue, and this activation is associated with cell cycle arrest, exit, or cell death. This suggests that ATR signaling may constitute a barrier to cancer (72-74, 225). Bypass of this barrier may be a double-edged sword for the cancer cell, as they may exhibit an increased dependency on the ATR pathway, analogous to oncogene addiction, to continue to replicate in the presence of oncogene-induced replication stress. ATR inhibition may be efficacious in these types of tumors. Furthermore, many current therapies are DNA damaging agents that increase the signaling burden on the ATR pathway, and ATR inhibition may increase their therapeutic index. In addition to these important clinical applications, a selective ATR inhibitor would also greatly advance basic research. Temporal studies of ATR function, which are difficult in genetic systems, would be possible.

I received a novel proprietary ATR inhibitor from AstraZeneca designated AZ20. While AZ has not disclosed the chemical structure of AZ20, it is an ATP analog. As a basic research tool, I used AZ20 to transiently inhibit ATR kinase activity during specific cell cycle phases and observed that ATR inhibition

perturbs DNA replication as expected from genetic studies. I also determined that ATR activity is required during prolonged replication fork stalling and during the recovery phase of DNA replication after replication stress. Finally, I began preliminary studies to examine the effectiveness of AZ20 as a single agent and found that AZ20 alone is cytostatic, likely due to off-target inhibition of mTOR. Instead, AZ20 sensitized cells to the replication stress agent HU, and ATM-deficiency sensitized cells to AZ20 treatment.

## Results

*Characterization of AZ20-mediated ATR inhibition*

I examined ATR-dependent Chk1 phosphorylation after HU treatment in U2OS cells to determine whether AZ20 inhibits ATR activity in cells. Chk1 phosphorylation increased after 4 hours of HU treatment (Figure 40a, Lane 1 vs 2). Simultaneous addition of AZ20 and HU inhibited Chk1 phosphorylation beginning at 1 μM with maximum inhibition occurring at 10μM (Figure 40a). Even at 10μM AZ20, inhibition of Chk1 phosphorylation was not complete.

I also determined the reversibility of ATR inhibition by co-treating cells with HU and 10μM AZ20 for 4 hours and then chasing into HU alone. At least by 2 hours of AZ20 removal, ATR inhibition is reversed and Chk1 phosphorylation levels increased (Figure 40a, lane 7 vs. 8). The reversal of inhibition is likely to occur much faster, but I did not analyze shorter chase times. Nonetheless, the reversibility of the inhibitor allows for transient inhibition of ATR.

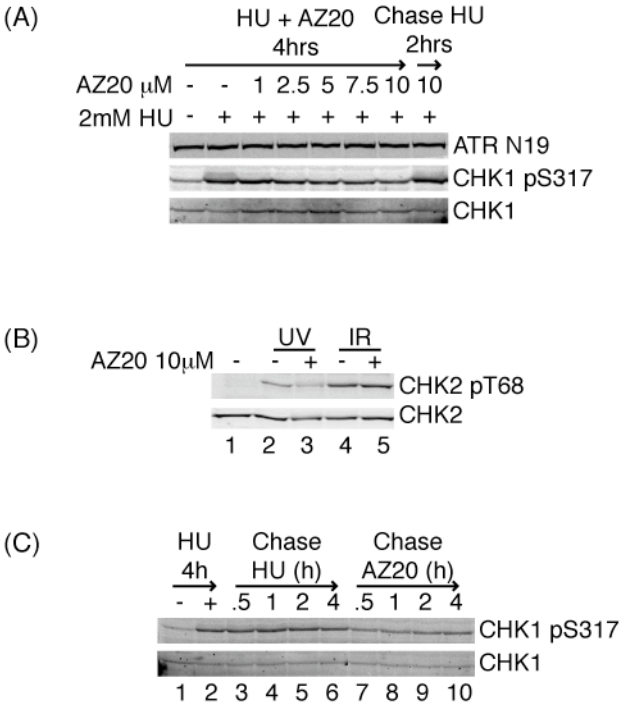


**Figure 40. AZ20 inhibits ATR.** (A-C) U2OS cell lysates were separated by SDS-PAGE and immunoblotted with the indicated antibodies. (A) Cells were co-treated with 2mM HU and AZ20 for 4 hours or co-treated for 4 hours and then chased into HU only for 2 hours. (B) Cells were co-treated with AZ20 and 50J/m$^2$ UV for 2 hours or 5Gy ionizing radiation (IR) for 1 hour. (C) Cells were initially treated with 2mM HU for 4 hours and then chased into HU alone or HU and 10$\mu$M AZ20 for the indicated time.

*AZ20 inhibits ATR but not ATM*

ATR and ATM are closely related DNA damage PIKK kinases with the highest degree of similarity occurring in the C-terminal kinase domain. AZ initially determined AZ20 to be 10-fold more selective for ATR versus ATM or mTOR in an *in vitro* kinase activity screen (personal communication). To confirm ATR selectively in cells, I examined whether AZ20 inhibited ATM-dependent Chk2 phosphorylation. ATM phosphorylated Chk2 after ionizing radiation (IR) in U2OS cells (Figure 40b, lane 1 vs. 4), and AZ20 treatment had no effect on this phosphorylation (Figure 40b, lane 4 vs. 5). In contrast AZ20 inhibited Chk2 phosphorylation after ultraviolet (UV) treatment (Figure 40b, lane 2 vs. 3), which is in agreement with previously published findings that Chk2 phosphorylation after UV is ATR-dependent. Therefore AZ20 specifically inhibits ATR and not ATM.

*AZ20 inhibits ATR rapidly*

To determine how quickly AZ20 inhibits ATR in cells, I treated U2OS cells with HU for 4 hours and then chased cells into HU alone or HU and AZ20 for the indicated times. Chk1 phosphorylation remained increased when HU treated cells were chased into HU (Figure 40c, lanes 2-6). In contrast, Chk1 phosphorylation decreased within 30 minutes of chasing into HU and AZ20 (Figure 40c, lane 3 vs. 7).

*AZ20 perturbs DNA replication*

ATR functions in S phase to promote completion of DNA replication through regulating replication origin firing and replication fork progression, stability, and restart. To analyze AZ20 effects on cell cycle progression in a synchronous population of cells, I utilized hTERT immortalized RPE cells, which undergo contact inhibition and reversible G0/G1 arrest (Figure 41a). I confirmed exit from the cell cycle by BrdU pulsing contact inhibited cells for 15 minutes prior to sample collection. The majority of contact inhibited cells contained 2N DNA content with very few BrdU positive cells (Figure 41b, 0 hour). Contact inhibited RPE cells re-enter the cell cycle when contact inhibition is relieved by passaging cells to non-confluent conditions. The burst in BrdU positive cells at 16 hours demonstrates this cell cycle re-entry, and cells progress through the cell cycle to 4N DNA content at 24 and 36 hours (Figure 41b, Top). Release of contact inhibited cells into AZ20 delayed the initial burst of BrdU incorporation by at least 8 hours and overall cell cycle progression, since by 36 hours there are also very few 4N DNA content cells (Figure 41b). At 36 hours AZ20 depressed BrdU incorporation. Strikingly, a distinct population of these BrdU positive cells exhibited grossly reduced incorporation further suggesting a disturbance in replication (Figure 41b, bottom 36h). These results are consistent with previously published genetic experiments.

In the previous experiment, AZ20 is present continuously after release from contact inhibition. Much like genetic manipulations of ATR, this makes it impossible to discern the effect of the drug on specifically S phase cells. To examine the effects of AZ20 specifically on cells in S phase, I released cells from contact inhibition into media only for 12 hours, which is prior to initial BrdU

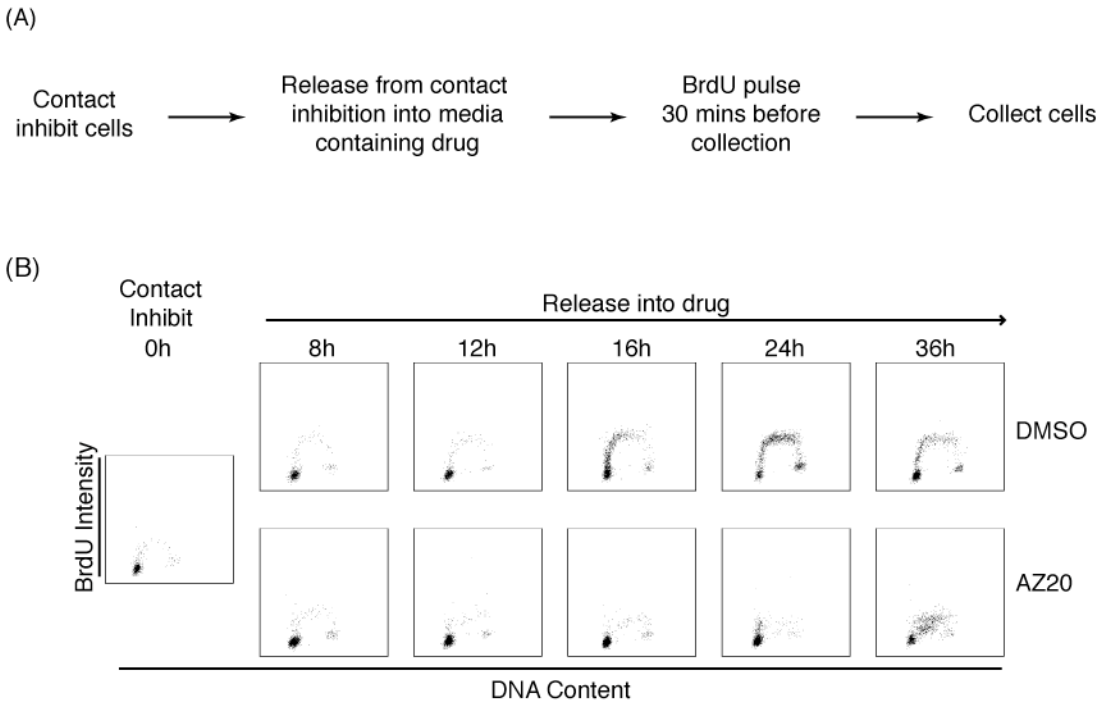


**Figure 41. AZ20 perturbs cell cycle progression.** (A) Schematic of experimental setup. RPE cells were contact inhibited (0h). Contact inhibited RPE cells were released from contact inhibition into DMSO control or 10$\mu$M AZ20 for the indicated times. Prior to harvesting at each time, cells were labeled with BrdU for 30 minutes. (B) BrdU and DNA content were analyzed by fluorescence activated scanning (FACS) using anti-BrdU-Alexafluor488 antibodies and propidium iodine, respectively.

incorporation (Figure 41b). After 12 hours of release into media, cells were chased into DMSO control or AZ20 (Figure 42a). Control cells progressed through S phase (Figure 42b, top) with BrdU positive cells at every time point and the appearance of 4N DNA content by 24 hours.

Cells chased into AZ20 exhibited a 4 hour delay in initial BrdU incorporation, which is not as pronounced as when cells were continuously released into AZ20. This suggests that AZ20 treatment in G0/G1 may contribute to the delay (addressed below). At 20 hours, AZ20 chased cells incorporated BrdU to a similar extent as control cells at 16 hours. However by 24 hours AZ20 chased cells exhibit depressed BrdU incorporation, consistent with results in Figure 41b (Figure 42b, bottom). Note, the difference in timing of the depressed BrdU incorporation (36 hour in Figure 41 and 24 hour in Figure 42) is likely due to the difference in delay of initial BrdU incorporation. Overall the data supports that AZ20 treatment in S phase perturbs DNA replication.

*AZ20 disrupts recovery from replication stress*

In addition to functioning during unperturbed replication, ATR genetically has been shown to be required for recovery of DNA replication following replication stress (18, 35). To assess whether AZ20 disrupts recovery of DNA synthesis after replication stress, I stalled replication forks in U2OS cells with 16 hours of HU treatment. This arrests cells in early S phase (Figure 43, 0 hour). I removed the HU and then released cells into DMSO control or AZ20 and nocodazole to prevent cells from exiting mitosis. DNA content analysis shows that control cells progress from 2N to 4N DNA by 10 hours after release from HU (Figure 43, black histograms). Cells released into AZ20 for 4 hours and 6 hours

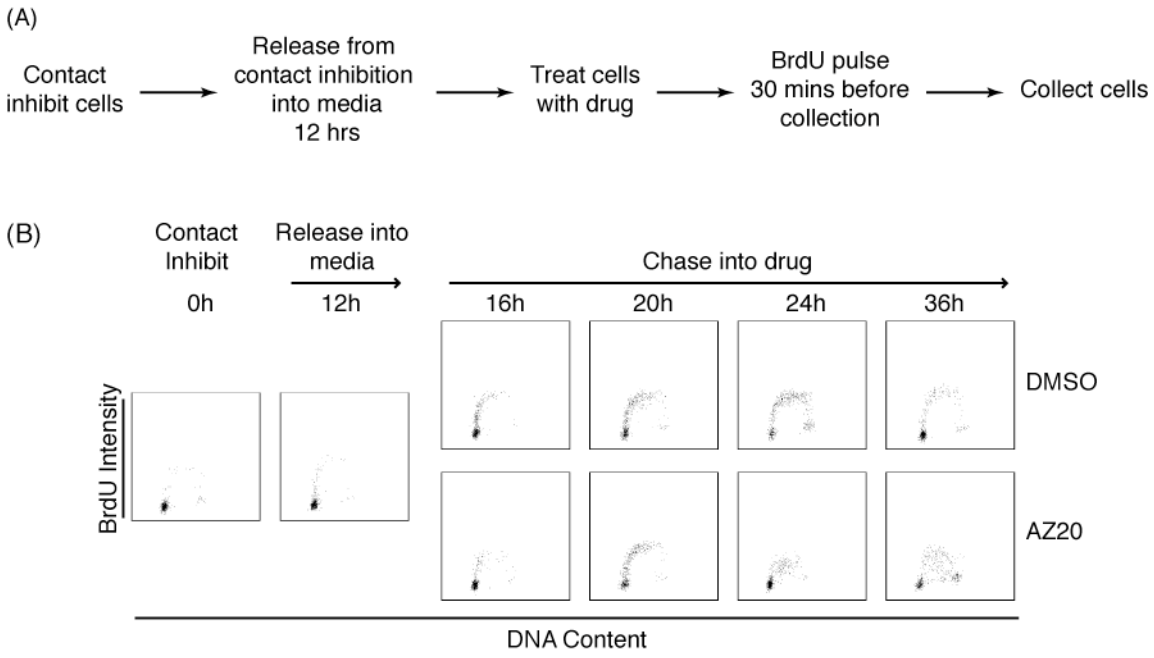


**Figure 42. ATR inhibition in S phase disrupts DNA replication.** (A) Schematic of experimental setup. RPE cells were contact inhibited (0h) and then released from contact inhibition into media alone for 12 hours. After 12 hours of release, cells were treated with DMSO or 10$\mu$M AZ20 and collected at the indicated times after release from contact inhibition. Prior to collection cells were labeled with BrdU for 30 minutes. (B) BrdU and DNA content were analyzed by FACS using anti-BrdU-Alexafluor488 antibodies and pridium iodine, respectively.

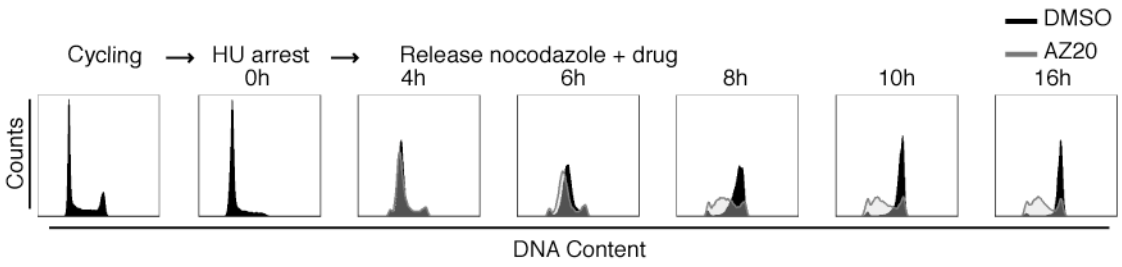


**Figure 43. ATR inhibition following a transient exposure to replication stress disrupts completion of DNA synthesis.** U2OS cells were arrested in early S phase with 2mM HU for 16 hours. Cells were then released into media containing DMSO or 10$\mu$M AZ20 and nocodazole for the times indicated. DNA content was analyzed by propidium iodide and FACS.

do not appear to have significant problems. However at 8 hours, cells released into AZ20 begin to accumulate in S phase (Figure 43, clear histogram). These cells do not progress to 4N DNA content even after 16 hours of release into AZ20. This data supports that AZ20 perturbs recovery from replication stress.

The function of ATR during prolonged replication fork stalling is not easily separable from DNA completion during recovery with genetics. To assess ATR function during a prolonged replication stall, I stalled replication forks with HU for 16 hours and then continued to stall forks either in HU and DMSO control or in HU and AZ20 for an additional 24 hours. Cells were then released into nocodazole, and DNA content was analyzed (Figure 44a). Cells stalled in the presence of HU and DMSO could resume DNA synthesis and a large percentage completed synthesis with 4N DNA content (Figure 44b, black histograms), although some cell death occurred likely due to the prolonged arrest. Strikingly, very few cells arrested in HU and AZ20 reached 4N DNA content when released (Figure 44b, clear histogram). In addition to cell death, a large percentage of AZ20 treated cells remain arrested. This data implies that ATR activity is also important during prolonged fork stalling possibly to prevent replication fork collapse and to prevent origins from firing.

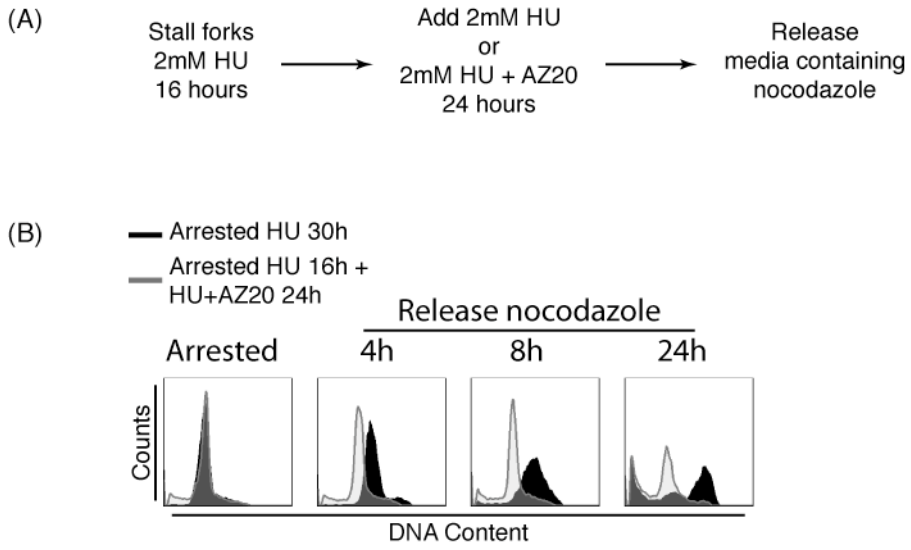


**Figure 44. ATR inhibition during prolonged replication fork stalling prevents completion of DNA synthesis.** (A) Schematic of experimental setup. U2OS cells were arrested in 2mM HU for 16 hours to stall replication forks and arrest cells in early S phase. After 16 hours, cells were then treated for an additional 24 hours with HU and DMSO control or HU and 10$\mu$M AZ20 (Arrested). Cells were then released into media containing nocodazole only for the indicated times. (B) DNA content was analyzed by propidium iodide and FACS.

*AZ20 delays entry into S phase*

In initial RPE release experiments, I observed a substantial delay in S phase entry when I released contact inhibited cells directly into AZ20 (Figure 41b). This effect was not as large when I treated cells with AZ20 only in S phase (Figure 42b), suggesting that ATR inhibition during G0/G1 contributes to the delay. To test this hypothesis, I released contact inhibited RPE cells immediately into DMSO control or AZ20 for 8 hours, chased cells into media, and BrdU pulsed cells 30 minutes prior to sample collection (Figure 45a). I chose the 8 hour treatment time, since released cells do not incorporate BrdU until 12-16 hours after release. Furthermore, from earlier characterization I determined that ATR inhibition was reversed within 2 hours of a chase. 20 hours after release, more than 50% of cells treated with DMSO during the initial 8 hours of release incorporated BrdU (Figure 45b and c). In contrast 25% of cells treated with AZ20 during the first 8 hours of release incorporated BrdU at 20 hours (Figure 45b and c). By 24 hours AZ20 treated cells reached percentages of BrdU positive cells observed in control cells at 20 hours. However, AZ20 treated cells did not exhibit a problem in replicating once they entered S phase, since they incorporated BrdU at similar intensities (data not shown). These results suggest that AZ20 treatment during G0 and G1 delays entry into S phase.

While I have shown that cells released from contact inhibition do not incorporate BrdU until some time between 12 and 16 hours, I wanted to rule out the possibility that AZ20 was being added during early time points of replication origin firing not discernable by BrdU incorporation. To do this, I treated cells released from contact inhibition for 4 hours at different windows during the first 12 hours of release (ie. 0-4hrs, 4-8hrs, and 8-12h; Figure 46a) and then chased into

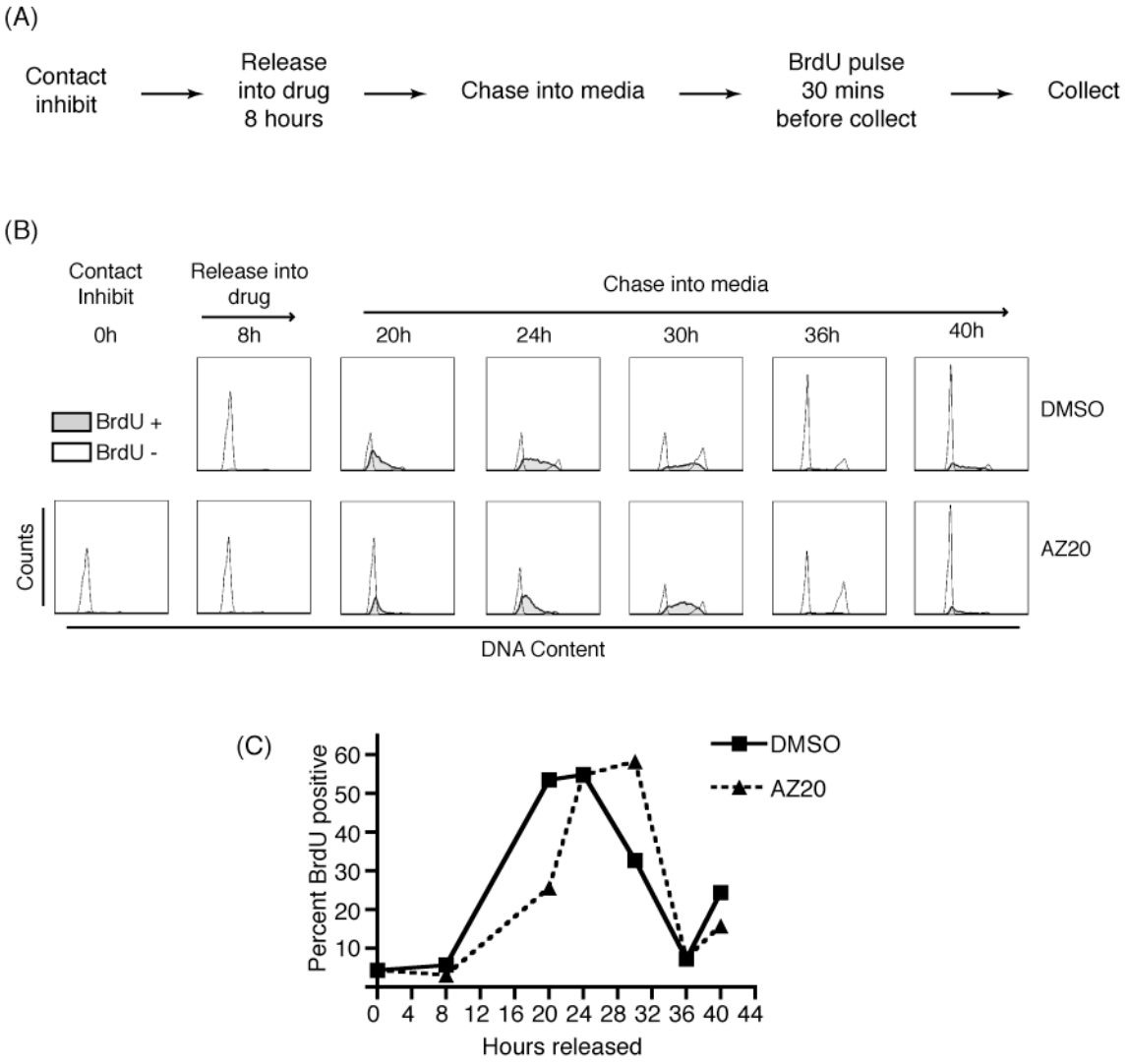


**Figure 45. AZ20 treatment during G0/G1 delays S phase entry.** (A) Schematic of experimental setup. RPE cells were contact inhibited (0h). Cells were released from contact inhibition into media containing DMSO or 10$\mu$M AZ20 for 8 hours. After 8 hours, AZ20 was removed and cells were chased into fresh media and collected at the indicated times after contact inhibition. Prior to collection cells were labeled with BrdU for 30 minutes. (B) BrdU and DNA content were analyzed by FACS using anti-BrdU-Alexafluor488 antibodies and pridium iodine, respectively. Histograms of DNA content were generated by gating BrdU negative (clear) and positive (shaded) cells. (C) BrdU positive cells at the indicated times in (B) were graphed.

media. Treating cells with AZ20 during the first four hours of release did not cause cells to delay BrdU incorporation (Figure 46b, 0-4 hour). Released contact inhibited cells are most likely progressing from G0 to G1 during this time. In contrast, releasing cells into media for the first four hours, then treating them with AZ20 for hours 4-8, and then releasing them into media caused a delay in S phase (Figure 46b). Similarly, releasing cells for the first 8 hours and then treating them with AZ20 from hours 8-12 and then releasing them into media also caused a delay in S phase (Figure 46b). These results indicate that a short treatment of four hours in G1 is sufficient to delay entry into S phase. Moreover treatment during hours 4-8 suggest that this delay is not due to inhibition of S phase cells that have fired origins but not incorporated significant amounts of BrdU.

I confirmed that the delay of entry into S phase was not specific to the RPE cell type. AZ20 treatment of primary human fibroblasts released from contact inhibition also delayed S phase entry (data not shown). The S phase delay is also not specific to the type of synchronization. In asynchronous U2OS cells, I BrdU pulsed cells at the start of the experiment to distinguish G1 (2N, BrdU negative) and S phase (BrdU positive cells) cells and then added AZ20 and nocodazole for the indicated times (Figure 47a). BrdU positive cells treated with DMSO control completed DNA synthesis by 12 hours (Figure 47b). The majority of BrdU positive cells treated with AZ20 also completed S phase but a portion of these cells also remained in S phase. This confirms RPE experiments showing that AZ20 treatment of S phase cells perturbs replication.

When examining the BrdU negative population, control cells progressed from 2N to 4N DNA content by 24 hours (Figure 47b). However, BrdU negative

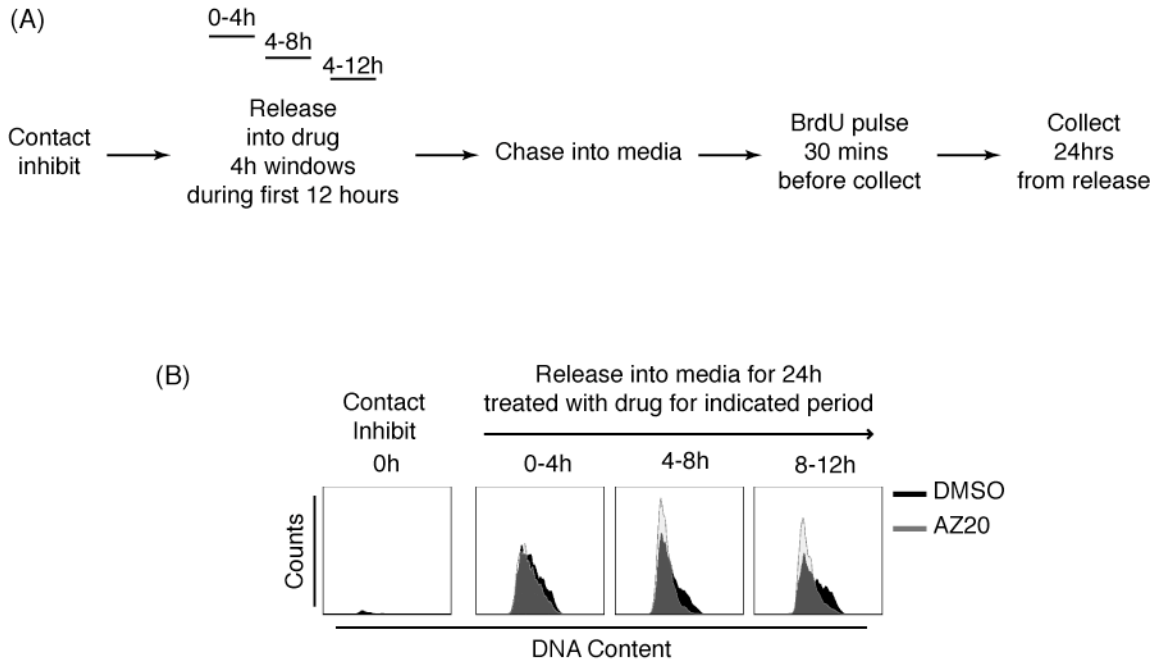


**Figure 46. AZ20 treatment during G1 delays S phase entry.** (A) Schematic of experimental setup. Contact inhibited RPE cells (0h) were released into DMSO or 10$\mu$M AZ20 for 4 hour time frames during the first 12 hours of release from contact inhibition. Cells were then chased into fresh media and harvested at 24 hours after release from contact inhibition. Prior to collection cells were labeled with BrdU for 30 minutes. (B) BrdU and DNA content were analyzed by FACS using anti-BrdU-Alexafluor488 antibodies and pridium iodine, respectively. Histograms depict DNA content of BrdU positive cells only.

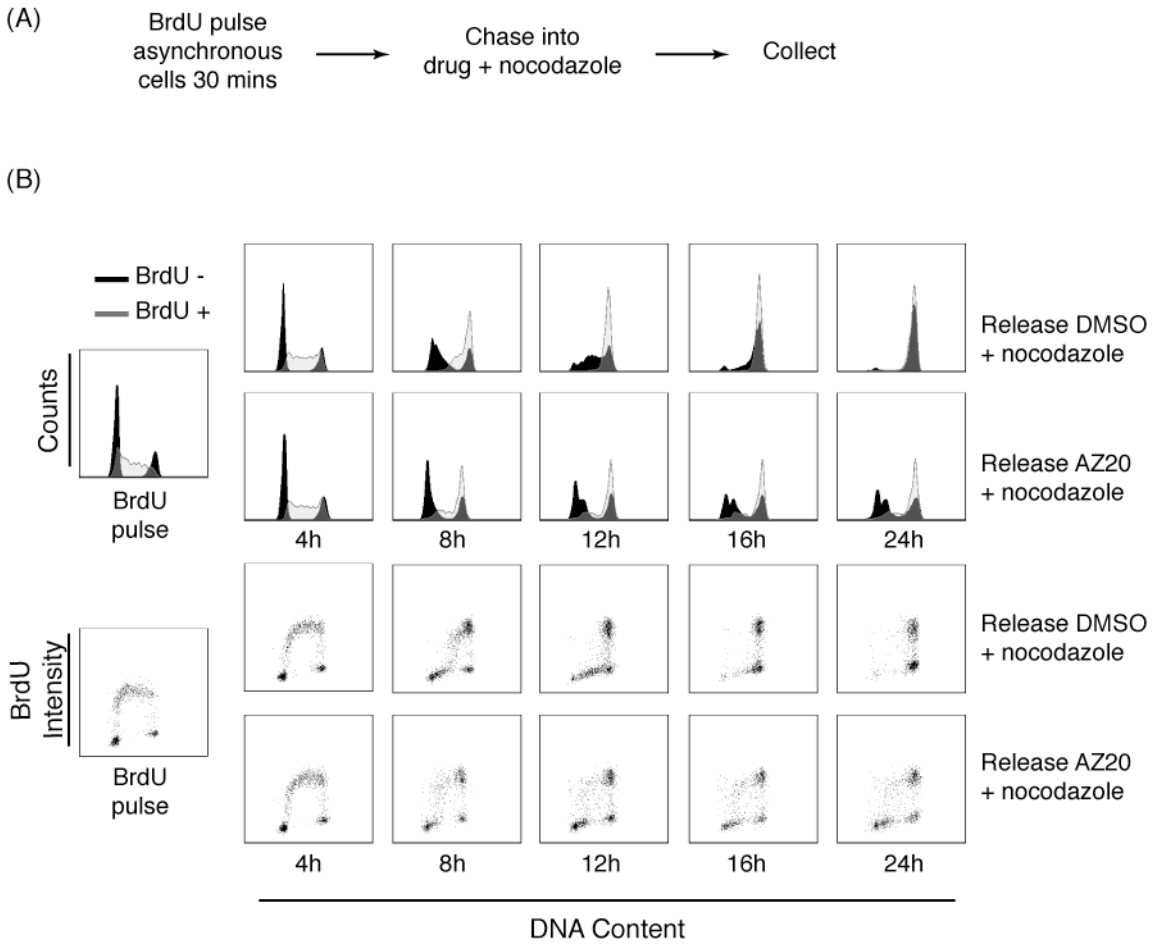


**Figure 47. AZ20 treatment of asynchronous U2OS cells perturbs DNA replication and delays S phase entry.** (A) Schematic of experimental setup. Asynchronous U2OS cells were first labeled with BrdU for 30 minutes. Cells were then grown in the presence of DMSO or 10 $\mu$M AZ20 and nocodazole for the indicated times. (B) BrdU and DNA content were analyzed by FACS using anti-BrdU-Alexafluor488 antibodies and pridium iodine, respectively. Histograms depict DNA content and were generated by gating BrdU negative (black) and positive (clear) cells. Results are also shown as BrdU intensity vs. DNA content.

AZ20 treated cells progressed from 2N to 4N DNA content at much slower rates than control cells, and a significant amount remained in G1 and early S phase (Figure 47b). This confirms that treating G1 cells slows entry into S phase. Additionally, any effect from AZ20 treatment of mitotic cells is unlikely to be visible in these experiments since I added nocodazole to the media.

*AZ20 delays RB phosphorylation*

No known function for ATR in G1 has been reported. One possibility is that ATR inhibition in G1 may cause DNA damage and enact a G1 checkpoint. Since ATM is the major kinase response for eliciting the G1 DNA damage checkpoint, I next examined whether ATM activity contributed to the G1 effects observed. Prolonged treatment of ATR in asynchronous U2OS causes cells to accumulate with 2N DNA content, which is indicative of the G1 delay. Co-administration of ATR and ATM inhibitors did not alleviate this accumulation, suggesting that the accumulation is not due to a G1 DNA damage checkpoint (Figure 48a).

I next examined whether AZ20 inhibited cyclin-dependent kinase (CDK) activity. In G1, Cyclin D-CDK4/6 phosphorylates the Retinoblastoma protein (RB), which relieves inhibition of the transcription factor E2F to promote transcription of genes required for S phase. I examined RB phosphorylation in RPE cells released from contact inhibition and observed an increase in RB phosphorylation at 12 hours (Figure 48b). AZ20 treatment transiently during the first 8 hours of release from contact inhibition caused a delay in RB phosphorylation (Figure 48b). This suggests that AZ20 delays entry into S phase by delaying RB phosphorylation in G1.

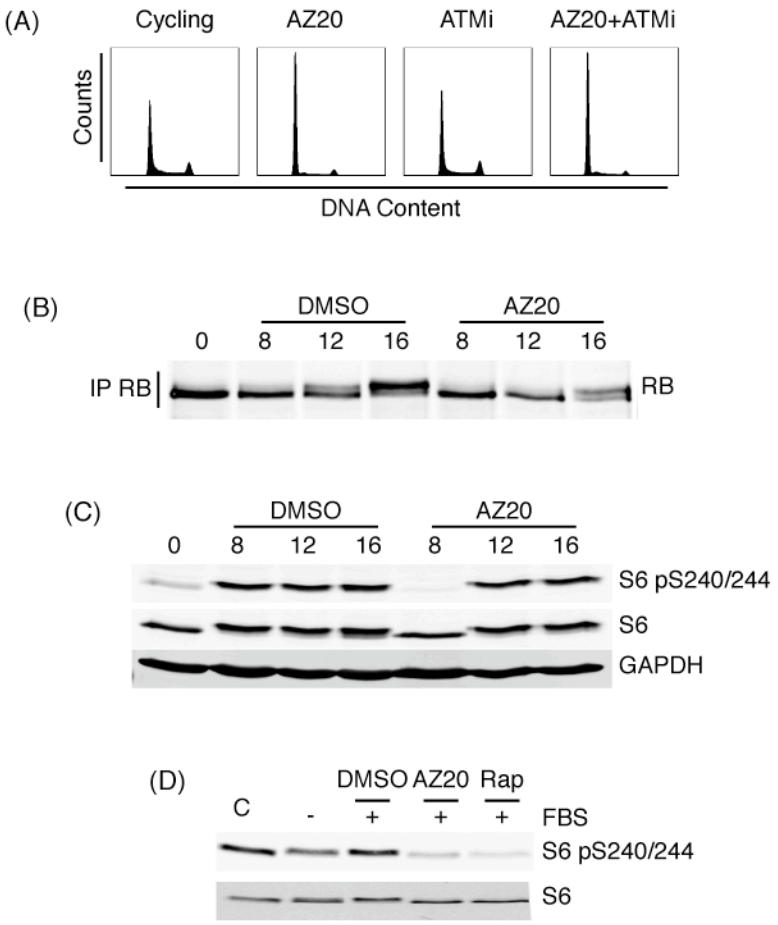


**Figure 48. AZ20 inhibits mTOR.** (A) Asynchronous U2OS cells were treated with DMSO, 10$\mu$M AZ20, 10$\mu$M of ATM inhibitor (KU55933), or 10$\mu$M AZ20 and ATM inhibitor for 16 hours. DNA content was analyzed by propidium idode and FACS. (B) Contact inhibited RPE cells were released into 10$\mu$M AZ20 for 8 hours and then chased into media for the times indicated after release from contact inhibition (see Figure 44a). RB was immunoprecipitated from cell lysates and immunoblotted with anti-RB antibodies. (C-D) Lysates were immunoblotted with phosphorylated-S6 ribosomal subunit and total S6. (C) Lysates from (B) were immunoblotted. (D) U2OS cells were serum starved for 16 hours. Cells were stimulated with media containing serum and DMSO, 10$\mu$M AZ20, or 100nM rapamycin for 30 minutes. C indicates lysate from cycling cells.

There is very little evidence for ATR-mediated promotion of Cyclin D-CDK4/6 activity. It is possible that AZ20 non-selectively inhibits CDK4/6. However, an ATR-related PIKK kinase, mTOR, regulates growth control, protein synthesis, and G1 progression in response to mitogenic signals (221). mTOR inhibition perturbs cyclin D accumulation in G1 cells (226, 227). Therefore I tested whether AZ20 G1 effects are off-target and due to mTOR inhibition. To examine mTOR inhibition, I examined phosphorylation of the S6 ribosomal protein subunit. S6 phosphorylation is visible 8 hours after release from contact inhibition in control RPE cells (Figure 48c). In cells treated transiently with AZ20 for the first 8 hours after release, S6 phosphorylation is delayed and does not appear until 12 hours (Figure 48c). I also confirmed mTOR inhibition in U2OS cells. Addition of serum to serum-starved U2OS cells induced S6 phosphorylation (Figure 48d). AZ20 treatment inhibited serum-induced S6 phosphorylation almost as potently as the mTOR inhibitor rapamycin (Figure 48d). From this data, I conclude that AZ20 is not ATR selective but also targets mTOR.

AZ20 inhibition of mTOR suggests that the delay in S phase entry is due to mTOR inhibition. In an attempt to distinguish whether ATR or mTOR inhibition is contributing to this phenotype, I first determined that the minimal concentration of AZ20 that causes the S phase delay is 500nM (Figure 49a). I then assayed for the concentration of AZ20 at which mTOR inhibition begins. Inhibition of mTOR-dependent S6 phosphorylation also begins at 500nM (Figure 49b). Furthermore, ATR-dependent Chk1 inhibition does not occur until 1μM (Figure 40a). Together, ATR and mTOR inhibition by AZ20 occur at similar ranges of drug concentration. This precludes me from determining the

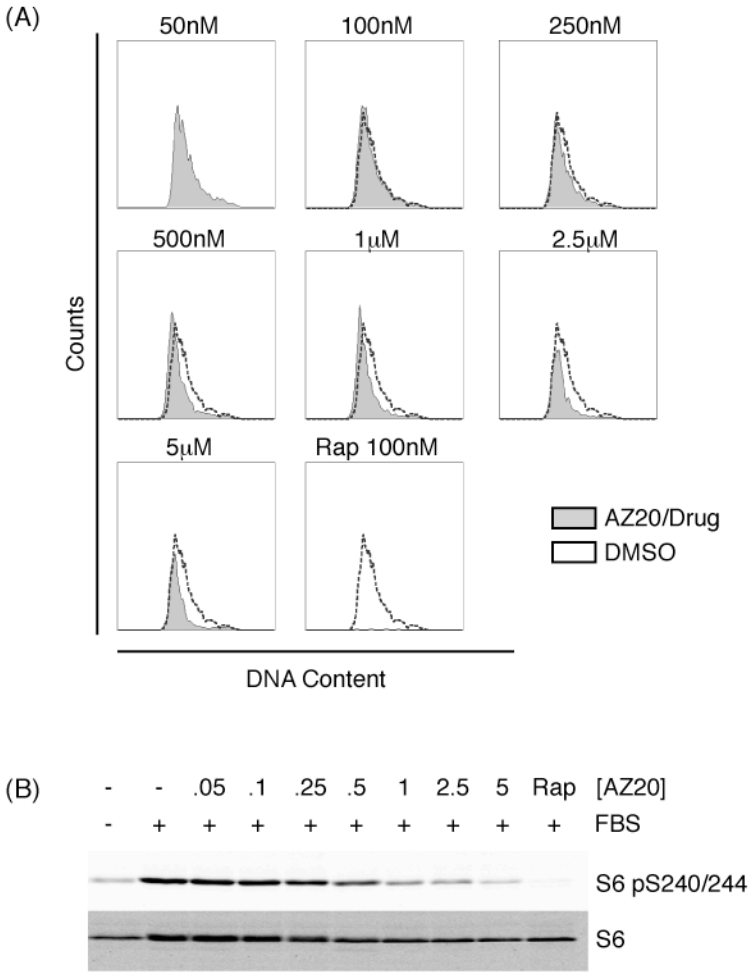


**Figure 49. AZ20 inhibits ATR and mTOR at similar concentrations.** (A) Contact inhibited RPE cells were released from contact inhibition into DMSO, increasing concentrations of AZ20, or 100nM of rapamycin for 8 hours. Cells were then chased into media alone and collected 20 hours after release from contact inhibition. Prior to collection, cells were labeled with BrdU for 30 minutes (see Figure 44a). BrdU and DNA content were analyzed by FACS using anti-BrdU-Alexafluor488 antibodies and pridium iodine, respectively. Histograms depict DNA content of BrdU positive cells only. Drug treated cells are shown as shaded histograms and overlay control cell histograms (clear). (B) U2OS cells were serum starved for 16 hours and then stimulated with media containing serum and indicated concentrations of AZ20 ($\mu$M) or 100nM rapamycin. Cell lysates were immunoblotted with indicated antibodies.

contribution of ATR and mTOR inhibition in G1 cells, although only mTOR of the two has well established roles in G1. Of note, S phase defects caused by AZ20 are not likely to be due to mTOR inhibition, as mTOR regulation of DNA replication has not been shown.

*Replication stress potentiates AZ20 cytotoxic effects*

Despite the non-selectively of AZ20, the drug did perturb replication and recovery from replication stress in S phase cells. Therefore, I assessed the cytotoxic affects of AZ20 treatment in U2OS cells. Static treatment of AZ20 alone caused very little cell death within 24 hours of treatment, since most cells accumulated in G1 and early S phase. Even after 72 hours of AZ20 treatment, only 21.4% of cells had sub-G0/G1 DNA content while most cells remained in G1 or S (Figure 50a). However, when cells are simultaneously treated with AZ20 and HU, 26.8% of cells died and by 72 hours 41.8% of cells underwent cell death (Figure 50a). HU alone at 72 hours only caused 28.3% cell death. This data suggests that AZ20 alone is cytostatic, likely because of mTOR inhibition slowing cells from entering S phase. However, replication stress enhanced cell killing by AZ20 compared to AZ20 or HU alone.

The above results suggest that increasing the replication stress burden of the cell increases the therapeutic index of AZ20. To further test this hypothesis, I arrested cells in HU and then released cells continuously into AZ20 or AZ20 and HU for 24, 48, and 72 hours. In each case, I also released cells into the treatments for only 24 hours and assessed cell death at 24, 48, and 72 hours. Cells released into DMSO control exhibited only 9.2% cell death at 72 hours. In contrast, release of cells into AZ20 caused 17.4%, 30.8%, and 57.6% cell death at 24, 48, and 72

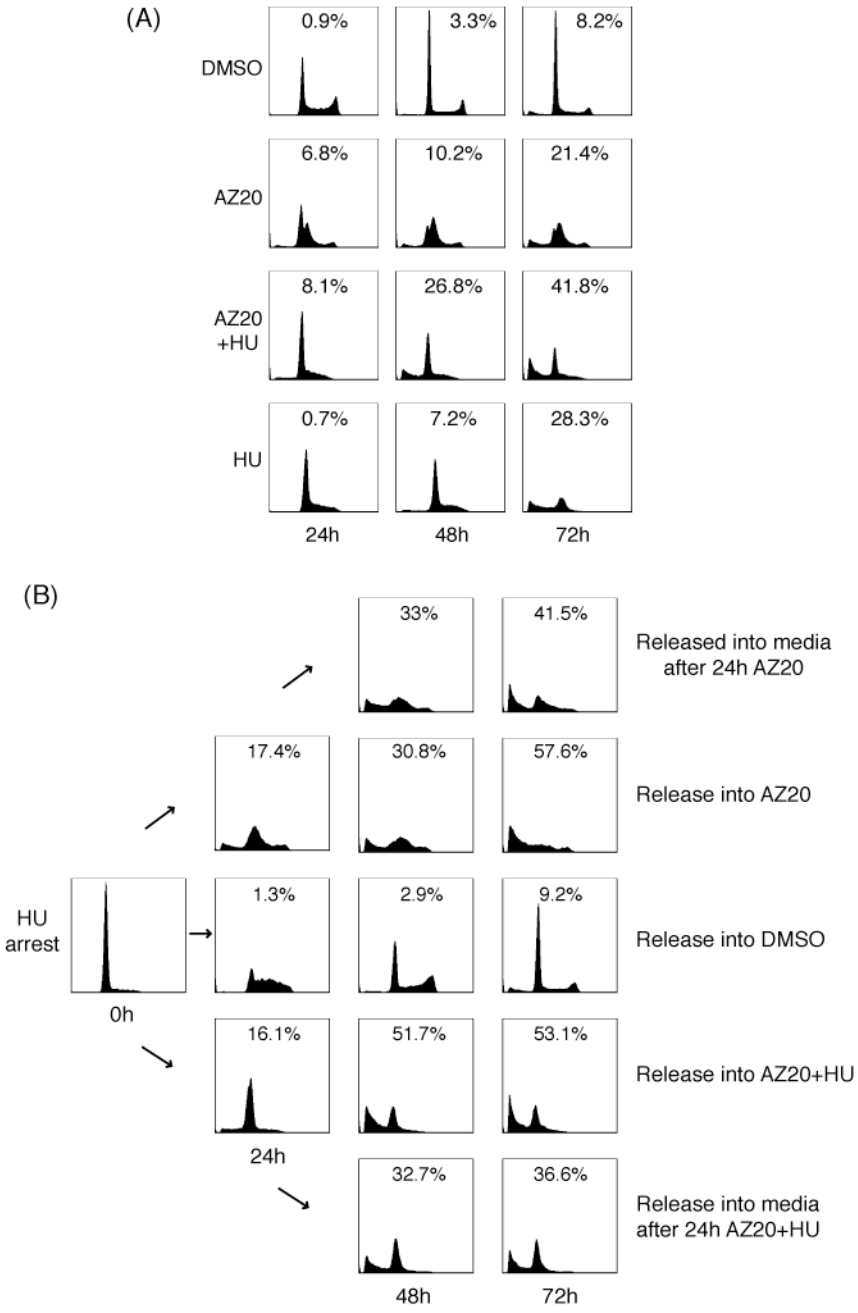


**Figure 50. DNA replication stress potentiates AZ20 cytotoxicity.** (A-B) Cell death was quantified by the determining the percentage of cells with less than 2N DNA content by propidium iodide and FACS. Percentages are displayed in the top corner of each histogram. (A) U2OS cells were treated with DMSO, 10$\mu$M AZ20, 10$\mu$M AZ20 and 2mM HU, or 2mM HU only for the indicated times. (B) U2OS cells were arrested with 2mM HU for 16 hours and then released into DMSO, 10$\mu$M AZ20, 10$\mu$M AZ20 and 2mM HU, or 2mM HU for the times indicated. Where indicated cells were released into drugs for only 24 hours and collected at the times indicated after release from HU.

hours respectively (Figure 50b). Only 24 hours of exposure to AZ20 after the release was sufficient to cause substantial cell death at 48 and 72 hours with 33% and 41.5% cell death respectively (Figure 50b). Release of cells into AZ20 and HU continuously caused 16.1%, 51.7%, and 53.1% cell death at 24, 48, and 72 hours. Release for only 24 hours into AZ20 and HU resulted in 32.7% and 36.6% cell death at 48 and 72 hours again showing that cell death increases even after just 24 hours of AZ20 treatment (Figure 50b). These data indicate that replication stress increases the therapeutic index of AZ20 and that the therapeutic window is in S phase cells.

*ATM deficiency increases AZ20 sensitivity*

Understanding the genetic determinants of AZ20 sensitivity is important in order to individualize therapy. I began some preliminary studies to assess whether p53 and ATM status affect AZ20 sensitivity. I assessed whether p53 deficiency could sensitize cells to AZ20 using an isogenic pair of HCT116 colon carcinoma $p53^{+/+}$ and $p53^{-/-}$ cell lines. The IC50 of AZ20 in $p53^{+/+}$ cells was 0.36μM and 0.15μM in $p53^{-/-}$ cells (Figure 51a). Thus, p53 status does not significantly sensitize cells to AZ20. In contrast to p53, ATM deficiency significantly sensitized cells to AZ20. Human fibroblasts isolated from an Ataxia Telangiectasia-Mutated patient integrated with a WT-ATM vector had an IC50 concentration of 0.7μM. ATM-deficient cells integrated with vector only were seven-fold more sensitive to AZ20 with an IC50 value of 0.1μM (Figure 51b). Sporadic Lymphomas and breast cancers exhibit high incidence of loss of ATM function and could be good candidates for ATR inhibition (23, 228).

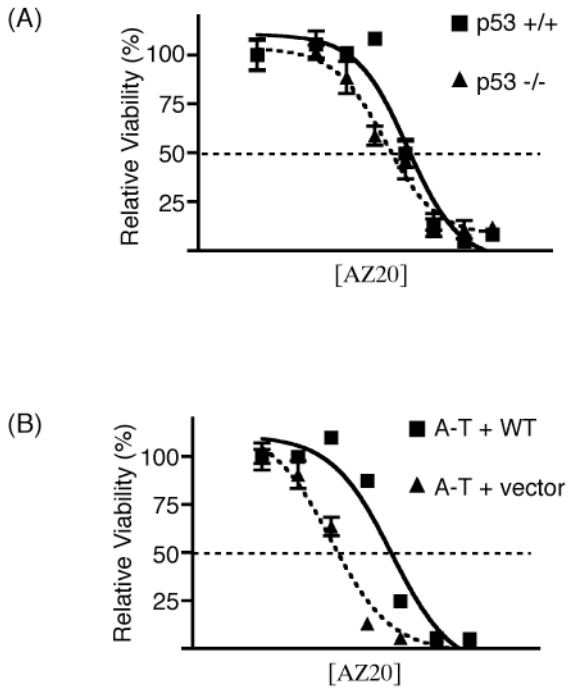


**Figure 51. ATM-deficiency sensitizes cells to AZ20 treatment.** (A-B) Cells were treated with increasing concentrations of AZ20. Viability was determined with an Alamar Blue assay. (A) HCT116 p53 wild type cells (IC50 = 0.36$\mu$M) or p53 null cells (IC50 = 0.15$\mu$M) were analyzed. (B) A-T cells integrated with wild-type ATM (IC50 = 0.7$\mu$M) or vector (IC50 = 0.1$\mu$M) were analyzed.

## Discussion

In this chapter I characterize a novel ATR inhibitor, AZ20, and use it to examine the temporal requirements of ATR in the response to replication stress. ATR activity is required both when replication forks are stalled and also during DNA replication after fork stalling agents are removed. Hydroxyurea potentiated AZ20-mediated cytotoxicity in U2OS cells. AZ20, while selective for ATR and not ATM, also inhibits the related PIKK mTOR. mTOR inhibition causes a G1 delay and delays entry into S phase where ATR inhibition would be most efficacious. Finally while p53-deficiency mildly sensitized cells to AZ20, ATM-deficiency sensitized cells to AZ20 seven-fold.

*Temporal requirements for ATR activity after replication stress*

In *S. cerevisiae*, experiments using inducible expression of $Rad53^{Chk1}$ show that loss of Rad53 function during fork stalling cannot be rescued by re-expression of Rad53 after fork stalling agents are removed due to irreversible fork collapse (142). Similarly using the ATR inhibitor, I find that transiently inhibiting ATR activity once replication forks are stalled greatly perturbs completion of replication when fork stalling agents and AZ20 are removed. This suggests that in mammalian cells ATR activity is also required for fork stability. Direct analysis of replication forks by DNA fiber labeling will be necessary to test this hypothesis. In addition, *RAD53* null defects can be rescued by deletion of the nuclease Exo1 while *MEC1* deficiency cannot (143). It would be interesting to compare Chk1 inhibition to ATR inhibition in mammalian cells and to also test whether nuclease inhibition can rescue these defects.

My data also supports that ATR activity is required during DNA replication after fork stalling agents are removed. One interesting observation in these experiments is differences in DNA content are not observed until 6 hours after inhibition of ATR in cells following release from replication stress. This is not due to the kinetics of ATR inhibition, as inhibition in cells occurs within 30 minutes. I also pre-treated cells for 1 hour prior to release and obtained similar results (not shown). This raises the question of what the function of ATR is during the recovery phase and where this early DNA synthesis is coming from. Is the DNA synthesis from restarted forks that lose stability in the absence of ATR activity? Alternatively, is there aberrant origin firing due to loss of ATR activity? Again DNA fiber labeling is required to examine the state of replication forks and origin firing. In addition to fiber labeling, purification of replication forks via the isolation of nascent DNA by iPOND under temporal inhibition of ATR activity will identify proteins that are involved in regulating replication fork stability, which are largely unknown (229).

*Clinical implication of AZ20*

Many studies have shown that activated oncogenes cause replication stress and activation of the ATR pathway in tumors (73, 74). Because ATR is an essential gene and is required to respond to replication stress, it is thought that inhibition of ATR signaling in tumors would be cytotoxic. I found that AZ20-mediated cytotoxicity was potentiated by replication stress in U2OS supporting this hypothesis. Another study using a different ATR inhibitor also showed increased DNA damage with overexpression of the oncogene cyclin E and ATR inhibition compared to vector expressing cells (205, 206). An important future

direction will be to test this hypothesis comprehensively in xenograft models using activated oncogenes and to explore the use of ATR inhibitors in combination with therapeutics that cause replication stress. In addition I found that ATR inhibition for only 24 hours was sufficient to cause significant cell death after an initial treatment of replication stress. This implies that scheduling of ATR inhibition in patients may be best after a replication stress agent such as cisplatin and only be required for a short period of time. Testing different treatment regimens will be important to minimize side-effects from ATR inhibition in rapidly proliferating non-malignant cells. Additionally, large scale screenings of tumor-derived cell lines may show a correlation between the efficacy of ATR inhibition and the state of replication stress in the cell line.

ATM-deficiency also potentiated AZ20-mediated cytotoxicity. This is likely due to the generation of double-strand breaks in the absence of ATR activity. ATM would normally respond to these double-strand breaks to mediate cell cycle checkpoints and DSB break repair. Loss of ATM and ATR could lead to the accumulation of DNA DSBs and cell death. This result predicts that tumor types that often exhibit inactivation ATM, such as lymphomas and sporadic breast cancers, would be sensitive to ATR inhibition (23, 228). Additionally, genome wide RNAi screens would be an important future direction to identify potential genetic backgrounds that would be sensitive to ATR inhibition.

*mTOR inhibition*

AZ20 treatment also causes mTOR inhibition and a G1 delay. Prolonged treatment of AZ20 alone caused cells to accumulate in G1 and entry into S phase is greatly delayed. AZ20 treatment alone did not substantially increase cell

death, likely due to preventing cells from entering S phase where ATR inhibition would be most efficacious. Synchronization of cells in early S phase with the replication stress agent hydroxyurea greatly sensitized cells to AZ20. This is probably due to both increased replication stress and synchronization of cells in S phase. Future derivatives of AZ20 and other available ATR inhibitors should be examined for mTOR inhibition, as mTOR inhibition may be counterproductive to ATR inhibition.

# CHAPTER VII

# SUMMARY AND FUTURE DIRECTIONS

## Summary

The hypothesis that phosphorylation regulates ATR at first glance is seemingly simple. However, definitively answering this question has been exceedingly difficult. My research constitutes one of the first concentrated efforts in studying phospho-regulation of ATR.

*ATR T1989 phosphorylation marks an active kinase*

Prior to my research it was unknown whether ATR was phosphorylated in response to DNA damage. In Chapter III, I identify and characterize the first DNA damage-regulated ATR phosphorylation site. DNA damage induces phosphorylation on ATR T1989. Ablation of T1989 phosphorylation causes a partial viability defect, but the function of this phosphorylation remains unclear. T1989 phosphorylation occurs concurrently with ATR-dependent Chk1 phosphorylation and requires ATR kinase activity and activation via the PIKK Regulatory Domain in cells. This supports that T1989 phosphorylation occurs on an activated ATR kinase. Monitoring T1989 phosphorylation with a phospho-peptide specific antibody can serve as a direct marker for ATR activity. This is a major advancement for studying ATR signaling.

*S and G2 functions of ATR are separable*

I test the hypothesis that candidate autophosphorylation sites regulate ATR activity in Chapter IV and uncover mutations that dissociate the S and G2 functions of ATR. Mutation of three candidate ATR autophosphorylation sites creates a 3A-ATR (T1566A/T1578A/T1578A) mutant protein that cannot complement cell viability and S phase defects due to *ATR* deletion. However, the G2 checkpoint remains intact in 3A-ATR expressing cells. 3A-ATR viability defects correlate with reduced ATR-dependent Chk1 phosphorylation and perturbed completion of DNA synthesis after replication stress. Thus, 3A-ATR mutations are the first identified and characterized mutations in human ATR that dissociate S and G2 phase activities.

3A-ATR experiments demonstrate that the G2 checkpoint activity of ATR is dispensable for the essential function of ATR to promote cell viability. The correlation between viability and replication stress response defects in 3A-ATR expressing cells suggest that the essential function of ATR in human cells is to respond to DNA replication stress in S phase. However, the function of 3A-ATR residues remains unknown.

*Identification of a novel regulatory region*

3A-ATR residues occur in a distinct inter-HEAT repeat loop adjacent to the ATR FAT domain. An analogous region also is present in ATM and DNA-PK and is targeted for critical autophosphorylation in these kinases. While I cannot conclude 3A-ATR residues are phosphorylated, my data suggests that the region is also important for ATR function. I also provide preliminary evidence supporting that the regulatory region is conserved in budding yeast.

*Additional regulatory steps exist in TopBP1-mediate activation of ATR*

16A-ATR is hyper-stimulated by the ATR Activation Domain (AAD) of TopBP1 *in vitro*. This is the first report of a hyper-stimulatable ATR kinase. I localize the responsible mutations to 6 candidate autophosphorylation sites that are distinct from the 3A-ATR mutant residues. Preliminary experiments also indicate that the hyper-stimulation of the ATR mutants is due to increased binding with the TopBP1 AAD. While the mechanism of hyper-stimulation is unclear, these data reveal that there may be additional regulatory steps in TopBP1-mediated activation of ATR.

*ATR kinase activity is important during replication fork stalling and completion of replication following fork stalling*

Genetic studies demonstrate that ATR is critical to respond to replication stress. These studies imply that ATR functions to stabilize stalled replication forks, regulate origin firing, and restart collapsed replication forks. Yet temporally it is unclear from genetic manipulation whether ATR activity is required during replication fork stalling, during replication recovery, or at both stages. In Chapter VI, I use a novel ATR inhibitor and discover that ATR is required under both conditions. However, the function of ATR during these stages of the replication stress response remains to be determined.

*Determinants of ATR inhibition sensitivity*

ATR inhibition with AZ20 increases cell death. However, release of cells from HU arrest into AZ20 causes a 5-fold increase in cell death compared to cells treated with HU alone. This suggests that the therapeutic index of ATR

inhibitors can be augmented with replication stress agents or in tumors with high levels of replication stress.

Genetically, ATM and p53 deficiency sensitize cells to ATR inhibition. p53 deficiency causes a 2-fold decrease in cell viability while ATM deficiency sensitizes cells to ATR inhibition 7-fold. This suggests that tumors with ATM mutations, such as sporadic breast and lymphomas, may be good candidates for therapies inhibiting ATR. Genome-wide screens for other genetic determinants of sensitivity to ATR inhibition will be an important future step.

AZ20 also inhibits the related PIKK mTOR. AZ20-mediated inhibition causes cells to accumulate in G1 and delays entry into S phase. This G1 accumulation is counterproductive for the cytotoxic effects of ATR inhibition, which is potentiated by DNA replication stress. As a consequence, AZ20 as a single agent was not very effective and future derivatives of ATR inhibitors should aim to not target mTOR.

## Future Directions

*ATR activation*

Activation of the ATR kinase requires independent localization of the ATR-ATRIP complex and ATR signaling factors to Replication Protein A-coated single-stranded DNA (RPA-ssDNA) (18). RPA-ssDNA can be considered analogous to a signaling scaffold to concentrate ATR signaling factors when there is DNA damage (Figure 52a). ATR-ATRIP recruitment to RPA-ssDNA occurs through an interaction between ATRIP and the 70kDa subunit of RPA (Figure 52b) (84, 87). Independent of ATR-ATRIP recruitment, the Rad17-RFC clamp loader loads the Rad9-Rad1-Hus1 (9-1-1) complex to a 5′ recessed junction, perhaps due to the interaction of Rad9 with the 70N domain of RPA (Figure 52b) (93-95). 9-1-1 recruitment facilitates localization of the ATR activator TopBP1. This proceeds through an interaction between TopBP1 BRCT repeats and the phosphorylated tail of Rad9 (230). TopBP1 interacts directly with the ATR PRD and a region on ATRIP (Figure 52c) (90). TopBP1 binding of ATR PRD presumably causes a conformational shift that increases ATR substrate affinity (110). Once activated, ATR phosphorylates substrates like Chk1 and concurrently ATR T1989 becomes phosphorylated in an ATR-dependent manner (Figure 52d) (191).

*Recruitment of ATR-ATRIP and ATR signaling factors*

Recent work demonstrates that artificial tethering of TopBP1-LacR to integrated Lac-O sequences in the absence of DNA damage is sufficient to activate ATR as measured by phosphorylation of the ATR substrate Chk1 (105).

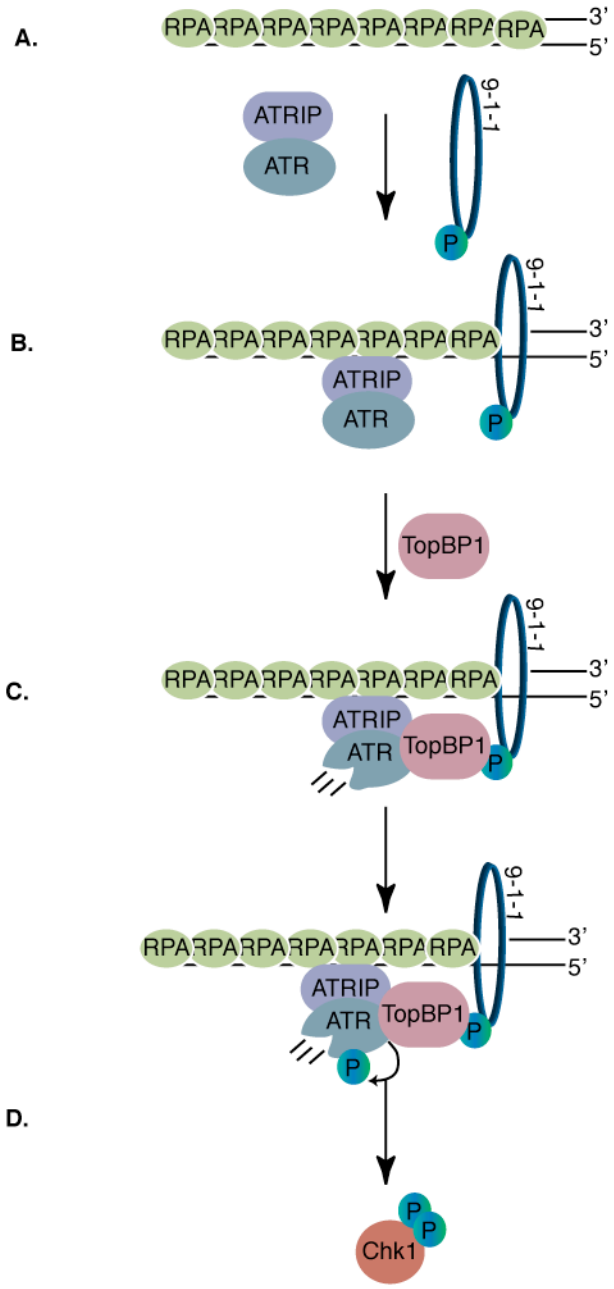


**Figure 52. Model of ATR activation.** (A) Generation of RPA-ssDNA. (B) Independent recruitment of ATR-ATRIP and Rad9-Rad1-Hus1 (9-1-1) complexes to RPA-ssDNA. ATRIP interaction with RPA facilitates ATR-ATRIP localization while the 9-1-1 complex is loaded in an ATP-dependent manner by a specialized clamp loading complex. (C) An interaction between the phosphorylated tail of Rad9 and the ATR activator protein TopBP1 recruits TopBP1 to ATR-ATRIP. The ATR activating domain (AAD) of TopBP1 binds the ATR PRD and ATRIP directly, activating the complex. (D) Activated ATR is concurrently phosphorylated at T1989 and phosphorylates its downstream targets including Chk1.

Other groups report similar results in yeast (104), and similar experiments tethering the ATM activator complex MRN demonstrate that concentration of MRN is sufficient to activate ATM (231). These data emphasize that concentrating the ATR kinase with its activator TopBP1 is sufficient for signaling.

While I have described a step-wise linear mode of ATR-ATRIP and TopBP1 recruitment to RPA-ssDNA, data in the field suggests that there are other modes of recruitment for both ATR-ATRIP and TopBP1 to RPA-ssDNA. In addition, localization may not be limited to the RPA-ssDNA scaffold.

An acidic checkpoint recruitment domain of ATRIP interacts with a basic cleft in the 70kDa subunit of RPA (87). Mutation of either of these domains prevents ATR-ATRIP binding to RPA-ssDNA with minimal consequences to checkpoint signaling (84). This supports that there may be alternative modes of ATR-ATRIP recruitment. For instance in both yeast and mammalian cells, Cdc6 interacts with ATRIP. Cdc6-deficiency perturbs ATR-ATRIP chromatin association and checkpoint signaling (232, 233). Whether this Cdc6-dependent chromatin association depends on RPA-ssDNA is not clear (Figure 53a).

Perhaps more intriguing than protein factors that may be semi-redundant or cooperative with RPA-ssDNA are RPA-ssDNA-independent mechanisms. ATR-dependent Chk1 phosphorylation in response to base alkylation in cells requires mismatch repair (MMR) proteins. In contrast, RPA-ssDNA generating agents such as HU do not depend on MMR proteins for ATR signaling (234). While processing alkylated bases may lead to RPA-ssDNA, evidence supports that MMR proteins MutSα and MutLα recruit ATR-ATRIP, TopBP1, and Chk1 to chromatin after base damage. Importantly, RPA, Rad17, and Rad9 were not enriched on chromatin in these experiments (235-238). This suggests that MMR

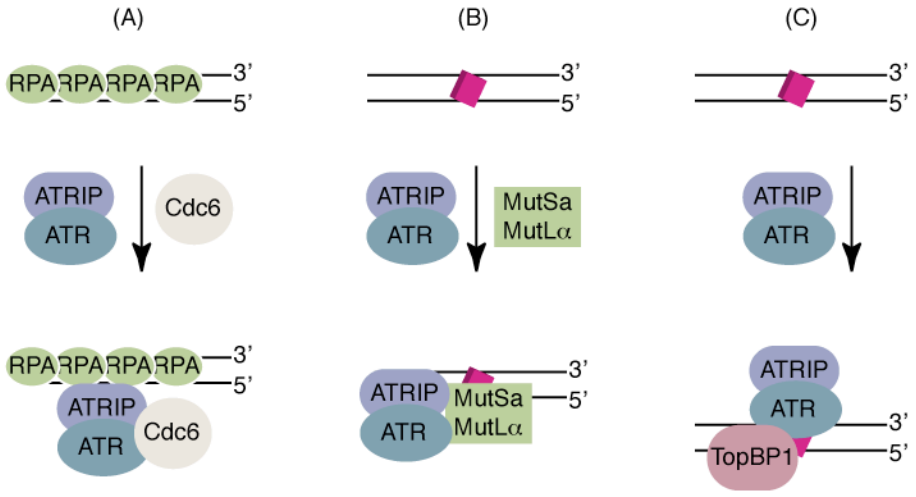


**Figure 53. Alternative mechanisms for ATR-ATRIP recruitment.** (A) Canonical recruitment of ATR-ATRIP to RPA-ssDNA via an interaction between ATRIP and RPA. Other protein factors, such as Cdc6, may contribute to recruitment. TopBP1 and Chk1 recruitment would occur as classically described. (B) Mismatch repair proteins, MutSα and MutLα, recognize and bind base adducts. Interaction between ATR-ATRIP and these proteins may localize ATR to base damaged DNA. TopBP1 and Chk1 also interact with the mismatch repair proteins (not drawn). (C) ATR HEAT repeats may directly recognize distortions in DNA caused by DNA damage. TopBP1 also may recognize
damaged DNA.

proteins bound to alkylated DNA may serve to scaffold ATR-ATRIP and TopBP1 (Figure 53b).

Finally, there is tantalizing evidence that ATR and TopBP1 may interact with DNA directly. ATR interacts with duplexed and UV-damaged DNA *in vitro,* and damaged DNA stimulates ATR activity (239, 240) Additionally, TopBP1 can bind damaged DNA *in vitro* (240). While no DNA binding domains have been described on ATR, the AlkD glycosylase binds DNA via its HEAT repeats (166), suggesting ATR may also bind DNA via its HEAT repeats (Figure 53c). Structural models of DNA-PK and ATM also support that HEAT repeats may contact DNA (218, 219). How TopBP1 might interact with DNA is not clear.

There is also 9-1-1 independent recruitment of TopBP1 to chromatin in the *Xenopus* egg extract system (114). Additionally, a novel protein called RHINO interacts with Rad9 and TopBP1 through distinct domains. Depletion of RHINO results in Chk1 phosphorylation defects after double strand breaks, suggesting that RHINO functions to promote TopBP1 recruitment (115). Alternatively, RHINO binding of Rad9 and TopBP1 may regulate either or both proteins allosterically.

It will be important to expand our understanding of how ATR-ATRIP and TopBP1 are brought together beyond the RPA-ssDNA scaffold. Base damage recruitment mechanisms are of particular interest because these types of lesions occur often during normal cellular metabolism and because many cancer therapeutics are base damaging agents (241). Understanding these other mechanisms of recruitment may provide novel drug targets.

*How does TopBP1 activate ATR?*

Mechanistic understanding of how TopBP1 activates ATR is lacking. It is postulated that TopBP1 binding to ATR induces a conformational change that increases substrate affinity for the kinase. This is based on the observation that TopBP1 greatly reduces the $K_m$ of ATR for its substrates (110). Typically kinases bind substrates in their active site and at distal docking sites (242). Binding of TopBP1 to ATR likely increases substrate affinity at the active site since it is a general activator of ATR towards all known substrates. Only structural information will provide a clear picture of how TopBP1 binding increases substrate affinity.

In addition to pushing towards an ATR structure, a screen for ATR activating mutations that bypass the requirement for TopBP1 would elucidate regions of the protein that may be involved in kinase activation. Theoretical alignments have been done on the structure of the PI3K kinase domain and the related PIKKs. While primary sequences are not similar, the predicted three-dimensional structure of the PIKK FAT, kinase, PRD, and FATC domains is similar to the PI3K helical, kinase, αK11, and αK12/αK13 domains (Figure 54a-b) (243). Oncogenic mutations in PI3K occur in the N-terminus of the helical domain. These mutations in the helical domain disrupt interactions between the p110 catalytic and p85 regulatory subunits of PI3K (244). Activating mutations in mTOR have been identified in yeast screens and in human tumors. These TOR mutations also occur in the FAT (helical) domain as well as in the kinase and PRD domain (245, 246). Similar to the PI3K mutations some of the mutations in the TOR FAT domain likely affect binding of regulatory proteins, such as the mTOR inhibitor rapamycin. Others mutations might affect conformation.

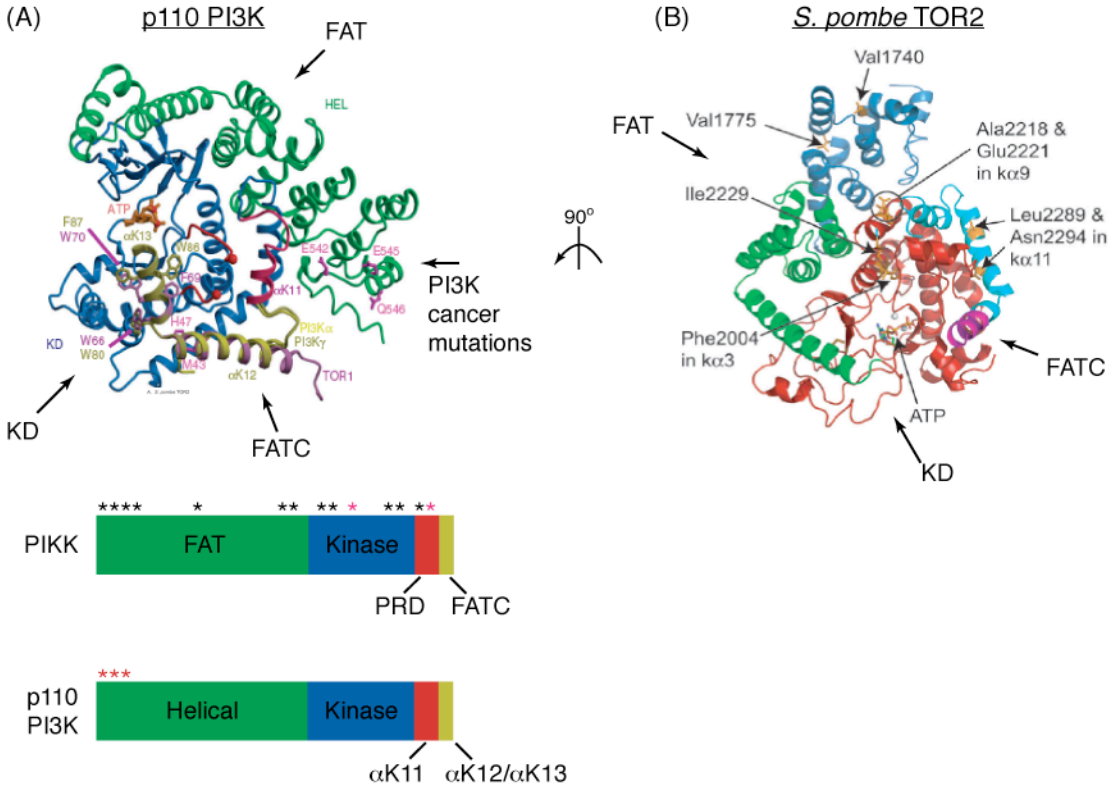


**Figure 54. Activating mutations in PI3K and TOR.** (A) Superimposition of the three-dimensional structure of the helical and kinase domain of the p110 catalytic subunit of PI3K onto the *S. cerevisiae* TOR1 FATC domain. Imagine reproduced and modified from (242). Helical domain is depicted in green, kinase domain in blue, αK11 in red, and αK12/K13 in yellow. Oncogenic PI3K mutated residues in the N-terminus of the helical domain E542, E545, Q546 are indicated. A schematic of domains of TOR proteins and the p110 catalytic are drawn below the structure. Black asterisks indicate positions of activation mutations. Red astericks denote mutations found in cancer. (B) Theorectical model of *S. pombe* TOR2 FAT (Green and blue), kinase (red), PRD (cyan), and FATC (magenta) domains reproduced and modified from (245).

Conducting a screen for activating ATR mutations would provide some hints into how the kinase is activated. We have yet to identify the equivalent PRD mutation in yeast Mec1$^{ATR}$. However a screen for Mec1 mutations that suppress HU sensitivity in the *ddc1Δdpb11-1* yeast strain may identify mutations that bypass the requirement for the two known ATR activators in yeast. Another possible genotype to conduct the screen with may be the use of the *ddc2$^{ATRIP}$-top* mutant which disrupts Mec1$^{ATR}$ activation by Dpb11$^{TopBP1}$. It would be difficult to conduct an *in vivo* screen with human ATR, but an *in vitro* kinase activity based screen with randomly mutagenized ATR might yield interesting results. Additionally, identification of activating residues may also help develop more specific ATR inhibitors. Still, only structural data can determine how these residues are involved in kinase activation.

*Regulation of TopBP1-mediated activation*

Regulation of TopBP1 binding to ATR occurs at the level of localizing the two proteins in close proximity as discussed above. However, there is evidence that additional mechanisms of regulation may exist. Phosphorylation of *Xenopus* TopBP1 by xATM on S1131 potentiates xATR-ATRIP activation after DNA double strand breaks (118). In addition, a phospho-mimicking mutation in the ATR activation domain of yeast TopBP1 also potentiates yeast ATR activation *in vitro* (112). Both of these phosphorylation events are thought to increase TopBP1 binding to ATR.

My observations that mutation of 6 candidate ATR autophosphorylation sites (6A-ATR) to alanine greatly increases TopBP1-mediated activation of ATR but not basal kinase activity *in vitro* also suggests that ATR dephosphorylation

regulates TopBP1-mediated activation. While I do not have direct evidence that these residues are phosphorylated, there is data to support that phosphatase activity is important for ATR signaling *in vivo* (222). Protein phosphatase 5 co-immunoprecipitates with ATR, and PP5 silencing perturbs ATR-dependent Chk1 phosphorylation after replication stress (222). The mutated residues in 6A-ATR occur in two distinct clusters, the N-terminal HEAT repeat region and the FAT domain. Since activating mutations in the mTOR FAT domain have been described (245, 246), it would not be surprising if the minimal mutations that cause the hyper-activation phenotype occur in the ATR FAT domain. Examination of the phenotype of a phospho-mimicking 6E-ATR will also be an important future direction. If phosphorylation of these sites were inhibitory, then the 6E-ATR mutant would exhibit ATR activation defects. 6A-ATR expressing cells also would be insensitive to PP5-silencing. Both ATM and DNA-PK interact with protein phosphatases and their signaling activities are regulated by phosphatases (247-249). Significantly, ATM also interacts with PP5, and *PP5* silencing causes ATM signaling defects (250). Study of protein phosphatases in ATR signaling may be an important future area of study and may reveal new insights into how TopBP1-mediated activation of ATR is regulated.

*Other ATR activating proteins?*

In budding yeast, both the homologs of TopBP1$^{Dpb11}$ and Rad9$^{Ddc1}$ can activate yeast ATR (103, 112). Whether human Rad9 can activate ATR-ATRIP remains to be tested. Yeast data also suggests that these protein activators function in distinct phases of the cell cycle and that there may be other proteins

activators (251). 3A-ATR mutations described in Chapter IV separate S and G2 functions of human ATR. One possibility is that these residues mediate ATR activation mediated by Rad9 or a novel protein activator. TopBP1 binds the ATR PRD to activate the kinase. Perhaps the 3A-ATR region mediates an interaction with another protein activator.

*Phospho-regulation of DNA damage PIKKs*

The catalytic domain of most protein kinases are structurally similar, consisting of two lobes forming a catalytic cleft at their interface. ATP and substrate binding in the catalytic cleft position ATP and the substrate in proximity to catalytic residues facilitating the phosphoryl transfer reaction. In addition an activation loop that occurs between the two lobes but outside the catalytic site also is important for activity of many kinases.

Phosphorylation regulates kinase activity by modulating access to the catalytic cleft and position of the catalytic residues. For instance, pseudosubstrates or protein conformation may occlude substrate access to the catalytic cleft. While many pseudosubstrates do not contain phospho-accepting residues, a few pseudosubstrates are phosphorylated to allow substrate access (252). More commonly, kinase phosphorylation and dephosphorylation can cause a conformational change promoting substrate access and binding (253). Phosphorylation in the activation loop also likely mediates or stabilizes a catalytic cleft conformation that favorably positions catalytic residues and potentiates catalysis (254). There are also a few cases where activation loop phosphorylation changes substrate binding (255). Phosphorylation can serve as phospho-binding sites for co-factors, activators, and substrates (256, 257). Finally

kinases often autophosphorylate once activated or as part of the activation process to mediate many of these described regulatory mechanisms (258).

Several of these mechanisms also regulate the PIKK kinases. ATM autophosphorylates on several residues, including S367, S1893, S1981, and S2996 (162, 180, 181). Mutation of any of these individually causes ATM signaling defects. S1981 in the ATM FAT domain has been best-studied, but the function of S1981 remains controversial. The Kastan group originally reported that S1981 autophosphorylation *in trans* mediates an inactive dimer to active monomer transition. Their data supports a model where the FAT domain interacts with and likely occludes the kinase domain as a dimer (Figure 55). Upon activation, S1981 autophosphorylation relieves this inhibition and promotes active monomer formation (162). However other groups report that ATM monomers can form without S1981 autophosphorylation. Instead DNA and the MRN complex are sufficient to facilitate dimer to monomer transitions *in vitro* (171).

DNA-PK is phosphorylated on over 30 residues of which many are autophosphorylation sites, including a highly conserved T3950. T3950 is a TQ and occurs in the activation loop based on comparisons to PI3K structures and secondary predictions of DNA-PK. Also T3950 resides between the classical DFG and APE motifs, which flank activation loops (187). ATR also contains DFG and APE motifs but lacks a conserved S/TQ (Figure 56). There are several conserved phospho-accepting residues, though, that may be phosphorylated. In future mutagenesis screens for activating mutations, this region may also be important to specifically target.

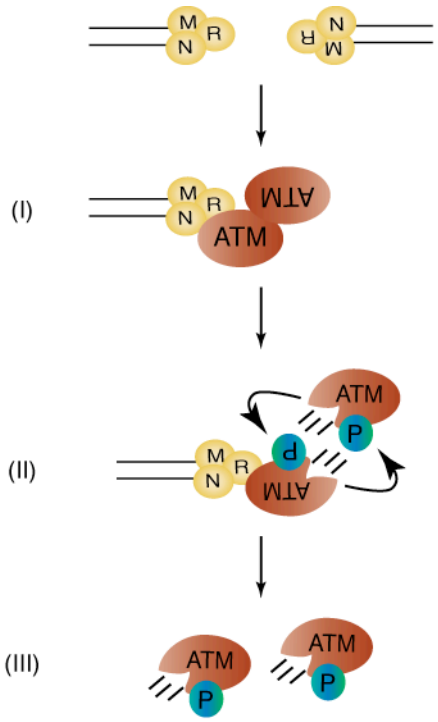


**Figure 55. Proposed model of ATM activation.** (I) Inactive ATM dimers are recruited to DNA double-strand breaks by the Mre11-Rad50-Nbs1 (MRN) complex. It is proposed that dimerization occurs via FAT-kinase domain interactions, which occlude the catalytic cleft. (II) The MRN complex activates ATM, and ATM autophosphorylates *in trans* on S1981 in the FAT domain. (III) The inactive dimer is converted to an active monomer. Whether S1981 autophosphorylation directly mediates this dimer to monomer transition is controversial. Note I have drawn only one DNA end and one MRN-ATM interaction, but it is not clear if the other inactive molecule of ATM also needs to interact with MRN. Also for simplicity, free monomers are depicted. However, ATM remains associated with chromatin due to interactions with MDC1.

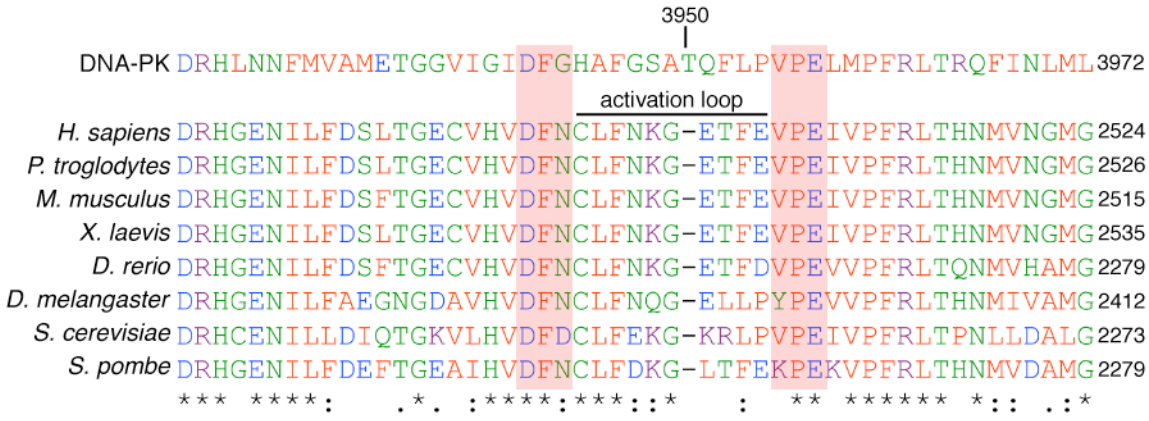


**Figure 56. Alignment of ATR activation loop.** ClustalW2 alignment of DNA-PK and ATR orthologs. T3950 indicates the DNA-PK activation loop autophosphorylation site. The DFG and APE motifs that flank activation loops are shaded in red. Amino acid properties are as follows: red – small, hydrophobic, aromatic except Y, blue – acidic, purple – basic except H, and green – hydroxyl, sufhydryl, amine, and G. Asterisks and dots denote the level of conservation among ATR orthologs only.

*A novel regulatory region*

In addition to T3950, only two other clusters of DNA-PK autophosphorylation have been extensively studied. One of these, the ABCDE cluster (T2609/S2612/T2638/T2647), occurs just N-terminal to the FAT domain and when mutated causes radiosensitivity (259). Based on *in vitro* data it is proposed that the ABCDE autophosphorylation cluster promotes kinase dissociation from Ku and DNA ends (Figure 57b) (182).

Mechanistically, DNA-PK autophosphorylation in the ABCDE cluster is thought to induce a conformational change in DNA-PK. This is based on low resolution structures that show movement of the C-terminal FAT, kinase, PRD, and FATC domains upon autophosphorylation (189). An unstructured flexible hinge region adjacent to the FAT domain is present in the DNA-PK crystal structure (Figure 57c) (218). Since the ABCDE cluster also occurs just N-terminal to the FAT domain, it is possible that ABCDE autophosphorylation occurs in this flexible hinge region. Indeed secondary predictions indicate that ABCDE sites occur in an inter-HEAT repeat loop, which is longer than a typical inter-repeat loop and predicted to contain little secondary structure (Figure 57a). An attractive model is that ABCDE autophosphorylation in the inter-HEAT repeat loop mediates the conformational change in the nearby FAT, kinase, PRD, and FATC domains.

Based on alignments by HEAT repeats (165), a region analogous to the extended inter-HEAT repeat region in DNA-PK also occurs in ATR and ATM (Figure 57a). In ATM and DNA-PK these loops are targeted for functional autophosphorylation (181, 184). 3A-ATR residues also occur in an extended inter-HEAT repeat loop adjacent to the ATR FAT domain. While 3A-ATR

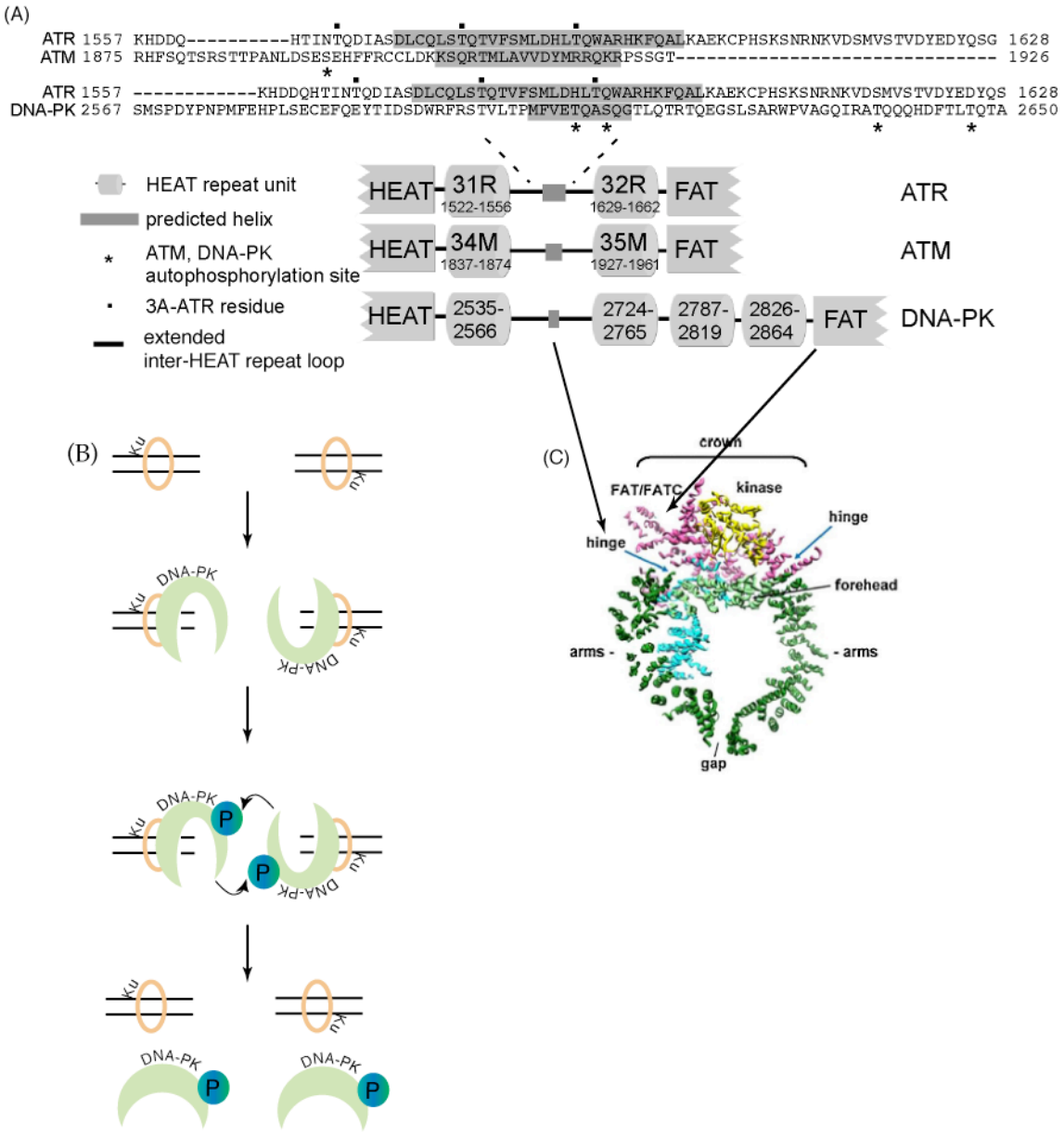


**Figure 57. An extended inter-HEAT repeat loop is a novel regulatory region shared among DNA damage PIKKs.** (A) Alignment of ATR and ATM by HEAT repeats as described by Perry and Kleckner (26). Secondary predictions generated by Jpred were used to align DNA-PK with ATR and ATM. (B) Model of the proposed function of DNA-PK ABCDE (T2609/S2612/T2638/T2647) autophosphorylation in this regulatory region. DNA-PK binding to DNA-bound Ku70/80 activates the kinase. ABCDE autophosphorylation causes DNA-PK to dissociate from Ku and DNA likely due to a conformation change observed in SAXS structures (189). (C) Reproduced and modified ribbon diagram of low resolution three-dimensional DNA-PK crystal structure from (218). N-terminal HEAT repeats are shown in green; FAT and FATC in magenta, putative DNA binding region in cyan, and kinase domain in yellow. Flexible unstructured hinge regions abut the FAT and FATC domain. The flexible region adjacent to the FAT domain may correspond to the extended inter-HEAT repeat loop in (A).

residues may not be phosphorylated, their mutation disrupted ATR function. This suggests that the region is also regulatory in ATR and identifies a previously unknown shared regulatory region among the DNA damage PIKKs.

The 3A-ATR region is present in all ATR orthologues. My preliminary data examining some of the conserved residues in the analogous region in $Mec1^{ATR}$ further support that this region is important for ATR function. One limitation of the FRVF1349AAAA mutant was that protein stability may have been affected by the mutations. In addition, there are other conserved residues in the region that could be examined. It is possible that a point mutation may give a similar phenotype without perturbing protein folding. If such a mutation were found, then a suppressor screen could provide interesting future directions to pursue.

*T1989 phosphorylation*

Three ATR phosphorylation sites appear in my mass spectrometry analysis and in several phospho-proteomic screens: S428, S435, and T1989. Of these, I find that T1989 is DNA damage-regulated, requires ATR kinase activity in cells, and occurs after ATR activation. T1989 is not essential for ATR signaling in cells, is not well conserved, and only causes a mild viability defect. Redundant phosphorylation may contribute to the lack of a phenotype.

Drawing parallels from other well studied kinases, T1989 phosphorylation in the ATR FAT domain may be part of signal amplification or possibly substrate selectivity. For instance, the Akt kinase contains two activating phosphorylation sites T308 in the activation loop and S473 on a hydrophobic motif outside the catalytic core. While T308 is required for Akt activation, S473 is not required for

growth factor stimulated Akt activity. However, S473 phosphorylation increases Akt kinase activity 10 fold (260). T1989 phosphorylation after TopBP1-mediated activation of ATR may function like Akt S473 phosphorylation and serve to amplify kinase activity. Defects in amplification may be more visible in normally proliferating cells with low levels of replication stress as compared to HU-treated cells. This could explain the mild viability defect but lack of checkpoint signaling defect with HU treatment. Examination of a phospho-mimicking T1989E ATR mutant *in vivo* may reveal that ATR-dependent signaling occurs with different kinetics.

Akt phosphorylation of some residues but not others in the FOXO proteins depends on S473 (261). This suggests that S473 phosphorylation may mediate substrate selectivity, or higher levels of kinase activity may be required to phosphorylate some substrates. Mutation of Serine 2035 in the mTOR FRB domain (rapamycin binding domain) also affects substrate selectivity (262). Note, the FRB domain occurs between the mTOR FAT and kinase domains and while given a distinct name, still consists of HEAT repeats. It is unclear if mTOR S2035 is phosphorylated, but this suggests that substrate selectivity in other PIKKs may be regulated by the FAT domain or regions nearby. While I observe no Chk1 phosphorylation defects, phosphorylation of other ATR targets may be perturbed with T1989 mutation. Alternatively, T1989 may not be part of the activation process. ATR oligomerizes, and phosphorylation in the FAT domain which is adjacent to the kinase domain may occur as a consequence of proximity and simply mark an active complex.

*Conflicting evidence for T1989 function*

The Lee group also reports that T1989 phosphorylation is DNA damage-regulated and is dependent on ATR kinase activity in cells. I demonstrate that T1989 phosphorylation is not essential for ATR activity or ATR signaling to Chk1. In contrast, the Lee study concludes that T1989 is essential for ATR function and Chk1 phosphorylation (263).

Lee *et al.* report that ATR flox cells integrated with a T1989A mutant cannot form colonies after *ATR* deletion in a colony formation assay. While I observe a mild colony forming defect, I can obtain many viable colonies from T1989A complemented ATR flox cells after excision of the floxed allele. These colonies can be expanded into cell lines, and they only express the integrated mutant as determined by RT-PCR and sequencing.

In my cellular complementation studies, I determine the expression levels of cell lines and importantly the percentage of cells within each line expressing exogenous ATR. The Lee study did not report whether the percent expressing exogenous ATR in their cell line is similar. This may be one source of discrepancy between our studies. Additionally, the cell cycle distribution of their mutant cell line is different from the wild-type cell line even prior to adenovirus infection or induction of exogenous protein expression.

Another major difference is that I do not observe defects in Chk1 phosphorylation on S317 after HU treatment in cells only expressing a T1989A mutant. However, the Lee group shows that Chk1 S345 phosphorylation after UV treatment requires T1989 phosphorylation. One possibility is that there may be differential requirements for T1989 phosphorylation after certain types of damage. Additionally as I described above, T1989 phosphorylation may dictate

substrate selectivity towards S345 but not S317 of Chk1. However if T1989 phosphorylation functioned in specific contexts, it is difficult to understand how it could be essential for ATR function.

Finally, Lee *et al.* do not provide an explanation for the essential function of T1989 yet the lack of conservation among ATR orthologues. This lack of conservation past primate ATR is particularly striking considering the FAT domain and activation mechanisms are well conserved. While the function of T1989 phosphorylation is unclear, data supports that it correlates with an active ATR kinase. An imperative future direction will be to assess the merit of T1989 phosphorylation as a predictive marker for response to therapies that cause DNA damage.

*Other post-translational modifications*

I have characterized T1989 and to some extent S428 and S435. I have also examined 16 candidate autophosphorylation sites. My *in vivo* phospho-peptide mapping studies illustrate that there are many more ATR phosphorylation sites that I have not characterized. A major challenge going forward will be to identify these phospho-residues and characterize their function. Other post-translational modifications may regulate ATR signaling as well. Regulatory acetylation catalyzed by Tip60 occurs in the ATM PRD (175, 176), but neither mutation of lysines in the ATR PRD nor *Tip60* silencing caused ATR signaling defects (90). While not a covalent modification, oxidation of conserved cysteine residues in the ATM FATC domain activates the ATM kinase independent of the MRN complex (264). While challenging, there remains much to be learned about ATR post-translational modifications.

*ATR function at replication forks*

New mechanistic insights in the ATR activation process are hampered by our lack of structural information. However, there has been rapid advancement in identifying new ATR functions using genetic ablation of ATR and mass spectrometry to identify ATR interacting proteins. Despite this, how ATR promotes fork stability and completion of replication after replication stress is not well understood. In addition when is ATR important? During fork stalling or during replication after stress? My inhibitor studies demonstrate that ATR activity is required during both times. However, my inhibitor studies do not address what the function of ATR is during these times.

For instance I observe that transient inhibition of ATR activity only when forks are stalled prevents cells from completing DNA replication after release from fork stalling agents. In fact, very little DNA incorporation is able to occur when cells are released from this condition, as observed by essentially no movement of the 2N DNA content peak after release. This suggests that there are very few competent replication forks. If forks irreversibly collapse, it would not explain why other origins cannot rescue them once the inhibitor is removed. The ATR-Chk1 pathway prevents new origin firing but allows dormant origin firing within pre-existing replication factors during replication stress (147, 265). Chk1 inhibitors also increase origin firing (266). One hypothesis is that too many origins have fired and have been exhausted. Future experiments examining DNA fibers under these conditions will give clues into the exact mechanism. Further, the development of iPOND, a technique that allows analysis of replication forks by purifying nascent DNA, will allow us to examine factors at the stalled forks (229). Recruitment of double-strand break repair proteins or other nucleases

would suggest that forks are collapsing or being remodeled in the absence of ATR.

*ATR signaling in the clinic*

I began to characterize one novel ATR inhibitor. During this time, three separate groups disclosed ATR inhibitors and reported the first characterization of these inhibitors in cells. Like AZ20, ATM and p53-deficiency sensitized cancer cells to ATR inhibition, and overexpression of the oncogene cyclin E in cells sensitized them to DDR inhibition (205, 206, 267). Important future directions in the use of ATR inhibitors in cancer therapy are to determine if certain molecular or genetic signatures can predict response to ATR inhibition. My discovery of ATR T1989 phosphorylation may provide a useful biomarker to answer these questions.

One issue with ATP analog kinase inhibitors, such as AZ20, is off-target inhibition of other related kinases. Another important approach for inhibiting ATR signaling will be to develop peptide based inhibitors (268). For instance, the RPA70N basic cleft mediates ATR-ATRIP recruitment to stalled forks as well as p53 and MRE11. The PRD may also be a promising peptide based inhibitor, since TopBP1 binding to ATR occurs in the PRD.

*ATR function at the centrosome*

While centrosome biology is well outside my area of study, I end my dissertation with a brief discussion on intriguing connections between ATR and centrosomes. Centrosomes are microtubule organizing centers whose function and number are crucial for chromosome segregation. Like the genome,

centrosome duplication occurs in S phase and must occur only once per cell cycle (269). Extra copies of centrosomes (supernumerary) has been observed in nearly early tumor type, and it is hypothesized that mis-segregation of chromosomes due to supernumerary centrosomes contributes to genomic instability (270). In addition to chromosome segregation, centrosome position determines cleavage plane orientation during cytokinesis for asymmetric cell division in some stem cells (271).

There is enticing evidence that ATR may regulate centrosomes. First, ATR localizes to the centrosome (272), and *ATR* silencing induces centrosome re-duplication (273). A large-scale screen for ATM and ATR substrates identified many centrosome components (127, 128). Third, a hypomorphic allele of *ATR* causes Seckel syndrome, and supernumerary centrosomes are observed in patient cells (274). Furthermore Seckel syndrome is a disease characterized by microcephaly and growth retardation. Autosomal recessive mutations in other centrosome proteins also cause microcephaly (275). It is thought that centrosome dysfunction disrupts cleavage plane orientation in neural crest stem cells during development, resulting in defects in asymmetric stem cell division and microcephaly (Figure 58a) (276). Other centrosome proteins such as Pericentrin, CEP152, CEP164, and CENPJ also cause Seckel syndrome (275). These centrosome proteins also function in ATR signaling, and many DNA damage response proteins localize and signal at the centrosome (272, 277-279).

These links between ATR and centrosome biology while tantalizing are preliminary. However, the hypothesis that ATR regulates centrosome function may be an interesting one to test. *ATR* deletion in mice results in stem cell exhaustion (280, 281). The widely accepted explanation is that this is due to

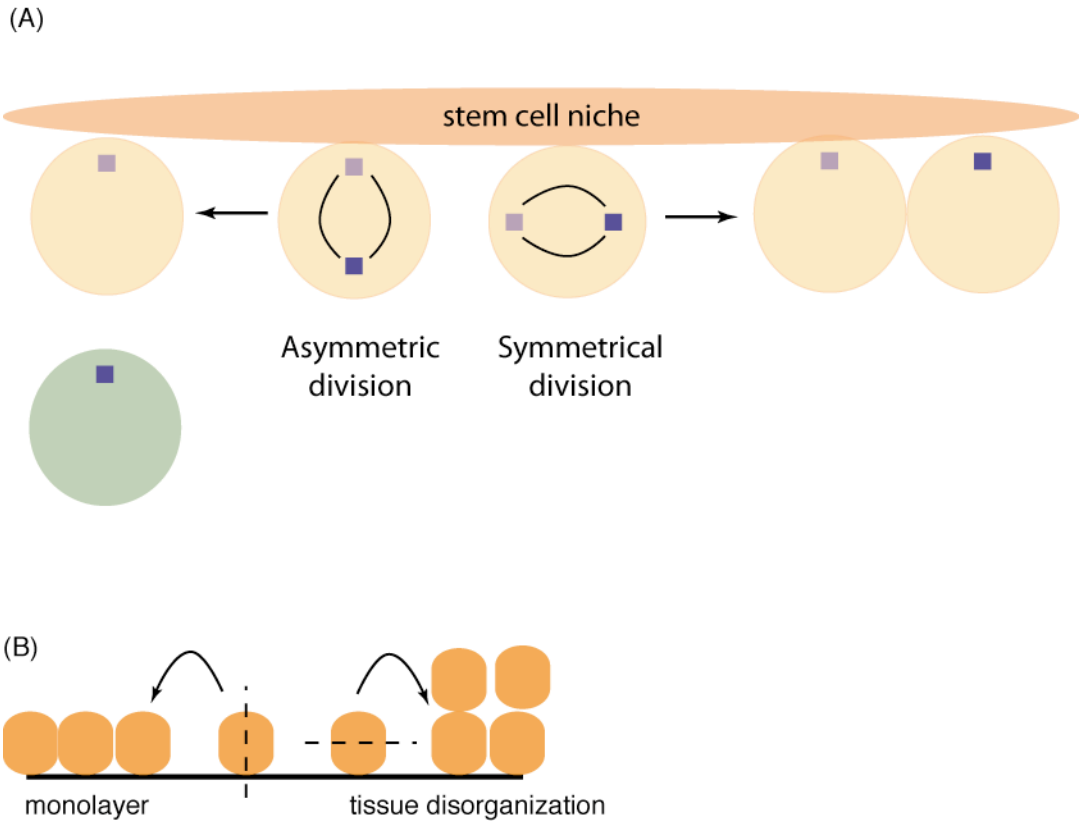


**Figure 58. Centrosome position and asymmetric stem cell division.** (A) One mechanism through which stem cells asymmetrically divide is by orienting spindle pole formation via centrosome positioning. Centrosome positions perpendicular to the external stem cell determinants results in one cell close to stem cell factors and one cell further away. Parallel centrosome orientation results in symmetric division with both cells close to stem determinants. Mis-orientation could perturb stem cell division and cause developmental defects. Supernumery also could disrupt correct cleavage orientation. (B) Changes in cleavage orientation may also contribute to cancer development. Apical-basal orientation of centrosomes may create tissue disorganization.

replication stress and proliferation defects in the stem cell niche. However, centrosome dysfunction due to *ATR* deletion could also deplete stem cells by perturbing asymmetric division of stem cells. If this were true, this would expand the field of ATR study greatly into stem cell and cancer stem cell biology. Supernumerary centrosomes are thought to contribute to chromosomal aberrations found in tumors, but perhaps mis-regulation of cleavage planes due to centrosome amplification contributes to the production of cancer stem cells and tissue disorganization (Figure 58b) (282).

Another reason why it is attractive to hypothesize that ATR may regulate centrosome duplication is that, like chromosome duplication, centrosome duplication occurs in S phase and must occur only once (Figure 59) (269). In some tumor-derived cell lines extreme lengthening of S phase with DNA synthesis inhibitors such as HU and aphidicolin induces centrosome re-duplication through some unknown mechanism (269). Since ATR is a master regulator of the S phase checkpoint, it may also coordinate centrosome duplication as part of the intra-S phase checkpoint to prevent re-duplication. The molecular mechanisms governing centrosome duplication are not well understood, making it difficult to speculate how ATR might regulate the process.

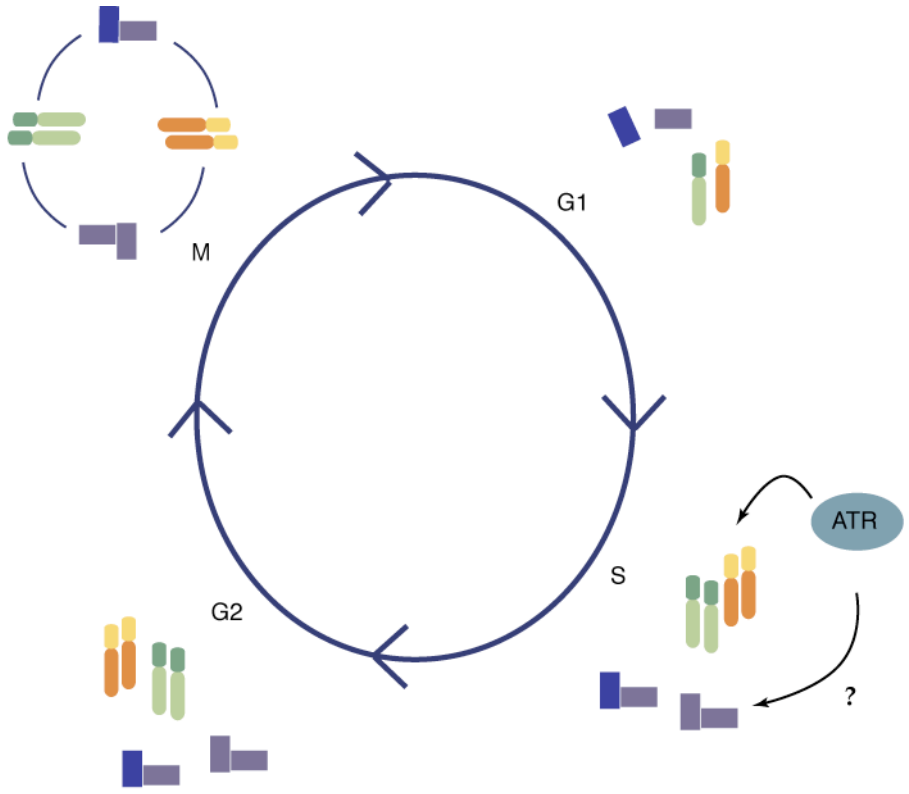


**Figure 59. Centrosome and chromosome duplication cycles.** Both centrosomes and chromosomes are duplicated in S phase and should be duplicated exactly once per cell cycle. Re-duplication of chromosomes or centrosomes leads to changes in ploidy and genome instability. Though purely speculative, ATR may coordinate chromosome and centrosome duplication when there is replication stress.

# APPENDIX A

## ATR S428 AND S435

*S428*

I and others identified S428 and S435 as ATR phosphorylation sites by mass spectrometry (Chapter III, (125, 126)). I examined the DNA damage-dependency of ATR S428 phosphorylation using a commercially available phospho-peptide specific antibody to S428 (Cell Signaling). Unlike T1989 phosphorylation, S428 phosphorylation did not increase after HU treatment (Figure 60a), suggesting S428 phosphorylation is not DNA damage-regulated. Caffeine, a non-specific inhibitor of ATR and ATM, inhibited HU-induced ATR-dependent Chk1 phosphorylation but did not reduce ATR S428 phosphorylation (Figure 60a). Since S428 is not damage-regulated and does not correlate with ATR activity, it is not a useful marker for active ATR.

My preliminary data indicates that ATR S428 phosphorylation is unlikely to be critical for the essential function of ATR to promote viability. I integrated WT-ATR and S428A mutant constructs into the $ATR^{flox/-}$TR cell line and examined colony formation following deletion of the floxed allele. 64% of WT-ATR cells formed colonies. Colony formation was not consistent between the two independent ATR-S428A cell lines. 62% of S428A2 cells formed colonies while only 29% of S428A1 cells formed colonies (Figure 60b). Western blot analysis of ATR expression levels revealed that S428A1 expresses substantially lower amounts of ATR protein compared to the WT-ATR integrant.

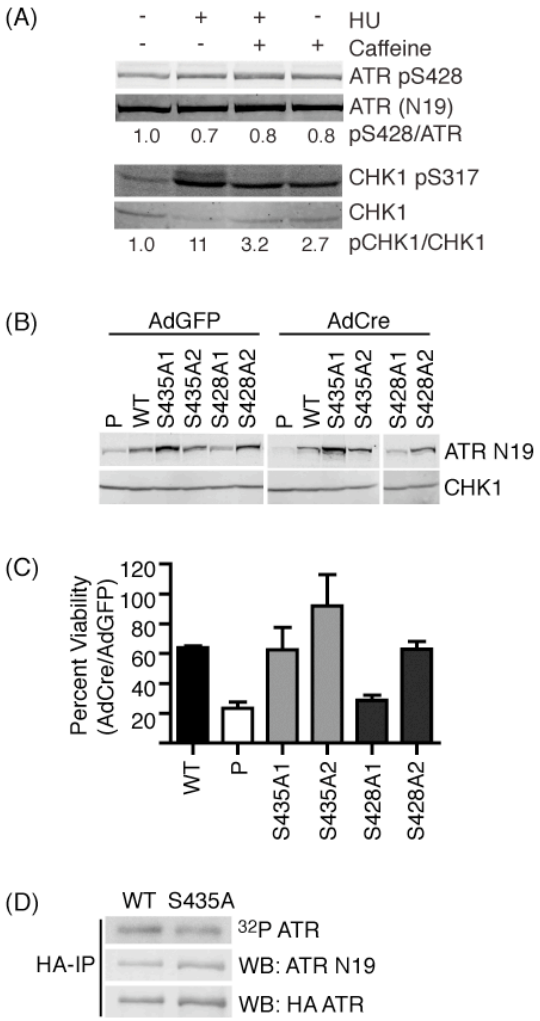


**Figure 60. S428 and S435 are dispensable for ATR function.** (A) 293T cells were treated with HU and caffeine as indicated for 6 hours. Total cell lysates were separated by SDS-PAGE and immunoblotted with the indicated antibodies. Infrared-conjugated secondary antibodies and an Odyssey instrument were used to quantify western blots. (B-C) Parental (P) ATR$^{flox/-}$TR, WT-ATR$^{flox/-}$TR, two clones of S428A-ATR$^{flox/-}$TR, and two clones of S435A-ATR$^{flox/-}$TR cells were treated with tetracycline and infected with adenovirus encoding Cre-recombinase or GFP control. (B) Cell lysates were immunoblotted for ATR and CHK1. (C) Infected cells were plated at low density and then cultured for 14 days in the presence of tetracycline. Surviving colonies were methylene blue stained and counted (n=5). (D) HA-immunoprecipitates from $^{32}$P labeled 293T cells transiently expressing HA-WT-ATR and HA-S435A-ATR were immunoblotted with the indicated antibodies. Blots were exposed to film to visualize $^{32}$P incorporation.

However, ATR expression in the S428A2 cell line, which supported viability similar to WT-ATR cells, is similar to the WT-ATR cell line (Figure 60a). Poor complementation of S428A1 may be a possible explanation for the low colony forming ability observed in S428A1 cells. Analysis of additional S428A-ATR$^{flox/-}$TR cell lines with similar expression to WT-ATR cells will be necessary to definitively determine whether S428 is important for ATR function.

*ATR S435*

An antibody to ATR S435 phosphorylation is not available. However, I confirmed that the S435 to alanine mutation reduces phosphorylation of the mutant protein by metabolically labeling HU-treated cells transiently expressing HA-epitope tagged WT-ATR and S435A-ATR with $^{32}$P-orthophosphate and HA-immunopurifying labeled HA-ATR. The S435A mutant incorporated less $^{32}$P *in vivo* compared to WT-ATR (Figure 60c), supporting that the mutation perturbs ATR phosphorylation. Whether DNA damage regulates this phosphorylation cannot be concluded from this experiment.

I assessed whether S435 is required for the essential function of ATR to promote viability using the genetic complementation assay. 23% of uncomplemented parental ATR$^{flox/-}$TR cells formed colonies after deletion of the floxed allele. Integration of WT-ATR rescued viability with 64% of cells forming colonies. Similarly, two independent S435A-ATR$^{flox/-}$ cell lines expressing at least the same amount of ATR protein as the WT-ATR cell line formed colonies at 62% and 92% (Figure 60b). This suggests that S435 is dispensable for the essential function of ATR.

S428 and S435 analysis suggest that the phosphorylation sites are dispensable for the essential function of ATR. However, the two phosphorylation sites may be functionally redundant. Analysis of a double S428A/S435A mutant may give different results. S435 is one of three consecutive serines, and redundancy or priming may be functioning at this site. I also only examined the effects of the mutations on cellular viability. ATR has many functions that may not be essential or readily observed in the genetic complementation assay. Examination of these mutants in different contexts and in different checkpoint assays may give different results.

# REFERENCES


1. Malumbres M & Barbacid M (2001) To cycle or not to cycle: a critical decision in cancer. Nat Rev Cancer 1(3):222-231.

2. Hanahan D & Weinberg RA (2000) The hallmarks of cancer. Cell 100(1):57-70.

3. Hanahan D & Weinberg RA (2011) Hallmarks of cancer: the next generation. Cell 144(5):646-674.

4. Jackson SP & Bartek J (2009) The DNA-damage response in human biology and disease. Nature 461(7267):1071-1078.

5. Kato J, Matsushime H, Hiebert SW, Ewen ME, & Sherr CJ (1993) Direct binding of cyclin D to the retinoblastoma gene product (pRb) and pRb phosphorylation by the cyclin D-dependent kinase CDK4. Genes Dev 7(3):331-342.

6. Sun A, Bagella L, Tutton S, Romano G, & Giordano A (2007) From G0 to S phase: a view of the roles played by the retinoblastoma (Rb) family members in the Rb-E2F pathway. J Cell Biochem 102(6):1400-1404.

7. Ekholm SV & Reed SI (2000) Regulation of G(1) cyclin-dependent kinases in the mammalian cell cycle. Curr Opin Cell Biol 12(6):676-684.

8. Randell JC, Bowers JL, Rodriguez HK, & Bell SP (2006) Sequential ATP hydrolysis by Cdc6 and ORC directs loading of the Mcm2-7 helicase. Mol Cell 21(1):29-39.

9. Bell SP & Dutta A (2002) DNA replication in eukaryotic cells. Annu Rev Biochem 71:333-374.

10. Machida YJ, Hamlin JL, & Dutta A (2005) Right place, right time, and only once: replication initiation in metazoans. Cell 123(1):13-24.

11. Walter J & Newport J (2000) Initiation of eukaryotic DNA replication: origin unwinding and sequential chromatin association of Cdc45, RPA, and DNA polymerase alpha. Mol Cell 5(4):617-627.

12. Pursell ZF, Isoz I, Lundstrom EB, Johansson E, & Kunkel TA (2007) Yeast DNA polymerase epsilon participates in leading-strand DNA replication. Science 317(5834):127-130.

13. Nick McElhinny SA, Gordenin DA, Stith CM, Burgers PM, & Kunkel TA (2008) Division of labor at the eukaryotic replication fork. Mol Cell 30(2):137-144.

14. Tanaka S & Araki H (2010) Regulation of the initiation step of DNA replication by cyclin-dependent kinases. Chromosoma 119(6):565-574.

15. Arias EE & Walter JC (2007) Strength in numbers: preventing rereplication via multiple mechanisms in eukaryotic cells. Genes Dev 21(5):497-518.

16. Rieder CL (2011) Mitosis in vertebrates: the G2/M and M/A transitions and their associated checkpoints. Chromosome Res 19(3):291-306.

17. Hartwell LH & Weinert TA (1989) Checkpoints: controls that ensure the order of cell cycle events. Science 246(4930):629-634.

18. Cimprich KA & Cortez D (2008) ATR: an essential regulator of genome integrity. Nat Rev Mol Cell Biol 9:616-627.

19. Kim ST, Lim DS, Canman CE, & Kastan MB (1999) Substrate specificities and identification of putative substrates of ATM kinase family members. J Biol Chem 274(53):37538-37543.

20. O'Neill T, Dwyer AJ, Ziv Y, Chan DW, Lees-Miller SP, Abraham RH, Lai JH, Hill D, Shiloh Y, Cantley LC, & Rathbun GA (2000) Utilization of oriented peptide libraries to identify substrate motifs selected by ATM. J Biol Chem 275(30):22719-22727.

21. Bartek J & Lukas J (2001) Mammalian G1- and S-phase checkpoints in response to DNA damage. Curr Opin Cell Biol 13(6):738-747.

22. Pietenpol JA & Stewart ZA (2002) Cell cycle checkpoint signaling: cell cycle arrest versus apoptosis. Toxicology 181-182:475-481.

23. Lavin MF (2008) Ataxia-telangiectasia: from a rare disorder to a paradigm for cell signalling and cancer. Nat Rev Mol Cell Biol 9(10):759-769.

24. Boutros R, Dozier C, & Ducommun B (2006) The when and wheres of CDC25 phosphatases. Curr Opin Cell Biol 18(2):185-191.

25. Boutros R, Lobjois V, & Ducommun B (2007) CDC25 phosphatases in cancer cells: key players? Good targets? Nat Rev Cancer 7(7):495-507.

26. Bartek J & Lukas J (2003) Chk1 and Chk2 kinases in checkpoint control and cancer. Cancer Cell 3(5):421-429.

27. Brown EJ & Baltimore D (2003) Essential and dispensable roles of ATR in cell cycle arrest and genome maintenance. Genes Dev 17(5):615-628.

28. Chen Y & Sanchez Y (2004) Chk1 in the DNA damage response: conserved roles from yeasts to mammals. DNA Repair (Amst) 3(8-9):1025-1032.

29. Cortez D & Elledge SJ (2000) Conducting the mitotic symphony. Nature 406(6794):354-356.

30. Branzei D & Foiani M (2010) Maintaining genome stability at the replication fork. Nat Rev Mol Cell Biol 11(3):208-219.

31. Cimprich KA (2003) Fragile sites: breaking up over a slowdown. Curr Biol 13(6):R231-233.

32. Cortez D (2005) Unwind and slow down: checkpoint activation by helicase and polymerase uncoupling. Genes Dev 19(9):1007-1012.

33. MacDougall CA, Byun TS, Van C, Yee MC, & Cimprich KA (2007) The structural determinants of checkpoint activation. Genes Dev 21(8):898-903.

34. Zhao H & Piwnica-Worms H (2001) ATR-mediated checkpoint pathways regulate phosphorylation and activation of human Chk1. Mol Cell Biol 21(13):4129-4139.

35. Paulsen RD & Cimprich KA (2007) The ATR pathway: fine-tuning the fork. DNA Repair (Amst) 6(7):953-966.

36. Cortez D, Guntuku S, Qin J, & Elledge SJ (2001) ATR and ATRIP: partners in checkpoint signaling. Science 294(5547):1713-1716.

37. Brown EJ & Baltimore D (2000) ATR disruption leads to chromosomal fragmentation and early embryonic lethality. Genes Dev 14(4):397-402.

38. de Klein A, Muijtjens M, van Os R, Verhoeven Y, Smit B, Carr AM, Lehmann AR, & Hoeijmakers JH (2000) Targeted disruption of the cell-cycle checkpoint gene ATR leads to early embryonic lethality in mice. Curr Biol 10(8):479-482.

39. Rudolph CJ, Upton AL, & Lloyd RG (2007) Replication fork stalling and cell cycle arrest in UV-irradiated Escherichia coli. Genes Dev 21(6):668-681.

40. Cobb JA, Schleker T, Rojas V, Bjergbaek L, Tercero JA, & Gasser SM (2005) Replisome instability, fork collapse, and gross chromosomal rearrangements arise synergistically from Mec1 kinase and RecQ helicase mutations. Genes Dev 19(24):3055-3069.

41. Sogo JM, Lopes M, & Foiani M (2002) Fork reversal and ssDNA accumulation at stalled replication forks owing to checkpoint defects. Science 297(5581):599-602.

42. Cortes-Ledesma F & Aguilera A (2006) Double-strand breaks arising by replication through a nick are repaired by cohesin-dependent sister-chromatid exchange. EMBO Rep 7(9):919-926.

43. Aguilera A & Klein HL (1988) Genetic control of intrachromosomal recombination in Saccharomyces cerevisiae. I. Isolation and genetic characterization of hyper-recombination mutations. Genetics 119(4):779-790.

44. Liang DT, Hodson JA, & Forsburg SL (1999) Reduced dosage of a single fission yeast MCM protein causes genetic instability and S phase delay. J Cell Sci 112(Pt 4):559-567.

45. Shima N, Alcaraz A, Liachko I, Buske TR, Andrews CA, Munroe RJ, Hartford SA, Tye BK, & Schimenti JC (2007) A viable allele of Mcm4 causes chromosome instability and mammary adenocarcinomas in mice. Nat Genet 39(1):93-98.

46. Chen C, Umezu K, & Kolodner RD (1998) Chromosomal rearrangements occur in S. cerevisiae rfa1 mutator mutants due to mutagenic lesions processed by double-strand-break repair. Mol Cell 2(1):9-22.

47. Myung K & Kolodner RD (2002) Suppression of genome instability by redundant S-phase checkpoint pathways in Saccharomyces cerevisiae. Proc Natl Acad Sci U S A 99(7):4500-4507.

48. Casper AM, Nghiem P, Arlt MF, & Glover TW (2002) ATR regulates fragile site stability. Cell 111(6):779-789.

49. Myung K, Smith S, Gupta A, & Kolodner RD (2005) Suppression of gross chromosomal rearrangements by the multiple functions of the Mre11-Rad50-Xrs2 complex in Saccharomyces cerevisiae. DNA Repair 4(5):606-617.

50. Pichierri P, Rosselli F, & Franchitto A (2003) Werner's syndrome protein is phosphorylated in an ATR/ATM-dependent manner following replication arrest and DNA damage induced during the S phase of the cell cycle. Oncogene 22(10):1491-1500.

51. Kolodner RD, Myung K, Datta A, & Chen C (2001) SGS1, the Saccharomyces cerevisiae homologue of BLM and WRN, suppresses genome instability and homeologous recombination. Nature Genetics 27(1):113-116.

52. Chu WK & Hickson ID (2009) RecQ helicases: multifunctional genome caretakers. Nat Rev Cancer 9(9):644-654.

53. O'Driscoll M, Ruiz-Perez VL, Woods CG, Jeggo PA, & Goodship JA (2003) A splicing mutation affecting expression of ataxia-telangiectasia and Rad3-related protein (ATR) results in Seckel syndrome. Nat Genet 33(4):497-501.

54. Alderton GK, Joenje H, Varon R, Borglum AD, Jeggo PA, & O'Driscoll M (2004) Seckel syndrome exhibits cellular features demonstrating defects in the ATR-signalling pathway. Hum Mol Genet 13(24):3127-3138.

55. Zighelboim I, Schmidt AP, Gao F, Thaker PH, Powell MA, Rader JS, Gibb RK, Mutch DG, & Goodfellow PJ (2009) ATR mutation in endometrioid endometrial cancer is associated with poor clinical outcomes. J Clin Oncol 27(19):3091-3096.

56. Menoyo A, Alazzouzi H, Espin E, Armengol M, Yamamoto H, & Schwartz S, Jr. (2001) Somatic mutations in the DNA damage-response genes ATR and CHK1 in sporadic stomach tumors with microsatellite instability. Cancer Res 61(21):7727-7730.

57. Liu H, Takeda S, Kumar R, Westergard TD, Brown EJ, Pandita TK, Cheng EH, & Hsieh JJ (2010) Phosphorylation of MLL by ATR is required for execution of mammalian S-phase checkpoint. Nature 467(7313):343-346.

58. Tibbetts RS, Cortez D, Brumbaugh KM, Scully R, Livingston D, Elledge SJ, & Abraham RT (2000) Functional interactions between BRCA1 and the checkpoint kinase ATR during genotoxic stress. Genes Dev 14(23):2989-3002.

59. Heinen CD, Schmutte C, & Fishel R (2002) DNA repair and tumorigenesis: lessons from hereditary cancer syndromes. Cancer Biol Ther 1(5):477-485.

60. Nowell PC (1976) The clonal evolution of tumor cell populations. Science 194(4260):23-28.

61. Loeb LA (1991) Mutator phenotype may be required for multistage carcinogenesis. Cancer Res 51(12):3075-3079.

62. Fishel R, Lescoe MK, Rao MR, Copeland NG, Jenkins NA, Garber J, Kane M, & Kolodner R (1993) The human mutator gene homolog MSH2 and its association with hereditary nonpolyposis colon cancer. Cell 75(5):1027-1038.

63. Kennedy RD & D'Andrea AD (2006) DNA repair pathways in clinical practice: lessons from pediatric cancer susceptibility syndromes. J Clin Oncol 24(23):3799-3808.

64. Ding L, Getz G, Wheeler DA, Mardis ER, McLellan MD, Cibulskis K, Sougnez C, Greulich H, Muzny DM, Morgan MB, Fulton L, Fulton RS, Zhang Q, Wendl MC, Lawrence MS, Larson DE, Chen K, Dooling DJ, Sabo A, Hawes AC, Shen H, Jhangiani SN, Lewis LR, Hall O, Zhu Y, Mathew T, Ren Y, Yao J, Scherer SE, Clerc K, Metcalf GA, Ng B, Milosavljevic A, Gonzalez-Garay ML, Osborne JR, Meyer R, Shi X, Tang Y, Koboldt DC, Lin L, Abbott R, Miner TL, Pohl C, Fewell G, Haipek C, Schmidt H, Dunford-Shore BH, Kraja A, Crosby SD, Sawyer CS, Vickery T, Sander S, Robinson J, Winckler W, Baldwin J, Chirieac LR, Dutt A, Fennell T, Hanna M, Johnson BE, Onofrio RC, Thomas RK, Tonon G, Weir BA, Zhao X, Ziaugra L, Zody MC, Giordano T, Orringer MB, Roth JA, Spitz MR, Wistuba, II, Ozenberger B, Good PJ, Chang AC, Beer DG, Watson MA, Ladanyi M, Broderick S, Yoshizawa A, Travis WD, Pao W, Province MA, Weinstock GM, Varmus HE, Gabriel SB, Lander ES, Gibbs RA, Meyerson M, & Wilson RK (2008) Somatic mutations affect key pathways in lung adenocarcinoma. Nature 455(7216):1069-1075.

65. Sjoblom T, Jones S, Wood LD, Parsons DW, Lin J, Barber TD, Mandelker D, Leary RJ, Ptak J, Silliman N, Szabo S, Buckhaults P, Farrell C, Meeh P, Markowitz SD, Willis J, Dawson D, Willson JK, Gazdar AF, Hartigan J, Wu L, Liu C, Parmigiani G, Park BH, Bachman KE, Papadopoulos N, Vogelstein B, Kinzler KW, & Velculescu VE (2006) The consensus coding sequences of human breast and colorectal cancers. Science 314(5797):268-274.

66. Wood LD, Parsons DW, Jones S, Lin J, Sjoblom T, Leary RJ, Shen D, Boca SM, Barber T, Ptak J, Silliman N, Szabo S, Dezso Z, Ustyanksky V, Nikolskaya T, Nikolsky Y, Karchin R, Wilson PA, Kaminker JS, Zhang Z, Croshaw R, Willis J, Dawson D, Shipitsin M, Willson JK, Sukumar S, Polyak K, Park BH, Pethiyagoda CL, Pant PV, Ballinger DG, Sparks AB, Hartigan J, Smith DR, Suh E, Papadopoulos N, Buckhaults P, Markowitz SD, Parmigiani G, Kinzler KW, Velculescu VE, & Vogelstein B (2007) The genomic landscapes of human breast and colorectal cancers. Science 318(5853):1108-1113.

67. Jones S, Zhang X, Parsons DW, Lin JC, Leary RJ, Angenendt P, Mankoo P, Carter H, Kamiyama H, Jimeno A, Hong SM, Fu B, Lin MT, Calhoun ES, Kamiyama M, Walter K, Nikolskaya T, Nikolsky Y, Hartigan J, Smith DR, Hidalgo M, Leach SD, Klein AP, Jaffee EM, Goggins M, Maitra A, Iacobuzio-Donahue C, Eshleman JR, Kern SE, Hruban RH, Karchin R, Papadopoulos N, Parmigiani G, Vogelstein B, Velculescu VE, & Kinzler KW (2008) Core signaling pathways in human pancreatic cancers revealed by global genomic analyses. Science 321(5897):1801-1806.

68. Parsons DW, Jones S, Zhang X, Lin JC, Leary RJ, Angenendt P, Mankoo P, Carter H, Siu IM, Gallia GL, Olivi A, McLendon R, Rasheed BA, Keir S, Nikolskaya T, Nikolsky Y, Busam DA, Tekleab H, Diaz LA, Jr., Hartigan J, Smith DR, Strausberg RL, Marie SK, Shinjo SM, Yan H, Riggins GJ, Bigner DD, Karchin R, Papadopoulos N, Parmigiani G, Vogelstein B, Velculescu VE, & Kinzler KW (2008) An integrated genomic analysis of human glioblastoma multiforme. Science 321(5897):1807-1812.

69. Negrini S, Gorgoulis VG, & Halazonetis TD (2010) Genomic instability--an evolving hallmark of cancer. Nat Rev Mol Cell Biol 11(3):220-228.

70. Bartkova J, Horejsi Z, Koed K, Kramer A, Tort F, Zieger K, Guldberg P, Sehested M, Nesland JM, Lukas C, Orntoft T, Lukas J, & Bartek J (2005) DNA damage response as a candidate anti-cancer barrier in early human tumorigenesis. Nature 434(7035):864-870.

71. Gorgoulis VG, Vassiliou LV, Karakaidos P, Zacharatos P, Kotsinas A, Liloglou T, Venere M, Ditullio RA, Jr., Kastrinakis NG, Levy B, Kletsas D, Yoneta A, Herlyn M, Kittas C, & Halazonetis TD (2005) Activation of the DNA damage checkpoint and genomic instability in human precancerous lesions. Nature 434(7035):907-913.

72. Bartkova J, Rezaei N, Liontos M, Karakaidos P, Kletsas D, Issaeva N, Vassiliou LV, Kolettas E, Niforou K, Zoumpourlis VC, Takaoka M, Nakagawa H, Tort F, Fugger K, Johansson F, Sehested M, Andersen CL, Dyrskjot L, Orntoft T, Lukas J, Kittas C, Helleday T, Halazonetis TD, Bartek J, & Gorgoulis VG (2006) Oncogene-induced senescence is part of the tumorigenesis barrier imposed by DNA damage checkpoints. Nature 444(7119):633-637.

73. Bartek J, Bartkova J, & Lukas J (2007) DNA damage signalling guards against activated oncogenes and tumour progression. Oncogene 26(56):7773-7779.

74. Halazonetis TD, Gorgoulis VG, & Bartek J (2008) An oncogene-induced DNA damage model for cancer development. Science 319(5868):1352-1355.

75. Glover TW, Arlt MF, Casper AM, & Durkin SG (2005) Mechanisms of common fragile site instability. Hum Mol Genet 14 Spec No. 2:R197-205.

76. Fanning E, Klimovich V, & Nager AR (2006) A dynamic model for replication protein A (RPA) function in DNA processing pathways. Nucleic Acids Res 34(15):4126-4137.

77. Liu JS, Kuo SR, & Melendy T (2006) Phosphorylation of replication protein A by S-phase checkpoint kinases. DNA Repair (Amst) 5(3):369-380.

78. Brush GS, Morrow DM, Hieter P, & Kelly TJ (1996) The ATM homologue MEC1 is required for phosphorylation of replication protein A in yeast. Proc Natl Acad Sci U S A 93(26):15075-15080.

79. Binz SK, Sheehan AM, & Wold MS (2004) Replication Protein A phosphorylation and the cellular response to DNA damage. DNA Repair (Amst) 3(8-9):1015-1024.

80. Cimprich KA (2007) Probing ATR activation with model DNA templates. Cell Cycle 6(19):2348-2354.

81. Byun TS, Pacek M, Yee MC, Walter JC, & Cimprich KA (2005) Functional uncoupling of MCM helicase and DNA polymerase activities activates the ATR-dependent checkpoint. Genes Dev 19(9):1040-1052.

82. Heller RC & Marians KJ (2006) Replication fork reactivation downstream of a blocked nascent leading strand. Nature 439(7076):557-562.

83. Huertas P (2010) DNA resection in eukaryotes: deciding how to fix the break. Nat Struct Mol Biol 17(1):11-16.

84. Ball HL, Myers JS, & Cortez D (2005) ATRIP Binding to RPA-ssDNA Promotes ATR-ATRIP Localization but Is Dispensable for Chk1 Phosphorylation. Mol Biol Cell 16:2372-2381.

85. Zou L & Elledge SJ (2003) Sensing DNA damage through ATRIP recognition of RPA-ssDNA complexes. Science 300(5625):1542-1548.

86. Barr SM, Leung CG, Chang EE, & Cimprich KA (2003) ATR kinase activity regulates the intranuclear translocation of ATR and RPA following ionizing radiation. Curr Biol 13(12):1047-1051.

87. Ball HL, Ehrhardt MR, Mordes DA, Glick GG, Chazin WJ, & Cortez D (2007) Function of a conserved checkpoint recruitment domain in ATRIP proteins. Mol Cell Biol 27(9):3367-3377.

88. Bomgarden RD, Yean D, Yee MC, & Cimprich KA (2004) A novel protein activity mediates DNA binding of an ATR-ATRIP complex. J Biol Chem 279(14):13346-13353.

89. Nam EA & Cortez D (2011) ATR signalling: more than meeting at the fork. Biochem J 436(3):527-536.

90. Mordes DA, Glick GG, Zhao R, & Cortez D (2008) TopBP1 activates ATR through ATRIP and a PIKK regulatory domain. Genes Dev 22(11):1478-1489.

91. Myers JS, Zhao R, Xu X, Ham AJ, & Cortez D (2007) Cyclin-dependent kinase 2 dependent phosphorylation of ATRIP regulates the G2-M checkpoint response to DNA damage. Cancer Res 67(14):6685-6690.

92. Venere M, Snyder A, Zgheib O, & Halazonetis TD (2007) Phosphorylation of ATR-interacting protein on Ser239 mediates an interaction with breast-ovarian cancer susceptibility 1 and checkpoint function. Cancer Res 67(13):6100-6105.

93. Ellison V & Stillman B (2003) Biochemical characterization of DNA damage checkpoint complexes: clamp loader and clamp complexes with specificity for 5' recessed DNA. PLoS Biol 1(2):E33.

94. Bermudez VP, Lindsey-Boltz LA, Cesare AJ, Maniwa Y, Griffith JD, Hurwitz J, & Sancar A (2003) Loading of the human 9-1-1 checkpoint complex onto DNA by the checkpoint clamp loader hRad17-replication factor C complex in vitro. Proc Natl Acad Sci U S A 100(4):1633-1638.

95. Xu X, Vaithiyalingam S, Glick GG, Mordes DA, Chazin WJ, & Cortez D (2008) The basic cleft of RPA70N binds multiple checkpoint proteins including RAD9 to regulate ATR signaling. Mol Cell Biol 28(24):7345-7353.

96. Iftode C & Borowiec JA (2000) 5' --> 3' molecular polarity of human replication protein A (hRPA) binding to pseudo-origin DNA substrates. Biochemistry 39(39):11970-11981.

97. de Laat WL, Appeldoorn E, Sugasawa K, Weterings E, Jaspers NG, & Hoeijmakers JH (1998) DNA-binding polarity of human replication protein A positions nucleases in nucleotide excision repair. Genes Dev 12(16):2598-2609.

98. Kim HS & Brill SJ (2001) Rfc4 interacts with Rpa1 and is required for both DNA replication and DNA damage checkpoints in Saccharomyces cerevisiae. Mol Cell Biol 21(11):3725-3737.

99. Michael WM, Ott R, Fanning E, & Newport J (2000) Activation of the DNA replication checkpoint through RNA synthesis by primase. Science 289(5487):2133-2137.

100. Van C, Yan S, Michael WM, Waga S, & Cimprich KA (2010) Continued primer synthesis at stalled replication forks contributes to checkpoint activation. J Cell Biol 189(2):233-246.

101. Delacroix S, Wagner JM, Kobayashi M, Yamamoto K, & Karnitz LM (2007) The Rad9-Hus1-Rad1 (9-1-1) clamp activates checkpoint signaling via TopBP1. Genes Dev 21(12):1472-1477.

102. Lee J, Kumagai A, & Dunphy WG (2007) The Rad9-Hus1-Rad1 checkpoint clamp regulates interaction of TopBP1 with ATR. J Biol Chem 282(38):28036-28044.

103. Navadgi-Patil VM & Burgers PM (2009) The unstructured C-terminal tail of the 9-1-1 clamp subunit Ddc1 activates Mec1/ATR via two distinct mechanisms. Mol Cell 36(5):743-753.

104. Bonilla CY, Melo JA, & Toczyski DP (2008) Colocalization of sensors is sufficient to activate the DNA damage checkpoint in the absence of damage. Mol Cell 30(3):267-276.

105. Lindsey-Boltz LA & Sancar A (2011) Tethering DNA damage checkpoint mediator proteins topoisomerase IIbeta-binding protein 1 (TopBP1) and Claspin to DNA activates ataxia-telangiectasia mutated and RAD3-related (ATR) phosphorylation of checkpoint kinase 1 (Chk1). J Biol Chem 286(22):19229-19236.

106. Hashimoto Y, Tsujimura T, Sugino A, & Takisawa H (2006) The phosphorylated C-terminal domain of Xenopus Cut5 directly mediates ATR-dependent activation of Chk1. Genes Cells 11(9):993-1007.

107. Yan S, Lindsay HD, & Michael WM (2006) Direct requirement for Xmus101 in ATR-mediated phosphorylation of Claspin bound Chk1 during checkpoint signaling. J Cell Biol 173(2):181-186.

108. Liu S, Bekker-Jensen S, Mailand N, Lukas C, Bartek J, & Lukas J (2006) Claspin operates downstream of TopBP1 to direct ATR signaling towards Chk1 activation. Mol Cell Biol 26(16):6056-6064.

109. Kumagai A, Lee J, Yoo HY, & Dunphy WG (2006) TopBP1 activates the ATR-ATRIP complex. Cell 124(5):943-955.

110. Mordes DA & Cortez D (2008) Activation of ATR and related PIKKs. Cell Cycle 7(18):2809-2812.

111. Toledo LI, Murga M, Gutierrez-Martinez P, Soria R, & Fernandez-Capetillo O (2008) ATR signaling can drive cells into senescence in the absence of DNA breaks. Genes Dev 22(3):297-302.

112. Mordes DA, Nam EA, & Cortez D (2008) Dpb11 activates the Mec1-Ddc2 complex. Proc Natl Acad Sci U S A 105(48):18730-18734.

113. Navadgi-Patil VM & Burgers PM (2008) Yeast DNA replication protein Dpb11 activates the Mec1/ATR checkpoint kinase. J Biol Chem 283(51):35853-35859.

114. Yan S & Michael WM (2009) TopBP1 and DNA polymerase-alpha directly recruit the 9-1-1 complex to stalled DNA replication forks. J Cell Biol 184(6):793-804.

115. Cotta-Ramusino C, McDonald ER, 3rd, Hurov K, Sowa ME, Harper JW, & Elledge SJ (2011) A DNA damage response screen identifies RHINO, a 9-1-1 and TopBP1 interacting protein required for ATR signaling. Science 332(6035):1313-1317.

116. Cescutti R, Negrini S, Kohzaki M, & Halazonetis TD (2010) TopBP1 functions with 53BP1 in the G1 DNA damage checkpoint. EMBO J 29(21):3723-3732.

117. Yoo HY, Kumagai A, Shevchenko A, Shevchenko A, & Dunphy WG (2007) Ataxia-telangiectasia mutated (ATM)-dependent activation of ATR occurs through phosphorylation of TopBP1 by ATM. J Biol Chem 282(24):17501-17506.

118. Yoo HY, Kumagai A, Shevchenko A, & Dunphy WG (2009) The Mre11-Rad50-Nbs1 complex mediates activation of TopBP1 by ATM. Mol Biol Cell 20(9):2351-2360.

119. Araki H, Leem SH, Phongdara A, & Sugino A (1995) Dpb11, which interacts with DNA polymerase II(epsilon) in Saccharomyces cerevisiae, has a dual role in S-phase progression and at a cell cycle checkpoint. Proc Natl Acad Sci U S A 92(25):11791-11795.

120. Masumoto H, Sugino A, & Araki H (2000) Dpb11 controls the association between DNA polymerases alpha and epsilon and the autonomously replicating sequence region of budding yeast. Mol Cell Biol 20(8):2809-2817.

121. Moyer SE, Lewis PW, & Botchan MR (2006) Isolation of the Cdc45/Mcm2-7/GINS (CMG) complex, a candidate for the eukaryotic DNA replication fork helicase. Proc Natl Acad Sci U S A 103(27):10236-10241.

122. Tanaka S, Umemori T, Hirai K, Muramatsu S, Kamimura Y, & Araki H (2007) CDK-dependent phosphorylation of Sld2 and Sld3 initiates DNA replication in budding yeast. Nature 445(7125):328-332.

123. Takayama Y, Kamimura Y, Okawa M, Muramatsu S, Sugino A, & Araki H (2003) GINS, a novel multiprotein complex required for chromosomal DNA replication in budding yeast. Genes Dev 17(9):1153-1165.

124. Hashimoto Y & Takisawa H (2003) Xenopus Cut5 is essential for a CDK-dependent process in the initiation of DNA replication. Embo J 22(10):2526-2535.

125. Daub H, Olsen JV, Bairlein M, Gnad F, Oppermann FS, Korner R, Greff Z, Keri G, Stemmann O, & Mann M (2008) Kinase-selective enrichment

enables quantitative phosphoproteomics of the kinome across the cell cycle. Mol Cell 31(3):438-448.

126. Dephoure N, Zhou C, Villen J, Beausoleil SA, Bakalarski CE, Elledge SJ, & Gygi SP (2008) A quantitative atlas of mitotic phosphorylation. Proc Natl Acad Sci U S A 105(31):10762-10767.

127. Matsuoka S, Ballif BA, Smogorzewska A, McDonald ER, 3rd, Hurov KE, Luo J, Bakalarski CE, Zhao Z, Solimini N, Lerenthal Y, Shiloh Y, Gygi SP, & Elledge SJ (2007) ATM and ATR substrate analysis reveals extensive protein networks responsive to DNA damage. Science 316(5828):1160-1166.

128. Stokes MP, Rush J, Macneill J, Ren JM, Sprott K, Nardone J, Yang V, Beausoleil SA, Gygi SP, Livingstone M, Zhang H, Polakiewicz RD, & Comb MJ (2007) Profiling of UV-induced ATM/ATR signaling pathways. Proc Natl Acad Sci U S A 104(50):19855-19860.

129. Takai H, Tominaga K, Motoyama N, Minamishima YA, Nagahama H, Tsukiyama T, Ikeda K, Nakayama K, Nakanishi M, & Nakayama K (2000) Aberrant cell cycle checkpoint function and early embryonic death in Chk1(-/-) mice. Genes Dev 14(12):1439-1447.

130. Liu Q, Guntuku S, Cui XS, Matsuoka S, Cortez D, Tamai K, Luo G, Carattini-Rivera S, DeMayo F, Bradley A, Donehower LA, & Elledge SJ (2000) Chk1 is an essential kinase that is regulated by Atr and required for the G(2)/M DNA damage checkpoint. Genes Dev 14(12):1448-1459.

131. Jia-Lin Ma N & Stern DF (2008) Regulation of the Rad53 protein kinase in signal amplification by oligomer assembly and disassembly. Cell Cycle 7(6):808-817.

132. Pellicioli A & Foiani M (2005) Signal transduction: how rad53 kinase is activated. Curr Biol 15(18):R769-771.

133. Kumagai A & Dunphy WG (2000) Claspin, a novel protein required for the activation of Chk1 during a DNA replication checkpoint response in Xenopus egg extracts. Mol Cell 6(4):839-849.

134. Lee J, Kumagai A, & Dunphy WG (2003) Claspin, a Chk1-regulatory protein, monitors DNA replication on chromatin independently of RPA, ATR, and Rad17. Mol Cell 11(2):329-340.

135. Unsal-Kacmaz K, Chastain PD, Qu PP, Minoo P, Cordeiro-Stone M, Sancar A, & Kaufmann WK (2007) The human Tim/Tipin complex coordinates an Intra-S checkpoint response to UV that slows replication fork displacement. Mol Cell Biol 27(8):3131-3142.

136. Unsal-Kacmaz K, Mullen TE, Kaufmann WK, & Sancar A (2005) Coupling of human circadian and cell cycles by the timeless protein. Mol Cell Biol 25(8):3109-3116.

137. Chou DM & Elledge SJ (2006) Tipin and Timeless form a mutually protective complex required for genotoxic stress resistance and checkpoint function. Proc Natl Acad Sci U S A 103(48):18143-18147.

138. Kemp MG, Akan Z, Yilmaz S, Grillo M, Smith-Roe SL, Kang TH, Cordeiro-Stone M, Kaufmann WK, Abraham RT, Sancar A, & Unsal-Kacmaz K (2010) Tipin-replication protein A interaction mediates Chk1 phosphorylation by ATR in response to genotoxic stress. J Biol Chem 285(22):16562-16571.

139. Santocanale C & Diffley JF (1998) A Mec1- and Rad53-dependent checkpoint controls late-firing origins of DNA replication. Nature 395(6702):615-618.

140. Shirahige K, Hori Y, Shiraishi K, Yamashita M, Takahashi K, Obuse C, Tsurimoto T, & Yoshikawa H (1998) Regulation of DNA-replication origins during cell-cycle progression. Nature 395(6702):618-621.

141. Tercero JA & Diffley JF (2001) Regulation of DNA replication fork progression through damaged DNA by the Mec1/Rad53 checkpoint. Nature 412(6846):553-557.

142. Lopes M, Cotta-Ramusino C, Pellicioli A, Liberi G, Plevani P, Muzi-Falconi M, Newlon CS, & Foiani M (2001) The DNA replication checkpoint response stabilizes stalled replication forks. Nature 412(6846):557-561.

143. Segurado M & Diffley JFX (2008) Separate roles for the DNA damage checkpoint protein kinases in stabilizing DNA replication forks. Genes Dev. 22(13):1816-1827.

144. Feijoo C, Hall-Jackson C, Wu R, Jenkins D, Leitch J, Gilbert DM, & Smythe C (2001) Activation of mammalian Chk1 during DNA replication arrest: a role for Chk1 in the intra-S phase checkpoint monitoring replication origin firing. J Cell Biol 154(5):913-923.

145. Shechter D, Costanzo V, & Gautier J (2004) ATR and ATM regulate the timing of DNA replication origin firing. Nat Cell Biol 6(7):648-655.

146. Maya-Mendoza A, Petermann E, Gillespie DA, Caldecott KW, & Jackson DA (2007) Chk1 regulates the density of active replication origins during the vertebrate S phase. Embo J 26(11):2719-2731.

147. Ge XQ & Blow JJ (2010) Chk1 inhibits replication factory activation but allows dormant origin firing in existing factories. J Cell Biol 191(7):1285-1297.

148. Cobb JA, Bjergbaek L, Shimada K, Frei C, & Gasser SM (2003) DNA polymerase stabilization at stalled replication forks requires Mec1 and the RecQ helicase Sgs1. Embo J 22(16):4325-4336.

149. Lucca C, Vanoli F, Cotta-Ramusino C, Pellicioli A, Liberi G, Haber J, & Foiani M (2004) Checkpoint-mediated control of replisome-fork association and signalling in response to replication pausing. Oncogene 23(6):1206-1213.

150. Trenz K, Smith E, Smith S, & Costanzo V (2006) ATM and ATR promote Mre11 dependent restart of collapsed replication forks and prevent accumulation of DNA breaks. Embo J 25(8):1764-1774.

151. Yoo HY, Shevchenko A, & Dunphy WG (2004) Mcm2 is a direct substrate of ATM and ATR during DNA damage and DNA replication checkpoint responses. J Biol Chem 279(51):53353-53364.

152. Cortez D, Glick G, & Elledge SJ (2004) Minichromosome maintenance proteins are direct targets of the ATM and ATR checkpoint kinases. Proc Natl Acad Sci U S A 101(27):10078-10083.

153. Ammazzalorso F, Pirzio LM, Bignami M, Franchitto A, & Pichierri P (2010) ATR and ATM differently regulate WRN to prevent DSBs at stalled replication forks and promote replication fork recovery. EMBO J 29(18):3156-3169.

154. Davies SL, North PS, Dart A, Lakin ND, & Hickson ID (2004) Phosphorylation of the Bloom's syndrome helicase and its role in recovery from S-phase arrest. Mol Cell Biol 24(3):1279-1291.

155. Hickson ID (2003) RecQ helicases: caretakers of the genome. Nat Rev Cancer 3(3):169-178.

156. Shimura T, Torres MJ, Martin MM, Rao VA, Pommier Y, Katsura M, Miyagawa K, & Aladjem MI (2008) Bloom's syndrome helicase and Mus81 are required to induce transient double-strand DNA breaks in response to DNA replication stress. J Mol Biol 375(4):1152-1164.

157. Lisby M, Barlow JH, Burgess RC, & Rothstein R (2004) Choreography of the DNA damage response: spatiotemporal relationships among checkpoint and repair proteins. Cell 118(6):699-713.

158. Desany BA, Alcasabas AA, Bachant JB, & Elledge SJ (1998) Recovery from DNA replicational stress is the essential function of the S-phase checkpoint pathway. Genes Dev 12(18):2956-2970.

159. Luciani MG, Oehlmann M, & Blow JJ (2004) Characterization of a novel ATR-dependent, Chk1-independent, intra-S-phase checkpoint that suppresses initiation of replication in Xenopus. J Cell Sci 117(Pt 25):6019-6030.

160. Lovejoy CA & Cortez D (2009) Common mechanisms of PIKK regulation. DNA Repair (Amst) 8(9):1004-1008.

161. Abraham RT (2004) PI 3-kinase related kinases: 'big' players in stress-induced signaling pathways. DNA Repair (Amst) 3(8-9):883-887.

162. Bakkenist CJ & Kastan MB (2003) DNA damage activates ATM through intermolecular autophosphorylation and dimer dissociation. Nature 421(6922):499-506.

163. Chen J, Zheng XF, Brown EJ, & Schreiber SL (1995) Identification of an 11-kDa FKBP12-rapamycin-binding domain within the 289-kDa FKBP12-rapamycin-associated protein and characterization of a critical serine residue. Proc Natl Acad Sci U S A 92(11):4947-4951.

164. Chiu MI, Katz H, & Berlin V (1994) RAPT1, a mammalian homolog of yeast Tor, interacts with the FKBP12/rapamycin complex. Proc Natl Acad Sci U S A 91(26):12574-12578.

165. Perry J & Kleckner N (2003) The ATRs, ATMs, and TORs are giant HEAT repeat proteins. Cell 112(2):151-155.

166. Rubinson EH, Gowda AS, Spratt TE, Gold B, & Eichman BF (2010) An unprecedented nucleic acid capture mechanism for excision of DNA damage. Nature 468(7322):406-411.

167. Sancak Y, Peterson TR, Shaul YD, Lindquist RA, Thoreen CC, Bar-Peled L, & Sabatini DM (2008) The Rag GTPases bind raptor and mediate amino acid signaling to mTORC1. Science 320(5882):1496-1501.

168. Sancak Y, Bar-Peled L, Zoncu R, Markhard AL, Nada S, & Sabatini DM (2010) Ragulator-Rag complex targets mTORC1 to the lysosomal surface and is necessary for its activation by amino acids. Cell 141(2):290-303.

169. Falck J, Coates J, & Jackson SP (2005) Conserved modes of recruitment of ATM, ATR and DNA-PKcs to sites of DNA damage. Nature 434(7033):605-611.

170. Lee JH & Paull TT (2004) Direct activation of the ATM protein kinase by the Mre11/Rad50/Nbs1 complex. Science 304(5667):93-96.

171. Lee JH & Paull TT (2005) ATM Activation by DNA Double-Strand Breaks Through the Mre11-Rad50-Nbs1 Complex. Science 308:551-554.

172. Meek K, Douglas P, Cui X, Ding Q, & Lees-Miller SP (2007) trans Autophosphorylation at DNA-dependent protein kinase's two major autophosphorylation site clusters facilitates end processing but not end joining. Mol Cell Biol 27(10):3881-3890.

173. Smith GC & Jackson SP (1999) The DNA-dependent protein kinase. Genes Dev 13(8):916-934.

174. Long X, Lin Y, Ortiz-Vega S, Yonezawa K, & Avruch J (2005) Rheb binds and regulates the mTOR kinase. Curr Biol 15(8):702-713.

175. Jiang X, Sun Y, Chen S, Roy K, & Price BD (2006) The FATC domains of PIKK proteins are functionally equivalent and participate in the Tip60-dependent activation of DNA-PKcs and ATM. J Biol Chem 281(23):15741-15746.

176. Sun Y, Xu Y, Roy K, & Price BD (2007) DNA damage induced acetylation of lysine 3016 of ATM activates ATM kinase activity. Mol Cell Biol 24:8502-8509.

177. Soliman GA, Acosta-Jaquez HA, Dunlop EA, Ekim B, Maj NE, Tee AR, & Fingar DC (2010) mTOR Ser-2481 autophosphorylation monitors mTORC-specific catalytic activity and clarifies rapamycin mechanism of action. J Biol Chem 285(11):7866-7879.

178. Acosta-Jaquez HA, Keller JA, Foster KG, Ekim B, Soliman GA, Feener EP, Ballif BA, & Fingar DC (2009) Site-specific mTOR phosphorylation promotes mTORC1-mediated signaling and cell growth. Mol Cell Biol 29(15):4308-4324.

179. Rosner M, Siegel N, Valli A, Fuchs C, & Hengstschlager M (2010) mTOR phosphorylated at S2448 binds to raptor and rictor. Amino Acids 38(1):223-228.

180. Kozlov SV, Graham ME, Jakob B, Tobias F, Kijas AW, Tanuji M, Chen P, Robinson PJ, Taucher-Scholz G, Suzuki K, So S, Chen D, & Lavin MF (2011) Autophosphorylation and ATM activation: additional sites add to the complexity. J Biol Chem 286(11):9107-9119.

181. Kozlov SV, Graham ME, Peng C, Chen P, Robinson PJ, & Lavin MF (2006) Involvement of novel autophosphorylation sites in ATM activation. EMBO J 25(15):3504-3514.

182. Dobbs TA, Tainer JA, & Lees-Miller SP (2010) A structural model for regulation of NHEJ by DNA-PKcs autophosphorylation. DNA Repair (Amst) 9(12):1307-1314.

183. Cui X, Yu Y, Gupta S, Cho YM, Lees-Miller SP, & Meek K (2005) Autophosphorylation of DNA-dependent protein kinase regulates DNA end processing and may also alter double-strand break repair pathway choice. Mol Cell Biol 25(24):10842-10852.

184. Chan DW, Chen BP, Prithivirajsingh S, Kurimasa A, Story MD, Qin J, & Chen DJ (2002) Autophosphorylation of the DNA-dependent protein kinase catalytic subunit is required for rejoining of DNA double-strand breaks. Genes Dev 16(18):2333-2338.

185. Pellegrini M, Celeste A, Difilippantonio S, Guo R, Wang W, Feigenbaum L, & Nussenzweig A (2006) Autophosphorylation at serine 1987 is dispensable for murine Atm activation in vivo. Nature 443(7108):222-225.

186. Merkle D, Douglas P, Moorhead GB, Leonenko Z, Yu Y, Cramb D, Bazett-Jones DP, & Lees-Miller SP (2002) The DNA-dependent protein kinase interacts with DNA to form a protein-DNA complex that is disrupted by phosphorylation. Biochemistry 41(42):12706-12714.

187. Douglas P, Cui X, Block WD, Yu Y, Gupta S, Ding Q, Ye R, Morrice N, Lees-Miller SP, & Meek K (2007) The DNA-dependent protein kinase catalytic subunit (DNA-PKcs) is phosphorylated in vivo on threonine 3950, a highly conserved amino acid in the protein kinase domain. Mol Cell Biol 27:1581-1591.

188. Uematsu N, Weterings E, Yano K, Morotomi-Yano K, Jakob B, Taucher-Scholz G, Mari PO, van Gent DC, Chen BP, & Chen DJ (2007) Autophosphorylation of DNA-PKCS regulates its dynamics at DNA double-strand breaks. J Cell Biol 177(2):219-229.

189. Hammel M, Yu Y, Mahaney BL, Cai B, Ye R, Phipps BM, Rambo RP, Hura GL, Pelikan M, So S, Abolfath RM, Chen DJ, Lees-Miller SP, & Tainer JA (2010) Ku and DNA-dependent protein kinase dynamic conformations and assembly regulate DNA binding and the initial non-homologous end joining complex. J Biol Chem 285(2):1414-1423.

190. Morris EP, Rivera-Calzada A, da Fonseca PC, Llorca O, Pearl LH, & Spagnolo L (2011) Evidence for a remodelling of DNA-PK upon autophosphorylation from electron microscopy studies. Nucleic Acids Res 39(13):5757-5767.

191. Nam EA, Zhao R, Glick GG, Bansbach CE, Friedman DB, & Cortez D (2011) T1989 phosphorylation is a marker of active ataxia telangiectasia-mutated and rad3-related (ATR) kinase. J Biol Chem.

192. Hickson I, Zhao Y, Richardson CJ, Green SJ, Martin NM, Orr AI, Reaper PM, Jackson SP, Curtin NJ, & Smith GC (2004) Identification and characterization of a novel and specific inhibitor of the ataxia-telangiectasia mutated kinase ATM. Cancer Res 64(24):9152-9159.

193. Leahy JJ, Golding BT, Griffin RJ, Hardcastle IR, Richardson C, Rigoreau L, & Smith GC (2004) Identification of a highly potent and selective DNA-dependent protein kinase (DNA-PK) inhibitor (NU7441) by screening of chromenone libraries. Bioorg Med Chem Lett 14(24):6083-6087.

194. Zabludoff SD, Deng C, Grondine MR, Sheehy AM, Ashwell S, Caleb BL, Green S, Haye HR, Horn CL, Janetka JW, Liu D, Mouchet E, Ready S, Rosenthal JL, Queva C, Schwartz GK, Taylor KJ, Tse AN, Walker GE, & White AM (2008) AZD7762, a novel checkpoint kinase inhibitor, drives checkpoint abrogation and potentiates DNA-targeted therapies. Mol Cancer Ther 7(9):2955-2966.

195. Chenna R, Sugawara H, Koike T, Lopez R, Gibson TJ, Higgins DG, & Thompson JD (2003) Multiple sequence alignment with the Clustal series of programs. Nucleic Acids Res 31(13):3497-3500.

196. Cole C, Barber JD, & Barton GJ (2008) The Jpred 3 secondary structure prediction server. Nucleic Acids Res 36(Web Server issue):W197-201.

197. Boyle WJ, van der Geer P, & Hunter T (1991) Phosphopeptide mapping and phosphoamino acid analysis by two-dimensional separation on thin-layer cellulose plates. Methods Enzymol 201:110-149.

198. Douglas P, Sapkota GP, Morrice N, Yu Y, Goodarzi AA, Merkle D, Meek K, Alessi DR, & Lees-Miller SP (2002) Identification of in vitro and in vivo phosphorylation sites in the catalytic subunit of the DNA-dependent protein kinase. Biochem J 368(Pt 1):243-251.

199. Neal JA, Dang V, Douglas P, Wold MS, Lees-Miller SP, & Meek K (2011) Inhibition of homologous recombination by DNA-dependent protein kinase requires kinase activity, is titratable, and is modulated by autophosphorylation. Mol Cell Biol 31(8):1719-1733.

200. Uziel T, Lerenthal Y, Moyal L, Andegeko Y, Mittelman L, & Shiloh Y (2003) Requirement of the MRN complex for ATM activation by DNA damage. Embo J 22(20):5612-5621.

201. Dupre A, Boyer-Chatenet L, & Gautier J (2006) Two-step activation of ATM by DNA and the Mre11-Rad50-Nbs1 complex. Nat Struct Mol Biol 13(5):451-457.

202. Ding Q, Reddy YV, Wang W, Woods T, Douglas P, Ramsden DA, Lees-Miller SP, & Meek K (2003) Autophosphorylation of the catalytic subunit of the DNA-dependent protein kinase is required for efficient end processing during DNA double-strand break repair. Mol Cell Biol 23(16):5836-5848.

203. Nagasawa H, Little JB, Lin YF, So S, Kurimasa A, Peng Y, Brogan JR, Chen DJ, Bedford JS, & Chen BP (2011) Differential role of DNA-PKcs phosphorylations and kinase activity in radiosensitivity and chromosomal instability. Radiat Res 175(1):83-89.

204. Ball HL & Cortez D (2005) ATRIP oligomerization is required for ATR-dependent checkpoint signaling. J Biol Chem 280(36):31390-31396.

205. Toledo LI, Murga M, Zur R, Soria R, Rodriguez A, Martinez S, Oyarzabal J, Pastor J, Bischoff JR, & Fernandez-Capetillo O (2011) A cell-based screen identifies ATR inhibitors with synthetic lethal properties for cancer-associated mutations. Nat Struct Mol Biol 18(6):721-727.

206. Reaper PM, Griffiths MR, Long JM, Charrier JD, Maccormick S, Charlton PA, Golec JM, & Pollard JR (2011) Selective killing of ATM- or p53-deficient cancer cells through inhibition of ATR. Nat Chem Biol 7(7):428-430.

207. Paciotti V, Clerici M, Scotti M, Lucchini G, & Longhese MP (2001) Characterization of mec1 kinase-deficient mutants and of new hypomorphic mec1 alleles impairing subsets of the DNA damage response pathway. Mol Cell Biol 21(12):3913-3925.

208. Choi JH, Lindsey-Boltz LA, Kemp M, Mason AC, Wold MS, & Sancar A (2010) Reconstitution of RPA-covered single-stranded DNA-activated ATR-Chk1 signaling. Proc Natl Acad Sci U S A 107(31):13660-13665.

209. Lindsey-Boltz LA, Sercin O, Choi JH, & Sancar A (2009) Reconstitution of human claspin-mediated phosphorylation of Chk1 by the ATR (ataxia telangiectasia-mutated and rad3-related) checkpoint kinase. J Biol Chem 284(48):33107-33114.

210. Kato R & Ogawa H (1994) An essential gene, ESR1, is required for mitotic cell growth, DNA repair and meiotic recombination in Saccharomyces cerevisiae. Nucleic Acids Res 22(15):3104-3112.

211. Zhao X, Muller EG, & Rothstein R (1998) A suppressor of two essential checkpoint genes identifies a novel protein that negatively affects dNTP pools. Mol Cell 2(3):329-340.

212. Zhao X, Chabes A, Domkin V, Thelander L, & Rothstein R (2001) The ribonucleotide reductase inhibitor Sml1 is a new target of the Mec1/Rad53 kinase cascade during growth and in response to DNA damage. Embo J 20(13):3544-3553.

213. Hakansson P, Hofer A, & Thelander L (2006) Regulation of mammalian ribonucleotide reduction and dNTP pools after DNA damage and in resting cells. J Biol Chem 281(12):7834-7841.

214. Sandrini MP & Piskur J (2005) Deoxyribonucleoside kinases: two enzyme families catalyze the same reaction. Trends Biochem Sci 30(5):225-228.

215. Fang Y, Tsao CC, Goodman BK, Furumai R, Tirado CA, Abraham RT, & Wang XF (2004) ATR functions as a gene dosage-dependent tumor suppressor on a mismatch repair-deficient background. Embo J 23(15):3164-3174.

216. Lewis KA, Mullany S, Thomas B, Chien J, Loewen R, Shridhar V, & Cliby WA (2005) Heterozygous ATR mutations in mismatch repair-deficient cancer cells have functional significance. Cancer Res 65(16):7091-7095.

217. Jardim MJ, Wang QH, Furumai R, Wakeman T, Goodman BK, & Wang XF (2009) Reduced ATR or Chk1 Expression Leads to Chromosome Instability and Chemosensitization of Mismatch Repair-deficient Colorectal Cancer Cells. Molecular Biology of the Cell 20(17):3801-3809.

218. Sibanda BL, Chirgadze DY, & Blundell TL (2010) Crystal structure of DNA-PKcs reveals a large open-ring cradle comprised of HEAT repeats. Nature 463(7277):118-121.

219. Williams DR, Lee KJ, Shi J, Chen DJ, & Stewart PL (2008) Cryo-EM Structure of the DNA-Dependent Protein Kinase Catalytic Subunit at Subnanometer Resolution Reveals alpha Helices and Insight into DNA Binding. Structure 16(3):468-477.

220. Spagnolo L, Rivera-Calzada A, Pearl LH, & Llorca O (2006) Three-dimensional structure of the human DNA-PKcs/Ku70/Ku80 complex assembled on DNA and its implications for DNA DSB repair. Mol Cell 22(4):511-519.

221. Wullschleger S, Loewith R, & Hall MN (2006) TOR signaling in growth and metabolism. Cell 124(3):471-484.

222. Zhang J, Bao S, Furumai R, Kucera KS, Ali A, Dean NM, & Wang XF (2005) Protein phosphatase 5 is required for ATR-mediated checkpoint activation. Mol Cell Biol 25(22):9910-9919.

223. Urano J, Sato T, Matsuo T, Otsubo Y, Yamamoto M, & Tamanoi F (2007) Point mutations in TOR confer Rheb-independent growth in fission yeast and nutrient-independent mammalian TOR signaling in mammalian cells. Proc Natl Acad Sci U S A 104(9):3514-3519.

224. Reinke A, Chen JC, Aronova S, & Powers T (2006) Caffeine targets TOR complex I and provides evidence for a regulatory link between the FRB and kinase domains of Tor1p. J Biol Chem 281(42):31616-31626.

225. Bartkova J, Hamerlik P, Stockhausen MT, Ehrmann J, Hlobilkova A, Laursen H, Kalita O, Kolar Z, Poulsen HS, Broholm H, Lukas J, & Bartek J (2010) Replication stress and oxidative damage contribute to aberrant constitutive activation of DNA damage signalling in human gliomas. Oncogene 29(36):5095-5102.

226. Dutcher JP (2004) Mammalian target of rapamycin inhibition. Clin Cancer Res 10(18 Pt 2):6382S-6387S.

227. Dutcher JP (2004) Mammalian target of rapamycin (mTOR) Inhibitors. Curr Oncol Rep 6(2):111-115.

228. Boultwood J (2001) Ataxia telangiectasia gene mutations in leukaemia and lymphoma. J Clin Pathol 54(7):512-516.

229. Sirbu BM, Couch FB, Feigerle JT, Bhaskara S, Hiebert SW, & Cortez D (2011) Analysis of protein dynamics at active, stalled, and collapsed replication forks. Genes Dev 25(12):1320-1327.

230. Parrilla-Castellar ER, Arlander SJ, & Karnitz L (2004) Dial 9-1-1 for DNA damage: the Rad9-Hus1-Rad1 (9-1-1) clamp complex. DNA Repair (Amst) 3(8-9):1009-1014.

231. Soutoglou E & Misteli T (2008) Activation of the Cellular DNA Damage Response in the Absence of DNA Lesions. Science 320:1507-1510.

232. Hermand D & Nurse P (2007) Cdc18 enforces long-term maintenance of the S phase checkpoint by anchoring the Rad3-Rad26 complex to chromatin. Mol Cell 26(4):553-563.

233. Yoshida K, Sugimoto N, Iwahori S, Yugawa T, Narisawa-Saito M, Kiyono T, & Fujita M (2010) CDC6 interaction with ATR regulates activation of a replication checkpoint in higher eukaryotic cells. J Cell Sci 123(Pt 2):225-235.

234. Stojic L, Mojas N, Cejka P, Di Pietro M, Ferrari S, Marra G, & Jiricny J (2004) Mismatch repair-dependent G2 checkpoint induced by low doses of SN1 type methylating agents requires the ATR kinase. Genes Dev 18(11):1331-1344.

235. Pabla N, Ma Z, McIlhatton MA, Fishel R, & Dong Z (2011) hMSH2 recruits ATR to DNA damage sites for activation during DNA damage-induced apoptosis. J Biol Chem 286(12):10411-10418.

236. Yoshioka K, Yoshioka Y, & Hsieh P (2006) ATR kinase activation mediated by MutSalpha and MutLalpha in response to cytotoxic O6-methylguanine adducts. Mol Cell 22(4):501-510.

237. Wang Y & Qin J (2003) MSH2 and ATR form a signaling module and regulate two branches of the damage response to DNA methylation. Proc Natl Acad Sci U S A 100(26):15387-15392.

238. Liu Y, Fang Y, Shao H, Lindsey-Boltz L, Sancar A, & Modrich P (2010) Interactions of human mismatch repair proteins MutSalpha and MutLalpha with proteins of the ATR-Chk1 pathway. J Biol Chem 285(8):5974-5982.

239. Unsal-Kacmaz K, Makhov AM, Griffith JD, & Sancar A (2002) Preferential binding of ATR protein to UV-damaged DNA. Proc Natl Acad Sci U S A 99(10):6673-6678.

240. Choi JH, Lindsey-Boltz LA, & Sancar A (2009) Cooperative activation of the ATR checkpoint kinase by TopBP1 and damaged DNA. Nucleic Acids Res 37(5):1501-1509.

241. Caporali S, Falcinelli S, Starace G, Russo MT, Bonmassar E, Jiricny J, & D'Atri S (2004) DNA damage induced by temozolomide signals to both ATM and ATR: role of the mismatch repair system. Mol Pharmacol 66(3):478-491.

242. Ubersax JA & Ferrell JE, Jr. (2007) Mechanisms of specificity in protein phosphorylation. Nat Rev Mol Cell Biol 8(7):530-541.

243. Lempiainen H & Halazonetis TD (2009) Emerging common themes in regulation of PIKKs and PI3Ks. EMBO J 28(20):3067-3073.

244. Huang CH, Mandelker D, Gabelli SB, & Amzel LM (2008) Insights into the oncogenic effects of PIK3CA mutations from the structure of p110alpha/p85alpha. Cell Cycle 7(9):1151-1156.

245. Hardt M, Chantaravisoot N, & Tamanoi F (2011) Activating mutations of TOR (target of rapamycin). Genes Cells 16(2):141-151.

246. Sturgill TW & Hall MN (2009) Activating mutations in TOR are in similar structures as oncogenic mutations in PI3KCalpha. ACS Chem Biol 4(12):999-1015.

247. Mi J, Dziegielewski J, Bolesta E, Brautigan DL, & Larner JM (2009) Activation of DNA-PK by ionizing radiation is mediated by protein phosphatase 6. PLoS One 4(2):e4395.

248. Wechsler T, Chen BP, Harper R, Morotomi-Yano K, Huang BC, Meek K, Cleaver JE, Chen DJ, & Wabl M (2004) DNA-PKcs function regulated specifically by protein phosphatase 5. Proc Natl Acad Sci U S A 101(5):1247-1252.

249. Peng A & Maller JL (2010) Serine/threonine phosphatases in the DNA damage response and cancer. Oncogene 29(45):5977-5988.

250. Ali A, Zhang J, Bao S, Liu I, Otterness D, Dean NM, Abraham RT, & Wang XF (2004) Requirement of protein phosphatase 5 in DNA-damage-induced ATM activation. Genes Dev 18(3):249-254.

251. Navadgi-Patil VM & Burgers PM (2009) A tale of two tails: activation of DNA damage checkpoint kinase Mec1/ATR by the 9-1-1 clamp and by Dpb11/TopBP1. DNA Repair (Amst) 8(9):996-1003.

252. Kobe B & Kemp BE (1999) Active site-directed protein regulation. Nature 402(6760):373-376.

253. Lee MH & Yang HY (2001) Negative regulators of cyclin-dependent kinases and their roles in cancers. Cell Mol Life Sci 58(12-13):1907-1922.

254. Adams JA (2003) Activation loop phosphorylation and catalysis in protein kinases: is there functional evidence for the autoinhibitor model? Biochemistry 42(3):601-607.

255. Hubbard SR (1997) Crystal structure of the activated insulin receptor tyrosine kinase in complex with peptide substrate and ATP analog. EMBO J 16(18):5572-5581.

256. Filippakopoulos P, Muller S, & Knapp S (2009) SH2 domains: modulators of nonreceptor tyrosine kinase activity. Curr Opin Struct Biol 19(6):643-649.

257. Hubbard SR (2002) Autoinhibitory mechanisms in receptor tyrosine kinases. Front Biosci 7:d330-340.

258. Pawson T (2002) Regulation and targets of receptor tyrosine kinases. Eur J Cancer 38 Suppl 5:S3-10.

259. Weterings E & Chen DJ (2007) DNA-dependent protein kinase in nonhomologous end joining: a lock with multiple keys? J Cell Biol 179(2):183-186.

260. Manning BD & Cantley LC (2007) AKT/PKB signaling: navigating downstream. Cell 129(7):1261-1274.

261. Jacinto E, Facchinetti V, Liu D, Soto N, Wei S, Jung SY, Huang Q, Qin J, & Su B (2006) SIN1/MIP1 maintains rictor-mTOR complex integrity and regulates Akt phosphorylation and substrate specificity. Cell 127(1):125-137.

262. McMahon LP, Choi KM, Lin TA, Abraham RT, & Lawrence JC, Jr. (2002) The rapamycin-binding domain governs substrate selectivity by the mammalian target of rapamycin. Mol Cell Biol 22(21):7428-7438.

263. Liu S, Shiotani B, Lahiri M, Marechal A, Tse A, Leung CC, Glover JN, Yang XH, & Zou L (2011) ATR Autophosphorylation as a Molecular Switch for Checkpoint Activation. Mol Cell 43(2):192-202.

264. Guo Z, Kozlov S, Lavin MF, Person MD, & Paull TT (2010) ATM activation by oxidative stress. Science 330(6003):517-521.

265. Trenz K, Errico A, & Costanzo V (2008) Plx1 is required for chromosomal DNA replication under stressful conditions. Embo J 27(6):876-885.

266. Petermann E, Woodcock M, & Helleday T (2010) Chk1 promotes replication fork progression by controlling replication initiation. Proc Natl Acad Sci U S A 107(37):16090-16095.

267. Peasland A, Wang LZ, Rowling E, Kyle S, Chen T, Hopkins A, Cliby WA, Sarkaria J, Beale G, Edmondson RJ, & Curtin NJ (2011) Identification and evaluation of a potent novel ATR inhibitor, NU6027, in breast and ovarian cancer cell lines. Br J Cancer 105(3):372-381.

268. Murray CW & Blundell TL (2010) Structural biology in fragment-based drug design. Curr Opin Struct Biol 20(4):497-507.

269. Nigg EA (2002) Centrosome aberrations: cause or consequence of cancer progression? Nat Rev Cancer 2(11):815-825.

270. Nigg EA (2006) Origins and consequences of centrosome aberrations in human cancers. Int J Cancer 119(12):2717-2723.

271. Knoblich JA (2010) Asymmetric cell division: recent developments and their implications for tumour biology. Nat Rev Mol Cell Biol 11(12):849-860.

272. Zhang S, Hemmerich P, & Grosse F (2007) Centrosomal localization of DNA damage checkpoint proteins. J Cell Biochem 101(2):451-465.

273. Collis SJ, Ciccia A, Deans AJ, Horejsi Z, Martin JS, Maslen SL, Skehel JM, Elledge SJ, West SC, & Boulton SJ (2008) FANCM and FAAP24 function in ATR-mediated checkpoint signaling independently of the Fanconi anemia core complex. Mol Cell 32(3):313-324.

274. Griffith E, Walker S, Martin CA, Vagnarelli P, Stiff T, Vernay B, Al Sanna N, Saggar A, Hamel B, Earnshaw WC, Jeggo PA, Jackson AP, & O'Driscoll M (2008) Mutations in pericentrin cause Seckel syndrome with defective ATR-dependent DNA damage signaling. Nat Genet 40(2):232-236.

275. O'Driscoll M, Jackson AP, & Jeggo PA (2006) Microcephalin: a causal link between impaired damage response signalling and microcephaly. Cell Cycle 5(20):2339-2344.

276. Nigg EA & Raff JW (2009) Centrioles, centrosomes, and cilia in health and disease. Cell 139(4):663-678.

277. Tibelius A, Marhold J, Zentgraf H, Heilig CE, Neitzel H, Ducommun B, Rauch A, Ho AD, Bartek J, & Kramer A (2009) Microcephalin and pericentrin regulate mitotic entry via centrosome-associated Chk1. J Cell Biol 185(7):1149-1157.

278. Kramer A, Mailand N, Lukas C, Syljuasen RG, Wilkinson CJ, Nigg EA, Bartek J, & Lukas J (2004) Centrosome-associated Chk1 prevents premature activation of cyclin-B-Cdk1 kinase. Nat Cell Biol 6(9):884-891.

279. Loffler H, Bochtler T, Fritz B, Tews B, Ho AD, Lukas J, Bartek J, & Kramer A (2007) DNA damage-induced accumulation of centrosomal Chk1 contributes to its checkpoint function. Cell Cycle 6(20):2541-2548.

280. Ruzankina Y, Pinzon-Guzman C, Asare A, Ong T, Pontano L, Cotsarelis G, Zediak VP, Velez M, Bhandoola A, & Brown EJ (2007) Deletion of the developmentally essential gene ATR in adult mice leads to age-related phenotypes and stem cell loss. Cell Stem Cell 1(1):113-126.

281. Murga M, Bunting S, Montana MF, Soria R, Mulero F, Canamero M, Lee Y, McKinnon PJ, Nussenzweig A, & Fernandez-Capetillo O (2009) A mouse model of ATR-Seckel shows embryonic replicative stress and accelerated aging. Nat Genet 41(8):891-898.

282. Pease JC & Tirnauer JS (2011) Mitotic spindle misorientation in cancer--out of alignment and into the fire. J Cell Sci 124(Pt 7):1007-1016.